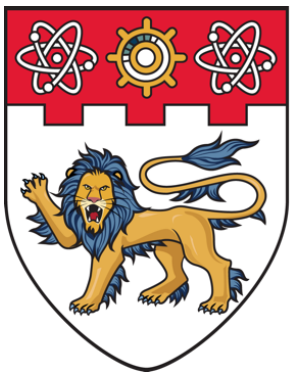

NANYANG TECHNOLOGICAL UNIVERSITY

SINGAPORE

ELUSIVE GROUP 14 ELEMENTAL SPECIES STABILISED BY AMIDINATO SILYLENES

MELDON WEE YI SHUO

SCHOOL OF CHEMISTRY, CHEMICAL ENGINEERING AND BIOTECHNOLOGY

2024

ELUSIVE GROUP 14 ELEMENTAL SPECIES STABILISED BY AMIDINATO SILYLENES

MELDON WEE YI SHUO

SCHOOL OF CHEMISTRY, CHEMICAL ENGINEERING AND BIOTECHNOLOGY

A thesis submitted to the Nanyang Technological University in partial fulfilment of the requirement for the degree of Doctor of Philosophy

2024

Statement of Originality

I hereby certify that the work embodied in this thesis is the result of original research done by me except where otherwise stated in this thesis. The thesis work has not been submitted for a degree or professional qualification to any other university or institution. I declare that this thesis is written by myself and is free of plagiarism and of sufficient grammatical clarity to be examined. I confirm that the investigations were conducted in accord with the ethics policies and integrity standards of Nanyang Technological University and that the research data are presented honestly and without prejudice.

. . 17/07/2023. . . . . .

Date Meldon Wee Yi Shuo

Supervisor Declaration Statement

I have reviewed the content and presentation style of this thesis and declare it of sufficient grammatical clarity to be examined. To the best of my knowledge, the thesis is free of plagiarism and the research and writing are those of the candidate's except as acknowledged in the Author Attribution Statement. I confirm that the investigations were conducted in accord with the ethics policies and integrity standards of Nanyang Technological University and that the research data are presented honestly and without prejudice.

. . 17/07/2023. . . . . .

Date Assoc. Prof. Dr. Cheuk-Wai So

Authorship Attribution Statement

This thesis **does not** contain any materials from papers published in peer-reviewed journals or from papers accepted at conferences in which I am listed as an author.

. . 17/07/2023. . . . . .

Date Meldon Wee Yi Shuo

Abstract

This thesis describes the synthesis and isolation of a series of Group 14 elemental clusters bearing challenging and unique structural characteristics, all stabilized by an amidinato silylene ligand system.

In Chapter 2, the synthesis of a remarkable heavier analogue of spiro[3.3]hepta-1,2,5,6-tetraene **2.4** is described. Its unique structure bearing two simultaneous strained cyclic allene moieties can also be described as simultaneous silylones, monatomic silicon(0) species stabilised by a tetradentate silylene ligand. Its reactivity to $W(CO)_5$·THF results in the formation of an bis(pentacarbonyl tungsten)-spiroheptasiladione adduct **2.8** demonstrating its Lewis Basicity. The structures of other co-products, **2.6** and **2.7**, from its synthesis shed light on its proposed synthetic pathway.

In Chapter 3, the transfer of digermanium(0) to amidinato silylene to from a digermadisilacyclobutadiene complex **3.2** is demonstrated. Stepwise growth of a germanium cluster is also demonstrated resulting the synthesis and isolation of a bis(trigermanium(0)) complex **3.3**. Preliminary results demonstrating the release of trigermanium (0) species towards the preparation of amorphous germanium nanoparticles are also described.

Acknowledgements

First goes to my supervisor Associate Professor Dr. Cheuk-Wai SO. I am deeply grateful to him for accepting me into his group. Through his patient guidance and thoughtful lessons, I was able to gain more than just scientific knowledge and laboratory skills. His insightful talks have lent me fresh perspectives into many of my troubles, and his unique outlook has taught me to think critically in all matters. He has been a significant factor in my growth during this period and for that I am ever grateful.

Secondly, goes to my lab colleagues—namely, our post-docs, Dr. ZHANG Teng and Dr. Rahul KUMAR Siwatch for their vast knowledge and thought-provoking discussions. Thank you to my graduated lab seniors, Dr. SHAN Yuliang, Dr. Luthfi ISMAIL, Dr. CHIA Cher Chiek, Dr. LEONG Bi-Xiang, Dr. FAN Jun for their support in the early stages of my PhD journey, helping me acquire the necessary skills to survive as well as lending me your ears when things got rough.

Thank you to my lab juniors and peers Miss. Melissa ONG Xin-Yi, Miss LEE Jiawen, Mr. TEO Yeow Chuan Nicholas, Miss QUEK Shina, Miss Isabel PHANG Si Jia and Miss KOH Anping. Thank you to all of you for many fruitful and whimsical discussions, be it lab-related or otherwise. I am grateful for your presence and support and occasional mealtime gatherings. The journey would not have been the same without you.

Third, goes to the central lab technical assistance. I thank Dr. LI Yongxin for patiently solving all my X-Ray crystal structures; I would also like to thank Miss GOH Ee Ling, Mr. Derek ONG and Mr. Keith LEUNG for their expertise in NMR. From further afield, at FACTS, I would like to thank Dr Samuel MORRIS, Dr TAY Yee Yan and Dr Teddy SALIM, for their patience in teaching me the ropes and helping me characterize many challenging samples. The Solid-State NMR team at PAP, Dr. James HOOPER and Dr. XUE Kai for their invaluable help deciphering and handling my precious solid state samples. I am also grateful to the research group of Dr. Ming-Der SU for his assistance with the theoretical calculations within this thesis.

Particular thanks go to teaching lab staffs—Miss SEOW Ai Hua, Miss LIM Yen Lin, Miss Nicole TAN, Miss Charlene POO and Mr. Edmund CHOW—and Mr. WANG Wee Jian. Your unwavering support has been absolutely invaluable, be it through essential lab supplies, services and teaching opportunities.

Fourthly, my PhD batch mates—Dr. LEONG Shi Xuan, Dr. PHAM Thang Loi, Dr. KWEK Jia Min Germain. It has been my honor to have been on this journey alongside you all. Thank you for being sympathetic listening ears, and a constant source of inspiration that allowed me to keep moving forward despite the odds.

Fifth to the people of Mumei Shudan Aikido Dojo and the NTU Aikido Club, especially, Serge BERAUD Sensei, Nathalie Marcias BERAUD Sensei, Hamzah Sensei, Wilson Sensei, Qai Sensei. Thank you so much for your guidance during this arduous journey. I have learned many lessons from you all, on and off the mats, and the skills and knowledge I have gained from them have helped me grow in many ways. Thank you for also giving me a space to work out my stress and to help me achieve my dreams of getting my Dan rank. To more trainings with everyone.

Sixth to the many friends that have been with me along the way – especially – Dr. WONG Zheng-Zing Jonathan, Miss Melissa ONG Xinyi and Dr. KWEK Jia Min Germain, for being my friends outside of lab that actually understand the struggles of the lab.

Seventh, to my thesis advisory committee members: Assoc. Prof. LEONG Weng Kee, Prof. LEUNG Pak-Hing and Dr. Felipe GARCIA. Thank you very much for your advice, insight, and moral support. It has been immensely helpful throughout the years and played a significant part in the completion of this journey

Additionally, I am indebted to the funds provided by the Nanyang President's Graduate Scholarship (NPGS) and Chief Teaching Assistantship (CTA) for fully subsidizing my fees and the many opportunities that arose from them.

Last, but certainly not least, I dedicate my gratitude towards my family for their unconditional support. It is through their care and concern that I am able to be where I am today.

Meldon Wee Yi Shuo (July 2023)

Table of Contents

List of Schemes

List of Figures

Figure A4.14 Raman spectrum of deposited Ge nanoparticles (12th day) onto a crystalline silicon wafer. Excitation wavelength: 514 nm. A broad peak at 270-310 cm^{-1} was observed, which corresponds to amorphous germanium.[55]

List of Tables

List of Abbreviations and Symbols

δ	NMR chemical shift in Hz
ε	molar absorptivity
°	Degree(s)
°C	Degrees Celsius
Å	Angstrom(s)
%	percentage
λ_{max}	maximum wavelength
Ar	Aryl
br	broad
Bbt	2,6-bis[bis-(trismethylsilyl)methyl]-4-[tris(trimethylsilyl)methyl]phenyl
calcd.	calculated
CAAC	Cyclic (alkyl)(amino) carbene
CAASi	Cyclic (alkyl)(amino) silylene
CDASi	Cyclic dialkyl silylene
cm-1	wavenumber
Cy	cyclohexyl
d	doublet
dec.	decomposed
DFT	Density-functional theory
Dipp	2,6-diisopropylphenyl
ESI	Electron Spray Ionization
et al.	and others
g	gram(s)
h	hour(s)
HOMO	Highest Occupied Molecular Orbital
HRMS	High Resolution Mass Spectrometry
Hz/MHz	hertz/megahertz
*i*Pr	isopropyl
IPr	1,3-bis(2,6-diisopropylphenyl) imidazol-2-ylidene
IR	Infrared

kcal	kilocalories
LUMO	Lowest Unoccupied Molecular Orbital
m	mulitplet
M	Molarity (mol dm^{-3})
m.p.	Melting point
Me	Methyl
mL	Millilitre(s)
μL	microlitre(s)
mmol/mol	millimole(s)/mole(s)
NHC	N-heterocyclic Carbene
NMR	Nuclear Magnetic Resonance
Ph	Phenyl
ppm	Parts per million
q	quartet
s	singlet
sept	septet
t	triplet
*t*Bu	*Tert*-butyl
THF	Tetrahydrofuran
TMS	trimethylsilyl (SiMe3)
UV/Vis	Ultraviolet-Visible
WBI	Wiberg Bond Index

Chapter 1

Introduction

1.1 Zero Oxidation State Silicon and Germanium Complexes

Elements can occur as allotropes, which differ in the number of atoms per structural unit, in their bonding, or both.[1] For example, oxygen can exist as dioxygen (O_2) but also as ozone (O_3), and carbon exists in forms based on hexagonal lattices (such as graphite, fullerenes, and nanotubes) but also on a tetrahedral lattice (diamond).[2] However, all allotropes are alike in that the atoms are in the zero-oxidation state. Aside from allotropes, the zero-oxidation state is classically found in pure bulk metals, as well as in transition metal complexes (Scheme 1.1) where single atoms are stabilized by ligands that donate electron pairs into their empty orbitals. However, such a state has been difficult to realize for main-group elements such as carbon, silicon and germanium.

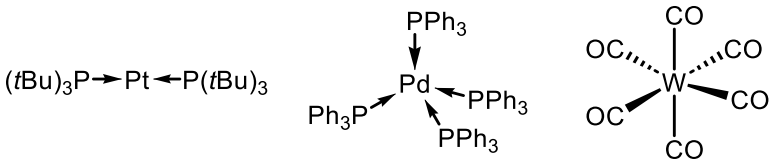

Scheme 1.1 Examples of transition metal (0) complexes

Molecular zero-oxidation-state silicon and germanium species are of fundamental importance owing to their highly intriguing electronic properties as well as their potential applications in small molecules activation. In these complexes, the silicon or germanium center is involved in a multiple bond and, at the same time, features a lone pair of electrons and vacant orbitals; these three attributes are usually associated with extreme instability. [3-7] However their greater solubility and reactivity facilitates further chemical transformations. As an illustration, soluble, ligand-coordinated metal (0) complexes undergo chemistry that is not possible using the insoluble elemental forms of the metal (homogeneous versus heterogeneous catalysis). Moreover, these

fundamental molecules could also serve as building blocks in the construction of more complex Group 14 cluster molecules with unconventional composition or serves as potential precursors in the synthesis of novel structures at the nanoscale.

To allow for the isolation of zero oxidation state silicon and germanium metal centres at ambient conditions, strongly σ-donating and/or π-accepting ligands are used to passivate these reactive centers. Furthermore, kinetic stabilization through ligands possessing steric bulk is required to preserve the reactive centers of these species

In this Chapter, we discuss the different approaches chemists have taken to synthesize and isolate a range of silicon(0) and germanium(0) elemental complexes as well as the experiments carried out to probe their unique reactivities.

1.2 Diatomic Group 14 Element(0) Complexes

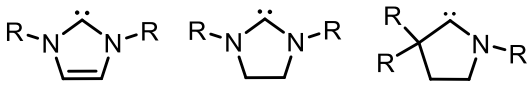

Scheme 1.2 N-heterocyclic carbenes and Cyclic (alkyl)(amino)carbenes

N-heterocyclic carbenes (NHCs) are strong σ-donating, but weak π-accepting two-electron donors (Scheme 1.2).[8-14] First discovered in 1991 by Arduengo, they possess a relatively simple synthetic design that allow for facile modifications for bespoke electronic and thermodynamic parameters of their transition metal complexes.[15]

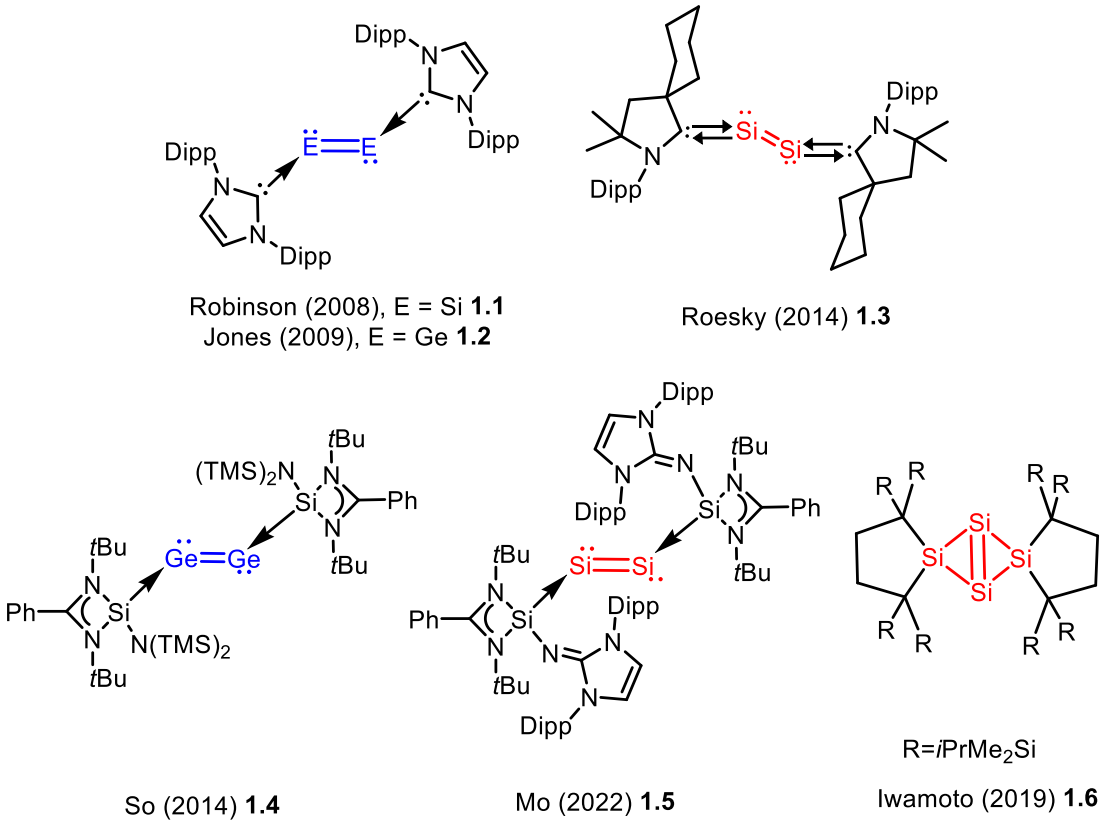

Scheme 1.3 Examples of isolated Lewis-base stabilized E(0) dimers

In 2008, Robinson et al. utilized a 1,3-bis(2,6-diisopropylphenyl) imidazol-2-ylidene NHC (IPr) to isolate a remarkable bis(NHC)-disilicon(0) complex

[IPr→Si=Si←IPr] **1.1** with a Si=Si double bond and a lone-pair of electrons on each silicon center (Scheme 1.4).[16] This was the first example of a stable, "bottleable" disilicon(0) complex, hailed by Dyker and Bertrand as the advent of a unique class of complexes, dubbed "soluble allotropes".[17] They were soluble in common organic solvents while retaining their unsaturated bonding structure.

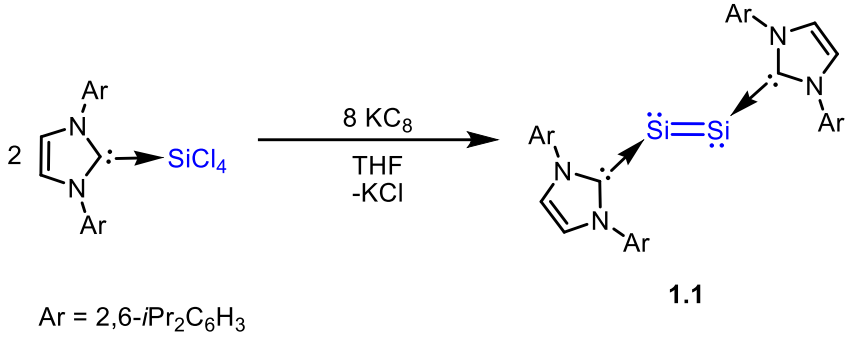

Scheme 1.4 Synthesis of complex 1.1

Robinson and co-workers probed the chemical nature of the disilicon(0) moiety. The strongly reducing nature of the Si=Si double bond was demonstrated through the reactivity of [IPr→Si=Si←IPr] toward BH_3.THF, chalcogens, CO_2, N_2O (Scheme 1.5).

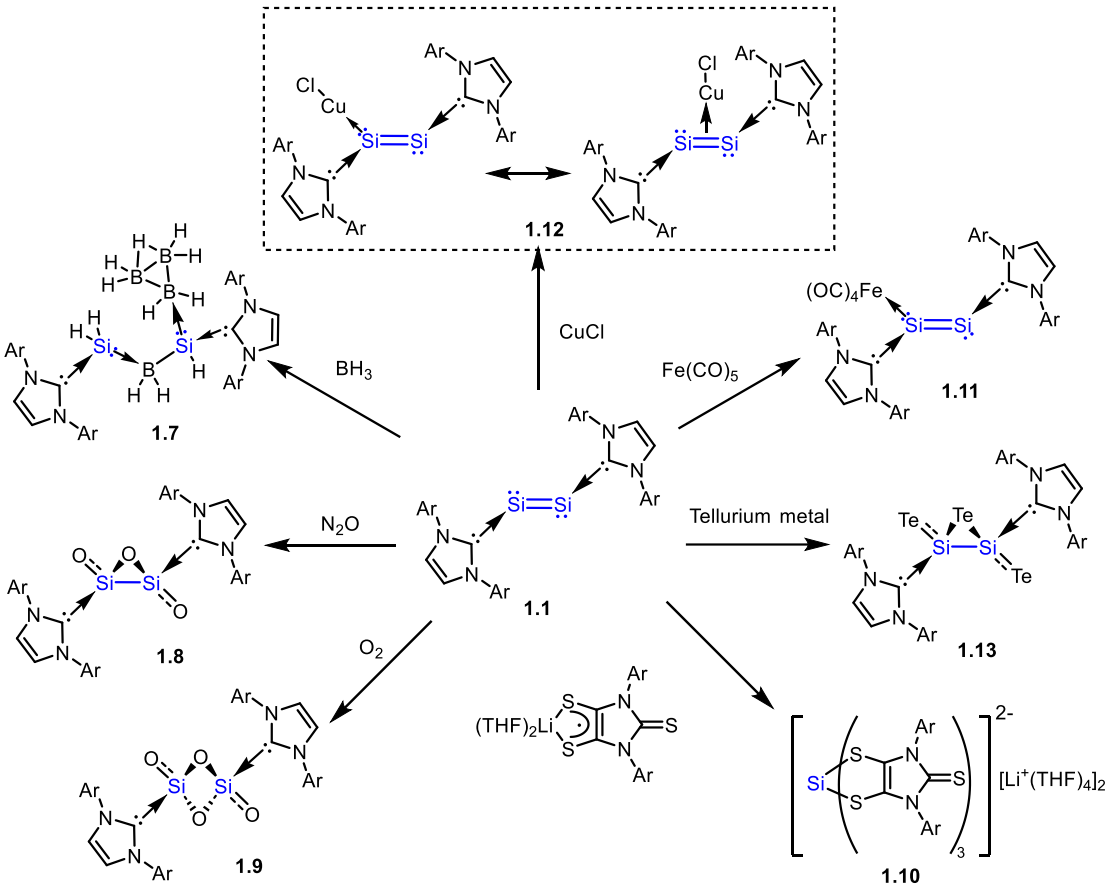

Scheme 1.5 Reactivity of complex 1.1

These reactions granted access to a range of other elusive chemical species, such as a Lewis acid and base-ligated parent silylene moiety (H_2Si) **1.7** upon reaction with BH_3.THF.[18] Reminiscent of surface oxidation of elemental silicon, they were also able to isolate molecular NHC-supported clusters of Si_2O_3 **1.8** and Si_2O_4 **1.9** by the reaction with N_2O and O_2 respectively.[19] Robinson and co-workers later demonstrated the coordinate bond nature of the IPr→Si bonds in the reaction of [IPr→Si=Si←IPr] with the lithium dithiolene radical, wherein dithiolene radical anion displaced NHC to form a dianionic silicon(IV) tris(dithiolene) complex **1.10**, providing the proof of a silicon(0) atom transfer reaction.[20] [IPr→Si=Si←IPr] also formed *σ*-complexes with pentacarbonyl iron(0) and copper(I) chloride through its lone pair of electrons.[21,22] This confirmed the existence of the lone pair on each silicon center, while also showing its potential to participate in the construction of larger, more complex molecules.

Interconversion of the $\sigma-\pi$ bonding interaction between the Si=Si double bond and the CuCl was observed in the latter, a significant observation reminiscent of similar $\sigma-\pi$ rearrangements observed in organometallic transition metal catalytic processes.[23] So and coworkers would later synthesize the tellurium analogue of the Si_2O_3 complex by direct reaction of the disilicon(0) analogue with tellurium metal,[24] a primary molecular example of Si_2Te_3, a p-type semiconductor material.[25-36]

Jones and co-workers later reported the germanium[37] and tin[38] analogues to this complex [IPr→E=E←IPr] (E = Ge, **1.2** and Sn, **1.14**), adopting a similar synthetic strategy utilizing the milder reducing agent Mg(I)Nacnac (Scheme 1.6).

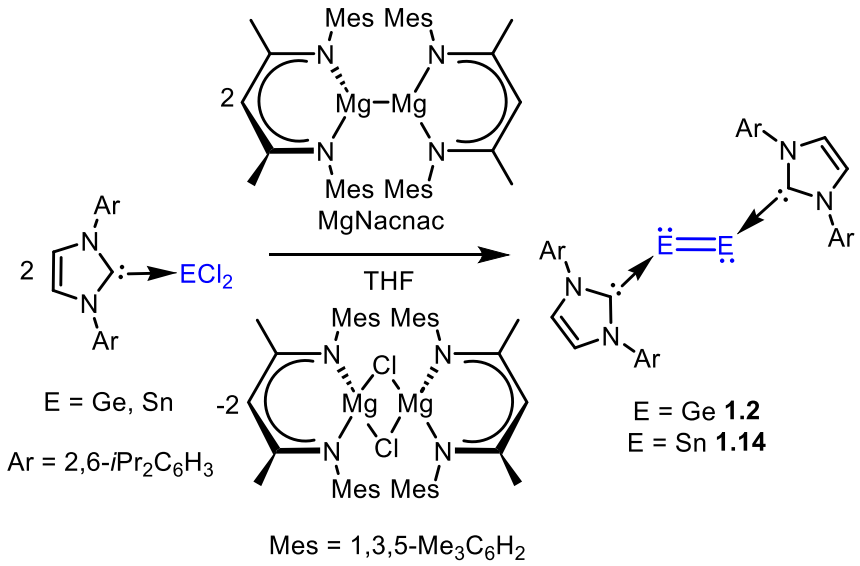

Scheme 1.6 Synthesis of complex 1.2 and 1.14

Cyclic (alkyl)(amino)carbenes (CAAC)[39, 40] were employed in the synthesis of diatomic Group 14 element(0). CAACs had one less nitrogen atom, replaced by a carbon atom. CAACs are comparatively stronger σ-donors. The central carbon atom experiences less electron-withdrawing inductive effect, making the σ lone-pair more available for donation. CAACs are also much stronger π-acceptors, due to reduced π-

donation from members in the ring into the vacant p orbital of the carbene carbon center (Scheme 1.7). [41-46]

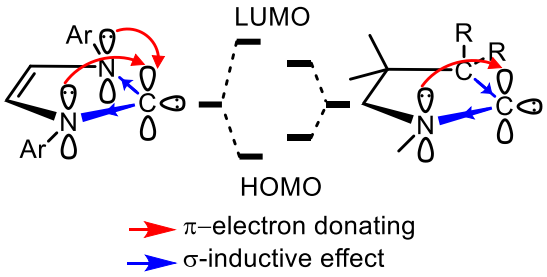

Scheme 1.7 Comparing NHC vs CAAC electronic effects

Roesky et al. used CAAC to isolate a bis(CAAC)-disilicon(0) [$CAAC_{Cy}$⇄Si=Si⇄$CAAC_{Cy}$] **1.3**, where the strong π-accepting ability of the CAACs enabled delocalization of the lone pairs on the Si(0) centers to the vacant *p* orbitals on the carbene centers, providing enhanced electronic stabilization of the disilicon(0) moiety (Scheme 1.8).[47] The double bond character in the C_{CAAC}–Si bonds increases concomitantly, leading to some triene electronic character. [48]

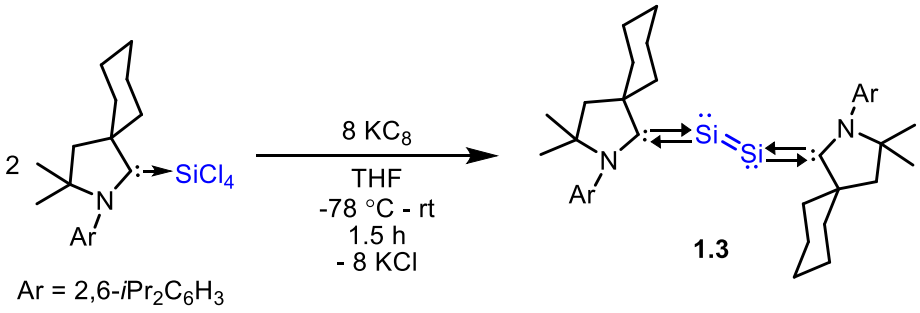

Scheme 1.8 Synthesis of complex 1.3

Persistent NHSis were first reported by Denk and West in 1994,[49] and since then there has been significant development in their application as strong σ-donating ligands in the field of organometallic chemistry.[50-57] Though similar in structure, stable silylenes have been found to exhibit electronic properties significantly different from their NHC counterparts. Computational studies comparing NHCs and known stable silylenes found that amidinate stabilized silylenes are significantly stronger donor ligands.[58,59] So and co-workers synthesized an N-heterocyclic silylene (NHSi) stabilised digermanium(0)

complex **1.4** [{PhC(N*t*Bu)$_2$}(NTMS$_2$) Si→Ge=Ge←Si(NTMS$_2$){(N*t*Bu)$_2$CPh}] from the reduction of an amidinato amidosilylene dichlorogermylene complex (Scheme 1.9). Mo et al. also employed an amidinato imidosilylene to isolate a bis(silylene)-disilicon(0) complex **1.5** [{PhC(N*t*Bu)$_2$}(NHI)Si→Si=Si←Si(NHI){(N*t*Bu)$_2$CPh}] (NHI =bis(2,6-(diisopropylphenyl)imidazolin-2-imino) (Scheme 1.9).[60] Iwamoto et al. illustrated that two bridging dialkylsilylene could establish side-on coordination with disilicon(0) to form a bicyclo[1.1.0]tetrasilabut-1(3)-ene **1.6** electronic structure with an inverted Si=Si double bond,[61] demonstrating that silylenes could also form bridging-type coordination; a feature unique to silylenes when compared with NHCs.

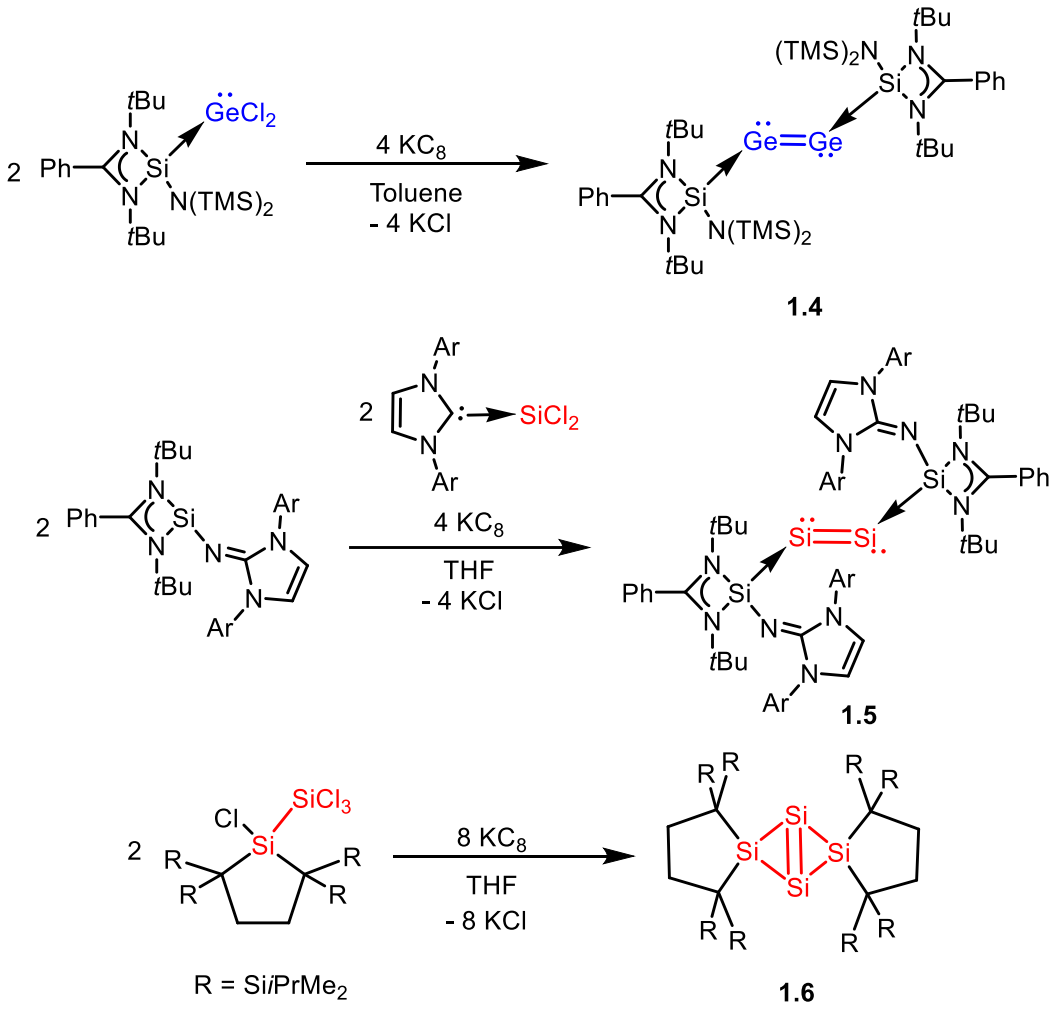

Scheme 1.9 Synthesis of NHSi-stabilised main group element complex 1.4, 1.5 and 1.6

1.3 Monoatomic Heavy Group 14 Element(0) Complexes

Another class of zero oxidation state group 14 element complexes is bis(Lewis base)-stabilized tetrylone[62-68] [L:→:E:←:L] with a strongly bent geometry, wherein the monoatomic E^0 center composes two lone pairs of electrons and forms two coordinative covalent bonds with two ligands.

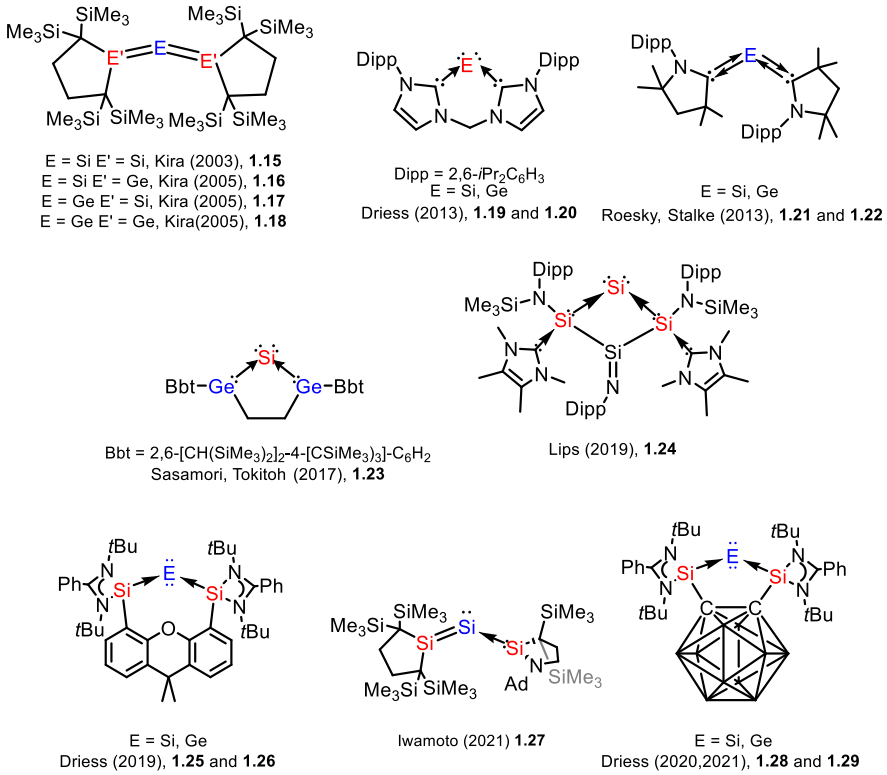

Scheme 1.10 Examples of tetrylone complexes

Synthesized by Ramirez 1961
Structure confirmed
by Vincent and Wheatley 1972

Electronic Structure
as suggested by Kaska 1973
Supported by theoretical
calculations Frenking 2006

Scheme 1.11 Carbodiphosphorane and its suggested "carbone" structure

The first example carbodiphosphorane (Ph_3PCPPh_3) was reported by Ramirez et al. in 1961, which was previously described as a double Wittig ylide containing electron sharing C-P bonds (Scheme 1.11).[69] Vincent and Wheatley successfully characterized it in 1972, confirming the bent nature of the P=C=P bond.[70] Kaska et al. would be the first to suggest using the donor-acceptor model as one of the resonance forms to describe the electronics that govern this structural configuration.[71] Both phosphane moieties are datively bonded to the central carbon (0) atom Later, Frenking et al. performed DFT calculations to support Kaska's claim 2006,[72] in which the HOMO (Highest Occupied Molecular Orbital) of Ph_3PCPPh_3 correspond to a π-type lone pair orbital and the HOMO-1 is an σ-type lone pair orbital. As a result, Ph_3PCPPh_3 can be considered as comprising single carbon atom with two lone pairs and forming donor–acceptor interactions with two two-electron-donating phosphines. The term ''carbones'' was subsequently suggested by Frenking for such monatomic C^0 complexes coordinated by two Lewis base donors.[73]

Kira et el. synthesized a series of heavier bent allenes analogues of composition [$R_2E=E=ER_2$] from dialkylsilylenes and dialkylgermylenes **1.15-1.18** (Scheme 1.10).[74-76] Although Kira et al. did not agree,[77] Frenking et al. interpreted these compounds as possessing similar electronic configuration to the carbone complexes, that is, the central atom bears a lone pair in an s-type orbital, with another residing in a p-type orbital delocalized into the vacant p-orbitals of the supporting tetrylenes.[78-80] As such, the terms silylone, germylone, stannylone, and plumbylone were suggested to label such bent allene complexes of the corresponding heavier group 14 elements in the zero oxidation state.

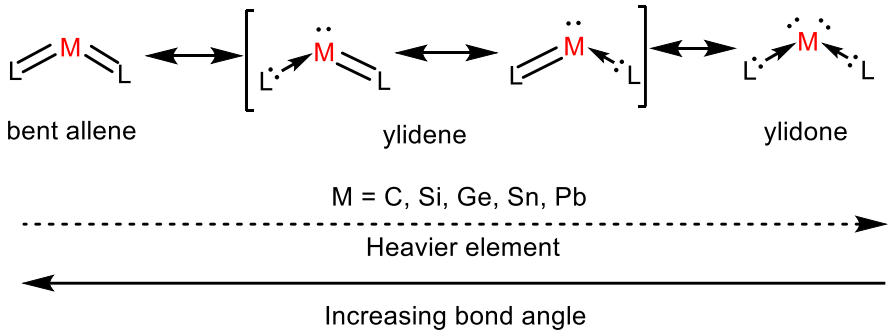

Scheme 1.12 de Proft's canonical resonance structures for tetrylones

Further theoretical studies by de Proft et al. utilized a maximum probability domain framework in combination with valence bond theory to describe the structure of monoatomic group 14 element(0) complexes (Scheme 1.12),[81] comprising three major canonical resonance structures: ylidone (L:→ :E: ← :L), ylidene (L: → :E = L ↔ L = E: ← :L), and bent allene (L = E = L). The ylidone structure contains symmetric [LP(σ)] and antisymmetric [LP(π)] lone pair (LP) electron orbitals with respect to the L−E−L plane, and the delocalization of the LP electrons to the vacant orbital of the ligands

increases the contribution of the ylidene and bent-allene characters. All three resonance structures exhibit different bond angles, reflecting the extent of s-p hybridization present about the central atom. The ylidone possesses the most acute bond angle of the three, reflecting the lowest degree of hybridization, making it the closest to a pseudo-elemental state.

With the aid of strong π-accepting ligands, Roesky et al. reported the synthesis of an acyclic bis(CAAC)-silylone complex **1.21** [$CAAC_{Me}$⇄Si⇄$CAAC_{Me}$] possessing diradicaloid character, due to significant delocalization of the p-type lone-pair into the carbene vacant p orbital (Scheme 1.13).[82,83] Iwamoto et al. reported an acyclic bis(CAASi)-silylone complex **1.30** (CAASi = cyclic (alkyl)(amino)silylene) adopting a π-localized ylidene structure in the solid state and a π-delocalized ylidene structure in solution.[84] This result further supports de Proft's earlier conclusion regarding the resonance forms of tetrylones, and highlights the important role played by the supporting ligands in favoring either of the major resonance forms.

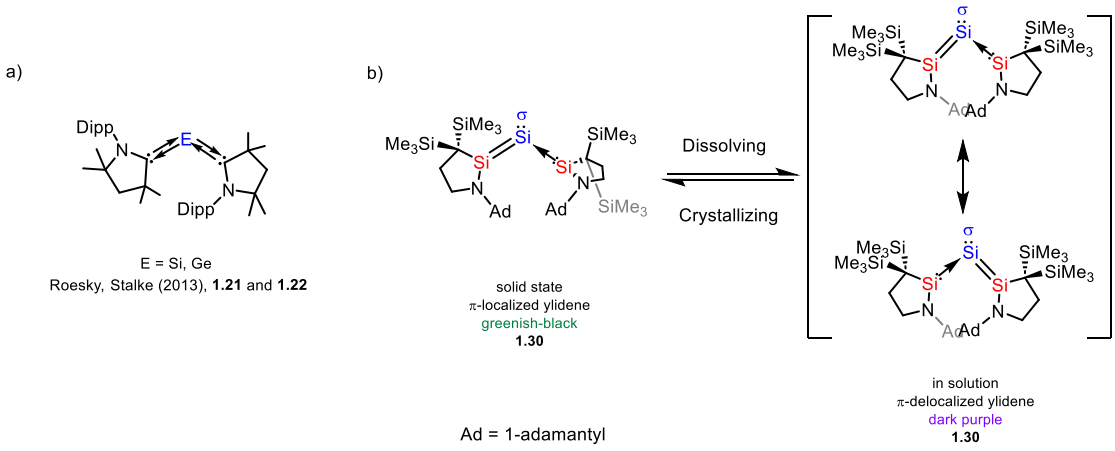

Scheme 1.13 a) Examples of bis(CAAC)-stabilized acylic tetrylones b) Conformational switch between solid state and solution state for acyclic tetrylone complex 1.30

Driess et al employed chelating bis(NHC)- and bis(amidinato silylene)–ligands to synthesize a series of silylones and germylones (Scheme 1.14).[85-91] The weak π-accepting ability of NHC and amidinato silylene, as well as the acute bond angle at the E(0) center exerted by the chelate effect of the ligands serve to enhance the "ylidone" character of the complex.[65,91]

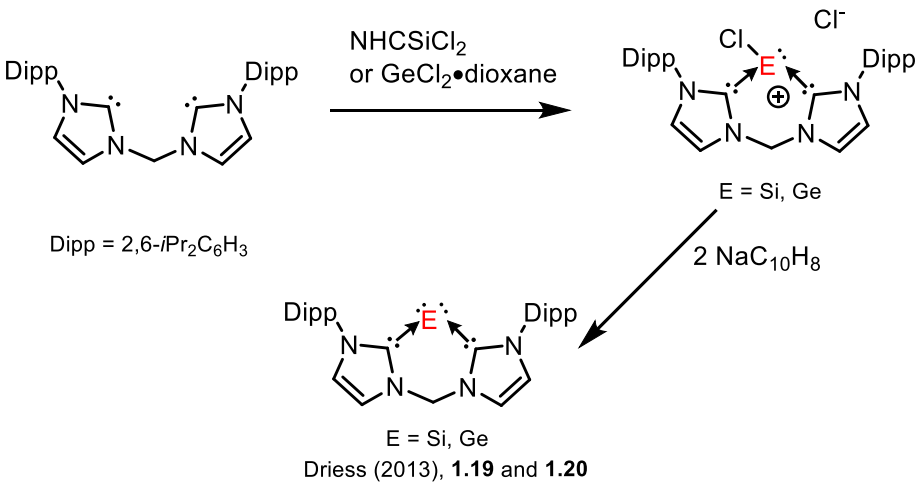

Scheme 1.14 Synthesis of cyclic tetrylone 1.19 and 1.20

Most notably, the coordination of bis(NHC)-silylone to two molecules of zinc (II) chloride **1.31**[63] and bis(amidinato silylene) germylone to two molecules of aluminum chloride **1.34** confirmed the presence of two lone pairs of electrons on the silicon(0) and germanium(0) centers (Scheme 1.15).[90]

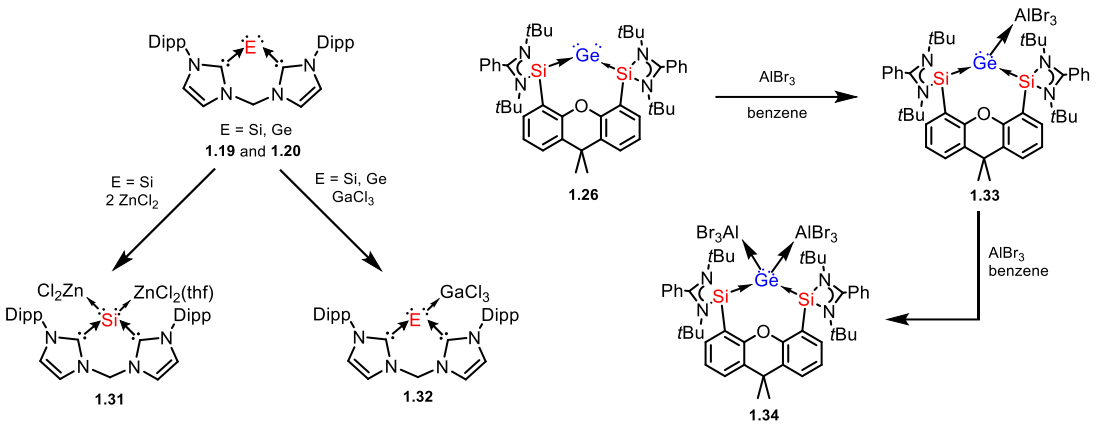

Scheme 1.15 Concurrent coordination to two Lewis acid metal centers of complex 1.19-20 and 1.26

The highly Lewis basic nature of the silicon (0) and germanium(0) centers was further demonstrated by their ability to coordinate to other transition metal and main group element centers, forming new metallic clusters such as a Ge_2Ni triatomic bimetallic cluster **1.35** containing both main group and transition metals (Scheme 1.16).[90]

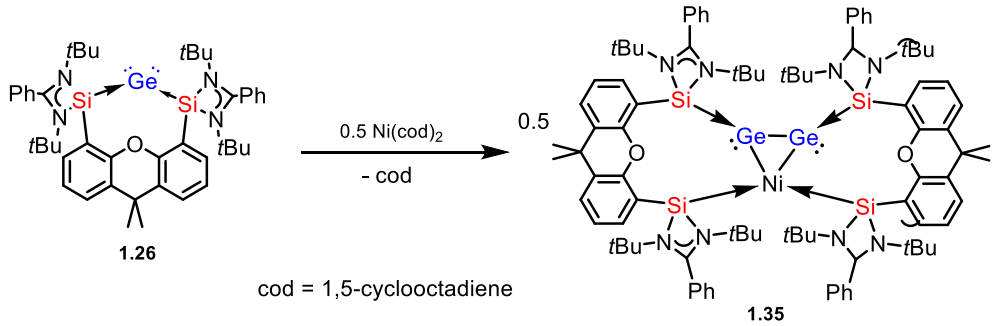

Scheme 1.16 Coordination of complex 1.26 and 1.29 to transition metal and main group element centers

1.19 also underwent oxidation with elemental chalcogens to form a series of bis(base)supported ECh_2 complexes (Scheme 1.17).[93] These are the first examples of molecular complexes bearing the empirical formula of silicon chalcogenides, a series of valuable semiconductor materials.

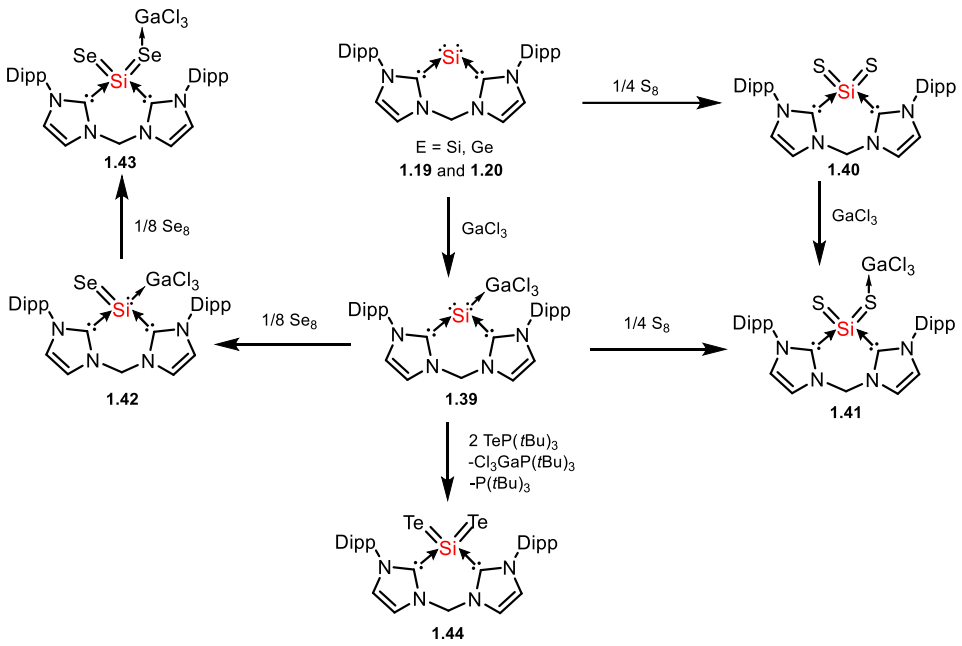

Scheme 1.17 Synthesis of a series of silicon chalcogenide monomer complexes

In combination with strong, bulky Lewis acids, they were able to form frustrated Lewis pairs capable of activating small molecules and enthalpically strong bonds such as breaking the H-H covalent bond in hydrogen gas, (**1.45** and **1.46**), and activating the C=C double bond of ethylene gas (**1.47**) (Scheme 1.18). [87, 90]

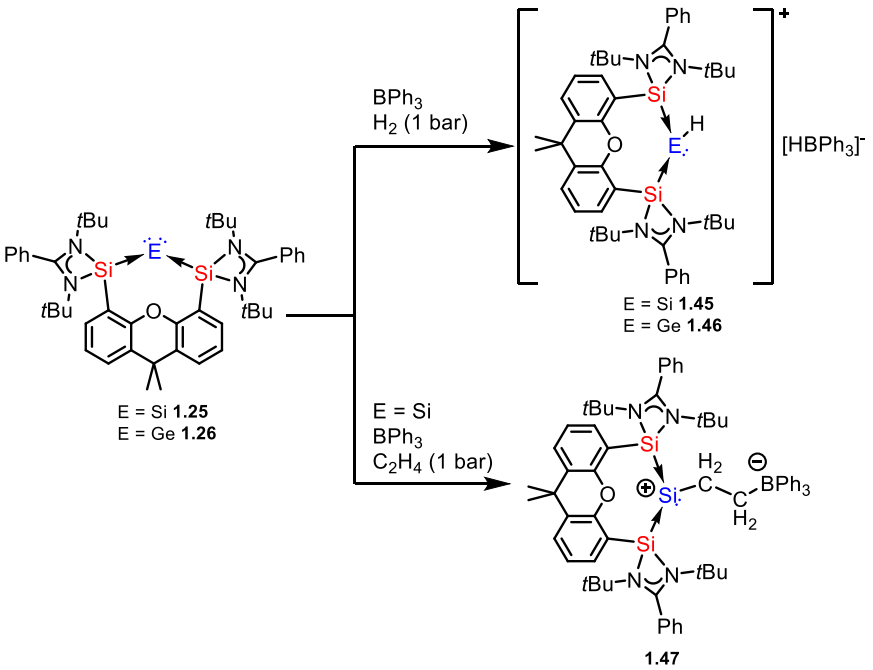

Scheme 1.18 Activation of small molecules by frustrated Lewis-pairs of 1.25 and 1.26 with BPh_3

More recently, they demonstrated that the redox non-innocence of a carborane backbone expanded the redox reactivity of the chelate-stabilized E(0) (Scheme 1.19).[88] Further reduction of the silylone **1.28** resulted in an intramolecular one-electron oxidation of the Si(0) center, resulting in the formation of an Si^{I}-Si^{I} bond, **1.48**, as well as the reduction of the carborane ligands.

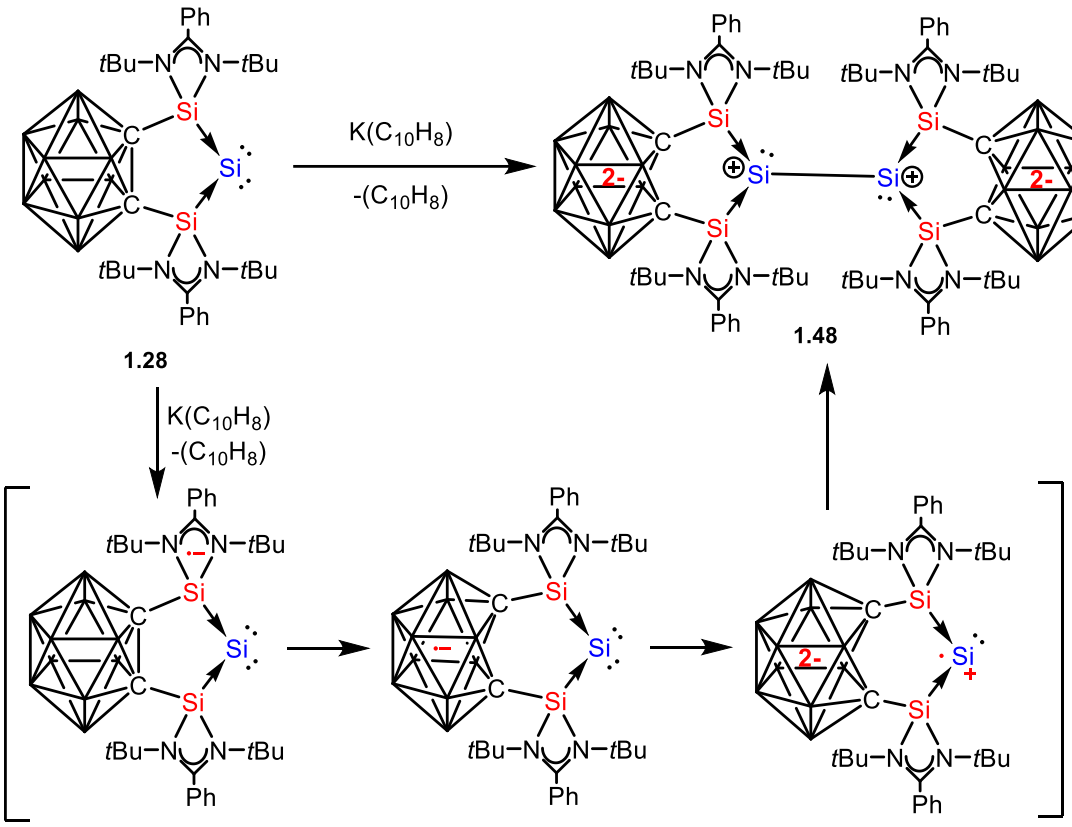

Scheme 1.19 Reduction of silylone 1.28

The germylone example **1.29** also underwent a one electron oxidation upon oxidation by $[Cp_2Fe][B(C_6H_3\{CF_3\}_2)_4]$, or intramolecularly upon reduction with KC_8, to form a Ge^I-Ge^I bond with a neutral (**1.49**) or negatively charged (**1.50**) carborane backbone, respectively(Scheme 1.20). [91]

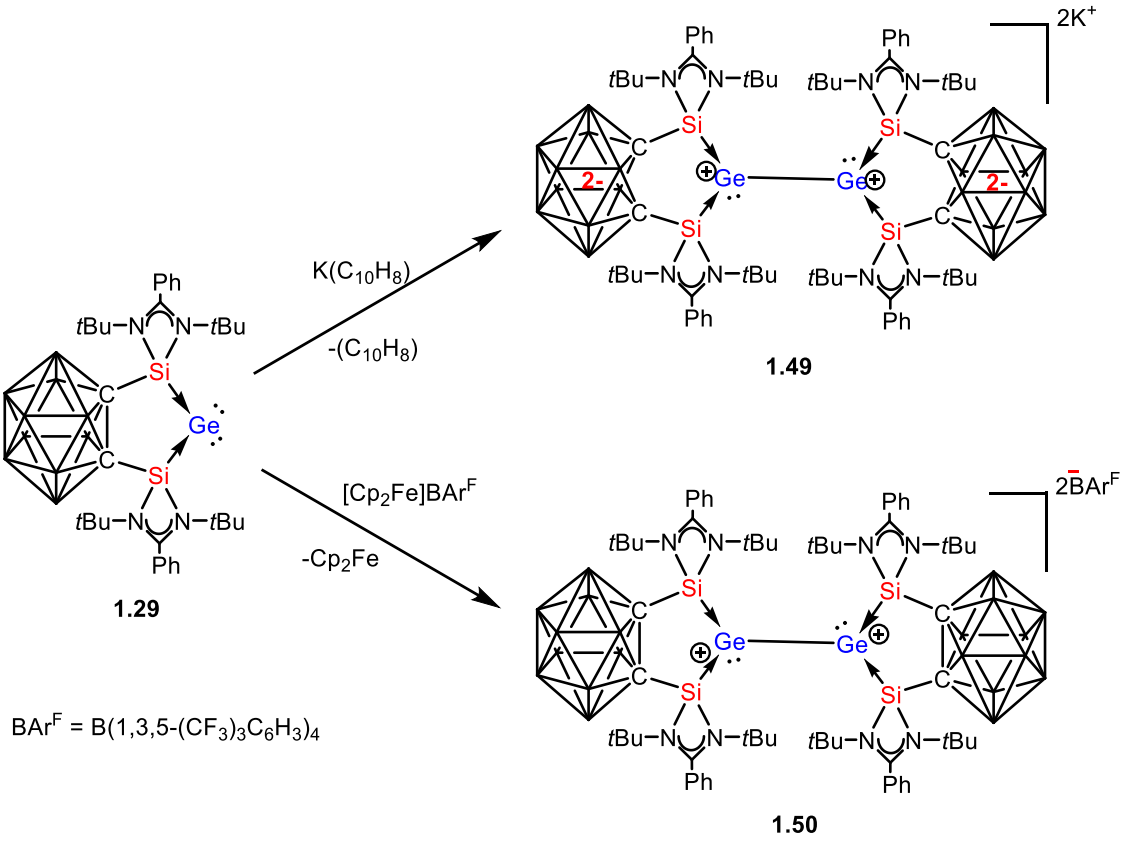

Scheme 1.20 Reduction and oxidation of germylone 1.29

1.4 Research Aim

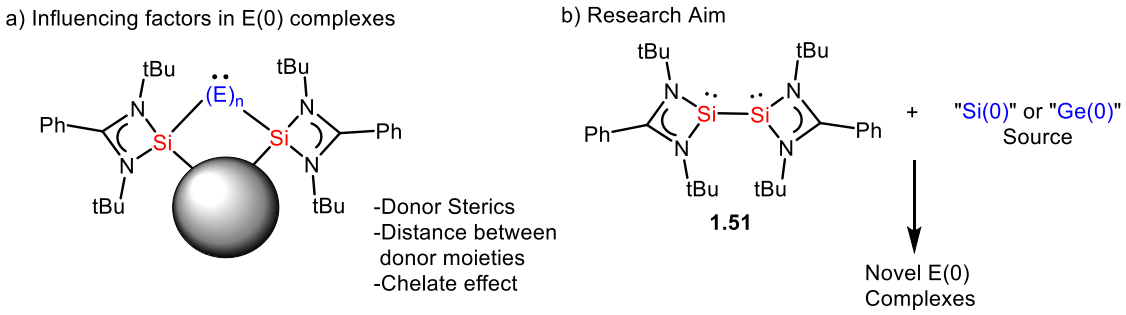

Scheme 1.21 a) Factors influencing E(0) complexes b) Research aim

In light of the abovementioned examples, it is apparent that a rational choice of ligand enables effective tuning of the electronic property and reactivity of zero oxidation state silicon and germanium complexes, and significantly impacts the resultant structure of the complexes formed. The chelate effect in bis(NHC) and bis(silylene) systems were found to be particularly effective for the isolation of monatomic E(0) species. The distance between the donor centers has also been observed to significantly contribute to the reactivity of the chelate system as well as the E(0) complexes formed. The characteristic nature of the linker moiety could provide varying degrees of steric control as well as significantly impact the electronic properties of the participating silylene moieties. This thesis aims to use amidinato disilyne (1.51), as a trapping reagent with sources of Si(0) and Ge(0) species to explore new synthetic avenues to access synthetically challenging molecular zero oxidation state silicon and germanium constructs.

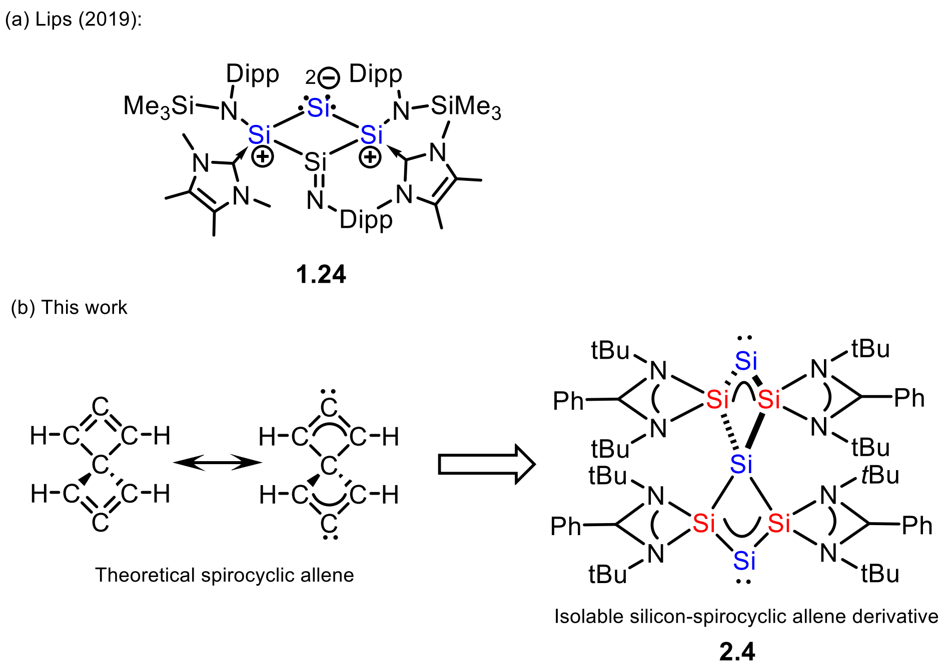

Scheme 1.22 Synthesis of first silicon analogue of spiro[3.3]heptasila-1,2,5,6-tetraene

As discussed earlier, the bond angle involved in the construction of the LE=E=EL moiety in tetrylone complexes has a significant impact on the character adopted by the tetrylone complex. This is a significant reason as to why chelate ligands are a key feature present in many examples of silylones. It would thus follow that decreasing the size of the linker moiety would result in a smaller bite angle present in the chelate ligand and hence a much tighter bond angle in the resultant tetrylone. So far, the example with the smallest linker for silylones was presented by Lips et al. (**1.24**) with a bis(carbene-stabilized-silylene) chelate ligand, forming a puckered four-membered ring with a single silicon atom as the linker (Scheme 1.22a).[94] We realize there is still potential that exists for chelates using a single silicon atom as a linker. The resultant four-membered cyclic silylone, as demonstrated in the Lips example (93.43°), would have a severely restrictied bond angle to less than or equal to 90 degrees.. We believe that a highly strained silylone could exhibit unique structural characteristics as well as significantly stronger sigma donor properties for coordination with electron rich

transition metal species. The synthesis and characterization of an all-silicon analogue of spiro[3.3]heptasila-1,2,5,6-tetraene is described in detail in Chapter 2 of this thesis (Scheme 1.22b).

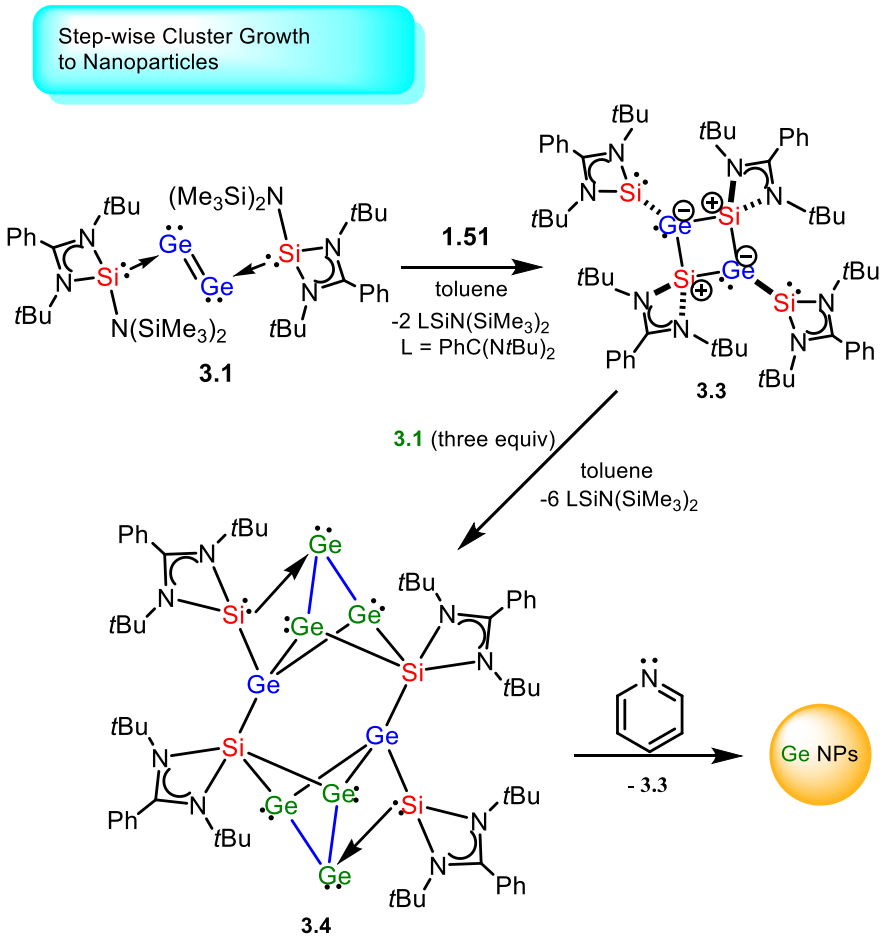

Scheme 1.23 Stepwise growth of germanium clusters

The isolation of many of these zero oxidation state elemental species, make use of ligands possessing high steric bulk. The thermodynamic stabilisation provided does allow for significant control over their formation, but it is noticeable that many of these species are limited to monatomic or diatomic species. At present, the only triatomic silicon cluster with a formally zero oxidation state was presented by Roesky et al. By

conducting the reduction of a CAAC-tetrachlorosilane adduct at lower temperatures, they were able to exclusively synthesize a $CAAC_3Si_3$ complex, with a unique triangular Si_3 cluster.[95] As the bidentate amidinato silylenes have been shown to be very effective at stabilizing monatomic species, we decided upon the amidinato disilyne as our ligand system. It could still provide sufficient electronic and thermodynamic stabilisation and possesses a reactive single bond between the two silicon centres which could trap the metal clusters we are hoping to isolate. The trapping of a trigermanium (0) cluster by bis(silylenyl)germylenes and its potential application as a nucleation seed in the synthesis of germanium nanoparticles is described in Chapter 3 of this thesis.

References

1. House, J. E.; House, K. A. Descriptive Inorganic Chemistry, 3rd ed.; Academic Press, **2016**.
2. Wiberg, E.; Wiberg, N.; Holleman, A. F., Inorganic chemistry, Academic Press, 2001
3. Honig, R. E., Sublimation Studies of Silicon in the Mass Spectrometer *J. Chem. Phys.* **1954**, *22*, 1610–1611
4. Honig, R. E., On the Heats of Sublimation and Evaporation of Germanium *J. Chem. Phys.* **1954**, *22*, 1610
5. Bloomfield, L. A.; Freeman, R. R.; Brown, W. L., Photofragmentation of Mass-Resolved Si^{+}_{2-12} Clusters *Phys. Rev. Lett.*, **1985**, *54*, 2246
6. Van Zee, R. J.; Ferrante, R. F.; Weltner W. Jr., *J. Chem. Phys*. **1985** *83*, 6181
7. Zhou M.; Jiang, L.; Xu, Q., Reactions of silicon atoms and small clusters with CO: Experimental and theoretical characterization of Si_nCO(n=1–5),Si_2CO(n=1–5), $Si_2(CO)_2$, $si_2(CO)_2$, c-Si_2(μ-o)(μ-CSi),c-Si_2(μ-O)(μ-CSi), and c-Si_2(μ-O)(μ-CCO)c-Si_2(μ-O)(μ-CCO) in solid argon. *J. Chem. Phys.* **2004**, *121*, 10474-10482.
8. Bourissou, D.; Guerret, O.; Gabbai, F. P.; Bertrand G. Stable Carbenes *Chem. Rev.* **2000**, *100*, 39-92.
9. Wang, Y.; Robinson, G. H. Carbene Stabilization of Highly Reactive Main-Group Molecules *Inorg. Chem.* **2011**, *50*, 12326-12337
10. Wang, Y.; Robinson, G. H. Carbene-stabilized main group diatomic allotropes *Dalton Trans.*, **2012**, *41*, 337-345.

11. Hopkinson, M. N.; Richter, C.; Schedler, M.; Glorius, F. An Overview of N-Heterocyclic Carbenes. *Nature* **2014**, *510*, 485–496.
12. Nesterov, V.; Reiter, D.; Bag, P.; Frisch, P.; Holzner, R.; Porzelt, A.; Inoue, S. NHCs in Main Group Chemistry. *Chem. Rev.* **2018**, *118*, 9678–9842.
13. Doddi, A.; Peters, M.; Tamm, M. N-Heterocyclic Carbene Adducts of Main Group Elements and Their Use as Ligands in Transition Metal Chemistry. *Chem. Rev.* **2019**, *119*, 6994-7112.
14. Wang, Y.; Robinson, G. H. Counterintuitive Chemistry: Carbene Stabilization of Zero-Oxidation State Main Group Species *J. Am. Chem. Soc.* **2023**, *145*, 5592-5612.
15. Arduengo, A. J.; III, Harlow, R. L.; Kline, M., A stable crystalline carbene. *J. Am. Chem. Soc.* **1991**, *113*, 361–363.
16. Wang, Y.; Xie, Y.; Wei, P.; King, R. B.; Schaefer, H. F., III; Schleyer, P. v. R.; Robinson, G. H. A Stable Silicon(0) Compound with a Si═Si Double Bond. *Science* **2008**, *321*, 1069– 1071.
17. Dyker, C.A.; Bertrand, G. Soluble Allotropes of Main-Group Elements. *Science* **2008**, *321*, 1050–1051.
18. Abraham, M. Y.; Wang, Y.; Xie, Y.; Wei, P.; Schaefer, H. F., III; Schleyer, P. v. R.; Robinson, G. H. Cleavage of Carbene-Stabilized Disilicon. *J. Am. Chem. Soc.* **2011**, *133*, 8874−8876.
19. Wang, Y.; Chen, M.; Xie, Y.; Wei, P.; Schaefer, H. F., III; Schleyer, P. v. R.; Robinson, G. H. Stabilization of elusive silicon oxides *Nature Chemistry*, **2015**, *7*, 509-513.
20. Wang, Y.; Tope, C. A.; Xie, Y.; Wei, P.; Urbauer, J. L.; Schaefer, H. F., III; Robinson, G. H. Carbene-Stabilized Disilicon as a Silicon-Transfer Agent:

Synthesis of a Dianionic Silicon Tris(dithiolene) Complex *Angew. Chem., Int. Ed.* **2020**, *59*, 8864-8867.

21. Hickox. H. P.; Wang, Y.; Xie, Y.; Chen, M.; Wei, P.; Schaefer, H. F., III; Robinson, G. H. Transition-Metal-Mediated Cleavage of a Si=Si Double Bond *Angew. Chem., Int. Ed.* **2015**, *54*, 10267-10270.
22. Chen, M.; Wang, Y.; Xie, Y.; Wei, P.; Gillard, R. J., Jr.; Schwartz. N. A.; Schaefer, H. F., III; Schleyer, P. v. R.; Robinson, G. H. Dynamic Complexation of Copper (I) Chloride by Carbene-Stabilized Disilicon *Chem. Eur. J.* **2014**, *20*, 9208-9211
23. Tatsumi, K.; Tsutsui, M. The σ−π Rearrangement: a Key Process in Organometallic Catalysis *J. Mol. Cat.* **1981**, *13*, 117-145.
24. Chan, Y.-C.; Leong, B.-X.; Li Y.; Yang, M.-C.; Li Y.; Su M.-D; So, C.-W. A dimeric NHC-Silicon Monotelluride: Synthesis, Isomerization, and Reactivity *Angew. Chem., Int. Ed.* **2017**, *56*, 11275-11652.
25. Wuttig, M.; Yamada, N. Phase-change materials for rewriteable data storage *Nat. Mater.* **2007**, *6*, 824 –83.
26. Lencer, D.; Salinga, M.; Grabowski, B.; Hickel, T.; Neugebauer, J.; Wuttig, M. A Map for Phase-Change Materials *Nat. Mater.* **2008**, *7*, 972 –977.
27. Tanaka, Y.; Ren, Z.; Sato, T.; Nakayama, K.; Souma, S.; Takahashi, T.; Segawa, K.; Ando, Y. Experimental Realization of a Topological Insulator in SnTe *Nat. Phys.* **2012**, *8*, 800 –803.
28. Sootsman, J. R.; Chung, D. Y.; Kanatzidis, M. G. New and Old Concepts in Thermoelectric Materials *Angew. Chem., Int. Ed.* **2009**, *48*, 8616 –8639; *Angew. Chem.* **2009**, *121*, 8768 –8792.

29. Snyder, G. J.; Toberer, E. S. Complex Thermoelectric Materials *Nat. Mater.* **2008**, *7*, 105 –114.

30. Mishra, R.; Mishra, P. K.; Phapale, S.; Babu, P. D.; Sastry, P. U.; Ravikumar, G.; Yadav, A. K. Evidences of the Existence of $SiTe_2$ Crystalline Phase and a Proposed New Si–Te Phase Diagram *J. Solid State Chem.* **2016**, *237*, 234 – 241.

31. Rau, J. W.; Kannewurf, C. R. Intrinsic Absorption and Photoconductivity in Single Crystal $SiTe_2$ *J. Phys. Chem. Solids* **1966**, *27*, 1097 –1101.

32. Exsteen, G.; Drowart, J.; Vander Auwera-Mahieu, A.; Callaerts, R. Thermodynamic Study of Silicon Sesquitelluride using a Mass Spectrometer *J. Phys. Chem.* **1967**, *71*, 4130 –4131.

33. Bailey, L. G. Preparation and Properties of Silicon Telluride *J. Phys. Chem. Solids***1966**, *27*, 1593 –1598.

34. Weiss, A.; Weiss, A. Siliciumchalkogenide. IV. Zur Kenntnis von Siliciumditellurid *Z. Anorg. Allg. Chem.* **1953**, *273*, 124 –128.

35. Steinberg, S.; Stoffel, R. P.; Dronskowski, R. Search for the Mysterious SiTe—An Examination of the Binary Si–Te System Using First-Principles-Based Methods *Cryst. Growth Des.* **2016**, *16*, 6152 –6155.

36. Segev, E.; Argaman, U.; Abutbul, R. E.; Golan, Y.; Makov, G. A new cubic prototype structure in the IV–VI monochalcogenide system: a DFT study *CrystEngComm* **2017**, *19*, 1751 –1761.

37. Sidiropoulos, A.; Jones, C.; Stasch, A.; Klein, S.; Frenking, G. N-Heterocyclic Carbene Stabilized Digermanium(0). *Angew. Chem., Int. Ed.* **2009**, *48*, 9701−9704.

38. Jones, C.; Sidiropoulos, A.; Holzmann, N.; Frenking, G.; Stasch, A. An N-Heterocyclic Carbene Adduct of Diatomic Tin, :Sn=Sn: *Chem. Commun.* **2012**, *48*, 9855−9857.

39. Lavallo, V.; Canac, Y.; DeHope, A.; Donnadieu, B.; Bertrand, G. A Rigid Cyclic (Alkyl)(amino)carbene Ligand Leads to Isolation of Low-Coordinate Transition-Metal Complexes. *Angew. Chem., Int. Ed.* **2005**, *44*, 7236– 7239

40. Lavallo, V.; Canac, Y.; Präsang, C.; Donnadieu, B.; Bertrand, G. Stable Cyclic (Alkyl)(Amino)Carbenes as Rigid or Flexible, Bulky, Electron-Rich Ligands for Transition-Metal Catalysts: A Quaternary Carbon Atom Makes the Difference *Angew. Chem., Int. Ed.* **2005**, *44*, 5705–5709.

41. Roy, S.; Mondal, K. C.; Roesky, H. W. Cyclic Alkyl(amino) Carbene Stabilized Complexes with Low Coordinate Metals of Enduring Nature. *Acc. Chem. Res.* **2016**, *49*, 357– 369

42. Tomás-Mendivil, E.; Hansmann, M. M.; Weinstein, C. M.; Jazzar, R.; Melaimi, M.; Bertrand, G. Bicyclic (Alkyl)(amino)carbenes (BICAACs): Stable Carbenes More Ambiphilic than CAACs *J. Am. Chem. Soc.* **2017**, *139*, 7753–7756.

43. Melaimi, M.; Jazzar, R.; Soleilhavoup, M.; Bertrand, G. Cyclic (Alkyl)(amino)carbenes (CAACs): Recent Developments. *Angew. Chem., Int. Ed.* **2017**, *56*, 10046– 10068

44. Weinstein, C. M.; Junor, G. P.; Tolentino, D. R.; Jazzar, R.; Melaimi, M.; Bertrand, G. Highly Ambiphilic Room Temperature Stable Six-Membered Cyclic (Alkyl)(amino)carbenes. *J. Am. Chem. Soc.* **2018**, *140*, 9255–9260

45. Welz, E.; Böhnke, J.; Dewhurst R. D.; Braunschweig, H.; Engels B. Unraveling the Dramatic Electrostructural Differences Between N-

Heterocyclic Carbene- and Cyclic (Alkyl)(amino)carbene-Stabilized Low-Valent Main Group Species *J. Am. Chem. Soc.* **2018**, *140*, 1258-12591.

46. Kushvaha, S. K.; Mishra A.; Roesky, H. W.; Mondal, K. C. Recent Advances in the Domain of Cyclic (Alkyl)(Amino) Carbenes **2022**, *17*, e2021013.
47. Mondal, K. C.; Samuel, P. P.; Roesky, H. W.; Aysin, R. R.; Leites, L. A.; Neudeck S.; Lübben J.; Dittrich, B.; Holzmann, N.; Hermann, M.; Frenking, G. One-Electron-Mediated Rearrangements of 2,3-Disiladicarbene *J. Am. Chem. Soc.* **2014**, *136*, 8919-8922.
48. Shan, Y.-L.; Yim, W.-L.; So, C.-W. An N-Heterocyclic Silylene-Stabilized Digermanium(0) Complex *Angew. Chem., Int. Ed.* **2014**, *53*, 13155-13158.
49. Denk, M.; Lennon, R.; Hayashi, R.; West, R.; Belyakov, A. V.; Verne, H. P.; Haaland, A.; Wagner, M.; Metzler, N. Synthesis and Structure of a Stable Silylene *J. Am. Chem. Soc.* **1994**, *116*, 2691-2692.
50. Sen, S. S.; Khan, S.; Samuel, P. P.; Roesky H. W. Chemistry of Functionalized Silylenes *Chem. Sci.* **2012**, *3*, 659-682.
51. Roesky, H. W. Chemistry of Low Valent silicon. *J. Organomet. Chem.* **2013**, *730*, 57-62.
52. Blom, B.; Stoelzel, M.; Driess, M. New Vistas in N-Heterocyclic Silylene (NHSi) Transition-Metal Coordination Chemistry: Syntheses, Structures and Reactivity towards Activation of Small Molecules *Chem. Eur. J.* **2013**, *19*, 40-62.
53. Sarmah, S.; Guha, A. K.; Phukan, A. K.; Kumar, A.; Gadre, S. R. Stabilization of Si(0) and Ge(0) Compounds by Different Silylenes and Germylenes: a Density Functional and Molecular Electrostatic Study. *Dalton Trans.* **2013**, *42*, 13200

54. Iwamoto, T.; Ishida, S. Stable Silylenes and Their Transition Metal Complexes. **2017**, 361-532.

55. Krahfuss, M. J.; Radius, U. N-Heterocyclic Silylenes as Ambiphilic Activators and Ligands. *Dalton Trans.* **2021**, *50*, 6752-6765.

56. Wang, L.; Li, Y.; Li Z.; Kira, M. Isolable Silylenes and their Diverse Reactivity *Coord. Chem. Rev.* **2022**, *457*.

57. Zhang, Y.; Wu, L.; Wang, H. Application of N-Heterocyclic Silylenes in Low-Valent Group 13, 14 and 15 Chemistry *Coord. Chem. Rev.* **2023**, *477*, 214942.

58. Benedek, Z.; Szilvási, T. Can Low-Valent Silicon Compounds be Better Transition Metal Ligands than Phosphines and NHCs?. *RSC Advances* **2015**, *5*, 5077-5086.

59. Nechaev, M. S. Tetrylenes: Electronic Structure, Stability, Reactivity and Ligand Properties – A Comparative DFT Study *Organometallics* **2021**, *40*, 3408-3423.

60. Du, S.; Jia, H.; Rong, H.; Song, H.; Cui, C.; Mo, Z. Synthesis and Reactivity of N-Heterocyclic Silylene Stabilized Disilicon(0) Complexes **2022**, *61*, e202115570.

61. Iwamoto, T.; Abe, T.; Sugimoto, K.; Hashizume, D.; Matsui, H.; Kishi, R.; Nakano, M.; Ishida, S. A Tetrasilicon Analogue of Bicyclo[1.1.0]but-1(3)-ene Containing a Si=Si Double Bond with an Inverted Geometry **2019**, *58*, 4371-4375.

62. Wilson, D. J. D.; Dutton. J. L. Recent Advances in the Field of Main-Group Mono- and Diatomic “Allotropes” Stabilised by Neutral Ligands. *Chem. Eur. J.* **2013**, *19*, 13626-13637.

63. Yao, S.; Xiong, Y.; Driess, M. A New Area in Main-Group Chemistry: Zerovalent Monoatomic Silicon Compounds and Their Analogues. *Acc. Chem. Res.* **2017**, *50*, 2026-2037.

64. Mahji, P. K.; Sasamori, T. Tetrylones: An Intriguing Class of Monoatomic Zero-Valent Group 14 Compounds *Chem. Eur. J.* **2018**, *24*, 9441-9455.

65. Yao, S.; Xiong, Y.; Saddington, A.; Driess, M. Entering New Chemical Space with Isolable Complexes of Single, Zero-Valent Silicon and Germanium Atoms *Chem. Commun.* **2021**, *57*, 10139-10153.

66. Ota, K.; Kinjo, R. Zero-Valent Species of Group 13-15 Elements *Chem* **2022**, *8*, 340-350.

67. Yadav, R.; Sinhababu, S.; Yadav, R.; Kundu, S. Base-Stabilized Formally Zero-Valent Mono and Diatomic Molecular Main-Group Compounds. *Dalton Trans.* **2022**, *51*, 2170-2202.

68. Liu, K.; Li, B.; Yu, J.; Shi. W. Carbone Derivatives of Group 14: A Class of Important Reactive Intermediates. *Acta Chim. Sin.* **2022**, *80*, 373.

69. Ramirez, F.; Desai, N. B.; Hansen, B.; McKelvie, N. Hexaphenylcarbodiphosphorane, $(C_6H_5)_3PCP(C_6H_5)_3$ *J. Am. Chem. Soc.* **1961**, *83*, 3539– 3540.

70. Vincent, A. T.; Wheatley, P. J. Crystal structure of bis(triphenylphosphoranylidene)methane [hexaphenylcarbodiphosphorane, Ph3P:C:PPh3] *J. Chem. Soc., Dalton Trans.*, **1972**, *5*, 617-622

71. Kaska, W. C.; Mitchell, D. K.; Reichelderfer Transition metal complexes of hexaphenylcarbodiphosphorane *J. Organomet. Chem.* **1973**, *47*, 391-402.

72. Tonner, R.; Öxler, F.; Neumüller, B.; Petz, W.; Frenking, G. Carbodiphosphoranes: The Chemistry of Divalent Carbon(0) *Angew. Chem., Int. Ed.* **2006**, *45*, 8038– 8042.

73. Klein, S.; Tonner, R.; Frenking, G. Carbodicarbenes and Related Divalent Carbon(0) Compounds *Chem. Eur. J.* **2010**, *16*, 10160-10170.

74. Ishida, S.; Iwamoto, T.; Kabuto, C.; Kira, M. A Stable Silicon-based Allene Analogue with a Formally sp-Hybridized Silicon Atom *Nature* **2003**, *421*, 725– 727.

75. Iwamoto, T.; Masuda, H.; Kabuto, C.; Kira, M. Trigermaallene and 1,3-Digermasilaallene *Organometallics* **2005**, *24*, 197– 199.

76. Iwamoto, T.; Abe, T.; Kabuto, C.; Kira, M. A Missing Allene of Heavy Group 14 Elements: 2-germadisilaallene *Chem. Commun.* **2005**, *41*, 5190-5192.

77. Kira, M.; Iwamoto, T.; Ishida, S.; Masuda, H.; Abe, T.; Kabuto, C. Unusual Bonding in Trisilaallene and Related Heavy Allenes *J. Am. Chem. Soc.* **2009**, *131*, 17135– 17144

78. Tonner, R.; Frenking, G. Divalent Carbon(0) Chemistry, Part 1: Parent Compounds *Chem. Eur. J.* **2008**, *14*, 3260-3272.

79. Takagi, N.; Shimizu, T.; Frenking, G. Divalent Silicon(0) Compounds *Chem. Eur. J.* **2009**, *15*, 3448-3456.

80. Takagi, N.; Tonner, R.; Frenking, G. Carbodiphosphorane Analogues $E(PPh_3)_2$ with E=C-Pb: A Theoretical Study with Implications for Ligand Design. *Chem. Eur. J.* **2012**, *18*, 1772-1780.

81. Turek, J.; Braïda, B.; De Proft, F. Bonding in Heavier Group 14 Zero-Valent Complexes – A Combined Maximum Probability Domain and Valence Bond Theory Approach *Chem. Eur. J.* **2017**, *23*, 14604-14613.

82. Mondal, K. C.; Roesky, H. W.; Schwarzer, M. C.; Frenking, G.; Niepötter, B.; Wolf, H.; Herbst-Irmer, R.; Stalke, D. A Stable Singlet Biradicaloid Siladicarbene: $(L:)_2Si$ *Angew. Chem., Int. Ed.* **2013**, *52*, 2963-2967.

83. Niepötter, B.; Herbst-Irmer, R.; Kratzert, D.; Samuel, P. P.; Mondal, K. C., Roesky, H. W. Jerabek, P.; Frenking, G.; Stalke, D. Experimental Charge Density of a Silylone *Angew. Chem., Int. Ed.* **2014**, *53*, 2766-2770.

84. Koike, T.; Nukazawa, T.; Iwamoto, T. Conformationally Switchable Silylone: Electron Redistribution Accompanied by Ligand Reorientation around a Monatomic Silicon *J. Am. Chem. Soc.* **2021**, *143*, 14332-14341.

85. Xiong, Y.; Yao, S.; Inoue, S.; Epping, J. D.; Driess, M. A Cyclic Silylone ("Siladicarbene") with an Electron-Rich Silicon(0) Atom *Angew. Chem., Int. Ed.* **2013**, *52*, 7147-7150.

86. Xiong, Y.; Yao, S.; Tan, G.; Inoue, S.; Driess, M. A Cyclic Germadicarbene ("Germylone") from Germyliumylidene *J. Am. Chem. Soc.* **2013**, *135*, 5004-5007.

87. Wang, Y.; Karni, M.; Yao, S.; Kaushansky, A.; Apeloig, Y.; Driess, M. Synthesis of an Isolable Bis(silylene)-Stabilized Silylone and Its Reactivity Toward Small Gaseous Molecules. *J. Am. Chem. Soc.* **2019**, *141*, 12916–12927,

88. Yao, S.; Kostenko, A.; Xiong, Y.; Ruzicka, A.; Driess, M. Redox Noninnocent Monoatomic Silicon(0) Complex ("Silylone"): Its One-Electron-Reduction Induces an Intramolecular One-Electron-Oxidation of Silicon(0) to Silicon(I). *J. Am. Chem. Soc.* **2020**, *142*, 12608– 12612.

89. Zhou, Y. P.; Karni, M.; Yao, S.; Apeloig, Y.; Driess, M. A Bis(silylenyl)pyridine Zero-Valent Germanium Complex and Its Remarkable Reactivity. *Angew. Chem., Int. Ed.* **2016**, *55*, 15096– 15099.

90. Wang, Y.; Karni, M.; Yao, S.; Apeloig, Y.; Driess, M. An Isolable Bis(silylene)-Stabilized Germylone and Its Reactivity. *J. Am. Chem. Soc.* **2019**, *141*, 1655– 1664.

91. Yao, S.; Kostenko, A.; Xiong, Y.; Lorent, C.; Ruzicka, A.; Driess, M. Changing the Reactivity of Zero- and Mono-Valent Germanium with a Redox Non-Innocent Bis(silylenyl)carborane Ligand. *Angew. Chem., Int. Ed.* **2021**, *60*, 14864– 14868.

92. Yao, S.; Saddington, A.; Xiong, Y.; Driess, M. Chelating Bis-silylenes As Powerful Ligands to Enable Unusual Low-Valent Main-Group Element Functions *Acc. Chem. Res.* **2023**, *56*, 475-488.

93. Burchert, A.; Müller, R.; Yao, S.; Schattenberg, C.; Xiong, Y.; Kaupp, M.; Driess, M. Taming Silicon Congeners of CO and CO_2: Synthesis of Monomeric Si^{II} and Si^{IV} Chalcogenide Complexes *Angew. Chem., Int. Ed.* **2017**, *56*, 6298– 6301.

94. Keuter, J.; Hepp, A.; Mück-Lichtenfeld, C.; Lips, F. Facile Access to an NHC-Coordinated Silicon Ring Compound with a Si═N Group and a Two-Coordinate Silicon Atom. *Angew. Chem., Int. Ed.* **2019**, *58*, 4395– 4399.

95. Mondal, K. C.; Roy, S.; Dittrich, B.; Andrada, D. M.; Frenking, G.; Roesky, H. W. A Triatomic Silicon(0) Cluster Stabilized by a Cyclic Alkyl(amino) Carbene *Angew. Chem., Int. Ed.* **2016**, *55*, 3158-3161.

Chapter 2

Synthesis and isolation of Spiroheptasiladione: Silicon analogue of Spirocyclic Allene

---

2.1 Introduction

Spirocyclic compounds contain two rings connected through a single shared atom.[1] They are inherently able to escape from planar chemical space due to their perpendicular rings.[2, 3] They furnish access to rigid and conformationally restricted structures when the spirocycles are composed of saturated small rings, such as cyclobutanes, oxetanes, azetidines, and thietanes. The conformation of bonding therein is rigorously well-defined in their spatial disposition, reducing the entropic cost when interacting with substrates, in particular, biological molecules that requires the adoption of a determined conformation. Thus, saturated spirocyclic scaffolds are popular in medicinal chemistry and shows pharmacological applications.[4-9]

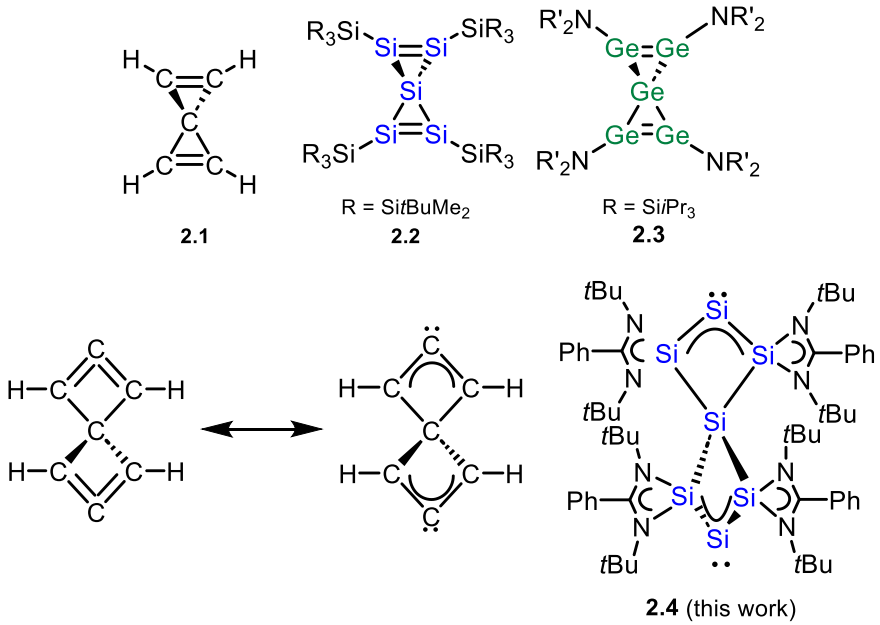

Scheme 2.1 Heavier analogues of spirocylic compounds

However, formation of the spirocyclic motif is always a synthetic challenge. Embedding carbon−carbon π-bonds within spirocyclic small ring systems leads to a high degree of strain.[10,11] The intrinsic high strain energy therefore, in principle, decreases the likelihood of their existence, but confers novel reactivity, often leading to both new modes of reaction as well as novel architectures in the resulting products. The smallest unsaturated spirocyclic molecules is spiropentadiene **2.1** (Scheme 2.1), a fundamentally important molecule in understanding the phenomena of spiroconjugation; through-space orbital interactions between two perpendicular π (π*) orbitals.[12] The spiropentadiene derivatives that have been synthesized so far are unstable and decompose at very low temperatures.[13-16] To stabilize such exotic spirocycles, replacing carbon atoms in the skeleton of these molecule with heavier group 14 elements, namely, silicon, germanium, tin or lead, would provide an opportunity to isolate their stable analogues at ambient conditions due to fundamentally different core electronic structure of heavy group 14 elements.[17,18] Silicon has been shown through theoretical studies to potentially relieve the high ring strain in such systems when incorporated into these scaffolds.[19-21]

Kira et al. isolated a spiropentasiladiene **2.2**,[22] a fully silicon analogue of the spiropentadiene backbone, which comprises of two perpendicular Si=Si double bonds, supporting the feasibility of spiroconjugation. Li, Driess and Wang et al. have reported the isolation of spiropentagermadiene **2.3**,[23] wherein σ-delocalization of the Ge_5 skeleton and the 2π-delocalized aromatic Ge_3 rings account for its high stability.

The next smallest unsaturated spirocyclic scaffolds is spiro[3.3]hepta-1,2,5,6-tetraene. It has received far less attention compared with other strained cyclic allenes,

despite having several advantages that warrant its further investigation. It possesses two strained allene moieties simultaneously. The acute bond angle at the central allene carbon is expected to break the degeneracy of orthogonal double bonds into one σ-symmetric lone pair and two delocalized π electrons akin to the electronic structure of carbodicarbenes.[24,25] The perpendicular π orbitals could further interact with each other through spiroconjugation. To date, such molecules have yet to be studied experimentally and theoretically, leading to a question of whether the spiro[3.3]hepta-1,2,5,6-tetraene backbone is feasible. Furthermore, because of its highly strained structure, the synthesis of spiro[3.3]hepta-1,2,5,6-tetraene should be one of the most difficult synthetic challenges. As illustrated in spiropentasiladiene **2.2** and spiropentagermadiene **2.3**, the incorporation of heavy group 14 elements into the spiro[3.3]hepta-1,2,5,6-tetraene scaffold could grant access to a stable derivative at ambient conditions. Herein, we report the synthesis of an amidinato spiroheptasiladione exhibiting this structure.

2.2 Results and discussion

The amidinato disilyne [LSi:]$_2$ (**1.51**, L = PhC(NtBu)$_2$)[26] was treated with (Me$_3$P)$_2$SiCl$_4$[27] and KC$_8$ in toluene at -78 ^{o}C, following which the mixture was warmed to 8 ^{o}C and reacted for 18 h to afford a mixture of spiroheptasiladione [Si{Si(LSi)$_4$}Si] (**2.4**), symmetrical tetrasilacyclobutadiene [(μ-LSi)$_2$Si$_2$(SiL)$_2$] (**2.5**) and unsymmetrical tetrasilacyclobutadiene [(μ-LSi)$_2$(SiSiL)(Sil)] (**2.6**), along with PMe3 as the by-product. The reaction mixture was extracted with pentane to isolate compound **2.6** as a dark red crystalline solid from the concentrated pentane filtrate. The residue was then extracted with 1:1 hexane and benzene to isolate compound **2.4** as a red crystalline solid from the concentrated hexane/benzene filtrate. The residue was further extracted with toluene to isolate compound **2.5** as black crystals from the concentrated toluene filtrate.

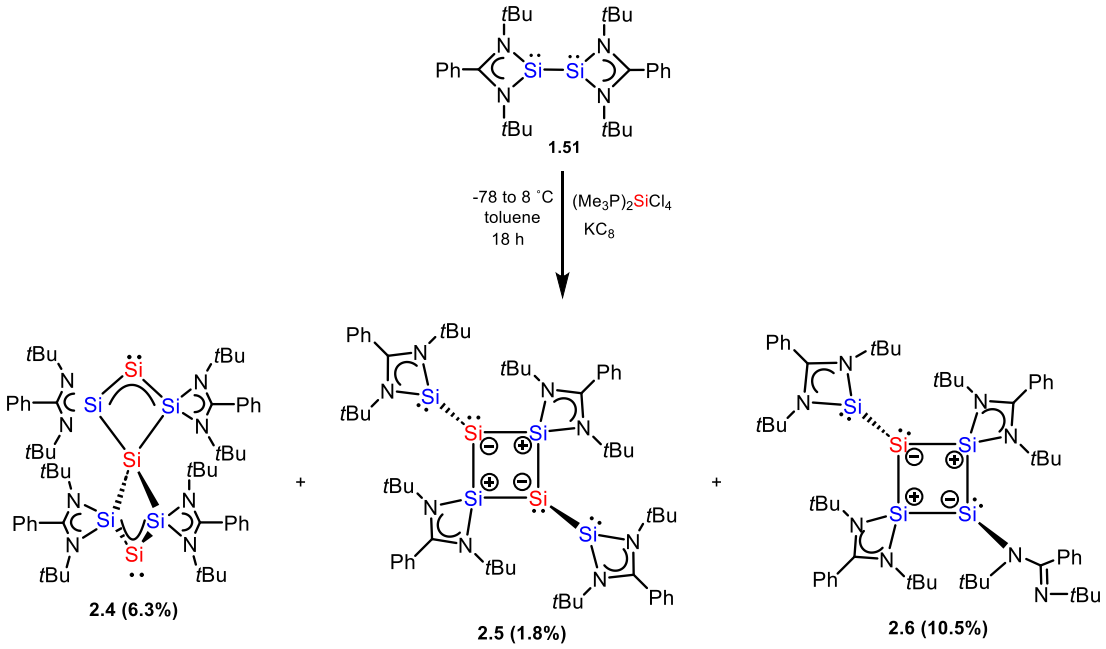

Scheme 2.2 Synthesis of spiroheptasiladione **2.4**, tetrasilacyclobutadiene analogues **2.5** and **2.6**

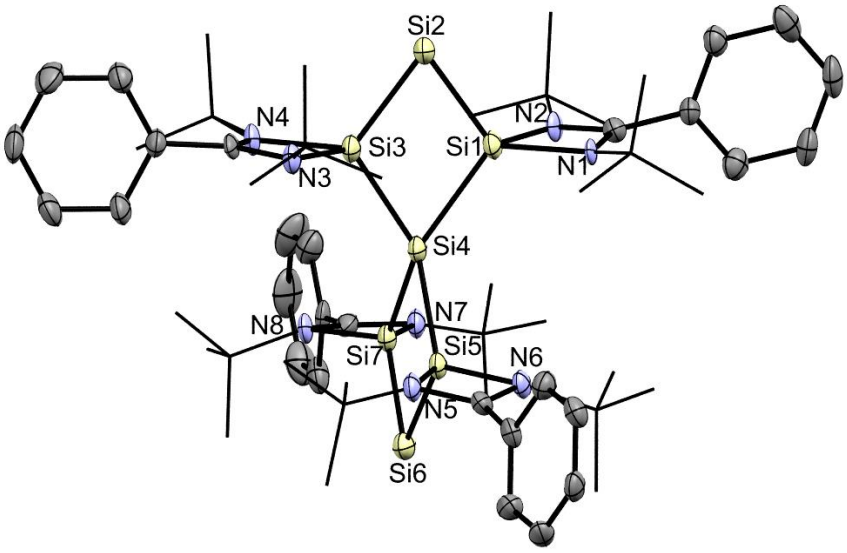

Figure 2.1 Molecular structure of **2.4** obtained by X-ray crystallography. Thermal ellipsoids are shown at 50 % probability. All hydrogen atoms are removed for clarity. Selected bond lengths (Å) and angles (deg): Si1-Si2 2.256(2), Si1-Si4 2.364(2), Si2-Si3 2.256(3), Si3-Si4 2.369(2), Si4-Si5 2.359(3), Si4-Si7 2.383(2), Si5-Si6 2.251(2), Si6-Si7 2.242(3), Si1-N1 1.888(5), Si1-N2 1.878(6), Si3-N3 1.888(6), Si3-N4 1.882(5), Si5-N5 1.874(6), Si5-N6 1.883(5), Si7-N7 1.892(6), Si7-N8 1.886(5), Si1-Si2-Si3 75.61(8), Si2-Si3-Si4 106.28(10), Si3-Si4-Si1 71.49(8), Si4-Si1-Si2 106.47(10), Si5-Si4-Si7 71.82(8), Si4-Si7-Si6 105.54(10), Si7-Si6-Si5 76.49(8), Si6-Si5-Si4 106.06(10).

Compound **2.4** is a highly air- and moisture-sensitive compound, having been observed to fully decolorize when left exposed to glovebox atmosphere (Ar, <0.1 ppm O_2, <0.1 ppm H_2O) overnight. It was fully characterized by NMR spectroscopy and X-ray crystallography. The molecular structure of compound **2.4** shows that the two silylone rings (Si1Si2Si3Si4 and Si4Si5Si6Si7) are planar and linked by the spiro-Si4 atom. These two planes are perpendicular to each other with a dihedral angle of 91.4(14)^o, which is larger than that in spiropentasiladiene (78.3(0)^o)[22] and spiropentagermadiene (70.2(15)^o).[23] The bond angles at the $Si_{silylone}$ atoms (Si3-Si2-Si1: 75.61(8)^o and Si-5-Si6-Si7 (76.49(8)^o) are the smallest among the cyclic bis(silylene)-ligated zero-valent silic–n complexes (82.75(2)^o - 104.38(3)^o),[28-42] indicating that the large energy separation between the s and p orbitals in the silicon atoms facilitate the

strongly bent geometry, which consequently breaks the degeneracy of orthogonal double bonds into one σ-symmetric lone pair and two delocalized π electrons. This accounts for the enhanced stability of compound **2.4**. The Si2-Si1 (2.256(2) Å, Si2-Si3 (2.256(3) Å), Si6-Si5 (2.251(2) Å), Si6-Si7 (2.242(3) Å) bond lengths fall in the high end of the Si=Si double bond length range (2.138 – 2.289 Å). They are similar to the 9,9-dimethyl-xanthene-4,5-diyl-substituted bis(amidinato silylene)-silylone complex **A** (2.2451(7) – 2.2586(7) Å)(Scheme 2.3)[37] and carborane-1,2-bis(amidinato silylene)-silylone complex **B** (2.225(6) – 2.2272(6) Å).[40] This shows that the π- electrons on the $Si_{silylone}$ atoms (Si2, Si6) are extensively delocalized along the Si1-Si2-Si3 and Si5-Si6-Si7 skeletons. The Si4-Si1 (2.364(2) Å), Si4-Si3 (2.369(2) Å), Si4-Si5 (2.359(3) Å), Si4-Si7 (2.383(2) Å) are typical of Si-Si single bonds.

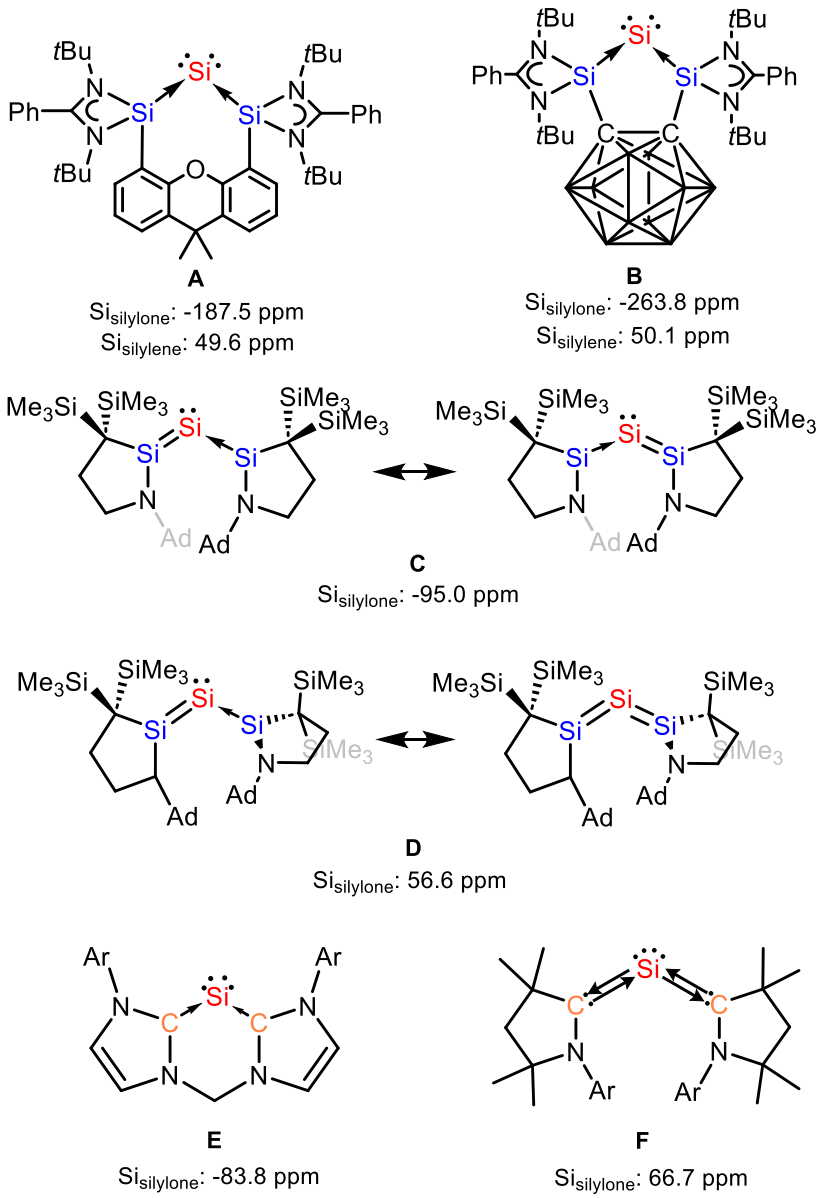

Scheme 2.3 Examples of similar silylone complexes

The ^{1}H NMR spectrum shows one set of signals due to the amidinate ligands. The ^{29}Si{^{1}H} NMR spectrum displays three resonances at -8.5, -7.5 and 31.5 ppm for the spiro-silicon, silylone, and amidinato silylene centers, respectively, which are in line with the gauge-inducing atomic orbital (GIAO) ^{29}Si NMR calculations ($Si_{spiro\text{-}silicon}$: -9.7, $Si_{silylone}$: -7.5, $Si_{silylene}$: 31.7 ppm; SO-ZORA-BP86/TZP//M06-2X/def2-SVP) and ^{29}Si CP-MAS NMR (spinning frequency: 12 kHz) spectroscopy ($Si_{spiro\text{-}silicon}$: 2.6, $Si_{silylone}$: -11.4, $Si_{silylene}$: 34.0 ppm). The ^{29}Si NMR signal for the $Si_{silylone}$

center (-7.5 ppm) is significantly downfield shifted in comparison with the silylone center of the 9,9-dimethyl-xanthene-4,5-diyl-substituted bis(amidinato silylene)-silylone complex **A** (-187.5 ppm)[37] and carborane-1,2-bis(amidinato silylene)-silylone complex **B** (-263.8 ppm),[40] indicating that the silylone center in compound **2.4** is less electron-rich. It is intermediate between that of the bis(CAASi)-silylone **C** (CAASi = cyclic (alkyl)(amino)silylene) with a π-delocalized ylidene structure (-95.0 ppm) and CDASi-silyone-CAASi **D** (CDASi = cyclic dialkylsilylene) with a twisted π-localized ylidene structure and some bent-allene character (56.6 ppm).[42] It is also intermediate between that of bis(NHC)-silylone **E** (-83.8 ppm)[33] and bis(CAAC)-silylone **F** (66.7 ppm).[42] The ^{29}Si NMR signal for the $Si_{silylene}$ (31.7 ppm) in compound **2.4** is upfield shifted in comparison with that of **A** (49.6 ppm)[37] and **B** (50.1 ppm).[40] The difference of ^{29}Si NMR chemical shifts between the $Si_{silylone}$ and $Si_{silylene}$ centers in compound **2.4** ($\Delta\delta$ = 31.5 ppm – (-7.5 ppm) = 39 ppm) is substantially smaller than of **A** ($\Delta\delta$ = 237.2 ppm) and **B** ($\Delta\delta$ = 313.9 ppm), indicating that **2.4** possesses relatively less polarized $Si_{silylene}$-$Si_{silylone}$ bond. The spectroscopic data implies that the π-type lone pair of electrons is extensively delocalized along the $Si_{silylene}$-$Si_{silylone}$-$Si_{silylene}$ skeleton. The ^{29}Si NMR signal for the $Si_{spiro\text{-}silicon}$ (-8.5 ppm) is downfield shifted in comparison with the upfield ^{29}Si NMR (~ -100 ppm) of the spiro-silicon center in spirooligosilanes (σ-electron delocalization).[43-47]

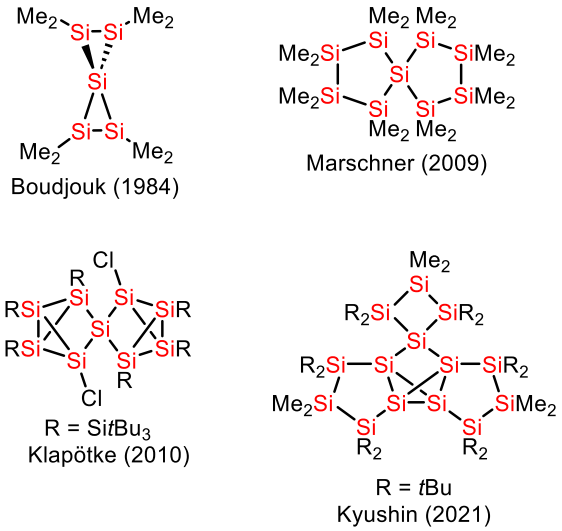

Scheme 2.4 Examples of spirooligosilanes

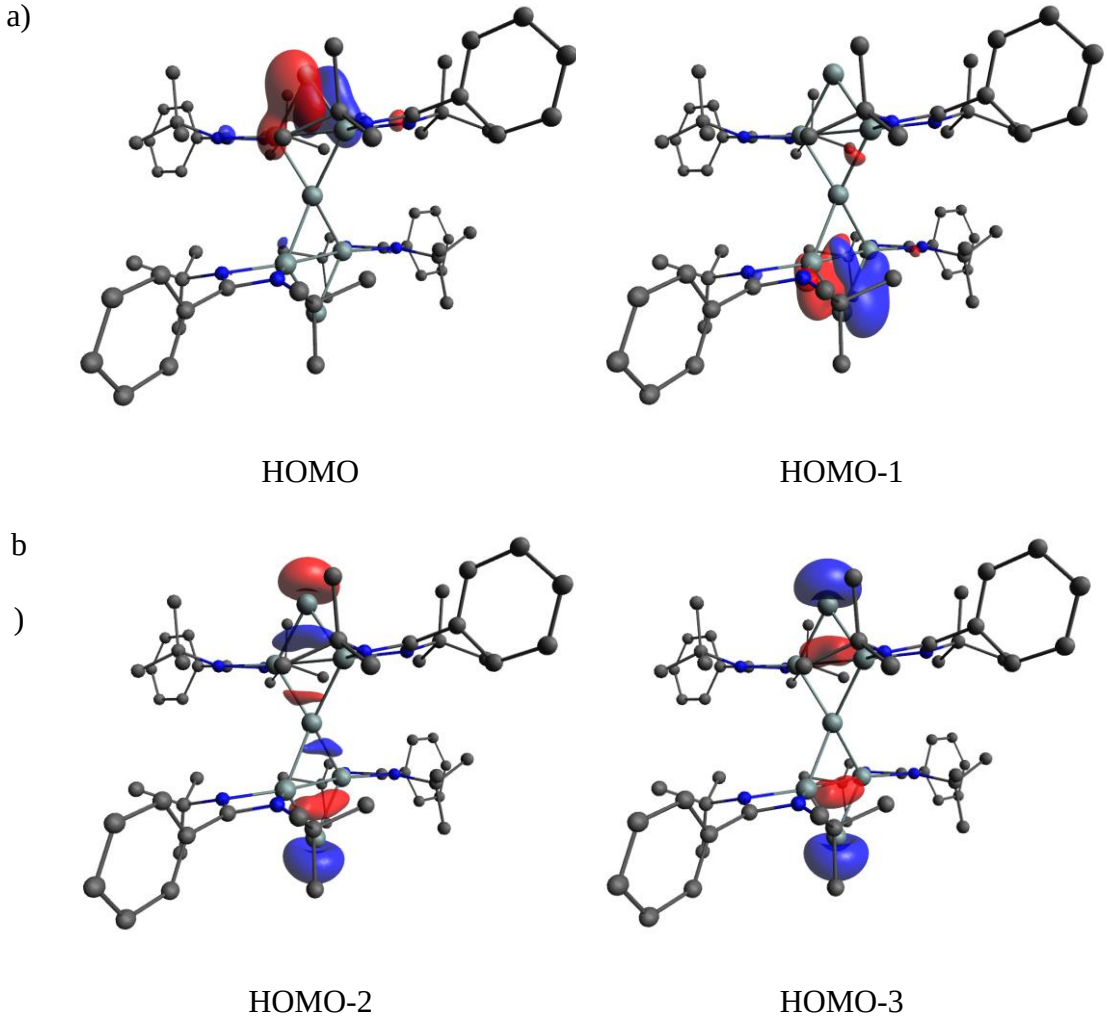

Figure 2.2 a) HOMO and HOMO-1 of compound **2.4** and b) HOMO-2 and HOMO-3 of compound **2.4** calculated at M06-2X/def2-SVP level of theory

DFT calculations (M06-2X/def2-SVP)[48,49] were performed to elucidate the electronic structure of compound **2.4**. Quasi-degenerate HOMO and HOMO-1 show the π-orbital on the Si1-Si2-Si3 and Si5-Si6-Si7 skeletons. HOMO-2 and HOMO-3 exhibit σ-type lone pair orbitals on the Si2 and Si6 atoms. HOMO-2, HOMO-6 and HOMO-7 display σ-delocalization in each Si-spiro ring. Accordingly, Natural Bond Orbital analysis[50-52] shows that there are σ-type lone pair orbitals on the Si2 and Si6 atoms, which are in high s-orbital character (Si2: $sp^{0.36}$; Si6: $sp^{0.37}$). The 3-center π-bonds are found on the Si1-Si2-Si3 and Si5-Si6-Si7 skeletons, where more than 50% of the π-electron density on the Si2 and Si6 atom is delocalized to adjacent silicon atoms (Si2: Si1 and Si3; Si6: Si5 and Si7). The extensive π-electron delocalization reduces electron density on the Si2 and Si6 atoms, which is in line with their low-field ^{29}Si NMR signals. The double bond character of the Si1-Si2, Si2-Si3, Si5-Si6 and Si6-Si7 bonds concomitantly increase as indicated by their Wiberg Bond Index (WBI: 1.14 – 1.15).[53-55] The WBI also shows that the Si-Si bonds formed by the spiro-Si4 atom are single bonds (WBI: 0.95).

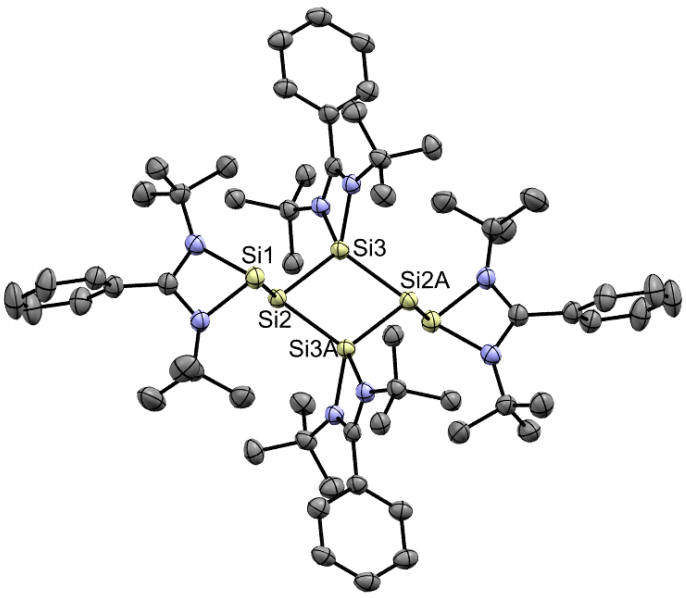

Figure 2.3 Molecular structure of **2.5** obtained by X-ray crystallography. Thermal ellipsoids are shown at 50 % probability. All hydrogen atoms are removed for clarity. Selected bond lengths (Å) and angles

(deg): Si2-Si3 2.3128(13), Si2-Si3A 2.3095(14), Si1-Si2 2.4079(14), Si2-Si3-Si2A 105.78(5), Si3-Si2-Si3A 74.22(5), Si1-Si2-Si3 112.40(5), Si1-Si2-Si3A 114.65(5), N2-Si1-N1 68.66(13), N2-Si1-Si2 99.03(10), N1-Si1-Si2 97.81(10).

Compound **2.5** is a tetrasilacyclobutadiene with an ylide electronic structure. Similar amidinate-stabilized heavier butadiene analogues have been reported.[56-59] Compound **2.5** is highly air and moisture-sensitive, instantly decolorizing upon exposure to ambient atmosphere. The molecular structure of compound **2.5** obtained by X-ray crystallography shows that it comprises a planar Si_4 four-membered ring. The amidinate ligands are bidentate bonded to the Si3A and Si3 atoms, which adopt a distorted tetrahedral geometry. The Si2 and Si2A atoms adopt a trigonal pyramidal geometry (sum of the bond angles, Si2/Si2A: 301.3°), indicating that there is a lone pair of electrons on the Si2 and Si2A atoms. The Si2-Si3 (2.3095(14) Å) and Si2-Si3A (2.3128(13) Å) bond lengths are typical of single bond lengths. Therefore, the planar Si_4 four-membered ring in compound **2.5** has an ylide structure. In addition, the Si2 and Si2A atoms are bonded with the amidinato silylene substituents. The Si1 and SiA atoms also adopt a trigonal pyramidal geometry (sum of the bond angles: 265.5°), which is consistent with a stereoactive lone pair on the Si1 and Si1A atoms. The Si1-Si2 bond length (2.4079(14) Å) is comparable with that of **1.51** (2.413(2) Å).

Compound **2.5** is sparingly soluble in most organic solvents and deuterated organic solvents after crystallization. Furthermore, the use of highly polar donor solvents such as pyridine and acetonitrile result in decomposition resulting in an intractable mixture, as observed by 1H NMR. As a result, the solution state ^{29}Si NMR signals of compound **2.5** in C_6D_6 could not be detected and instead the solid state ^{29}Si CP-MAS NMR (spinning frequency: 14 kHz) spectroscopy was performed, where two

resonances at -81.4 and 91.3 ppm are attributable to the three-coordinate and four-coordinate silicon atoms in the Si_4 four-membered ring. The large difference in chemical shift suggests that there is a ylide structure in the Si_4 four-membered ring. Similar large difference in chemical shift is found in the ^{29}Si solid state NMR spectrum of the terta-aryl substituted tetrasilacyclobutadiene $[(EMind)_4Si_4]$(-52, -50, 300 and 308 ppm).[56] In addition, the ^{29}Si NMR CP-MAS spectrum of **2.5** displays a sharp singlet at 57.7 ppm corresponding to the exocyclic Si1/SiA centers, which shows a upfield shift compared with that of **1.51** (76.3 ppm).

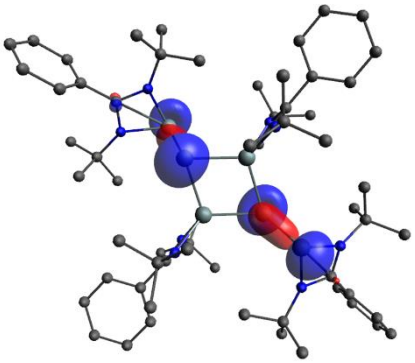

HOMO (ε = -4.065 eV)

(Top View)

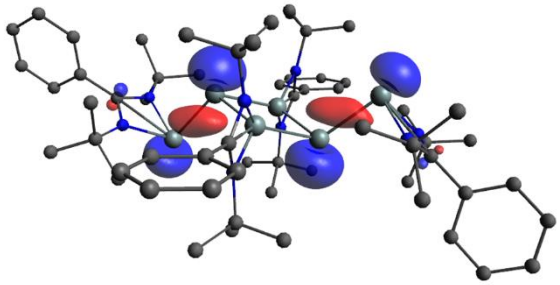

HOMO (ε = -4.065 eV)

(Side View)

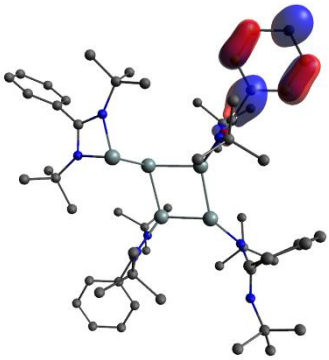

LUMO (ε = 0.023 eV)

Figure 2.4 Selected MOs of compound **2.5** calculated at M06-2X/def2-SVP level of theory

DFT calculations (M06-2X/def2-SVP) were performed to elucidate the electronic structure of compound **2.5** (Figure 2.4). The HOMO arises from lone pair orbitals at the three-coordinate Si atoms of the Si_4 four-membered ring and the exocyclic Si atoms. The HOMO-2 shows the endocyclic Si-Si σ orbitals. Accordingly, NBO shows that the Lewis structures of the Si4 rings have four occupied σ orbitals for the endocyclic Si-Si bonds. The Wiberg bond index (WBI) indicates that the bond orders of the endocyclic (WBI:) and exocyclic Si-Si bonds (WBI: 0.90) are equal and single bonds. Moreover, the lone pair orbitals on the endocyclic (Si2: $sp^{0.57}$, Si2A: $sp^{0.65}$ hybrids) and exocyclic three-coordinate Si atoms (Si1: $sp^{0.37}$) are high in s-character, with some directionality. The NPA charges (Si3: 0.925, Si3A: 0.903; Si2: -0.550, Si2A: -0.584 e) show that the Si_4 four-membered ring has a charge-separated structure. Overall, the results show that compound **2.5** has a planar rhombic tetrasilacyclobutadiene ylide electronic structure.

Compound **2.6** has a similar cyclobutadiene ylide electronic structure. The $^{29}Si\{^1H\}$ NMR spectrum of **2.6** displays a large difference in chemical shift for the four-coordinate (58.8 ppm) and three-coordinate silicon centers (-97.4 and -163.2 ppm) of the Si_4 four-membered ring, in addition to a singlet at 101.7 ppm attributable to the exocyclic Si center.

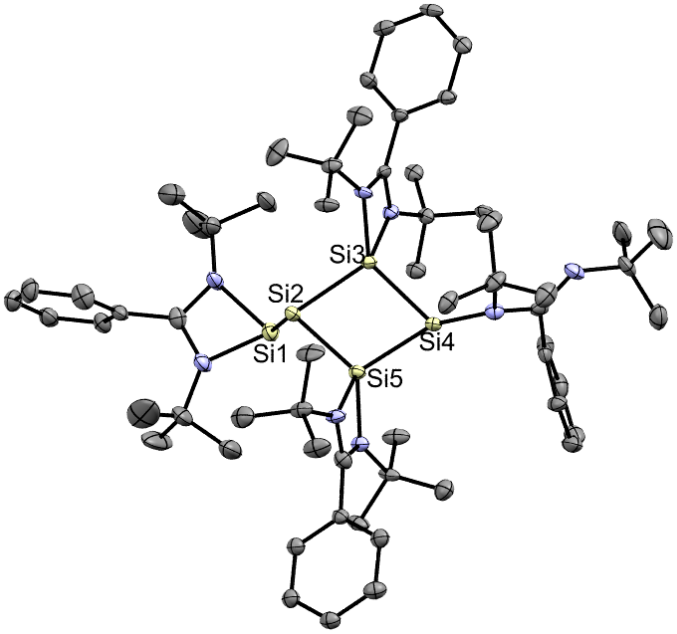

Figure 2.5 Molecular structure of **2.6** obtained by X-ray crystallography. Thermal ellipsoids are shown at 50 % probability. All hydrogen atoms are removed for clarity. Selected bond lengths (Å) and angles (deg): Si2-Si3 2.317(2), Si3-Si4 2.286(2), Si4-Si5 2.299(2), Si2-Si5 2.338(2), Si1-Si2 2.424(2), Si2-Si3-Si4 101.82(8), Si3-Si4-Si5 78.34(7), Si4-Si5-Si2 100.80(8), Si5-Si2-Si3 76.95(7), Si1-Si2-Si3 108.03(8), Si1-Si2-Si5 112.01(9).

Compound **2.6** composes a puckered Si_4 four-membered ring (dihedral angle: 17.1°). The Si4 and Si2 centers adopt a trigonal pyramidal geometry (sum of the bond angles, Si2: 297°, Si4: 337.4°), indicating that there is a lone pair of electrons on the Si2 and Si4 atoms. The Si3-Si4 (2.286(2) Å) and Si4-Si5 (2.299(2) Å) bonds are shorter than the Si2-Si3 (2.317(2) Å) and Si2-Si5 (2.338(2) Å) bonds, indicating that the lone pair of electrons on the Si4 atom is slightly delocalized to the Si3 and Si5 atoms. Thus, the Si2-Si3 and Si2-Si5 bonds are typical of single bonds, while the Si3-Si4 (2.286(2) Å) and Si4-Si5 (2.299(2) Å) bonds have slight double bond character.

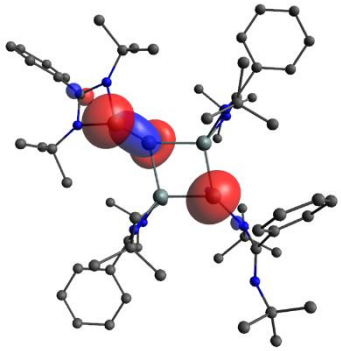

HOMO (ε = -4.317 eV)

(Top View)

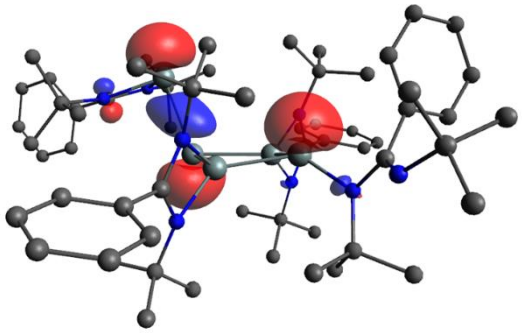

HOMO (ε = -4.317 eV)

(Side View)

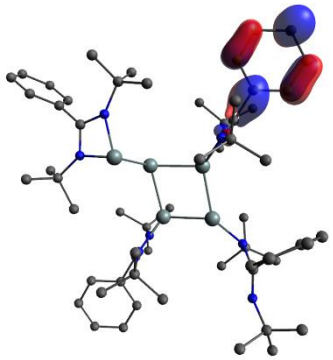

LUMO (ε = 0.014 eV)

Figure 2.6 Selected MOs of compound **2.6** calculated at M06-2X/def2-SVP level of theory

DFT calculations show that the HOMO arises from lone pair orbitals at the three-coordinate Si atoms of the Si_4 four-membered ring and the exocyclic Si atoms. Accordingly, NBO analysis shows that a lone pair orbital on the endocyclic Si2 ($sp^{0.54}$) and exocyclic Si1 ($sp^{0.36}$) atoms. The Si2-Si3 (WBI: 1.01) and Si2-Si5 (WBI: 1.03) bonds are single bonds. The Si3-Si4 bond composes a π orbital generated by the mixing of Si p orbitals, which is strongly polarized toward the Si4 atom (17.63% Si3 + 82.37% Si4). This illustrates that the lone pair of electrons on the Si4 atom slightly delocalize to the Si3 and Si5 atoms, leading to slight double bond character (WBI: Si3-Si4: 1.13; Si5-Si4: 1.13).

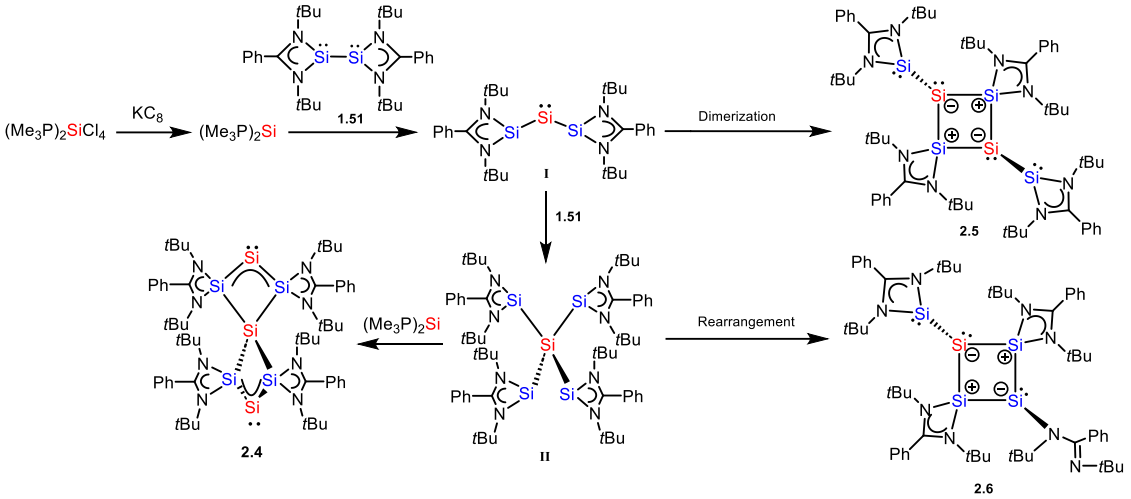

Scheme 2.5 Proposed reaction mechanism for the synthesis of complex **2.4**

A passing comparison of compounds **2.5** and **2.6** would consider them to be closely related ylides, however they are invaluable in providing a clearer understanding of the formation mechanism of **2.4**. By varying the temperature at which this reaction was carried out we were able to drive the reaction selectively towards either **2.5** or **2.6**. When the reaction of **1.51**, $(PMe_3)_2SiCl_4$ and KC_8 in toluene was performed at -40 °C for 16 h to form compound **2.6** as the sole kinetic product. On the other hand, when reflux condition was employed, only compound **2.5** was afforded as the sole thermodynamic product. Compound **2.4** were not observed in these conditions. These results suggest that the formation of these complexes could proceed through the same intermediate through different kinetic pathways. We recognize that the charge-separated structure of **2.5** can be understood as the dimerization product of bis(silylenyl)silylene, **I** (Scheme 2.5). Depicted using the donor-acceptor model, the lone pair from an amidinato silylene moiety of **I** donates into the vacant p orbital on the central silylene center of another molecule of **I,** thus forming compound **2.5**. Whereas for **2.6**, it would appear to be an oxidative addition product, whereby one molecule of **I** inserts, via the central silylene center, into the Si-Si bond of **1.51**. While we initially anticipated this

transformation could directly afford compound **2.6** via a concerted mechanism, the partially dissociated amidinate moiety suggested otherwise, potentially as a result of a rearrangement from an intermediate structure. We, therefore, suggested that it should pass through one more intermediate **II**, a tetrakis(amidinatosilylenyl) silane. Intermediate **II** would be a key intermediate that could naturally lead to the unique structure observed in compound **2.4**.

DFT calculations (M06-2X-D3(BJ)/def2-SVP level of theory) show that **I** proceeds through a lower kinetic barrier (9.2 kcal/mol) to form the kinetic product [$(LSi)_4Si$] (**II**), while the dimerization process passes through a higher kinetic barrier (25.1 kcal/mol) to form the thermodynamic product **2.5**. **II** then quickly undergoes a thermodynamic rearrangement to give compound **2.6**. Therefore, the calculated reaction pathway is in agreement with the kinetic selectivity between **2.5** and **2.6**, suggesting that the reaction is highly likely to pass through the two proposed intermediates. While all attempts have been made to identify the proposed source of Si(0) atoms, $(PMe_3)_2Si$, we were unfortunately unable to observe its formation spectroscopically. As such we are hesitant to propose its involvement in the reaction mechanism that results in the formation of **2.4**. Nevertheless, with the observation of **2.4** exclusively occurring at intermediate temperatures (8 °C), it would logically suggest that **2.4** is formed from the same intermediate **II**, in competition with the rearrangement into **2.6**.

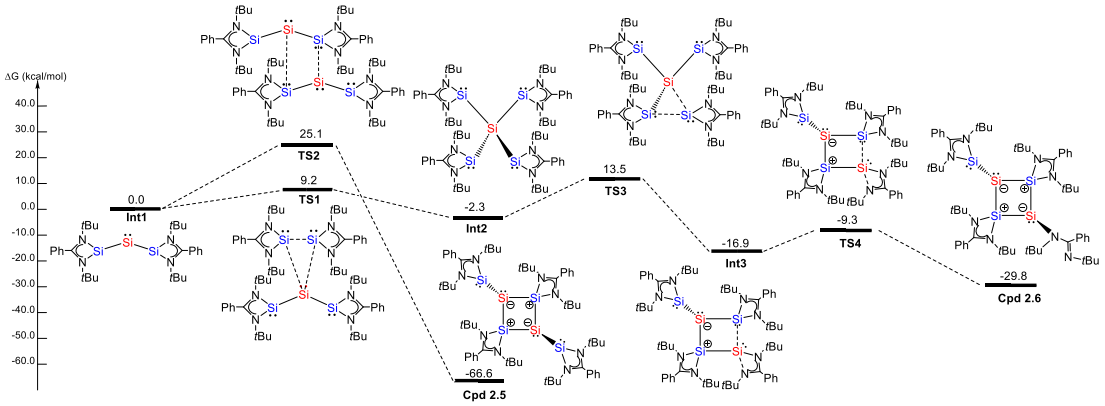

Scheme 2.6 Reaction pathway for the formation of intermediate **II** and compounds **2.5 and 2.6** calculated at M06-2X/def2-SVP level of theory

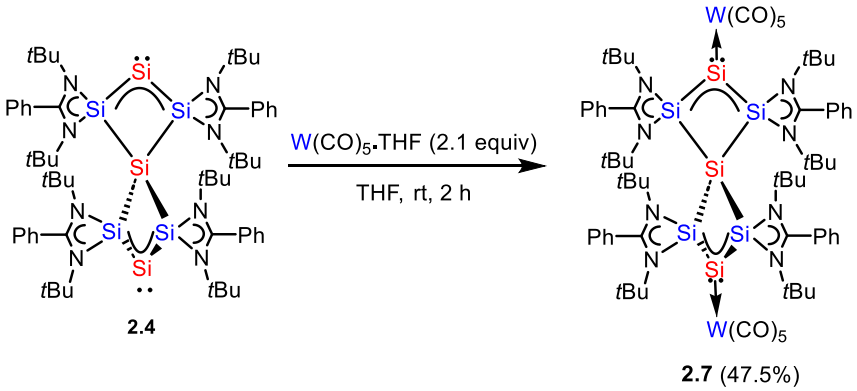

Scheme 2.7 Reaction of **2.4** with $W(CO)_5$·THF in formation of complex **2.7**

The unique structure of **2.4** prompted us to investigate its properties as a donor, as the first ditopic silicon donor. The presence of σ-type lone pair orbitals on the silicon atoms in compound **2.4** was illustrated by its reaction with two equivalents of $W(CO)_5$·THF in THF at room temperature, where bis(pentacarbonyl tungsten)-spiroheptasiladione adduct $[(OC)_5W{\leftarrow}Si\{Si(LSi)_4\}Si{\rightarrow}W(CO)_5]$ (**2.7**) is obtained.

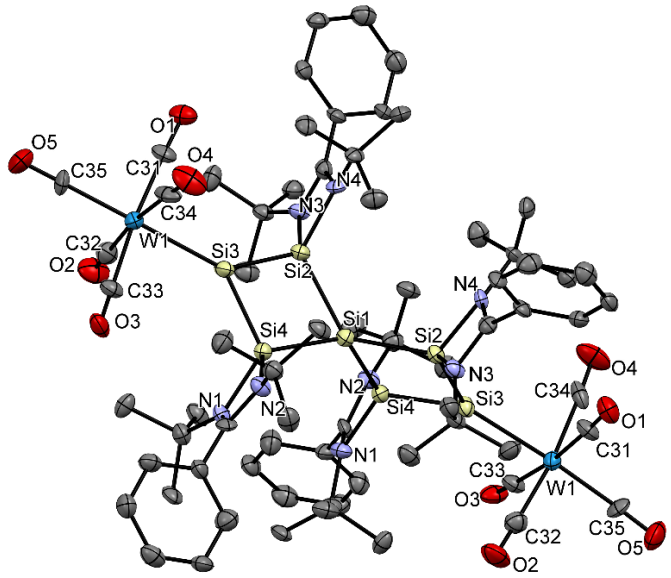

Figure 2.7 Molecular structure of **2.7** obtained by X-ray crystallography. Thermal ellipsoids are shown at 50 % probability. All hydrogen atoms are removed for clarity. Selected bond lengths (Å) and angles (deg): Si3-Si2 2.219(4), Si3-Si4 2.238(4), Si1-Si2 2.364(3), Si1-Si4 2.354(4), Si3-W1 2.574(3), W1-C35 2.014(9), C35-O5 1.134(12), Si3-Si2-Si1 100.71(14), Si2-Si1-Si4 76.70(9), Si3-Si4-Si1 100.47(14), Si2-Si3-Si4 82.12(13), Si2-Si3-W1 138.58(14), Si4-Si3-W1 139.14(15**)**

The molecular structure of compound **2.7** determined by X-ray crystallography shows that two planar silylone rings (si1Si2Si3Si4 and Si1Si2ASi3ASi4A) are remain almost perpendicular to each other with a dihedral angle of 87.9°, which is comparable with that of **2.4**. The bond angles at the $Si_{silylone}$ atoms (82.12(13)°) are larger than those of **2.4**, while The Si2-Si3 (2.219(4) Å) and Si3-Si4 (2.238(4) Å) bonds are almost identical to that of compound **2.4**, preserving their double bond character, suggesting significant electron delocalization is retained within the ring. The Si3-W1 bond (2.574(3) Å) is in the range of Si→W coordinative covalent bond in silylene-tungsten pentacarbonyl complexes [2.337−2.636 Å].[60-63]

The ^{29}Si{1H} NMR signal for the silylone centers (-27.6 ppm) in compound **2.7** is curiously upfield shifted in comparison with that of compound **2.4**. Upon coordination,

it is generally expected that electron density is drawn away from the donor center, which would result in a significant downfield shift of the ^{29}Si NMR resonances as is commonly observed in reported silylene-$W(CO)_5$ complexes. However, a similar upfield shift was found in the synthesis of the bis(NHC)-silylone-$GaCl_3$ adduct (-119.0 ppm) by the reaction of **E** (-83.8 ppm) with $GaCl_3$ (Scheme 2.3).[64] In reference to the X-ray crystallographic data, the retention of the double bond character of the Si2-Si3 and Si3-Si4 bonds in **2.7** would suggest significant pi delocalization over the central Si atom. Furthermore, the widening of the Si-Si-Si bond angle would suggest and increase in the p character of the filled orbital of the central Si atom, enhancing any pi-donating effects from the adjacent silylene moieties. In addition, the ^{29}Si NMR signal for the $Si_{spiro\text{-}silicon}$ (--87.9 ppm) becomes comparable with the upfield ^{29}Si NMR (~ -100 ppm) of the spiro-silicon center in spirooligosilanes after complexation. The ^{29}Si NMR resonance for the amidinate-bonded silicon center (28.2 ppm) does not shift significantly compared with that of compound **2.4** (31.7 ppm). While it could be suggested that the increase in electron density arises from backbonding from the tungsten metal center, the FT-IR (CaF cell) spectrum of **2.7** refutes this notion and supports the strong donating ability of **2.4.** The presence of sharp bands at 2036, 1916 and 1903 cm^{-1} and one broad band at 1887 cm^{-1} corresponding to the cis-CO and trans-CO stretches are bathochromic shifted compared to those of $W(CO)_5$·THF (1929 and 1892 cm^{-1}), respectively. This is in stark contrast with the hypsochromic shift observed in N-heterocyclic silylene tungsten complexes reported by West et al. (2069 cm^{-1}, 2011 cm^{-1} and 1980 cm^{-1}), which is consistent with significant backbonding from the tungsten metal into the vacant p orbital of the coordinating silylene (Scheme 2.8) .[65] Hence, this provides further evidence that **2.4** can be interpreted as simultaneous trisilaallene moieties, or two simulateneous

silylone center, as the significant pi delocalization over the central silicon center prevents back-bonding from the metal center.

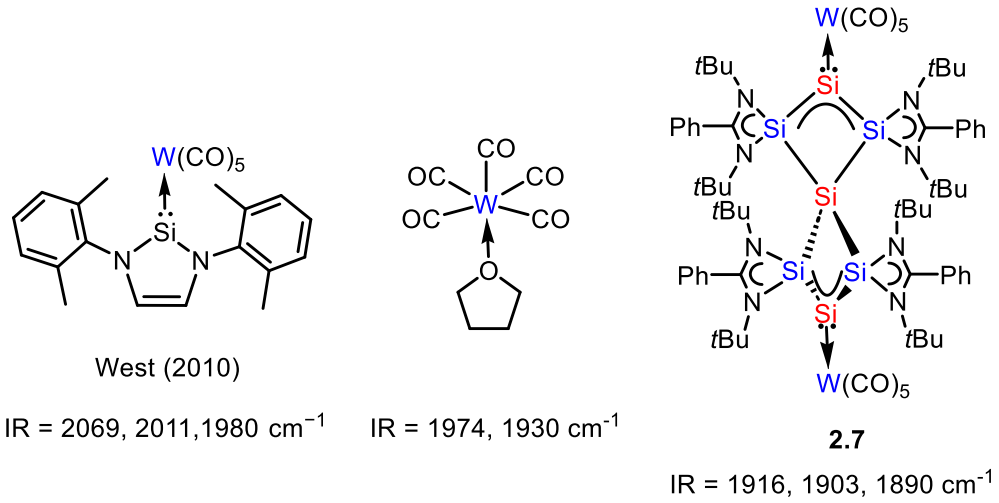

Scheme 2.8 Comparison of IR frequencies between **2.7**, $W(CO)_5$·THF and West's NHSi-$W(CO)_5$.

Attempts were made to react **2.4** with other transition metal Lewis acids to further probe its Lewis basicity. However, reaction with metal halides, such as $[(cod)RhCl]_2$, resulted in immediate decomposition of **2.4** to give the monochlorosilylene LSiCl (L= $PhC(N^tBu)_2$) and an intractable mixture. Reacting **2.4** with chalcogenides was not as trivial as previously thought, and gave complex mixtures that have thus far resisted purification.

2.3 Conclusion

In conclusion, we described the successful synthesis of the heavier analogue of spiro[3.3]hepta-1,2,5,6-tetraene, spiroheptasiladione complex **2.4**. Its structure is remarkable for a number of reasons. First, the spiro[3.3]hepta-1,2,5,6-tetraene scaffold has yet to be synthesized, with complex **2.4** serving as the first synthetic example of any complex bearing such a structure. Second, complex **2.4** can also be considered as the first bis-silylone, based on Frenking's model for heavier bent allenes described in the Introduction chapter, bearing two simultaneous silicon(0) centers that are physically separated within the same molecule. Last, the central seven-atom silicon cluster at the core of complex **2.4** is itself a unique structure seldom observed in the cluster chemistry of semi-metals such as silicon. Its ability to act as a strong Lewis base donor was demonstrated in its reaction to form complex **2.7**, simultaneously demonstrating a lack of proton termination on the central silicon atom.

The synthesis of tetrasilacyclobutadiene **2.5** and ylide **2.6** have allowed us to further probe the mechanism behind the formation of complex **2.4**, providing greater insight into the formation of such complexes which could provide new direction in the synthesis of similar complexes. Investigation of further reactivities of all complexes is not included due to time constraints but are currently underway.

2.4 Experimental Procedures

General Procedures. All manipulations were carried out under an inert atmosphere of argon gas by standard Schlenk techniques. Toluene was dried over and distilled over Na/k alloy prior to use. [LSi:]$_2$ (**1.51**, L = PhC(N*t*Bu)$_2$),[26] LSiCl[66] and $(Me_3P)_2SiCl_4$[27] were prepared according to the literature procedures. C_6D_6 and THF-d_8 was dried and distilled over K metal. The NMR spectra were recorded on a JEOL ECA 400 spectrometer and Bruker 400 spectrometer. High resolution mass spectrometry was performed by the Division of Chemistry and Biological Chemistry, Nanyang Technological University using a Waters Q-tof Premier mass spectrometer. Melting points were measured in sealed glass tubes and were not corrected.

Reduction of $(Me_3P)_2SiCl_4$ with KC_8 and 1.51: Toluene (20 mL), chilled to -78 ˚C, was added to a mixture of [LSi:]$_2$ **1.51** (L = PhC(N*t*Bu)$_2$) (519 mg, 1.0 mmol), $(Me_3P)_2SiCl_4$ (161 mg, 0.5 mmol) and KC_8 (283 mg, 2.1 mmol) at-78 ˚C. The resulting mixture was stirred for 18 hours at 8˚C to afford a mixture of a dark red suspension. The reaction mixture was filtered and residue was washed with pentane (3 x 10 mL) and extracted with hexane/benzene (1:1, 2 x 20 mL). The extracts were concentrated to 2 mL and left to stand overnight to afford **2.4** as red block crystals in 6.3% yield (12 mg).

Further extraction of the residue with toluene (2 x 20 mL) gave a purple solution. The solution was concentrated by half and left to stand overnight to afford tetrasilacyclobutadiene **2.5** as black block crystals in 1.8% yield (5 mg).

The filtrate was dried and extracted with pentane (1 x 20 mL). The red solution obtained was filtered and concentrated to a third of its volume and left to stand overnight at room temperature to afford dark red block crystals of ylide **2.6**. Yield: 54 mg (22.8 %).

Compound **2.4:** Mp: 248.9 °C (decomposed). ^{1}H NMR (395.9 MHz, 24 °C, C_6D_6, ppm): δ = 1.67 (s, 72H, *t*Bu), 6.93-6.96 (m, 2H), 6.97-6.99 (m, 2H), 6.99-7.02, (m, 3H), 7.05-7.09 (m, 3H), 7.29-7.36 (m, 8H); ^{13}C{^{1}H} NMR (100.5 MHz, c_6D_6, 25°C): d = 32.3 (C*Me*$_3$), 55.4 (*C*Me$_3$), 127.0, 128.8, 129.4, 134.6 (Ph), 166.9 (NCN) ppm; ^{29}Si NMR (160.5 MHz, 24 °C, C_6D_6, ppm): δ = -8.5 (spiro Si), -7.5 (terminal Si) 31.5 (amidinate Si). HRMS (ESI), *m/z* calcd: 1120.5830 $[M+H]^+$; found: 1120.5842.

Compound **2.5:** Mp: 159.8 °C (decomposed). ^{1}H NMR (395.9 MHz, 24 °C, C_6D_6, ppm): δ = 1.22 (s, 36H, *t*Bu), 1–43 (s, 36H, *t*Bu), 7.01 - 7.09 (m, 18H, Ar-*H*), 7.31 – 7.37 (m, 2H, Ar-*H*); ^{1}H NMR (395.9 MHz, 24 °C, d_5-pyridine, ppm): δ = 1.16 (s, 36H, *t*Bu), 1.59 (s, 36H, *t*Bu), 7.30 – 7.49 (m, 20H, Ar-*H*); ^{13}C{^{1}H} NMR (100.5 MHz, d_5-pyridine, 25°C): d = 29.3, 33.0 (C*Me*$_3$), 51.4, 53.0 (*C*Me$_3$), 125.8, 128.0, 128.1, 128.7, 128.7, 129.4, (Ph), 140.9, 153.8 (NCN) ppm; ^{29}Si NMR (160.5 MHz, 24 °C, C_6D_6, ppm): δ = -7.9 (three-coordinate Si), 40.9 (four-coordinate Si). HRMS (ESI), *m/z* calcd: 1064.6293 $[M+H]^+$; found: 1064.6291.

Compound **2.6:** Mp: 277.3 °C (decomposed). ^{1}H NMR (395.9 MHz, 24 °C, C_6D_6, ppm): δ = 1.46 (s, 18H), 1.51 (s, 36H), 1.72 (brs, 18H), 6.87-7.08 (m, 10H), 7.22-7.28 (m, 5H), 7.36-7.41 (m, 3H), 7.77-7.79 (m, 2H); ^{13}C{^{1}H} NMR (100.5 MHz, C_6D_6, 25°C): d = 14.60, 23.06, 32.35, 33.05, 33.11, 34.77 (C*Me*$_3$), 53.11, 55.24 (*C*Me$_3$), 127.00, 127.16, 127.74, 127.89, 129.19, 129.24, 129.88, 130.18, 130.67, 131.27, 132.17, 134.73, 136.60,

145.06 (*C*-Ar), 149.06, 160.15, 168.53 (N*C*N); ^{29}Si NMR (160.5 MHz, 24 °C, C_6D_6, ppm): δ = -163.2 (LSi*Si*Si), -97.4 (Si*Si*N^{t}Bu), 58.8 (LSiSi*Si*), 101.7(L*Si*SiSi). HRMS (ESI), *m/z* calcd: 1092.6064 $[M+H]^+$; found: 1092.6061.

Alternative synthesis of 2.5:

Toluene (70 mL) was added to LSiCl (591 mg, 2.0 mmol) and KC_8 (433 mg, 3.2 mmol) at room temperature. The mixture was immediately placed into a preheated oil-bath at 120 ˚C and stirred under reflux for 16 hrs. The deep purple mixture was filtered hot and left to cool overnight to yield black block-like crystals of **2.5** in 14 % yield (51 mg).

Alternative synthesis of 2.6:

Cold toluene (40 mL) was added to a 100 mL Schlenk flask containing LSi-SiL (260 mg, 0.5 mmol), $(PMe_3)_2SiCl_4$ (53.7 mg, 0.17 mmol) and KC_8 (135 mg, 1.0 mmol) at -78°C. The flask was warmed to -40°C and stirred for 16 h. The flask was allowed to warm up slowly to room temperature and stirred for 24 h. The reaction mixture was filtered, and all volatiles were removed. The solids were extracted with pentane (8 mL) to give a dark red solution. The solution was kept for 4 days at room temperature to afford dark red needles of **2.6** (new Si4) in 21% yield (37 mg).

Synthesis of compound 2.7:

Tungsten hexacarbonyl (13.1 mg, 0.037 mmol) was dissolved in tetrahydrofuran (20 mL) at room temperature and irradiated for approx. 24 hrs with a 15W UV bulb with

periodic degassing. FT-IR spectra of the solution was taken to ascertain complete formation of $W(CO)_5$•THF. The bright yellow solution was completely added to **2.4** (21 mg, 0.019 mmol) at room temperature to give a deep orange-red solution. After stirring for 16 hours, the reaction mixture was filtered, concentrated to a third of its original volume. Orange-red crystals of **2.7** (16 mg, 0.008 mmol, 47.5%) was isolated after standing the mixture overnight.

Compound **2.7:** Mp: 173.6°C (decomposed). ^{1}H NMR (395.9 MHz, 24 °C, THF-d_8, ppm): δ= 1.54 (s, 72H), 7.17 (dt, J = 7.6, 1.6 Hz, 4H), 7.42-7.50 (m, 4H), 7.50-7.59 (m, 8H), 7.62 (dt, J = 7.5, 1.7 Hz, 4H), ^{13}C{^{1}H} NMR (100.5 MHz, THf-d_8, 25°C): d = 32.4 (C*Me*$_3$), 57.0 (*C*Me$_3$), 127.1, 129.1, 129.5, 130.0, 131.2, 133.5 (Ph), 173.2 (NCN), 202.7 (cis-CO) ppm; ^{29}Si NMR (160.5 MHz, 24 °C, THF-d_8, ppm): δ = -87.9 (spiro Si), -27.6 (terminal Si), 28.2(amidinate Si). FT-IR (CaF liquid cell, THF, cm^{-1}): 2036, 1916, 1903, 1887. HRMS (ESI), *m/z* calcd: 1768.4340 [$M+H$]$^{+}$; found: 1768.4336.

Solid-State NMR and Discussion

Methodology

Solid State NMR experiments for compound **2.4** were conducted at 11.7 T (υ_0 (^{29}Si) = 99.33 MHz) on a 500 MHz JEOL NMR spectrometer (JNM-ECZL500G) and equipped with a 3.2 mm double-resonance HXMAS probe (JEOL Ltd., Tokyo, Japan). CPMAS pulse sequences with high power proton decoupling, ^{1}H pulse lengths of 2.7 μs (determined on adamantane$_{(s)}$) and recycle delays of 20 s were utilized. The ^{29}Si(^{1}H) CPMAS was acquired at one MAS frequencies of 12 KHz. The ^{29}Si data was data referenced with respect to $Me_4Si_{(aq)}$ (δ_{iso} = 0 ppm).

Solid state NMR experiments in this study for compound **2.5** were completed on a Bruker Avance III HD 600 MHz spectrometer with a Bruker 4 mm HXY MAS probe. Spectral processing and simulation of NMR spectra was achieved via the *Topspin* software package. The ^{29}Si and ^{13}C NMR experiments were completed at 14.1 T (υ_0 (^{29}Si) = 119.24 MHz; υ_0 (^{13}C) = 150.92 MHz) utilising CPMAS pulse sequences with high power proton decoupling, ^{1}H pulse lengths of 2.7 μs (determined on adamantane$_{(s)}$) and recycle delays of 3 s.

The ^{29}Si(^{1}H) CPMAS experiments utilised a contact pulse length of 4500 s (optimised on kaolinite$_{(s)}$) and was acquired with an MAS frequency of 14 KHz. The ^{29}Si data was data referenced with respect to $Me_4Si_{(aq)}$ (δ_{iso} = 0 ppm). The ^{13}C(^{1}H) CPMAS experiment utilised a contact pulse length of 6000 s (optimised on adamantane$_{(s)}$) with an MAS frequency of 12 KHz and resulting data was referenced with respect to adamantane$_{(s)}$ (δ_{iso} = 38.48, 40.49 ppm).

X-ray Data Collection and Structural Refinement.

Intensity data for all compounds were collected by using a Bruker APEX II diffractometer. The structures were solved by direct-phase determination (SHELXS-97) and refined for all data by full-matrix least-squares methods on F^2.[68] All non-hydrogen atoms were subjected to anisotropic refinement. The hydrogen atoms were generated geometrically and allowed to ride on their respective parent atoms; they were assigned appropriate isotopic thermal parameters and included in the structure-factor calculations. All non-hydrogen atoms were refined with anisotropic thermal parameters.

Theoretical studies

Computational Methodology.

All the calculations were performed using the Gaussian16 program package.[69] The geometries of compounds **2.4**, **2.5** and **2.6** were optimized using M06-2X[70] with def2-SVP[71] basis set.[72] The optimized geometry of compounds **2.4**, **2.5** and **2.6** is consistent with the X-ray crystallographic data. The Natural Bond Orbital Analysis (NBO) [73] has been carried out at M06-2X/def2-SVP level of theory for Natural Population Analysis (NPA)[74] and Wiberg Bond indices (WBI)[75]. Quantom Theory of Atoms-in-Molecules (QTAIM)[76] analysis of compound **2.4** was performed using MultiWfn[77] program suite at M06-2X/def2-SVP level of theory. Frequency calculations for the synthesis of compound **2.4**, intermediates, transition states and related products **2.5** and **2.6** were carried out at the M06-2X-D3(BJ)/def2-SVP level of theory with empirical dispersion corrections of Grimme (D3) [78] with Becke-Johnson (BJ) damping.[79] NMR analysis of DFT calculations were performed at SO-ZORA-BP86/TZP levels[80-87] using the ADF system.[88,89]

References

1. Moss, G. P. Extension and Revision of the Nomenclature for Spiro Compounds *Pure Appl. Chem.* **1999**, *71*, 531-558.
2. Carreira, E. M.; Fessard, T. C. Four-membered Ring-Containing Spirocycles: Synthetic Strategies and Opportunities *Chem. Rev.* **2014**, *114*, 8257-8322.
3. Lovering, F.; Bikker, J.; Humblet, C. Escape from Flatland: Increasing Saturation as an Approach to Improving Clinical Success *J. Med. Chem.* **2009**, *52*, 6752-6756.
4. Minkin, V. I. Photo-, Thermo-, Solvato-, and Electrochromic Spiroheterocyclic Compounds *Chem. Rev.* **2004**, *104*, 2751-2776.
5. Aho, J. E.; Pihko, P. M.; Rissa, T. K. Nonanomeric Spiroketals in Natural Products: Structures, Sources, and Synthetic Strategies *Chem. Rev.* **2005**, *105*, 4406-4440.
6. Galliford, C. V.; Scheidt K. A. Pyrrolidinyl-Spirooxindole Natural Products as Inspirations for the Development of Potential Therapeutic Agents *Angew. Chem., Int. Ed.* **2007**, *46*, 8748-8758.
7. Trost, B. M.; Brennan, M. K. Asymmetric Syntheses of Oxindole and Indole Spirocyclic Alkaloid Natural Products *Synthesis* **2009**, *18*, 3003-3025.
8. Ding, A.; Meazza, M.; Guo, H.; Yang, J. W.; Rios, R. New Development in the Enantioselective Synthesis of Spiro Compounds. *Chem. Soc. Rev.* **2018**, *47*, 5946– 5996.
9. Dampalla, C. S.; Rathnayake, A. D.; Galasiti Kankanamalage, A. C.; Kim, Y.; Perera, K. D.; Nguyen, H. N.; Miller, M. J.; Madden, T. K.; Picard, H. R.; Thurman, H. A.; Kashipathy, M. M.; Liu, L.; Battaile, K. P.; Lovell, S.; Chang, K.-O.; Groutas, W. C. Structure-Guided Design of Potent Spirocyclic

Inhibitors of Severe Acute Respiratory Syndrome Coronavirus-2 3C-like Protease. *J. Med. Chem.* **2022**, *65*, 7818-7832.

10. Von Baeyer, A. Ueber Polyacetylenverbindungen *Ber. Dtsch. Chem. Ges.* **1885**, *18*, 2269-2281.
11. Wiberg, K. B. The Concept of Strain in Organic Chemistry *Angew. Chem., Int. Ed.* **1986**, *25*, 312-322.
12. Simmons, H. E.; Fukunaga, T. Spiroconjugation *J. Am. Chem. Soc.* **1967**, *89*, 5208-5215.
13. Billups, W. E.; Haley, M. M. Spiropentadiene *J. Am. Chem. Soc.* **1991**, *113*, 5084-5085.
14. Saini, R. K.; Litosh, V. A.; Daniels, A. A.; Billups, W. E. Synthesis and Characterisatio of 1,4-dichlorospiropentadiene *Tetrahedron Lett.* **1999**, *40*, 6157-6158.
15. Billups, W. E.; Litosh, V. A.; Saini, R. K.; Daniels, A. D. Synthesis of Oxaspiropentene *Org. Lett.* **1999**, *1*, 115-116.
16. Tian, X.; Bo, X.-X.; Ding, Y.-H. All-nitrogen Spiropentadiene – N_5^+ *J. Chem. Phys.* **2021**, *155*, 174304.
17. Power, P. P. Main-group elements as transition metals. *Nature* **2010**, *463*, 171– 177.
18. Kutzelnigg, W. Chemical Bonding in Higher Main Group Elements. *Angew. Chem., Int. Ed. Engl.* **1984**, *23*, 272– 295.
19. Naruse, Y.; Ma, J.; Takeuchi, K.; Nohara, T.; Inagaki, S. π-Relaxation of the ring strain: design of polycyclic unsaturated silicon molecules *Tetrahedron* **2006**, *62*, 4491-4497.

20. Bande, A.; Michl, J. Conformational Dependence of σ-Electron Delocalization in Linear Chains: Permethylated Oligosilanes. *Chem. - Eur. J.* **2009**, *15*, 8504– 8517.

21. Miller, R. D.; Michl, J. Polysilane high polymers. *Chem. Rev.* **1989**, *89*, 1359– 1410.

22. Iwamoto, T.; Tamura, M.; Kabuto, C.; Kira, M. A Stable Bicyclic Compound with Two Si = Si Double Bonds. *Science* **2000**, *290*, 504.

23. Guo, Y.; Xia, Z.; Liu, J.; Yu, J.; Yao, S.; Shi, W.; Hu, K.; Chen, S.; Wang, Y; Li, A.; Driess, M.; Wang, W. A Tetra-amido-Protected Ge_5-Spiropentadiene *J. Am. Chem. Soc.* **2019**, *141*, 19252-19256.

24. Tonner R.; Frenking, G. C(NHC)2: Divalent Carbon(0) Compounds with N-Heterocyclic Carbene Ligands—Theoretical Evidence for a Class of Molecules with Promising Chemical Properties *Angew. Chem., Int. Ed.* **2007**, 8695-8698.

25. Dyker, C. A.; Lavallo, V.; Donnadieu, B.; Bertrand, G. Synthesis of an Extremely Bent Acyclic Allene (A "Carbodicarbene"): A Strong Donor Ligand *Angew. Chem., Int. Ed.* **2008**, *47*, 3206-3209.

26. Sen, S. S.; Jana, A.; Roesky, H. W.; Schulzke, C. A Remarkable Base-Stabilized Bis(silylene) with a Silicon(I)-Silicon(I) Bond *Angew. Chem., Int. Ed.* **2009**, *48*, 8536-8538.

27. Levason, W.; Pugh, D.; Reid, G. Phosphine and diphosphine complexes of silicon(IV) halides *Inorg. Chem.* **2013**, *52*, 5185– 5193.

28. Ishida, S.; Iwamoto, T.; Kabuto, C.; Kira, M. A Stable Silicon-based Allene Analogue with a Formally sp-Hybridized Silicon Atom *Nature* **2003**, *421*, 725– 727.

29. Iwamoto, T.; Masuda, H.; Kabuto, C.; Kira, M. Trigermaallene and 1,3-Digermasilaallene *Organometallics* **2005**, *24*, 197– 199.
30. Iwamoto, T.; Abe, T.; Kabuto, C.; Kira, M. A Missing Allene of Heavy Group 14 Elements: 2-germadisilaallene *Chem. Commun.* **2005**, *41*, 5190-5192.
31. Kira, M.; Iwamoto, T.; Ishida, S.; Masuda, H.; Abe, T.; Kabuto, C. Unusual Bonding in Trisilaallene and Related Heavy Allenes *J. Am. Chem. Soc.* **2009**, *131*, 17135– 17144
32. Mondal, K. C.; Roesky, H. W.; Schwarzer, M. C.; Frenking, G.; Niepötter, B.; Wolf, H.; Herbst-Irmer, R.; Stalke, D. A Stable Singlet Biradicaloid Siladicarbene: $(L:)_2Si$ *Angew. Chem., Int. Ed.* **2013**, *52*, 2963-2967.
33. Xiong, Y.; Yao, S.; Inoue, S.; Epping, J. D.; Driess, M. A Cyclic Silylone ("Siladicarbene") with an Electron-Rich Silicon(0) Atom *Angew. Chem., Int. Ed.* **2013**, *52*, 7147-7150.
34. Xiong, Y.; Yao, S.; Tan, G.; Inoue, S.; Driess, M. A Cyclic Germadicarbene ("Germylone") from Germyliumylidene *J. Am. Chem. Soc.* **2013**, *135*, 5004-5007.
35. Zhou, Y. P.; Karni, M.; Yao, S.; Apeloig, Y.; Driess, M. A Bis(silylenyl)pyridine Zero-Valent Germanium Complex and Its Remarkable Reactivity. *Angew. Chem., Int. Ed.* **2016**, *55*, 15096– 15099.
36. Sugahara, T.; Sasamori, T.; Tokitoh, N. Highly Bent 1,3-Digerma-2-silaallene *Angew. Chem. Int. Ed.* **2017**, *56*, 9920-9923.
37. Wang, Y.; Karni, M.; Yao, S.; Kaushansky, A.; Apeloig, Y.; Driess, M. Synthesis of an Isolable Bis(silylene)-Stabilized Silylone and Its Reactivity Toward Small Gaseous Molecules. *J. Am. Chem. Soc.* **2019**, *141*, 12916–12927,

38. Keuter, J.; Hepp, A.; Mück-Lichtenfeld, C.; Lips, F. Facile Access to an NHC-Coordinated Silicon Ring Compound with a Si═N Group and a Two-Coordinate Silicon Atom. *Angew. Chem., Int. Ed.* **2019**, *58*, 4395– 4399.
39. Wang, Y.; Karni, M.; Yao, S.; Apeloig, Y.; Driess, M. An Isolable Bis(silylene)-Stabilized Germylone and Its Reactivity. *J. Am. Chem. Soc.* **2019**, *141*, 1655– 1664.
40. Yao, S.; Kostenko, A.; Xiong, Y.; Ruzicka, A.; Driess, M. Redox Noninnocent Monoatomic Silicon(0) Complex ("Silylone"): Its One-Electron-Reduction Induces an Intramolecular One-Electron-Oxidation of Silicon(0) to Silicon(I). *J. Am. Chem. Soc.* **2020**, *142*, 12608– 12612.
41. Yao, S.; Kostenko, A.; Xiong, Y.; Lorent, C.; Ruzicka, A.; Driess, M. Changing the Reactivity of Zero- and Mono-Valent Germanium with a Redox Non-Innocent Bis(silylenyl)carborane Ligand. *Angew. Chem., Int. Ed.* **2021**, *60*, 14864– 14868.
42. Koike, T.; Nukazawa, T.; Iwamoto, T. Conformationally Switchable Silylone: Electron Redistribution Accompanied by Ligand Reorientation around a Monatomic Silicon *J. Am. Chem. Soc.* **2021**, *143*, 14332-14341.
43. Boudjouk, P.; Sooriyakumaran, R. The Synthesis of the First Spiropentasilane, Octamethylsiropentasilane *J. Chem. Soc., Chem. Commun.* **1984**, *12*, 777– 778.
44. Hlina, J.; Mechtler, C.; Wagner, H.; Baumgartner, J.; Marschner, C. Multiple Silyl Exchange Reactions: A Way to Spirooligosilanes *Organometallics* **2009**, *28*, 4065-4071.
45. Iwamoto, T.; Furiya, Y.; Kobayashi, H.; Isobe, H.; Kira, M. Synthesis and Facile Ring Expansion of Silylenecyclotetrasilane. *Organometallics* **2010**, *29*, 1869– 1872.

46. Klapötke, T. M.; Vasisht, S. K.; Mayer, P. Spirocycle (Si*t*Bu$_3$)$_6$Si$_9$Cl$_2$: The First of Its Kind among Group 14 Elements. *Eur. J. Inorg. Chem.* **2010**, 3256– 3260.
47. Tsurusaki, A.; Kamiyama, J.; Kyushin, S. Tetrasilane-Bridged Bicyclo[4.1.0]heptasil-1(6)-ene. *J. Am. Chem. Soc.* **2014**, *136*, 12896– 12898.
48. Zhao, Y.; Truhlar, D. G. The M06 Suite of Density Functionals for Main Group Thermochemistry, Thermochemical Kinetics, Noncovalent Interactions, Excited States, and Transition Elements: Two New Functionals and Systematic Testing of Four M06-class Functionals and 12 Other Functionals *Theor Chem Acc.* **2008**, *120*, 215–241.
49. Weigend, F.; Ahlrichs, R. Balanced Basis Sets of Split Valence, Triple Zeta Valence and Quadruple Zeta Valence Quality for H to Rn: Design and Assessment of Accuracy *Phys. Chem. Chem. Phys.* **2005**, *7*, 3297-3305.
50. Foster, J. P.; Weinhold, F. Natural Hybrid Orbitals *J. Am. Chem. Soc.* **1980**, *102*, 7211-7218.
51. Reed, A. E.; Weinhold, F. Natural Bond Orbital Analysis of Near-Hartree–Fock Water Dimer *J. Chem. Phys.* **1983**, *78*, 4066– 4073.
52. Reed, A. E.; Curtiss, L. A.; Weinhold, F. Intermolecular Interactions from a Natural Bond Orbital, Donor-Acceptor Viewpoint *Chem. Rev.* **1988**, *88*, 899-926.
53. Wiberg, K. B. Application of the Pople-Santry-Segal CNDO Method to the Cyclopropylcarbinyl and Cyclobutyl Cation and to Bicyclobutane *Tetrahedron* **1968**, *24*, 1083– 1096.

54. Harper, L. K.; Shoaf, A. L.; Bayse, C. A. Predicting Trigger Bonds in Explosive Materials through Wiberg Bond Index Analysis *ChemPhysChem* **2015**, *16*, 3886-3892.

55. Mayer, I. Bond Order and Valence Indices: a Personal Account *J. Comput. Chem.* **2007**, *28*, 204-221.

56. Suzuki, K.; Matsuo, T.; Hashizume, D.; Fueno, H.; Tanaka, K.; Tamao, K. A planar rhombic charge-separated tetrasilacyclobutadiene *Science* **2011**, *331*, 1306– 1309.

57. Inoue, S.; Epping, J. D.; Irran, E.; Driess, M. Formation of a donor-stabilized tetrasilacyclobutadiene dication by a Lewis acid assisted reaction of an N-heterocyclic chloro silylene *J. Am. Chem. Soc.* **2011**, *133*, 8514– 8517.

58. Zhang, S.-H.; Xi, H.-W.; Lim, K. H.; So, C.-W. An extensive n, π, σ-electron delocalized Si_4 ring *Angew. Chem., Int. Ed.* **2013**, *52*, 12364– 12367.

59. Sun, X.; Simler, T.; Yadav, R.; Köppe, R.; Roesky, P. W. A Stable Aromatic Tetrasilacyclobutadiene Dication *J. Am. Chem. Soc.* **2019**, *141*, 14987-14990.

60. Schmedake, T. A.; Haaf, M.; Paradise, B. J.; Millevolte, A. J.; Powell, D. R.; West, R. Electronic and Steric Properties of Stable Silylene Ligands in Metal(0) Carbonyl Complexes *J. Organomet. Chem.* **2001**, *636*, 17-25.

61. Takanashi, K.; Lee, V. Y.; Yokoyama, T.; Sekiguchi, A. Base-Free Molybdenum and Tungsten Bicyclic Silylene Complexes Stabilized by a Homoaromatic Contribution *J. Am. Chem. Soc.* **2009**, *131*, 916-917.

62. Krahfuß, M. J.; Nitsch, J.; Bickelhaupt, F. M.; Marder, T. B.; Radius, U. N-Heterocyclic Silylenes as Ligands in Transition Metal Carbonyl Chemistry: Nature of Their Bonding and Supposed Innocence *Chem. Eur. J.* **2020**, *26*, 11276-11292.

63. Guddorf, B. J.; Feldt, M.; Hepp, A.; Daniliuc, C. G.; Lips, F. Reactivity of an NHC-Coordinated Trisilacyclopropylidene with Transition Metal Carbonyl Compounds *Organometallics* **2020**, *39*, 4387-4394.

64. Xiong, Y.; Yao, S.; Müller, R.; Kaupp, M; Driess, M. From Silylone to an Isolable Monomeric Silicon Disulfide Complex *Angew. Chem., Int. Ed.* **2015**, *54*, 10254-10257.

65. Zark, P.; Schäfer, A.; Mitra, A.; Haase, D.; Saak, W.; West, R.; Müller, T. Synthesis and reactivity of *N*-aryl substituted *N*-heterocyclic silylenes *J. Organomet. Chem.* **2010**, *695*, 398-408

66. So, C.-W.; Roesky, H.W.; Magull, J.; Oswald, R.B. Synthesis and Characterization of [PhC(NtBu)2]SiCl: A Stable Monomeric Chlorosilylene *Angew. Chem. Int. Ed.* **2006**, *45*, 3948-3950

67. For the zwitterionic structure of other heavier cyclobutadiene analogues, see a) Yeong, H.-X.; Zhang, S.-H.; Xi, H.-W.; Guo, J.-D.; Lim, K. H.; Nagase, S.; So, C.-W. An Amidinate-Stabilized Germatrisilacyclobutadiene Ylide *Chem. - Eur. J.* **2012**, *18*, 2685-2691; b) Yeong, H.-X.; Xi, H.-W.; Li, Y.; Kunnappilly, S. B.; Chen, B.; Lau, K.-C.; Hirao, H.; Lim, K. H.; So, C.-W.; Zwitterionic Base-Stabilized Digermadistannacyclobutadiene and Tetragermacyclobutadiene *Chem. - Eur. J.* **2013**, *19*, 14726-14731.

68. Sheldrick, G. M. SADABS V2014/4 (Bruker AXS Inc.) University of Göttingen, Göttingen, Germany, **2014**.

69. Frisch, M. J.; Trucks, G. W.; Schlegel, H. B.; Scuseria, G. E.; Robb, M. A.; Cheeseman, J. R.; Scalmani, G.; Barone, V.; Mennucci, B.; Petersson, G. A.; Nakatsuji, H.; Caricato, M.; Li, X.;H. P. Hratchian, H. P.; Izmaylov, A. F.; Bloino, J.; Zheng, G.; Sonnenberg, J. L.; Hada, M.; Ehara, M.; Toyota, K.;

Fukuda, R.; Hasegawa, J.; Ishida, M.; Nakajima, T.; Honda, Y.; Kitao, O.; Nakai, H.; Vreven, T.; Montgomery, J. A., Jr.; Peralta, J. E.; Ogliaro, F.; Bearpark, M.; Heyd, J. J.; Brothers, E.; Kudin, K. N.; Staroverov, V. N.; Keith, T.; Kobayashi, R.; Normand, J.; Raghavachari, K.; Rendell, A.; Burant, J. C. Iyengar, S. S.; Tomasi, J.; Cossi, M.; Rega, N.; Millam, J. M.; Klene, M.; Knox, J. E.; Cross, J. B.; Bakken, V.; Adamo, C.; Jaramillo, J.; Gomperts, R.; Stratmann, R. E.; Yazyev, O.; Austin, A. J.; Cammi, R.; Pomelli, C.; Ochterski, J. W.; Martin, R. L.; Morokuma, K.; Zakrzewski, V. G.; Voth, G. A.; Salvador, P.; Dannenberg, J. J.; Dapprich, S.; Daniels, A. D.; Farkas, O.; Foresman, J. B.; Ortiz, J. V.; Cioslowski, J.; Fox, D. J. Gaussian 09 (Revision B.01), Gaussian, Inc., Wallingford CT, **2010**.

70. Zhao, Y.; Truhlar, D. G. *Theor. Chem. Acc.* **2008**, *120*, 215-241.
71. Weigend, F.; Hser, M.; Patzelt, H.; Ahlrichs, R. *Chem. Phys. Lett.* **1998**, *294*, 143.
72. a) Krishnan, R.; Binkley, J. S.; Seeger, R.; Pople, J. A. *J. Chem. Phys.* **1980**, *72*, 650-654; b) McLean, A. D.; Chandler, G. S. *J. Chem. Phys.* **1980**, *72*, 5639-5648; c) Curtiss, L. A.; McGrath, M. P.; Blandeau, J.-P.; Davis, N. E.; Binning, R. C., Jr.; Radom, L. *J. Chem. Phys.* **1995**, *103*, 6104-6113.
73. a) Reed, A. E.; Curtiss, L. A.; Weinhold, F. *Chem. Rev.* **1988**, *88*, 899; b) Glendening, E. D.; Reed, A. E.; Carpenter, J. E.; Weinhold, F. NBO Version 5.9.
74. Reed, A. E.; Weinstock, R. B.; Weinhold, F. *J. Chem. Phys.* **1985**, *83*, 735.
75. Wiberg, K. B. *Tetrahedron* **1968**, *24*, 1083.
76. a) Bader, R. F. W. Atoms in Molecules - A Quantum Theory; Oxford University Press: Oxford, 1990; b) Jonas, V.; Frenking, G.; Reetz, M. T. *J. Am. Chem. Soc.* **1994**, *116*, 8741.

77. Lu, T.; Chen, F. J. *Mol. Graphics Modell*. **2012**, *38*, 314.

78. Grimme, S.; Antony, J.; Ehrlich, S.; Krieg, H. *J. Chem. Phys.* **2010**, *132*, 154104.

79. Grimme, S.; Ehrlich, S.; Goerigk, L. *J. Comput. Chem* **2011**, *32*, 1456.

80. van Lenthe, E.; Baerends, E. J.; Snijders, J. G. *J. Chem. Phys.* **1993**, *99*, 4597–4610.

81. Wolff, S. K.; Ziegler, T.; van Lenthe, E.; Baerends, E. J. *J. Chem. Phys.* **1999**, *110*, 7689– 7698.

82. van Lenthe, E.; Snijders, J. G.; Baerends, E. J. *J. Chem. Phys.* **1996**, *105*, 6505–6516.

83. Becke, A. D. *Phys. Rev. A: At., Mol., Opt. Phys.* **1988**, *38*, 3098– 3100.

84. Perdew, J. P. *Phys. Rev. B: Condens. Matter Mater. Phys.* **1986**, *33*, 8822– 8824.

85. Van Lenthe, E.; Baerends, E. J. *J. Comput. Chem.* **2003**, *24*, 1142– 1156.

86. Perdew, J. P.; Burke, K.; Ernzerhof, M. *Phys. Rev. Lett.* **1996**, *77*, 3865– 3868.

87. Bursch, M.; Gasevic, T.; Stückrath, J. B.; Grimme, S. *Inorg. Chem.* **2021** *60*, 272-285.

88. te Velde, G.; Bickelhaupt, F. M.; Baerends, E. J.; Fonseca Guerra, C.; van Gisbergen, S. J. A.; Snijders, J. G.; Ziegler, T. *J. Comput. Chem.* **2001**, *22*, 931– 967.

89. *ADF* 2019.303; SCM, Theoretical Chemistry, Vrije Universiteit: Amsterdam, The Netherlands, **2019**.

Chapter 3

Synthesis and isolation of a trigermanium(0) complex and its related compounds

---

Chapter 3 Synthesis of a Amidinato-Silylene-Supported Germanium Cluster

Chapter 3.1 Introduction

Ever since the advent of nanotechnology, the formation mechanism of monodisperse particles have been a subject of significant study. LaMer and Dinegar hypothesized the Critical Nucleation Theory (CNT) in 1950 as a general growth model for colloidal nanocluster formation, wherein monodispersed nanoparticles are formed through a burst nucleation step, with a near infinite rate of formation, followed by a slow step of diffusion-controlled Ostwald ripening resulting in growth in particle size over time.[1]

In 1994, Finke and co-workers synthesised polyoxoanion-stabilized iridium nanoparticles and observed nucleation rates that were gentler and more continuous than the near infinite rate described in CNT.[2] Further kinetic studies on this iridium system led to the development of an alternative growth model, namely the Finke-Watzky (FW) autocatalytic model, comprising two pseudoelementary steps: (i) a slow(rate-determining), continuous nucleation step and (ii) an autocatalytic surface growth step, where the precursor molecule is deposited directly on the surface of the critical nuclei resulting in a particle size growth.[3,4] This model was shown to better fit kinetics observed in the formation of transition metal nanoparticles, which are believed to

possess stronger interatomic interactions, as opposed to the thiol sol nanoparticles studied by LaMer in their seminal work which are expected to be weakly associating.[5,6]

In recent years, in tandem with the development of the FW model, there has been increasing evidence to support the formation of critical nuclei in the synthesis of strongly bonded nanoparticles.[7-11] Many of these oligoatomic nuclei, containing anywhere from 2 to 10 atoms, have been isolated in a range of transition and noble metal nanoparticle syntheses. Application of this kinetic model to the study of main group p-block element nanoparticles is still relatively in its infancy. There is, thus, significant value to capture, isolate and study any oligomeric main group elemental species that could potentially act as seeds for nanoparticle synthesis.

Silicon and germanium are of particular interest to us given their role in a wide range of semiconductor materials.[12] With the increasing importance of quantum dots,[13-16] there is a need to better understand the mechanism behind their synthesis. With this knowledge, more control over size, shape and composition can be granted to the industrial chemist. Computational studies have been carried out to predict the structure of a range of oligoatomic clusters.[17,18] They are expected to require electronic stabilization if they are to be isolated and handled under ambient laboratory conditions as many of them are metastable and prone to fragmentation and agglomeration.[17,19] To tackle this, strong Lewis base donors, namely N-heterocyclic carbenes and amidinato silylenes, were used to coordinate with main-group elements(0) to enhance their stability.[20-22] This approach resulted in the formation of remarkable monoatomic and diatomic main-group element complexes in recent years (Figure 3.1a).[22-38]

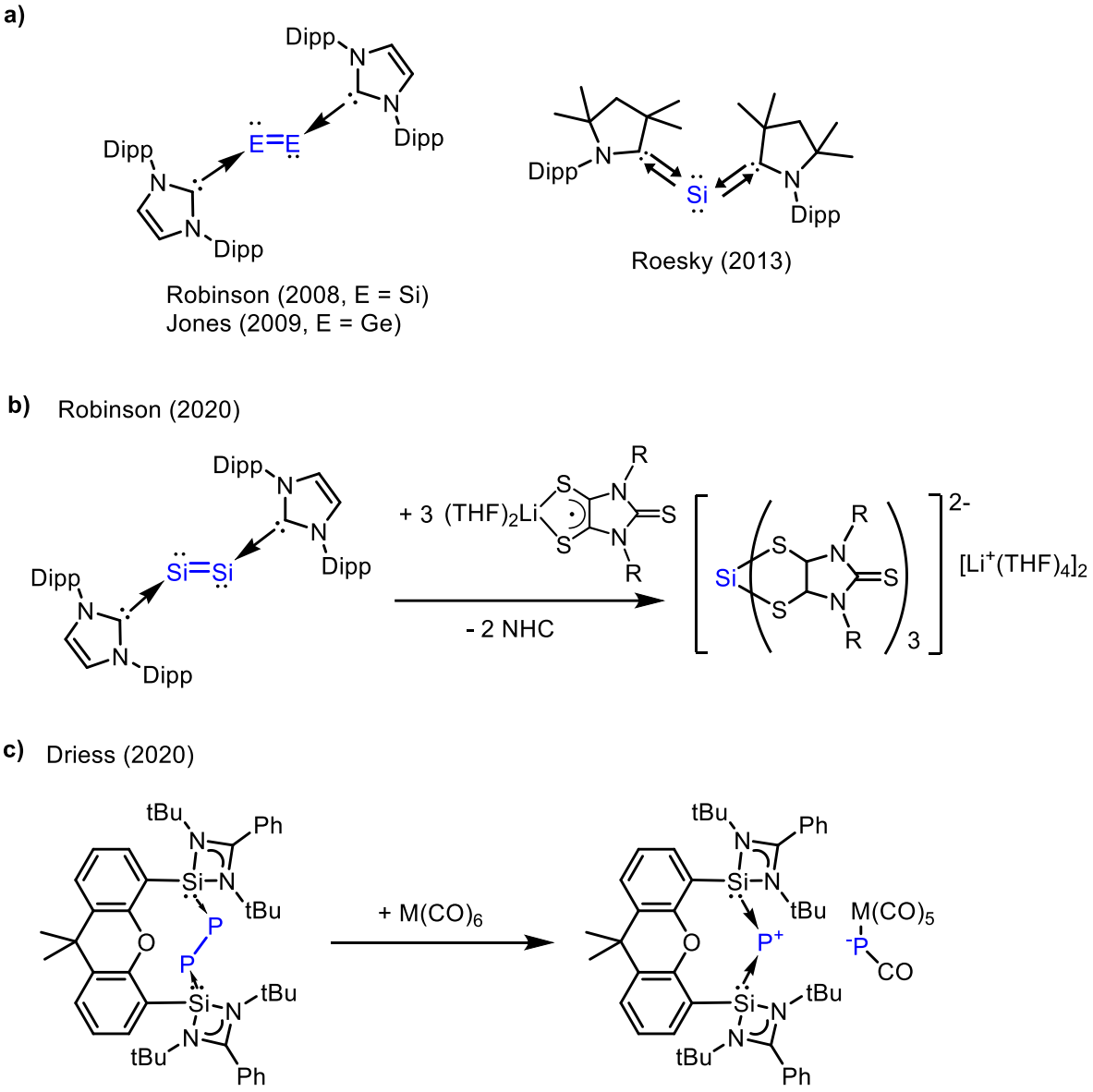

Scheme 3.1 a) Examples of NHC-monoatomic and diatomic main group element(0) complexes; b) functionalization of disilicon(0) with lithium dithiolene radical and c) abstraction of a monophosphide anion with $M(CO)_6$

In these complexes, the σ-donating and π-accepting properties, as well as the steric environment of Lewis base donors have a strong effect on the size, electronic property and reactivity of main-group element(0). The strong stabilization effect exerted by the Lewis base donors, however, leads to a dilemma- the release of the elemental species from the complexes, which is required for further functionalization and important if they are to be employed as critical nuclei, becomes exceedingly difficult,

requiring the crossing of a very high energy barrier or the presence of highly reactive substrates. Robinson, et al., reported that the NHC-disilicon(0) complex served as a silicon(0) transfer agent in its reaction with a highly reactive lithium dithiolene radical (Scheme 3.1b).[39] Driess, et al., showed that a strong donor, NHC and carbon monoxide is essential to mediate the abstraction of a monophosphorus anion from the bis(silylene)-diphosphorus(0) compound (Scheme 3.1c).[40]

Through the study of these spectacular examples, we are certain that each unique Lewis donor system employed allows to the isolation of one type of main-group element allotrope. Consequently, conversion from one form to another by changing Lewis donors should be possible. However, the strong confinement of monoatomic and oligoatomic main-group element allotrope by Lewis base donors inhibits transfer between allotropic species and thus prevents aggregation to form larger elemental systems.

We believe that the isolation of a main-group allotrope "seed" requires a Lewis base donor system that provides sufficient thermodynamic and kinetic stabilization, while also being sufficiently labile, such that it can be substituted, allowing the seed to aggregate. Such flexibility would allow for subsequent expansion or release of the main-group allotrope moiety. We have addressed this synthetic challenge by finding a series of Lewis donors that is able to balance both these attributes in the transfer and aggregation from diatom to nanoparticle.

Our group has previously isolated an amidinato amidosilylene-digermanium(0) complex **3.1** (Scheme 3.2).[41] We anticipated that the monodentate amidinato silylene while providing adequate thermodynamic and kinetic stabilization, is also being sufficiently labile; it could thus serve as a promising candidate in the transfer and aggregation of germanium allotropes in the presence of silylenes or other Lewis base

donors at ambient conditions. Herein, we report that the amidinato amidosilylene-digermanium(0) complex **3.1** transferred the digermanium(0) moiety to an amidinato disilyne **1.51**[42] to form a digermadisilacyclobutadiene **3.2**. Its dissociation into two bis(silylenyl)germylenes mediated the aggregation of the digermanium(0) moiety from compound **3.1** to form the bis(trigermanium(0)) complex **3.3** (Scheme 3.2). Further transfer and aggregation of the trigermanium(0) moiety resulted in the formation of germanium(0) nanoparticles.

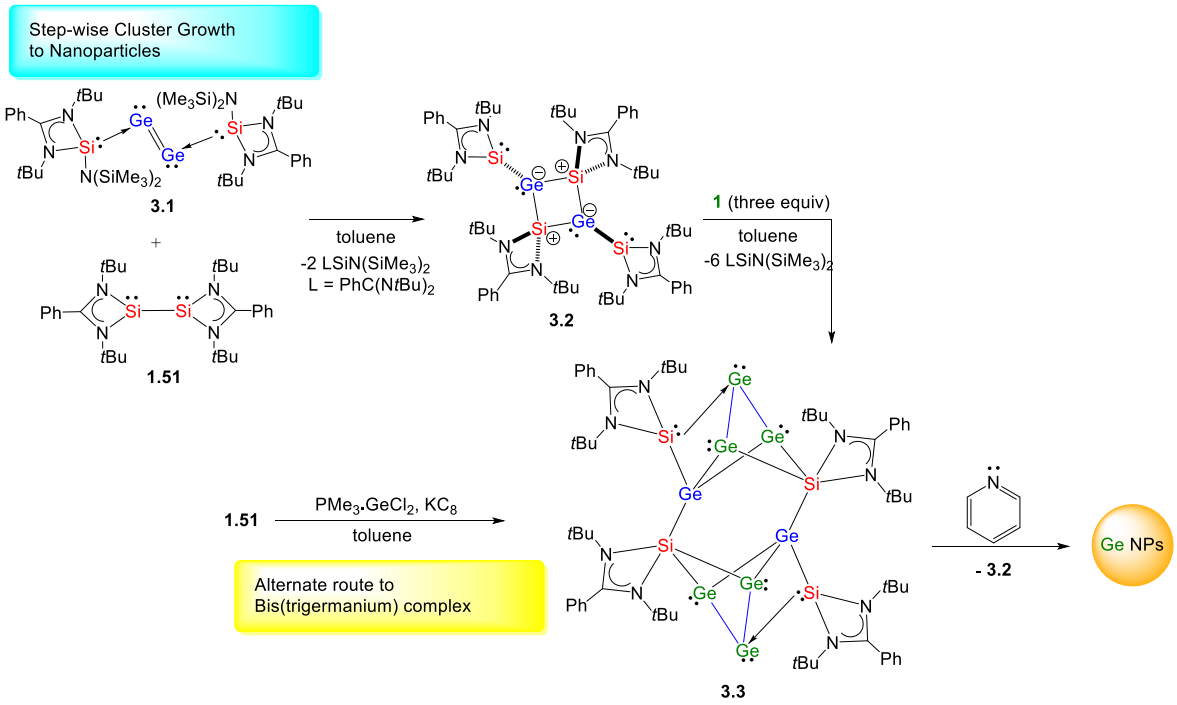

Scheme 3.2. Transfer and aggregation of germanium(0)

3.2 Results and Discussion

3.2.1 Transfer of digermanium(0) to the amidinato disilyne

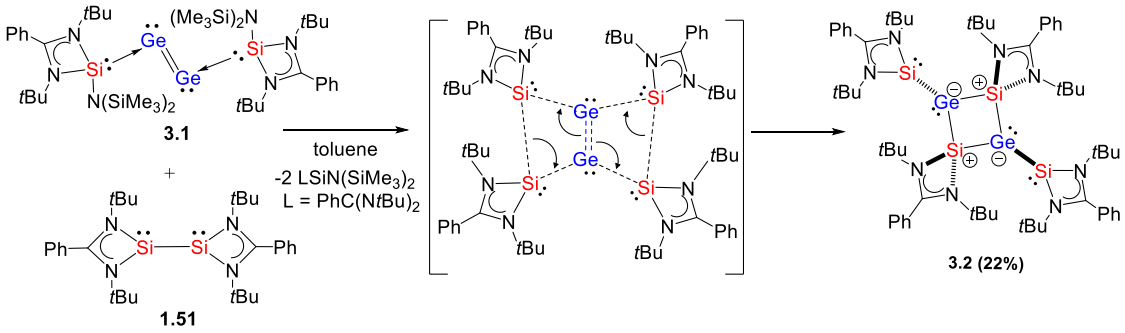

Scheme 3.3 Proposed mechanism for the formation of **3.2**

The amidinato disilyne compound[42] **1.51** was utilized to displace the amidinato amidosilylene ligand in compound **3.1**. Two equivalents of **1.51** was reacted with **3.1** in toluene at room temperature to afford a mixture of the amidinato digermadisilacyclobutadiene $[(LSi)_2Ge]_2$ (**3.2**, L = $PhC(NtBu)_2$) and amidinato amidosilylene $[LSiN(SiMe_3)_2]$. In this reaction, the amidinato amidosilylene ligand in **3.1** was displaced by compound **1.51**. The resulting digermanium(0) moiety did not coordinate with the Si donors of compound **3.1**, instead it underwent a double insertion with two Si^{I}-Si^{I} bonds of two molecules of **3.1** resulting in the cleavage of Ge=Ge double bond to form compound **3.2** (Scheme 3.3). The results support our hypothesis that compound **3.1** could act as a digermanium(0) transfer reagent. Additionally, compound **1.51** is able to trap the digermanium(0) moiety.

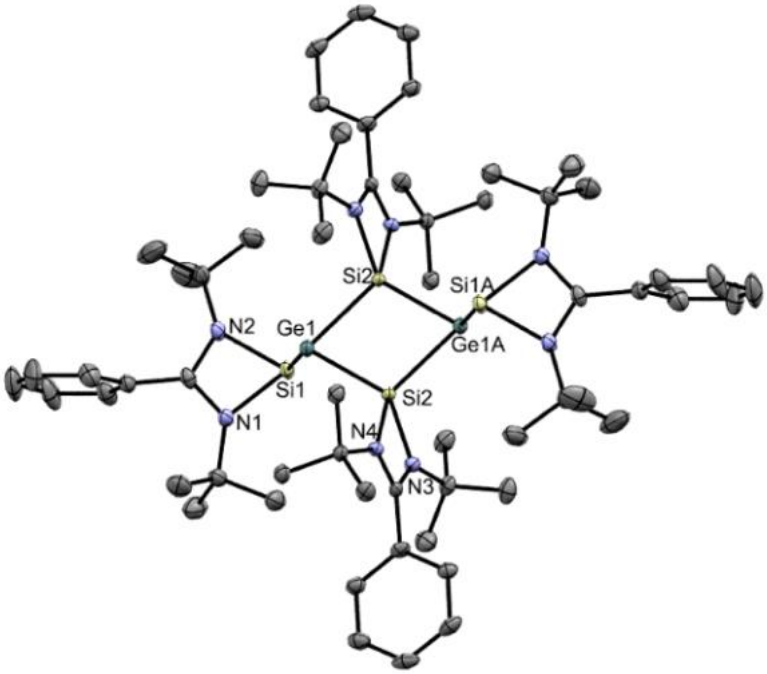

Figure 3.1 X-ray crystal structure of **3.2** (50% ellipsoids probability). Hydrogen atoms are omitted for clarity. Selected bond lengths (Å) and angles (º): Ge1-Si2 2.3852(11), Ge1-Si2A 2.3844(11), Ge1-Si1 2.4673(13), Ge1-Si2-Ge1A 106.82(4), Si2A-Ge1-Si2 73.18(4), Si2A-Ge1-Si1 109.50(4), Si2-Ge1-Si1 111.83(4), N1-Si1-N2 68.18(14), N1-Si1-Ge1 97.18(12), N2-Si1-Ge1 96.14(11)

Compound **3.2** was isolated as black blocks (Yield of crystals: 22%) from the concentrated reaction mixture. The $^{29}Si\{^{1}H\}$ NMR spectrum of **3.2** shows two signals at δ = -7.9 and 40.9 ppm corresponding to the three- and four-coordinate silicon centers, respectively. The molecular structure obtained from single-crystal X-ray diffraction studies shows that the Ge_2Si_2 core is planar and rhombic; the combined sum of internal bond angles adding up to 360º. The amidinate ligands remain bidentate coordinated to the Si2 and Si2A atoms, both adopting a distorted tetrahedral geometry. The Ge1-Si2 (2.3852(11) Å) and Ge1-Si2A bond lengths (2.3844(11) Å) are comparable to typical Si-Ge single bond lengths (2.356(4) – 2.510(2) Å).[43] As the four-membered ring is composed of single bonds, the Ge_2Si_2 core can be considered to possess a zwitterionic structure to account for the unsaturated Ge atoms. Both the Ge1 and exocyclic Si1 atoms

have three bond pairs, with average bond angles less than 107° (average bond angle around Ge: 98.2°, Si: 87.2°), which are consistent with a highly distorted trigonal pyrmidal geometry. This geometry is consistent with the presence of a single stereoactive lone pairs on each of the Ge atoms and exocyclic-silylene Si atoms. The extreme distortion of geometry can be attributed to the restrictions imparted by the 4-membered ring systems that Ge1 and Si1 are each a part of.

(a)

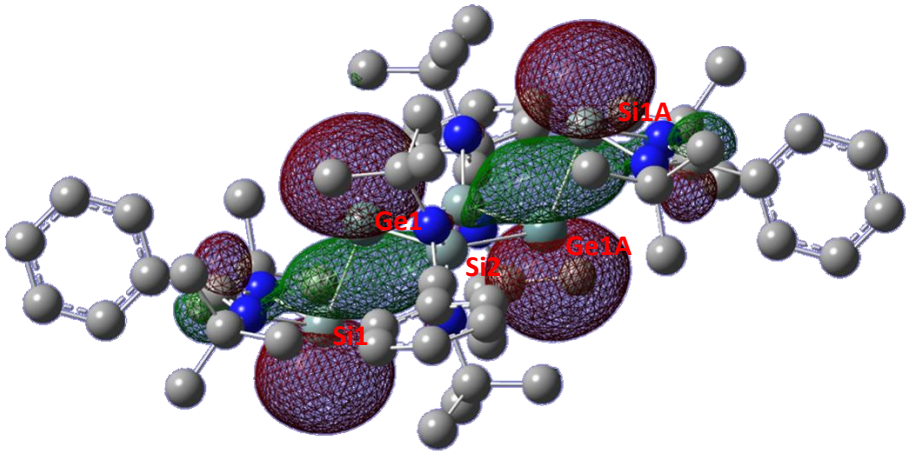

(b)

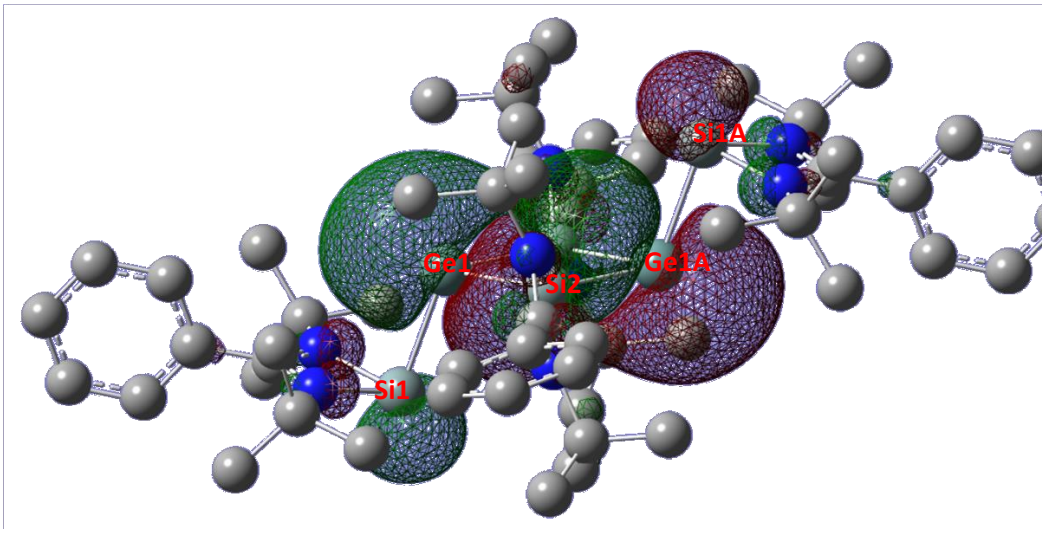

Figure 3.2 The a)HOMO and b)HOMO-1 of compound **3.2**

Theoretical studies were performed at M06-2X/6-311G(d) level of theory to understand the bonding in **3.2**. The HOMO of **3.2** comprises two exocyclic Ge1-Si1 and

Ge1A-Si1A σ orbitals. The HOMO-1 mainly arises from the combinations of lone pair orbitals on the three-coordinate Si1/1A and Ge1/1A atoms (Figure 3.1). These orbitals are in agreement with the observed trigonal pyrimidal geometry around the Si1/1A and Ge1/1A atoms and provide additional support to the presence of their stereoactive lone pairs. The Wiberg bond index (WBI) indicates that the endocyclic Ge-Si bonds (WBI: 1.05, 1.04) are single bonds, in good agreement with the observed crystal structure. Moreover, the NPA charges of **3.2** (Ge1/1A: -0.61, Si2/2A: 1.02) show that the Ge_2Si_2 four-membered ring has a charge-separated structure, which is also in agreement with our analysis of the crystal structure of **3.3**

3.2.2 Transfer and aggregation of digermanium(0) on the amidinato digermadisilacyclobutadiene

We believe that the zwitterionic structure, as well as the exocyclic silicon donor moiety, could enable compound **3.2** to act as a multi-functional ligand. In addition, the Ge atom in **3.2** could act as a "seed" for aggregation of digermanium(0) to form a larger cluster. To prove our concept, compound **3.2** was treated with three equivalents of amidinato amidosilylene-digermanium(0) complex **3.1** in toluene at room temperature to afford a mixture of the amidinato silylene-germanium cluster $[\{(LSi)_2Ge\}Ge_3]_2$ (**3.3**) and amidinato amidosilylene $[LSiN(SiMe_3)_2]$. **3.3** is considered as two trigermanium(0) coordinated with bis(silylenyl)germylenes due to the fact that the trigermanium(0) moiety can be transferred out to form compound **3.2** (Scheme **3.2** and see below). Compound **3.3** is the first example of a heavier zwitterionic cyclobutadiene analogue that can undergo dissociation and proceed to trap and aggregate main-group element allotropes.

In the reaction of **3.1** and **3.2**, we propose that digermanium(0) is transferred from **3.1** and it undergoes a [1+2] cycloaddition with the Ge lone pair in compound **3.2**. Such an interaction results in the cleavage of the endocyclic Si-Ge bonds to form a three-membered germanium ring intermediate "$(LSi:)_2Ge(Ge_2)$" (Scheme 2). It further reacts with digermanium(0) to form complex **3.3**.

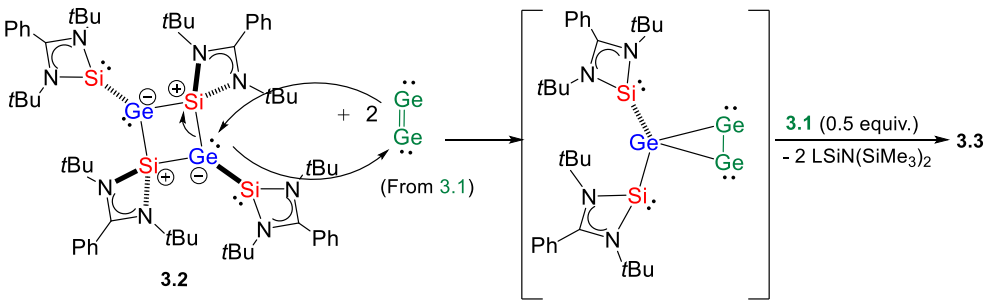

Scheme 3.4 Proposed mechanism for the formation of **3.3**

Compound **3.3** could be synthesized by an alternative route. The reaction of **1.51**, $PMe_3 \cdot GeCl_2$ and KC_8 in a molar ratio of 3 : 8 : 14 in toluene for 16 hours afforded a mixture of **3.2** (a few crystals), **3.3** (major product) and free Pme_3. In this reaction, PMe_3 is expected to act in a similar role to the amidinato amidosilylene [$LSiN(SiMe_3)_2$]; it stabilizes transient Ge(0) moieties generated from the reduction. While we were unable to observe the formation of a phosphine-digermanium(0) derivative in solution, however this approach avoids the need to separate compound **3.3** and $LSiN(SiMe_3)_2$ by recrystallization, as PMe_3 is removed during workup. Compound **3.3** was isolated as a red crystalline solid from its concentrated toluene solution. The ^{29}Si CPMAS NMR spectroscopy shows two signals at 34 and 85 ppm for bridging and terminal Si donors. They are in the downfield region similar to that of compound **1.51** (δ = 30.8 ppm).

The X-ray crystal structure of **3.3** comprises two Ge_3 (Ge1Ge2Ge3 and Ge1AGe2AGe3A) units that are supported by the terminal Si (Si1, Si1A), bridging Ge (Ge4, Ge4A) and bridging Si atoms (Si2, Si2A). The Ge-Ge bond lengths of the Ge_3 unit (Ge1-Ge2: 2.5338(7) Å; Ge2-Ge3: 2.5335(7) Å) are longer than reported Ge-Ge single bonds (average 2.44 Å).[44] The trigermanium configuration observed deviates significantly from the optimized structure of the free Ge_3 cluster optimized by Xu et al..[17] The cluster observed in **3.3** has a smaller bond angle than calculated (this work: 64.40(2), calculated: 84.6) and longer single bonds (calculated: 2.325 Å). This implies a significant degree of perturbation of the structure, which we attribute to the stabilizing donor interactions from the surrounding silylene and gerymylene moieties. The Ge1···Ge3 distance is 2.7003(9) Å, while smaller than the theoretical value (3.130 Å), is significantly larger than any reported Ge-Ge single bonds, which most likely suggests that there is, at most, minimal if not no interaction between the Ge1 and Ge3 atoms. The

Ge-Ge bonds (Ge4-Ge1: 2.4735(7), Ge4-Ge3: 2.4810(6) Å), which are formed by the bridging Ge4 atom and Ge_3 unit, are shorter than the Ge1-Ge2 and Ge2-Ge3 bonds. The Si1-Ge2 bond (2.4012(11) Å), which is formed by the terminal Si1 donor and Ge_3 unit, is comparable with the Si^{II}-Ge^0 donor-acceptor bond (2.406(2) Å) in **3.1**.[41] The Si2-Ge bonds (Si2-Ge1: 2.5249(12); Si2-Ge3: 2.5502(11) Å), which are formed by the bridging Si2 donor and Ge_3 unit, are significantly longer than the Si1-Ge2 bond, suggesting weaker bridging-type interactions.

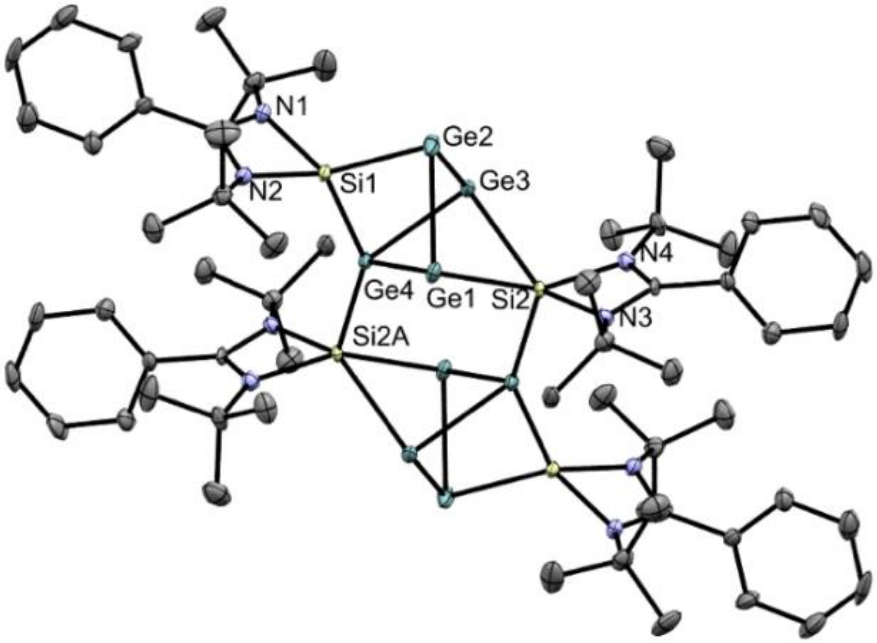

Figure 3.3 X-ray crystal structure of **3.3** (50% ellipsoids probability). Hydrogen atoms and solvent molecules are omitted for clarity. Selected bond lengths (Å) and angles (º): Ge1-Ge2 2.5338(7), Ge2-Ge3 2.5335(7), Si1-Ge2 2.4012(11), Si2-Ge1 2.5249(12), Si2-Ge3 2.5503(11), Ge4-Ge1 2.4735(7), Ge4-Ge3 2.4810(6), Si1-Ge4 2.3365(12), Si2A-Ge4 2.3855(11); Ge1-Ge2-Ge3 64.403(19), Ge2-Ge3-Ge4 89.03(2), Ge2-Ge1-Ge4 89.19(2), Ge1-Ge4-Ge3 66.055(19), Si1-Ge2-Ge1 75.13(3), Si1-Ge2-Ge3 78.43(3), Ge2-Ge1-Si2 101.58(3), Ge2-Ge3-Si2 100.89(3), Ge3-Si2-Ge1 64.29(3). Ge1···Ge3 distance: 2.7004(7) Å.

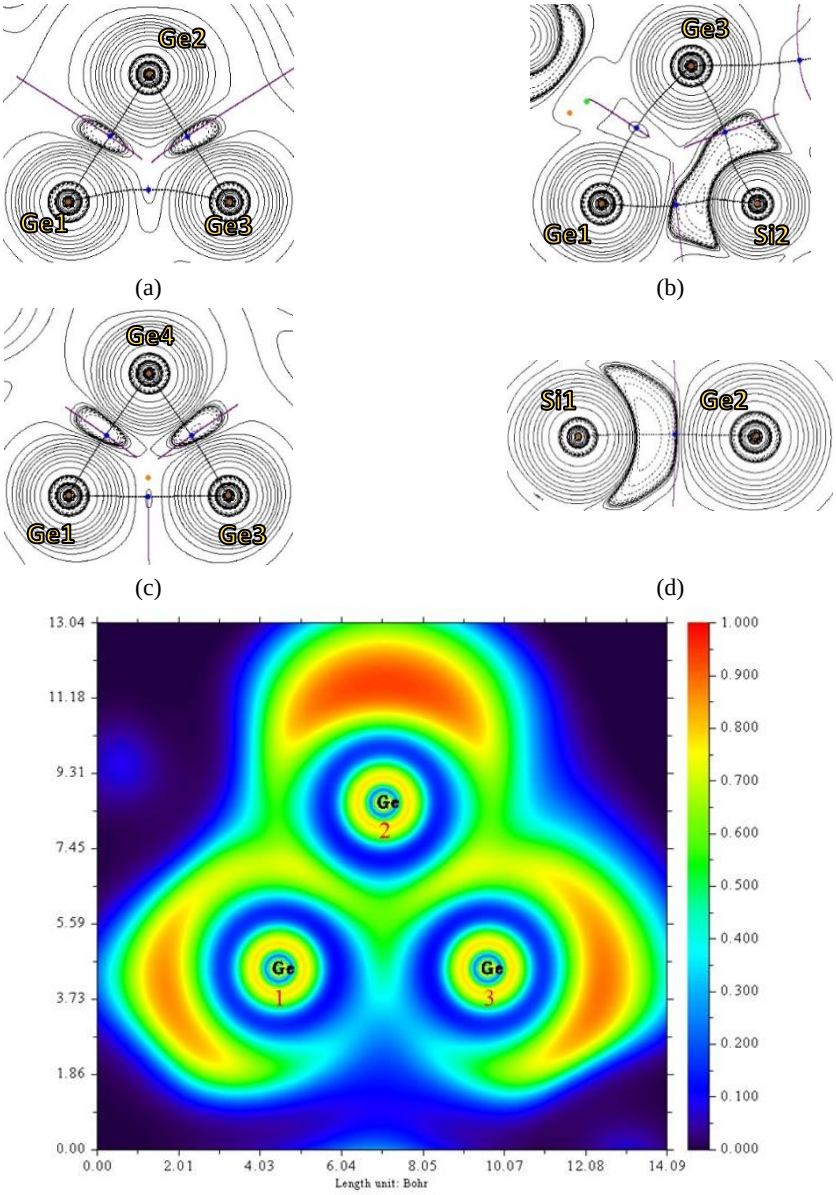

Figure 3.4 The contour plots of the Laplacian distribution of the (a) Ge1Ge2Ge3, (b) Ge1Si2Ge3, (c) Ge1Ge4Ge3, (d) Si1Ge2 skeleton calculated at M06-2X/def2-SVP level of theory. e) ELF color-filled map of the Ge1Ge2Ge3 skeleton.

To obtain a clearer understanding of the nature of the germanium cluster and the bonding situation present in **3.3**, theoretical studies were performed at M06-2X/def2-SVP level of theory. Bader's quantum theory of atoms in molecules (QTAIM)

calculations was carried out to investigate the bonding situation surrounding the trigermanium cluster. Regions of significant charge concentration were observed between the Ge1-Ge2 and Ge2-Ge3 atoms, suggesting bonds of a covalent nature, while there is no covalent bonding between the Ge1 and Ge3 atoms due to no obvious charge concentration between them (Figure 3.4a). Accordingly, NBO analysis shows that the Ge1-Ge2 and Ge2-Ge3 bonds are formed by the overlapping of the *p* orbital on the Ge2 atom with the *p*-rich sp hybrids on the Ge1 and Ge3 atoms (Ge1: $s^{0.12}p^{0.88}$, Ge3: $s^{0.13}p^{0.87}$), respectively. The Si1 atom donates its lone pair electrons (NBO: $sp^{1.25}$ hybrids) to the vacant *p* orbital on the Ge2 atom, which is illustrated by the contour plot of the Laplacian distribution (Figure 3.4d). Moreover, the Si2 atom donates its lone pair electrons (NBO: $sp^{2.62}$ hybrids) to the vacant *p* orbitals on the Ge1 and Ge3 atoms (Figure 3.4b), which is illustrated by the contour plot of the Laplacian distribution. Furthermore, the Ge4 atom bridges Ge3 and Ge4 atoms, resulting in the formation of the Ge4-Ge3 and Ge4-Ge1 bonds (Figure 3.4c). QTAIM calculations show that the Ge4-Ge3 and Ge4-Ge1 bonds are polar and covalent (Figure 3.4c). NBO analysis illustrates that the natural orbitals involved in these bonds are different. The Ge4-Ge3 bond is due to the overlapping of the $sp^{3.17}$ hybrids on the Ge4 atom with the *p*-rich $s^{0.12}p^{0.88}$ hybrids on the Ge3 atom, while the Ge4-Ge1 bond is formed by the overlapping of the *p*-rich hybrids on both Ge4 ($s^{0.15}p^{0.85}$) and Ge1 ($s^{0.12}p^{0.88}$) atoms. The NBO analysis also highlights the largely unhybridized nature of Ge1, Ge2 and Ge3. All interactions from these three atomic centers involve orbitals exhibiting high p-type character with minimal hybrid contributions from s-type orbitals. This would suggest an almost pure element-like state of each atoms, which encourages us to consider these atoms to formally be of oxidation state (0).

Electron localization function (ELF) calculations (Figure 3.4e) also show a single maxima on each of the Ge1, Ge2 and Ge3 atoms pointed outward from the cluster(Figure 3.3 for the numbering system) suggesting a lone pair of electrons (an area of significant electron localization is present on each of the Ge atoms. The NBO analysis of the lone pairs (Ge1: $s^{0.71}p^{0.29}$; Ge2: $s^{0.74}p^{0.26}$; Ge3: $s^{0.70}p^{0.30}$) show that they reside in an hybrid orbital possessing high s character.

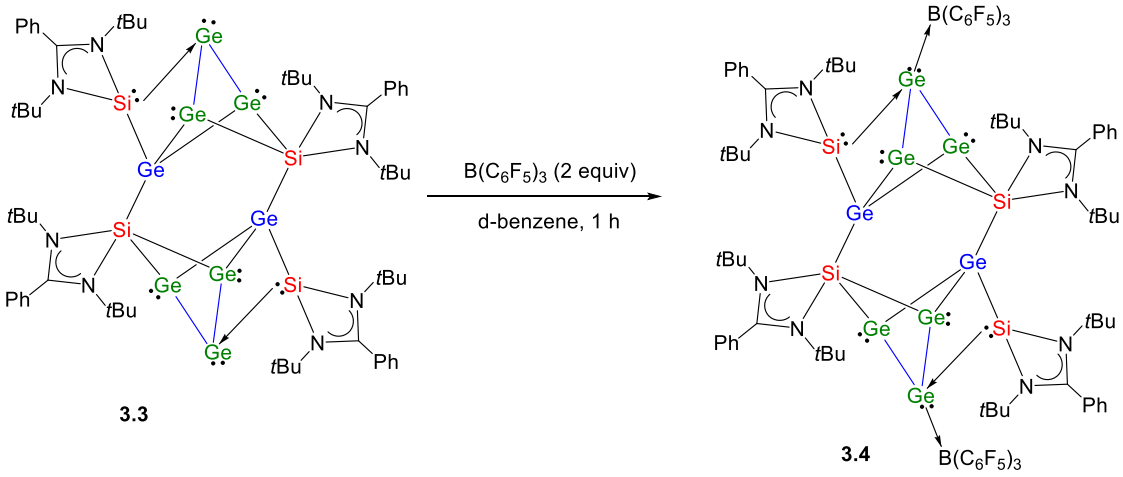

Scheme 3.5 Synthesis of tris(pentafluorophenyl)borane adduct **3.4**

The presence of σ-type lone pair orbitals on the germanium atoms at the vertex of the trigermanium cluster in compound **3.3** was illustrated by its reaction with two equivalents of trispentafluorophenylborane (BCF) in d-benzene at room temperature, furnishing the BCF-amidinato silylene-germanium cluster adduct (**3.4**) as bright orange crystals (Scheme 3.5).

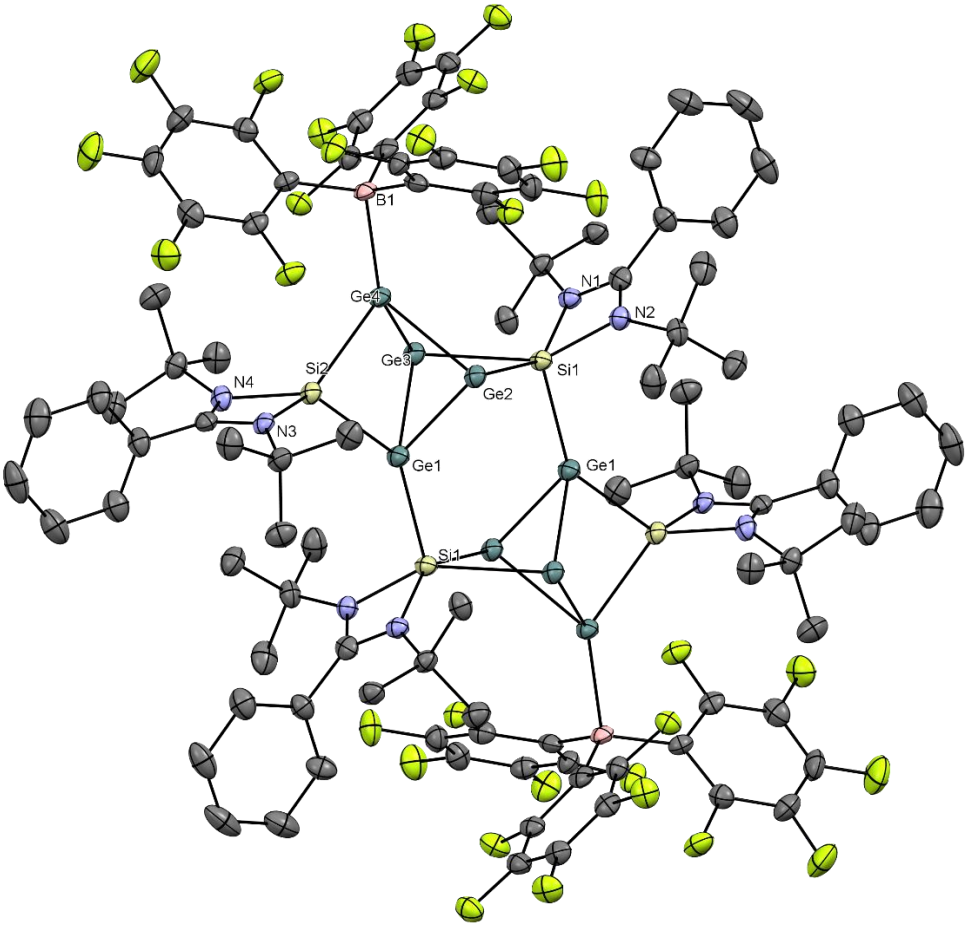

Figure 3.5 X-ray crystal structure of **3.4** (50% ellipsoids probability). Hydrogen atoms and solvent molecules are omitted for clarity. Selected bond lengths (Å) and angles (º): Ge1-Ge2 2.4699(6), Ge1-Ge3 2.476(1), Si1-Ge1 2.368(1), Si2-Ge1 2.330(1), Ge2-Ge4 2.4943(8), Ge2-Si1 2.579(2), Ge4-Ge3 2.5001(7), Si1-Ge3 2.544(1), B1-Ge4 2.205(5); Ge2-Ge4-Ge3 67.99(2), Ge1-Ge2-Ge4 82.64(2), Ge1-Ge3-Ge4 82.41(2), Ge2-Ge1-Ge3 68.76(2), Ge1-Si2-Ge4 88.71(5), Si1-Ge2-Ge4 100.91(4), Si1-Ge3-Ge4 101.73(4), Si2-Ge4-Ge3 81.39(4), , Ge2-Si1-Ge3 64.29(3), B1-Ge4-Si2 132.7(2), Ge3-Ge4-B1 134.0(1), Ge2-Ge4-B1 131.9(1). Ge1···Ge3 distance: 2.7926(9) Å.

The molecular structure of Compound **3.4** was characterized by X-ray crystallography. The two Ge_3 clusters (Ge2Ge3Ge4) are structurally comparable with those of **3.3**. The bond angles for Ge2Ge4Ge3 (67.99(2)º) is slightly larger than those of **3.3** (64.403(19)). The Ge2-Ge4 (2.4943(8) Å) and Ge3-Ge4 (2.5001(7) Å) are slightly shortened in comparison to those of compound **3.3**. The Ge4-B1 bond (2.205(5) Å) is

on the longer end in the range of Ge→B coordinative covalent bond in Ge^{II}-borane adduct [2.156−2.265 Å].

The ^{19}F NMR spectroscopy shows three signals at -126.0, -161.1 and -165.0 ppm. The chemical shift difference between the meta and para ^{19}F signals ($\Delta\delta_{m,p}$ = 4.9) is consistent with other reported examples of neutral and anionic tetracoordinated perfluoroaryl boranes and borates. ($\Delta\delta_{m,p}$ = 3.7 – 9.7) as opposed to neutral tricoordinate BCF ($\Delta\delta_{m,p}$ = 20.1).[45] ^{11}B NMR spectroscopy shows a broad signal at -12.7 ppm in good agreement with other reported Ge^{II}-BCF adducts.[46-51]

3.2.3 Transfer and aggregation of trigermanium(0) from the amidinato silylene-germanium cluster 4 to form Ge nanoparticles

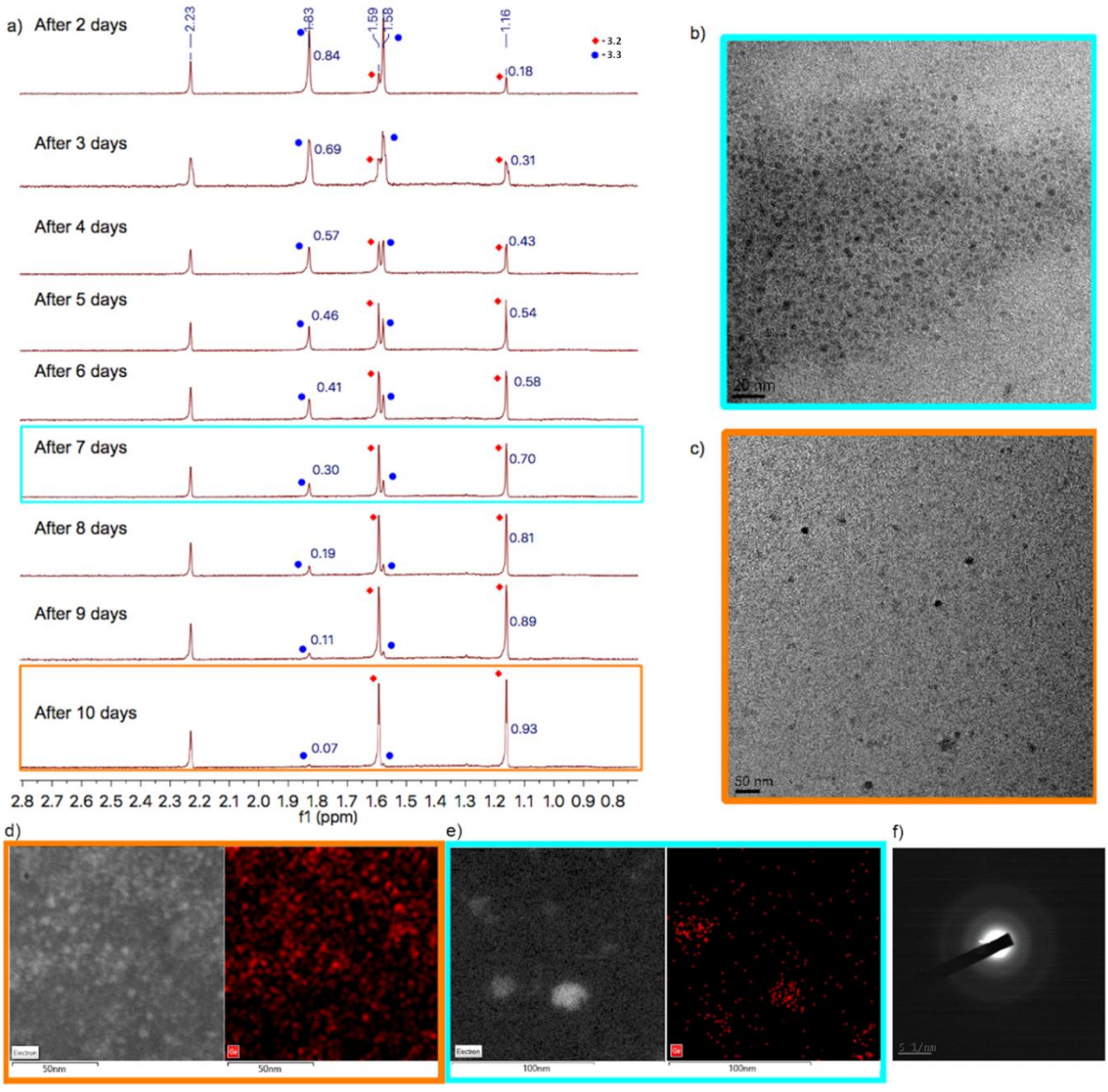

Figure 3.6 (a) ^{1}H NMR spectra showing conversion of **3.3** to **3.2** over 10 days, b) TEM micrograph of Ge nanoparticles on the seventh day of conversion, c) TEM micrograph of Ge nanoparticles on the tenth day of conversion, d) HAADF TEM micrographs and Ge Kα1 EDS map of germanium nanoparticles on the seventh day of conversion e) germanium nanoparticles on the tenth day of conversion showing only germanium residing in nanoparticles, f) SAED micrograph

On the basis of the X-ray crystal structure of **3.3**, we hypothesized that the Ge4 atom acts as both donor and acceptor similar to a bridging CO ligand, which bridges Ge3 and Ge4 atoms of the Ge_3 moiety, resulting in the formation of the Ge4-Ge3 and Ge4-Ge1 bonds. When there is a strong and less sterically hindered Lewis base donor, it could attack the vacant orbital on the Ge4 atom and hence disrupt the interaction between the bis(silylenyl)germylene and trigermanium(0) moiety, resulting in the displacement of the trigermanium(0) moiety for further aggregation.

In search of strong and less sterically hindered Lewis base donor, we anticipated that pyridine should be a promising candidate for the displacement of trigermanium(0) moieties from compound **3.3**. To test this hypothesis, compound **3.3** was dissolved in d_5-pyridine at room temperature and the solution was observed changed from red-orange to yellow-orange over time. Monitoring by ^{1}H NMR spectroscopy showed the signals of **3.3** gradually decreased, with the concurrent appearance and growth in the signals of **3.2**(Figure 3.6a),. No other significant side-products were observed over the course of 10 days. This indicates that elemental germanium is released as trigermanium(0) clusters instead of mono- and diatomic species. In addition, visual observation of the reaction under a microscope showed no visible deposition of metallic germanium; the reaction solution remained clear throughout. These results suggest that a slow release of trigermanium(0) occurred and its aggregation did not lead to the deposition of bulk germanium, indicating the possible formation of nanoparticles. It is also important to note that the regeneration of compound **3.2** also indicates that compound **3.3** is indeed composed of two trigermanium(0) moieties bonded with two bis(silylenyl)germylenes, thus confirming our initial assessment of its structure.

The formation of germanium nanoparticles was confirmed by transmission electron microscopy (TEM). On the seventh day of the reaction, 70 % conversion was

observed. Electron micrography measurements of more than 100 quasi-spherical particles in this sample gave the average size of nanoparticles formed at 70% conversion to be 4.53 ± 0.6 nm in diameter (Figure 3.6b). On the tenth day of the reaction, 100 % conversion was observed. Electron micrography measurements of the sample at 100% conversionshows the formation of larger nanoparticles with an average diameter of 11.1 ± 2.3 nm (Figure 3.6c). Energy-dispersive X-ray spectroscopy (EDS) shows only germanium residing in areas containing these nanoparticles (Figure 3.6 d,e). The selected area diffraction (SAED) image shows two diffuse rings characteristic of amorphous Ge, due to short range order of the crystal structure resulting in two broad diffraction peaks(Figure 3.6f).[52] High-resolution TEM yielded no observable crystal domains, confirming the lack of crystallinity in the Ge nanoparticles. X-ray Photoelectron Spectroscopy was carried out to ascertain the oxidation state of the Ge nanoparticles obtained.[53] While all attempts to minimize surface oxidation were taken, based on the Ge 3d data, a significant extent of oxidation was observed, resulting in only 30% of the nanoparticles comprising of Ge(0) metal.

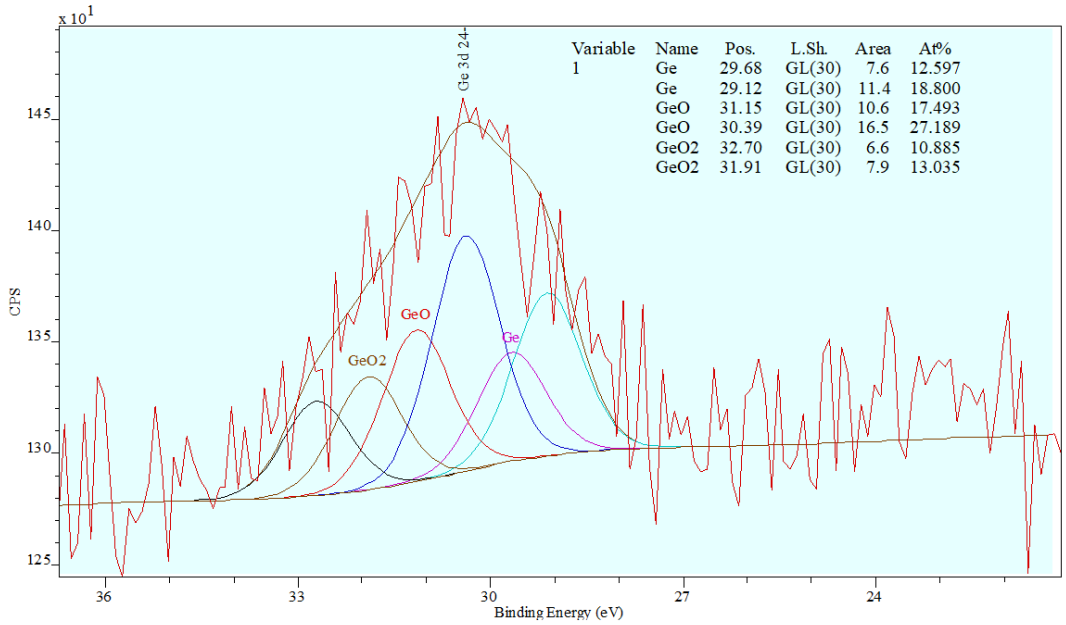

Figure 3.6. Representat[iv]e Ge 3d XPS data for 7th day samples. Spectrum was collected with an Al source (1486.69 eV), 50 scans, and pass energy 20 eV.

We propose that pyridine first donates its lone pair of electrons to the germanium atom of bis(silylenyl)germylene in compound **3.3**, but the steric effect exerted by the amidinate ligand make such interaction difficult, leading to slow release of trigemanium(0) cluster and regeneration of compound **3.2**. The trigermanium(0) then aggregates to form Ge nanoparticles. The amorphous nature of the resultant nanoparticles can be attributed to the slow release of trigermanium(0) clusters. Large excess of pyridine in the reaction prevents elemental germanium from reversibly reacting with compound **3.2** to form back compound **3.3**. Improved passivation of the nanoparticle surface could reduce the extent of surface oxidation, as described above, if strongly binding surfactants were introduced into the synthesis process. However, as a proof of concept, we have obtained evidence that a step-wise transfer of germanium(0) precursors can indeed result in the formation of amorphous Ge(0) nanoparticles. This represents the first observable example from an oligogermanium allotrope that has hitherto not been reported, even for other Group 14 element allotrope complexes.

3.3 Conclusion

We have demonstrated the first observable stepwise growth of germanium nanoparticles, beginning from a diatom to a small germanium cluster and ending with the formation of amorphous nanoparticles. The amidinato amidosilylene-digermanium(0) complex is an excellent digermanium(0) transfer reagent, which reacted with the silicon(I) derivative to form the digermadisilacyclobutadiene **3.2**. It is capable of dissociation, to form silylene-germanium complex **3.3** through the capture of three digermanium(0) moieties, and later re-association after releasing trigermanium(0) clusters in pyridine. The trigermanium(0) clusters further aggregate in pyridine to form amorphous Ge nanoparticles. This series of transformations demonstrate the importance of ligand selection if chemists are interested in employing element (0) clusters in further application. While strong stabilization from Lewis base ligands and bulky side chains are essential in the isolation of these species, a careful balance is required to allow for further reactivity, access to new geometric structures, and other applications. It is promising to also observe the first stepwise transfer of trigermanium (0) clusters which suggests potential applications in the development of pure germanium materials. It could also see additional potential in the development of new mixed metal materials with well defined elemental compositions if reacted with the appropriate metal source.

. The further applications of this trapping mode of germanium allotropes, as observed between compound **3.3** and Ge nanoparticles, are currently under investigation. Experimentation with other passivating surfactants is also underway.

3.4 Experimental procedures

General Procedures: All manipulations were carried out under an inert atmosphere of argon gas by standard Schlenk techniques. Toluene was dried over and distilled over Na/k alloy prior to use. $[LSi:]_2$ (**3.2**, L = $PhC(NtBu)_2$),[S3] $[L\{(Me_3Si)_2N\}Si(Ge=Ge)Si\{N(SiMe_3)_2\}L]$ (**3.1**)[S4] and $[LSiNMe_2]$[S5] were prepared according to the literature procedures. C_6D_6 and THF-d_8 were dried and distilled over K metal prior to use. The NMR spectra were recorded on a JEOL ECA 400 spectrometer and Bruker 400 spectrometer. 11B and 19F NMR spectra are referenced to BF3(OEt2), and CFCl3, respectively. High resolution mass spectrometry was performed by the Division of Chemistry and Biological Chemistry, Nanyang Technological University using a Waters Q-tof Premier mass spectrometer. Melting points were measured in sealed glass tubes and were not corrected. Transmission election microscopy (TEM) images of the nanoparticles were obtained with a JEOL JEM-1400 Electron Microscopy operating at 100 kV. High angle annular dark-field (HAADF) images and energy-dispersive spectroscopy (EDS) were obtained on a JEOL 2100F ZrO/W(100) Schottky-type Microscope operating at 200 kV. TEM samples were prepared by diluting 0.1 mL aliquots of the suspended nanoparticles in 0.1 mL toluene and drop-casting onto Formvar-coated copper TEM grids. Size-distribution histograms were constructed by measuring the longest length for more than 100 nanoparticles (when possible). X-ray photoelectron spectroscopy (XPS) spectra were obtained using a Phoibos 100 spectrometer with a monochromatic Al X-ray radiation source. The scanning range was from 0 –1200 eV. The C 1s binding energy peak at 284.4 eV was used for XPS calibration. Processing of high-resolution spectra was carried out using CasaXPS (Vamas) software. After calibration, the extrinsic loss structure in the background from each spectrum was subtracted using a Shirley-type background. The elemental

germanium peaks were fitted with a fixed spin-orbit splitting of 0.58 eV. Raman spectroscopy was performed using a STELLAR-PRO-L SELECT 300 Raman microscope with a He–Ne laser (λ = 514 nm).

$[(LSi)_2Ge]_2$ (**3.2**): Toluene (30 mL) was added to a mixture of $[L\{(Me_3Si)_2N\}Si(Ge{=}Ge)Si\{N(SiMe_3)_2\}L]$ (**3.1**, 0.19 g, 0.20 mmol) and **1.51** (0.21 g, 0.40 mmol) at ambient temperature. The resulting red mixture was stirred for 16 hours to afford a mixture of **3.2** and $[LSiN(SiMe_3)_2]$. The reaction mixture was filtered and the filtrate was concentrated to afford red crystals of compound **3.2**. Yield: 0.054 g (22.8 % based on the weight of red crystals). After one day, the mother liquor must be filtered and the filtrate afforded a mixture of red crystals of **3.2** and colorless crystals of $[LSiN(SiMe_3)_2]$.

Mp: 124.3 °C (decomposed). ^{1}H NMR (399.5 MHz, C_6D_6, 25°C): ^{1}H NMR (395.9 MHz, 24 °C, C_6D_6, ppm): δ = 1.22 (s, 36H, *t*Bu), 1–43 (s, 36H, *t*Bu), 7.09 - 7.01 (m, 18H, Ar-*H*), 7.37 – 7.31 (m, 2H, Ar-*H*); ^{1}H NMR (395.9 MHz, 24 °C, d_5-pyridine, ppm): δ = 1.16 (s, 36H, *t*Bu), 1.59 (s, 36H, *t*Bu), 7.49 – 7.30 (m, 20H, Ar-*H*); ^{13}C{^{1}H} NMR (100.5 MHz, d_5-pyridine, 25°C): δ = 29.3, 33.0 (C*Me*$_3$), 51.4, 53.0 (*C*Me$_3$), 125.8, 128.0, 128.1, 128.7, 128.7, 129.4, (Ph), 140.9, 153.8 (NCN) ppm. ^{29}Si NMR (160.5 MHz, 24 °C, C_6D_6, ppm): δ = -7.9 (three-coordinate Si), 40.9 (four-coordinate Si). HRMS (ESI), *m/z* calcd: 1185.5024 $[M+H]^+$; found: 1185.5066.

$[\{(LSi)_2Ge\}Ge_3]_2$ (3.3):

Synthesis of compound 3.3. Toluene (20 mL) was added to a mixture of **3.1** (0.38 g, 0.37 mmol) and **3.2** (0.15 g, 0.12 mmol) at ambient temperature. The resulting red mixture was stirred for 16 hours. It was filtered and the filtrate was concentrated to afford red crystals of compound **3.3** (Yield: 0.023g, 11.3%). After one day, the mother

liquor was filtered and the filtrate afforded colorless crystals of [LSiN($SiMe_3$)$_2$]. Mp: 113.8 °C (decomposed). ^{1}H NMR (395.9 MHz, pyridine-d5, 25°C): d = 1.83 (s, 36H, *t*Bu), 1.57 (s, 36H, *t*Bu), 6.66-7.02 (m, 20H, Ph) ppm. ^{29}Si{^{1}H} CPMAS NMR : d = 34.1 (Si_{bridge}), 85.2 ($Si_{terminal}$) ppm. HRMS (ESI), *m/z* calcd: 1622.0399 $[M+H]^+$; found: 1622.0399.

Alternative synthetic route for compound 3.4:

A stirring toluic (30 mL) solution of $PMe_3{\cdot}GeCl_2$ (0.11 g, 0.51 mmol) was added to a mixture of **1.51** (0.10 g, 0.19 mmol) and KC_8 (0.12, 0.89 mmol) at -78° C. The resulting red mixture was stirred at 0° C for 16 hours. The reaction mixture was filtered and the filtrate was concentrated to afford red crystals of compound **3.3**. Subsequent filtering and concentrating affords additional crops of red crystals together with the formation of black crystals of **3.2**. Yield of 3.4: 0.034 g (33.5%, based on the cumulative weight of red crystals isolated)

Synthesis of compound 3.4

Tris(pentafluorophenyl)borane (0.0060 g, 0.0037 mmol) was added to a suspension of the trigermanium(0) complex (0.0038 g, 0.0073 mmol) in C6D6 (0.4 mL). A bright orange colour began to develop in the solution, which was stirred at room temperature for 1 hour. The bright orange solution was filtered and concentrated to half its volume, whereupon it has left to stand overnight. Orange plate-like crystals (0.003 g, 0.0018 mmol)of x-ray diffraction quality were obtained in 51% yield.

^{1}H NMR (500.1 MHz, C_6D_6, 25°C): d = 1.16 (s, 36H, *t*Bu), 1.52 (s, 36H, *t*Bu), 6.88, 6.91, 6.95-7.00, 7.07, 7.14-7.16, 7.32, 7.45, 7.70 ppm.^{19}F{^{1}H} (470.6 MHz, C_6D_6, 25°C): d = -165.0, -161.1, -126.0 ppm ^{11}B{^{1}H} (128.4 MHz, C_6D_6, 25°C): d = -12.7.

Preparation of Ge nanoparticles:

A J-young NMR tube was charged with 0.0034g (0.002 mmol) of compound **3.3**, after which 0.35 mL of d5-pyridine was added. This mixture was left to stand at room temperature and was monitored every 24 hours. After 7 and 10 days, the nanoparticles were isolated by centrifugation and deposited onto copper TEM grids for analysis.

Solid-State NMR and Discussion

Methodology

All solid state NMR experiments in this study were completed on a Bruker Avance III HD 600 MHz spectrometer with a Bruker 4 mm HXY MAS probe. Spectral processing and simulation of NMR spectra was achieved via the *Topspin* software package. The ^{29}Si and ^{13}C NMR experiments were completed at 14.1 T (υ_0 (^{29}Si) = 119.24 MHz; υ_0 (^{13}C) = 150.92 MHz) utilising CPMAS pulse sequences with high power proton decoupling, ^{1}H $\pi/2$ pulse lengths of 2.7 μs (determined on adamantane$_{(s)}$) and recycle delays of 3 s.

The ^{29}Si(^{1}H) CPMAS experiments utilised a contact pulse length of 4500 s (optimised on kaolinite$_{(s)}$) and was acquired at two MAS frequencies, 12 and 10 KHz, to assist in the simulation of CSA sideband manifolds. The ^{29}Si data was data referenced with respect to $Me_4Si_{(aq)}$ (δ_{iso} = 0 ppm). The ^{13}C(^{1}H) CPMAS experiment utilised a contact pulse length of 6000 s (optimised on adamantane$_{(s)}$) with an MAS frequency of 12 KHz and resulting data was referenced with respect to adamantane$_{(s)}$ (δ_{iso} = 38.48, 40.49 ppm).

Results

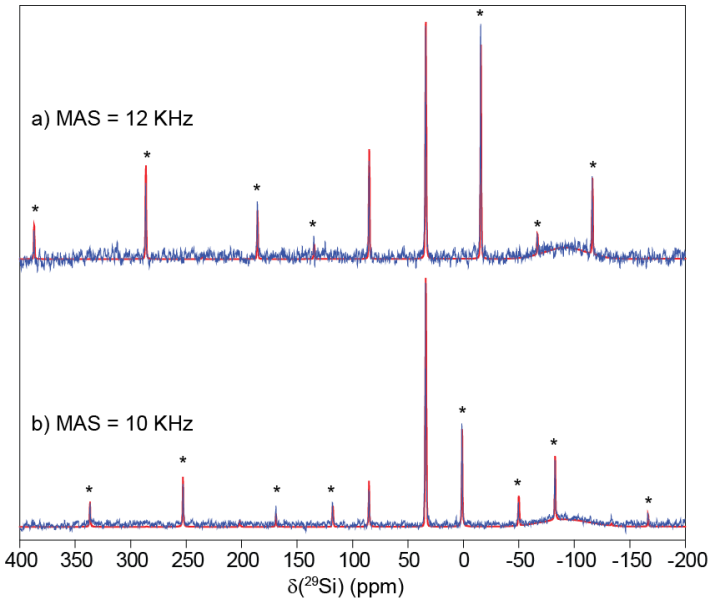

Figure 3.7 $^{29}Si(^{1}H)$ CPMAS NMR spectra of compound **3.3** at MAS frequencies of 12 KHz and 10 KHz. Experimental and simulated spectra are in blue and red respectively, with spinning sideband manifolds marked by asterisks.

Assignment	$\delta_{iso}(^{29}Si)$ (ppm)	$\delta_{CSA}(^{29}Si)$ (ppm)	$\eta_{CSA}(^{29}Si)$ (KHz)
1	85.2	375	0.05
2	34.1	100	0.10
grease	-91.6	-	-

Table 3.1 The ^{29}Si NMR simulation parameters of the $^{29}Si(^{1}H)$ CPMAS NMR spectra of compound **3.3**.

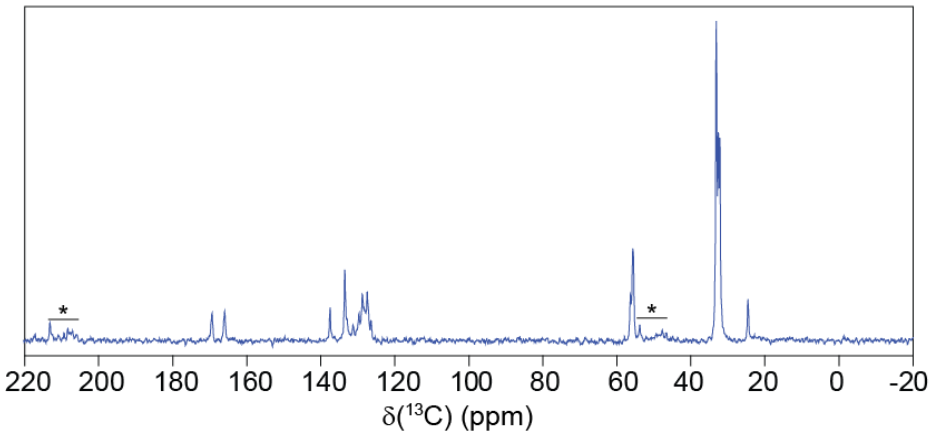

Figure 3.8 $^{13}C(^{1}H)$ CPMAS NMR spectra of compound **3.3** at an MAS frequency of 12 KHz. Spinning sideband manifolds are marked by asterisks.

Solid-state NMR Data Discussion

The ^{29}Si CPMAS NMR data shows two narrow resonances at 85 and 34 ppm. The 85 ppm resonance has a large enough chemical shift anisotropy that the CSA powder pattern is visible in the spinning sideband manifolds even at 12 KHz MAS. These two resonances represent the two similar Si environments in the complex, with the 34 ppm resonance corresponding to the bridging Si atom, and the 85 ppm resonance corresponding to the terminal Si atom.

The amorphous ^{29}Si resonance at -92 ppm can be attributed to silicon grease impurities.

The ^{13}C NMR reflects the organic functional groups present. Resonances at 126-138 ppm represent the phenyl carbons; 32-34 and 56 ppm represent the tertbutyl carbons; and 166 and 169 represents the N bridging carbon. The two clear resonances for the latter site can be explained due to the two different Si sites that the organic functional group attaches to.

X-ray Photoelectron Spectra (XPS)

Discussion of XPS data:

Initial XPS experiments (Figure A4.8) were able to show the presence of elemental germanium in a roughly 3:7 ratio to germanium oxide, attributed to exposure to air during the transfer of the sample into the XPS. Upon increasing loading, we observed an increase in sodium and calcium contaminants observed in our spectrums (Figure A4.10). These are attributed to the molecular sieves and CaH_2 used in the drying process of our solvents. Drying the nanoparticles and resuspended in redistilled methanol to remove these contaminants. We observed that we were only successful in removing the sodium contaminant (Figure A4.12). However, the germanium content remained relatively consistent across samples.

1. X-ray Data Collection and Structural Refinement.

Intensity data for all compounds were collected by using a Bruker APEX II diffractometer. The structures were solved by direct-phase determination (SHELXS-97) and refined for all data by full-matrix least-squares methods on F^2.[S7] All non-hydrogen atoms were subjected to anisotropic refinement. The hydrogen atoms were generated geometrically and allowed to ride on their respective parent atoms; they were assigned appropriate isotopic thermal parameters and included in the structure-factor calculations. All non-hydrogen atoms were refined with anisotropic thermal parameters. CCDC-1579032(**3.2**) and 1577528 (**3.3**) contain the supplementary crystallographic data for this paper. The data can be obtained free of charge from the Cambridge Crystallography Data Center via www.ccdc.cam.ac.uk/data_request/cif.

Theoretical studies

Computational Methodology. All the calculations were performed using Gaussian09 program package.[S8] The geometries of compound **3.3** were optimized using M06-2X[S9] with def2-SVP basis set.[S10] The geometry of compound **3.2** was optimized using M06-2X[S9] with 6-311G(d) basis set.[S11] The Natural Bond Orbital analysis (NBO)[S12] has been carried out at M06-2X/def2-SVP level of theory for compounds **3.3** and at M06-2X/6-311G(d) level of theory for compound **3.2**. QTAIM[S13] and ELF[S14] analysis of compounds **3.3** were performed using the MultiWfn[S15] program suite at M06-2X/def2-SVP level of theory. The optimized geometries of compounds **3.2** and **3.3** are consistent with the X-ray crystallographic data.

References

1. LaMer, V. K.; Dinegar, R. H. Theory, Production and Mechanism of Formation of Monodispersed Hydrosols. *J. Am. Chem. Soc.* **1950**, *72*, 4847−4854.
2. Lin Y.; Finke R. G., Novel Polyoxoanion-and Bu_4N^+ - Stabilized, Isolable, and Redissolvable, 20–30 Å $Ir_{\sim 300-900}$ Nanoclusters: The Kinetically Controlled Synthesis, Characterization, and Mechanism of Formation of Organic Solvent-Soluble, Reproducible Size, and Reproducible Catalytic Activity Metal Nanoclusters, *J. Am. Chem. Soc.*, **1994**, *116*, 8335–8353
3. Watzky, M. A.; Finke R. G., Transition Metal Nanocluster Formation Kinetic and Mechanistic Studies. A New Mechanism When Hydrogen Is the Reductant: Slow, Continuous Nucleation and Fast Autocatalytic Surface Growth, *J. Am. Chem. Soc.* **1997**, *119* (43), 10382–10400
4. Watzky, M. A.; Finke R. G., Nanocluster Size-Control and "Magic Number" Investigations. Experimental Tests of the "Living-Metal Polymer" Concept and of Mechanism-Based Size-Control Predictions Leading to the Syntheses of Iridium(0) Nanoclusters Centering about Four Sequential Magic Numbers, *Chem. Mater.* **1997**, *9*(12), 3083–3095
5. Laxson W. W.; Finke R. G., Nucleation is Second Order: An Apparent Kinetically Effective Nucleus of Two for $Ir(0)_n$ Nanoparticle Formation from $[(1,5\text{-COD})Ir^{I}\cdot P_2W_{15}Nb_3O_{62}]^{8-}$ Plus Hydrogen, *J. Am. Chem. Soc.*, **2014**, *136*, 1760'–17615.
6. Whitehead, C. B.; Özkar, S.; Finke, R. G., LaMer's 1950 model of particle formation: a review and critical analysis of its classical nucleation and fluctuation theory basis, of competing models and mechanisms for phase-changes and particle formation, and then of its application to silver halide,

semiconductor, metal, and metal-oxide nanoparticles, *Mater. Adv.*, **2021**, *2*, 186-235.

7. Ershov, B. G.; Janata, E.; Henglein, A., Growth of silver particles in aqueous solution: long-lived "magic" clusters and ionic strength effects, *J. Phys. Chem.*, **1993**, *97*, 339-343.
8. Henglein, A.; Giersig, M., Formation of Colloidal Silver Nanoparticles: Capping Action of Citrate, *J. Phys. Chem. B*, **1999**, *103*, 9533-9539.
9. Stamplecoskie, K. G.; Scaiano, J. C., Kinetics of the Formation of Silver Dimers: Early Stages in the Formation of Silver Nanoparticles, *J. Am. Chem. Soc.*, **2011**, *133*, 3913-3920.
10. Yao, S.; Yuan, Y.; Xiao, C.; Li, W.; Kou, Y.; Dyson, P. J.; Yan, N.; Asakura, H.; Teramura, K.; Tanaka, T. Insights into the Formation Mechanism of Rhodium Nanocubes. *J. Phys. Chem. C* **2012**, *116* (28), 15076–15086.
11. Biegel, M.; Schikarski, T.; Cardenas Lopez, P.; Gromotka, L.; Lübbert, C.; Völkl, A.; Damm, C.; Walter, J.; Peukert, W. Efficient Quenching Sheds Light on Early Stages of Gold Nanoparticle Formation. *RSC Advances* **2023**, *13* (26), 18001–18013.
12. Hollingsworth, J. A.; Klimov, V. I. "Soft" Chemical Synthesis and Manipulation of Semiconductor Nanocrystals. In *Semiconductor and Metal Nanocrystals: Synthesis and Electronic and Optical Properties*, Klimov, V. I., Eds.; Marcel Dekker, 2004; pp 1-64.
13. Alferov, Zh. I.; The History and Future of Semiconductor Heterostructures *Semiconductors* **1998**, *32*, 1– 14.
14. Ashoori, R. C. Electrons in Artificial Atoms *Nature* **1996**, *379*, 413– 419.

15. Cotta, M. A. Quantum Dots and Their Applications: What Lies Ahead? *ACS Appl. Nano Mater.* **2020**, *3*, 4920-4924.
16. Efros, A. L.; Brus, L. E. Nanocrystal Quantum Dots: From Discovery to Modern Development *ACS Nano* **2021**, *15*, 6192-6210.
17. Xu, W.; Zhao, Y.; Li, Q.; Xie, Y.; Schaefer, H. F., III. The Germanium Clusters Ge_n (n = 1-6) and their Anions: Structures, Thermochemistry and Electron Affinities *Mol. Phys.* **2004**, *102*, 579-598.
18. Zhao, L.-Z.; Lu W.-C.; Qin, W.; Zang, Q.-J.; Wang, C. Z.; Ho, K. M. Fragmentation Behavior of Ge_n Clusters ($2 \leqslant n \leqslant 33$) *Chem. Phys. Chem.* **2008**, *4-6*, 225-231.
19. Schnepf, A. Metalloid Clusters. In *Clusters – Contemporary Insight in Structure and Bonding*, Dehnen, S., Eds.; Vol. 174, Springer, Berlin, 2017, pp. 135– 200.
20. Nesterov, V.; Reiter, D.; Bag, P.; Frisch, P.; Holzner, R.; Porzelt, A.; Inoue, S. NHCs in main group chemistry. *Chem. Rev.* **2018**, *118*, 9678-9842.
21. Roy, S.; Mondal, K. C.; Roesky, H. W Cyclic Alkyl(amino) Carbene Stabilized complexes with low coordinate metals of enduring nature. *Acc. Chem. Res.* **2016**, *49*, 357-369.
22. Yao, S.; Xiong, Y.; Driess, M. A New Area in Main-Group Chemistry: Zerovalent Monoatomic Silicon Compounds and their Analogues *Acc. Chem. Res.* **2017**, *50*, 2026-2037.
23. Dyker, C. A.; Lavallo, V.; Donnadieu, B.; Bertrand, G. Synthesis of an Extremely Bent Acyclic Allene (A "carbodicarbene"): a Strong Donor Ligand. *Angew. Chem., Int. Ed.* **2008**, *47*, 3206-3209.

24. Wang, Y.; Xie, Y.; Wei, P.; King, R. B.; Schaefer, H. F., III; Schleyer, P. v. R.; Robinson, G. H. A stable silicon(0) compound with a Si=Si double bond. *Science* **2008**, *321*, 1069-1071.

25. Xiong, Y.; Yao, S.; Inoue, S.; Epping, J. D.; Driess, M. A Cyclic Silylone ("siladicarbene") with an Electron-Rich Silicon(0) Atom. *Angew. Chem., Int. Ed.* **2013**, *52*, 7147-7150 (2013).

26. Xiong, Y.; Yao, S.; Tan, G.; Inoue, S.; Driess, M. A Cyclic Germadicarbene ("germylone") from Germyliumylidene. *J. Am. Chem. Soc.* **2013**, *135*, 5004-5007.

27. Li, Y.; Mondal, K. C.; Roesky, H. W.; Zhu, H.; Stollberg, P.; Herbst-Irmer, R.; Stalke, D.; Andrada, D. M. Acyclic Germylones: Congeners of Allenes with a Central Germanium Atom. *J. Am. Chem. Soc.* **2013**, *135*, 12422-12428.

28. Su, B.; Ganguly, R.; Li, Y.; Kinjo, R. Isolation of an Imino-N-heterocyclic carbene/germanium(0) Adduct: A Mesoionic Germylene Equivalent. *Angew. Chem., Int. Ed.* **2014**, *53*, 13106-13109.

29. Sidiropoulos, A.; Jones, C.; Stasch, A.; Klein, S.; Frenking, G. N-heterocyclic Carbene Stabilized Digermanium(0). *Angew. Chem., Int. Ed.* **2009**, *48*, 9701.

30. Jones, C.; Sidiropoulos, A.; Holzmann, N.; Frenking, G.; Stasch, A. An N-heterocyclic Carbene Adduct of Diatomic Tin, :Sn=Sn:. *Chem. Comm.* **2012**, *48*, 9855-9857.

31. Masuda, J. D.; Schoeller, W. W.; Donnadieu, B.; Bertrand, G. Carbene Activation of P4 and Subsequent Derivatization. *Angew. Chem., Int. Ed.* **2007**, *46*, 7052-7055.

32. Wang, Y.; Xie, Y.; Wei, P.; King, R. B.; Schaefer, H. F., III; Schleyer, P. v. R.; Robinson, G. H. Carbene-stabilized Diphosphorus. *J. Am. Chem. Soc.* **2008**, *130*, 14970-14971

33. Abraham, M. Y.; Wang, Y.; Xie, Y.; Wei, P.; Schaefer, H. F., III; Schleyer, P. v. R.; Robinson, G. H. Carbene stabiliza–ion of diarsenic: from hypervalency to allotropy. *Chem. - Eur. J.* **2010**, *16*, 432-435.

34. Kretschmer, R.; Ruiz, D. A.; Moore, C. E.; Rheingold, A. L.; Bertrand, G. One-, Two-, and Three-Electron Reduction of a Cyclic Alkyl(amino)carbene-$SbCl_3$ Adduct. *Angew. Chem., Int. Ed.* **2014**, *53*, 8176-8179.

35. Zhou, Y.-P.; Karni, M.; Yao, S.; Apeloig, Y.; Driess, M. A Bis(silylenyl)pyridine Zero-Valent Germanium Complex and Its Remarkable Reactivity. *Angew. Chem., Int. Ed.* **2016**, *55*, 15096-15099.

36. Yao, S.; Kostenko, A.; Xiong, Y.; Ruzicka, A.; Driess, M. Redox Noninnocent Monoatomic Silicon(0) Complex ("Silylone"): Its One-electron-reduction Induces an Intramolecular One-electron-oxidation of Silicon(0) to Silicon(I) *J. Am. Chem. Soc.* **2020**, *142*, 12608-12612.

37. Wang, Y.; Karni, M.; Yao, S.; Kaushansky, A.; Apeloig, Y.; Driess, M. Synthesis of an Isolable Bis(silylene)-stabilized Silylone and Its Reactivity Towards Gaseous Molecules. *J. Am. Chem. Soc.* **2019**, *141*, 12916-12927.

38. Wang, Y.; Karni, M.; Yao, S.; Apeloig, Y.; Driess, M. An Isolable Bis(silylene)-stabilized Germylone and Its Reactivity. *J. Am. Chem. Soc.* **2019**, *141*, 1655-1664.

39. Wang, Y.; Tope, C. A.; Xie, Y.; Wei, P.; Urbauer, J. L.; Schaefer, H. F., III; Robinson, G. H. Carbene-stabilized Disilicon as a Silicon-transfer agent:

Synthesis of a Dianionic Silicon Tris(dithiolene) Complex *Angew. Chem., Int. Ed.* **2020**, *59*, 8864-8867.

40. Wang, Y.; Szilvasi, T.; Yao, S.; Driess, M. A Bis(silylene)-stabilized Diphosphorus Compound and its Reactivity as a Monophosphorus Anion Transfer Reagent. *Nat. Chem.* **2020**, *12*, 801-807.
41. Shan, Y. -L.; Yim, W.-L; So, C. -W. An N-heterocyclic Silylene-stabilized Digermanium(0) Complex. *Angew. Chem. Int. Ed.* **2014** *53*, 13155-13158.
42. Sen, S. S.; Jana, A.; Roesky, H. W.; Schulzke, C. A remarkable base-stabilized bis(silylene) with a silicon(I)–silicon(I) Bond. *Angew. Chem. Int. Ed.* **2009**, *48*, 8536-8538.
43. Baines, K. M.; Stibbs, W. G. The Molecular Structure of Organogermanium Compounds. *Coord. Chem. Rev.* **1995**, *145*, 157-200.
44. Yeong, H.-X.; Zhang, S.-H.; Xi, H.-W.; Guo J.-D.; Lim, K. H.; Nagase, S.; So, C.-W. An Amid–nato-stabilized Germatrisilacyclobutadiene Ylide. *Chem. - Eur. J.* **2012**, *18*, 2685-2691.
45. Beringhelli, T.; Donghi, D.; Maggioni, D.; D'Alfonso, G. Solution Structure, Dynamics and Speciation of Perfluoroaryl Boranes through ^{1}H, ^{11}B and ^{19}F NMR Spectroscopy *Coord. Chem. Rev.* **2008**, *252*, 2292-2313.
46. Siriwardane, U.; Islam, M. S.; Maguire, J. A.; Hosmane, N. S. Synthesis and structure of 2,3-bis(trimethylsilyl)-5-(trichlorogermyl)-2,3-dicarba-1-germa-closo-heptaborane. (6). A novel, potential intermediate for extended germacarboranes of mixed valences *Organometallics* **1998**, *7*, 1893-1895.
47. Rasika Dias, H. V.; Wang, Z. Germanium-Containing Heterobicyclic 10-π-Electron Ring Systems. Synthesis and Characterization of Neutral and Cationic

Germanium(II) Derivatives of Aminotroponiminates *J. Am. Chem. Soc.* **1997**, *119*, 4650-4655.

48. Leung, W.-P.; Chiu, W.-K.; Mak, T. C. W. Synthesis and Structural Characterization of Metallogermylenes, Cp-Substituted Germylene, and a Germanium(II)-Borane Adduct from Pyridyl-1-azaallyl Germanium(II) Chloride *Organometallics* **2012**, *31*, 6966-6971.
49. Del Rio, N.; Lopez-Reyes, M.; Baceiredo, A.; Saffon-Merceron, N.; Lutters, D.; Müller, T.; Kato, T. N,P-Heterocyclic Germylene/B(C6F5)3 Adducts: A Lewis Pair with Multi-reactive Sites *Angew. Chem., Int. Ed.* **2017**, *56*, 1365-1370.
50. Dong, Z.; Cramer, H. H.; Schmidtmann, M.; Paul, L. A.; Siewert, I.; Müller, T. Evidence for a Single Electron Shift in a Lewis Acid-Base Reaction *J. Am. Chem. Soc.* **2018**, *140*, 15419-15424.
51. Welch, G. C.; Prieto, R.; Dureen, M. A.; Lough, A. J.; Labeodan, O. A.; Höltrichter-Rössmann, T.; Stephan, D. W. Reactions of Phosphines with Electron Deficient Boranes *Dalton Trans* **2009**, *9*, 1559-1570.
52. Chiu, H. W.; Chervin, C. N. & Kauzlarich, S. M. Phase Changes in Ge Nanoparticles *Chem. Mater.* **2005**, *17*, 4858-4864.
53. Matthew, J. Surface Analysis by Auger and X-Ray Photoelectron Spectroscopy. D. Briggs and J. T. Grant (Eds). IMPublications, Chichester, UK and SurfaceSpectra, Manchester, UK, 2003. 900 Pp., ISBN 1-901019-04-7, 900 Pp. *Surface and Interface Analysis* **2004**, 36 (13), 1647–1647.
54. For the zwitterionic structure of other heavier cyclobutadiene analogues, see a) Yeong, H.-X.; Zhang, S.-H.; Xi, H.-W.; Guo, J.-D.– Lim, K. H.; Nagase, S.; So, C.-W. An Amidinate-Stabilized Germatrisilacyclobutadiene Ylide *Chem. - Eur. J.* **2012**, *18*, 2685-2691; b) Yeong, H.-X.; Xi, H.-W.; Li, Y.; Kunnappilly, S. B. ;

Chen, B. ; Lau, K.-C.– Hirao, H.; Lim, K. H.; So, C.-W. Zwitterionic Base-Stabilized Digermadistannacyclobutadiene and Tetragermacyclobutadiene *Chem. - Eur. J.* **2013**, *19*, 14726-14731.

55. Bentlohner, M. M.; Waibel, M.; Zeller, P.; Sarkar, K.; Müller-Buschbaum, P.; Fattakhova-Rohlfing, D.; Fässler, T. F. *Angew. Chem. Int. Ed.* **2016**, *55*, 2441
56. Sheldrick, G. M. SADABS V2014/4 (Bruker AXS Inc.) University of Göttingen, Göttingen, Germany, 2014.
57. Frisch, M. J.; Trucks, G. W.; Schlegel, H. B.; Scuseria, G. E.; Robb, M. A.; Cheeseman, J. R.; Scalmani, G.; Barone, V.; Mennucci, B.; Petersson, G. A.; Nakatsuji, H.; Caricato, M.; Li, X.;H. P. Hratchian, H. P.; Izmaylov, A. F.; Bloino, J.; Zheng, G.; Sonnenberg, J. L.; Hada, M.; Ehara, M.; Toyota, K.; Fukuda, R.; Hasegawa, J.; Ishida, M.; Nakajima, T.; Honda, Y.; Kitao, O.; Nakai, H.; Vreven, T.; Montgomery, J. A., Jr.; Peralta, J. E.; Ogliaro, F.; Bearpark, M.; Heyd, J. J.; Brothers, E.; Kudin, K. N.; Staroverov, V. N.; Keith, T.; Kobayashi, R.; Normand, J.; Raghavachari, K.; Rendell, A.; Burant, J. C. Iyengar, S. S.; Tomasi, J.; Cossi, M.; Rega, N.; Millam, J. M.; Klene, M.; Knox, J. E.; Cross, J. B.; Bakken, V.; Adamo, C.; Jaramillo, J.; Gomperts, R.; Stratmann, R. E.; Yazyev, O.; Austin, A. J.; Cammi, R.; Pomelli, C.; Ochterski, J. W.; Martin, R. L.; Morokuma, K.; Zakrzewski, V. G.; Voth, G. A.; Salvador, P.; Dannenberg, J. J.; Dapprich, S.; Daniels, A. D.; Farkas, O.; Foresman, J. B.; Ortiz, J. V.; Cioslowski, J.; Fox, D. J. Gaussian 09 (Revision B.01), Gaussian, Inc., Wallingford CT, 2010.
58. Zhao, Y.; Truhlar, D. G. *Theor. Chem. Acc.* **2008**, *120*, 215-241.
59. Weigend, F.; Hser, M.; Patzelt, H.; Ahlrichs, R. *Chem. Phys. Lett.* **1998**, *294*, 143.

60. a) Krishnan, R.; Binkley, J. S.; Seeger, R.; Pople, J. A. *J. Chem. Phys.* **1980**, *72*, 650-654; b) McLean, A. D.; Chandler, G. S. *J. Chem. Phys.* **1980**, *72*, 5639-5648; c) Curtiss, L. A.; McGrath, M. P.; Blandeau, J.-P.; Davis, N. E.; Binning, R. C., Jr.; Radom, L. *J. Chem. Phys.* **1995**, *103*, 6104-6113.
61. a) Reed, A. E.; Curtiss, L. A.; Weinhold, F. *Chem. Rev.* **1988**, *88*, 899; b) Glendening, E. D.; Reed, A. E.; Carpenter, J. E.; Weinhold– F. NBO Version 5.9.
62. Bader, R. F. W. Atoms in Molecules - A Quantum Theory; Oxford University Press: Oxford, 1990; b) Jonas, V.; Frenking, G.; Reetz, M. T. *J. Am. Chem. Soc.* **1994**, *116*, 8741.
63. Becke, A. D.; Edgecombe, K. E. *J. Chem. Phys.* **1990**, *92*, 5397–5403.
64. Lu, T.; Chen, F. J. Mol. *Mol. Graphics Modell.* **2012**, *38*, 314.

Chapter 4

Conclusion

This thesis sought to employ amidinate disilyne as a trapping reagent in reaction with sources Si(0) and Ge(0) species, in the interest of establishing new synthetic avenues towards new and challenging zero oxidation silicon and germanium molecular constructs.

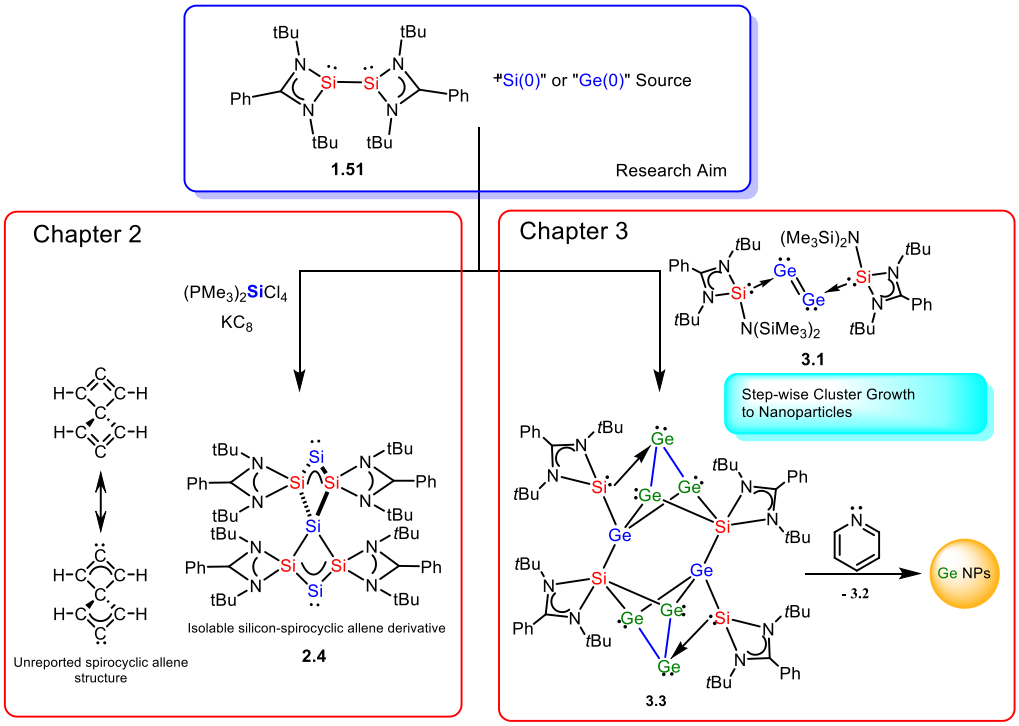

Scheme 4.1 Thesis aim and resultant complexes

In Chapter 2, we successfully synthesized the complex **2.4**. A structurally remarkable complex that could be interpreted in two ways. One, as the heavier silicon analogue of spiro[3.3]hepta-1,2,5,6-tetraene. With the carbon analogue still not yet reported, **2.4** represents the first example of a stable molecule possessing two simultaneous strained cyclic allene moieties. Alternatively, it can also be described as a silylone complex if the donor-acceptor model is applied. This represents another first in the series of known silylone complexes as the only example exhibiting currently two

simultaneous and separate silylone moieties. The occupancy of the p orbital on the silylone moiety was confirmed with the synthesis of tungsten pentacarbonyl complex **2.7**, exhibiting red-shifted CO IR resonances, ruling out the possibility of pi-backbonding from the tungsten metal. With the isolation of tetrasilacyclobutadiene analogues **2.5** and **2.6** from the same reaction, we were able to gain a deeper understanding of the formation mechanism of **2.4**. Potentially, with this knowledge, we will be able to apply a similar strategy in the development of similar homometallic and heterometallic spiro-complexes. Given the role spiro compounds play in the development of organic light emitting diode technologies, the extensive incorporation of silicon and germanium into spiro-scaffolds could see further advances in applications in optoelectronics.[1-5]

In Chapter 3, we reported first transfer of a bisgermanium (0) species in the synthesis of a digermadisilatetracyclobutadiene complex **3.2**, as well as the continued transfer of digermanium (0) species resulting in the the synthesis of a bis(trigermanium(0)) complex **3.3**. Complex **3.3** has also been demonstrated to release the bound trigermanium cluster resulting in the formation of germanium nanoparticles in pyridine. To date, transfer and release of Ge (0) species for the synthesis of larger clusters have yet to be described. This result is the first report of such a transformation occurring, and a significant step forward in our understanding regarding the mechanisms behind cluster formation in main group elements. This development could significantly change our approach to new main group element cluster complexes or even new semiconductor materials. Already, complex **3.3** presents an opportunity to form mixed metal or semiconductor clusters with controlled elemental ratios. We suggest that the preparation of metal chalcogenide clusters of the formula GeCh (Ch = S, Se, Te) would be one of the first approaches.[6-8] We expect the trigermanium cluster to be reactive

towards elemental chalcogenides, given the presence of its three lone pairs. We would expect either the direct synthesis of the GeCh semiconductor material or isolate a small oligomeric GeCh cluster complex, which would be similar to an NHC-stabilized SiTe complex previously reported by our group.[9] For now, further analysis needs to be done to properly ascertain the nature of the obtained germanium nanoparticles, and experiments involving different surfactants are currently underway to minimize surface oxidation during analysis of these nanoparticles.

In conclusion, we successfully demonstrated the synthesis of novel main group cluster-like complexes, using the amidinato disilyne scaffold, showing the importance of ligand design in cluster formation while also breaking new ground in the types of possible molecular structures that we can construct. We are excited to see where this synthetic strategy can go-expanding towards other members of the p-block, applying our current complexes in materials or optoelectronic contexts, or the synthesis of new mixed-metal clusters.

References

1. Qu, Y-.K.; Zheng, Q.; Fan, J.; Liao, L-.S.; Jiang, Z-.Q. Spiro Compounds for Organic Light-Emitting Diodes. *Acc. Mater. Res.* **2021**, *2*, 12, 1261-1271
2. Saragi, T. P. I.; Spehr, T.; Siebert, A.; Fuhrmann-Lieker, T.; Salbeck, J. Spiro Compounds for Organic Optoelectronics. *Chem. Rev.* **2007**, *107*, 1011– 1065
3. Pusztai, E.; Toulokhonova, I. S.; Temple, N.; Albright, H.; Zakai, U. I.; Guo, S.; Guzei, I. A.; Hu, R.; West, R. Synthesis and Photophysical Properties of Asymettric Substituted Silafluorenes *Organometallics*, **2013**, *32*, 9, 2529-2535
4. Li. C.; Wu. L.; Xu, W.; Song, J.; Shi, J.; Yu, P.; Kan, Y.; Wang, H. Silicon Spiro Double Helicene-like Compounds Based on Dithieno[2,3-b:3′,2′-d]thiophene: Syntheses and Crystal Structures *J. Org. Chem.* **2015**, *80*, 21, 11156–11161
5. Chan, C-.Y.; Wong, Yi-.C; Chan, M-.Y.; Cheung, S-.H.; So, S-.K.; Yam, V. W-.W. Bifunctional Heterocyclic Spiro Derivatives for Organic Optoelectronic Devices *ACS Appl. Mater. Interfaces* **2016**, *8*, 37, 24782–24792
6. Zhou, X.; Zhang, Q.; Gan, L.; Li, H; Xiong, J.; Zhai, T. Booming Development of Group IV-VI Semiconductors: Fresh Blood of 2D Family *Adv. Sci.* **2016**, *3*, 12, 1600177
7. Tan, D.; Lim, H. E.; Wang, F.; Mohamed, N. B.; Mouri, S.; Zhang, W.; Miyauchi, Y.; Ohfuchi, M.; Matsuda, K. Anisotropic optical and electronic properties of two-dimensional layered germanium sulfide *Nano Res.* **2017**, *10*, 546-555
8. Roychowdhury, S.; Samanta, M.; Perumal, S.; Biswas, K. Germanium Chalcogenide Thermoelectrics: Electronic Structure Modulation and Low Lattice Thermal Conductivity *Chem. Mater.* **2018**, *30*, 17, 5799-5813

9. Chan, Y-.C.; Leong, B-.X.; Li, Y.; Yang, M-.C.; Li, Y.; Su, M-.D.; So, C-.W. A Dimeric NHC-Silicon Monotelluride: Synthesis, Isomerization, and Reactivity *Angew. Chem., Int. Ed.* **2017**, *56*, 38, 11565-11569

Appendix

A.1 NMR Spectrum

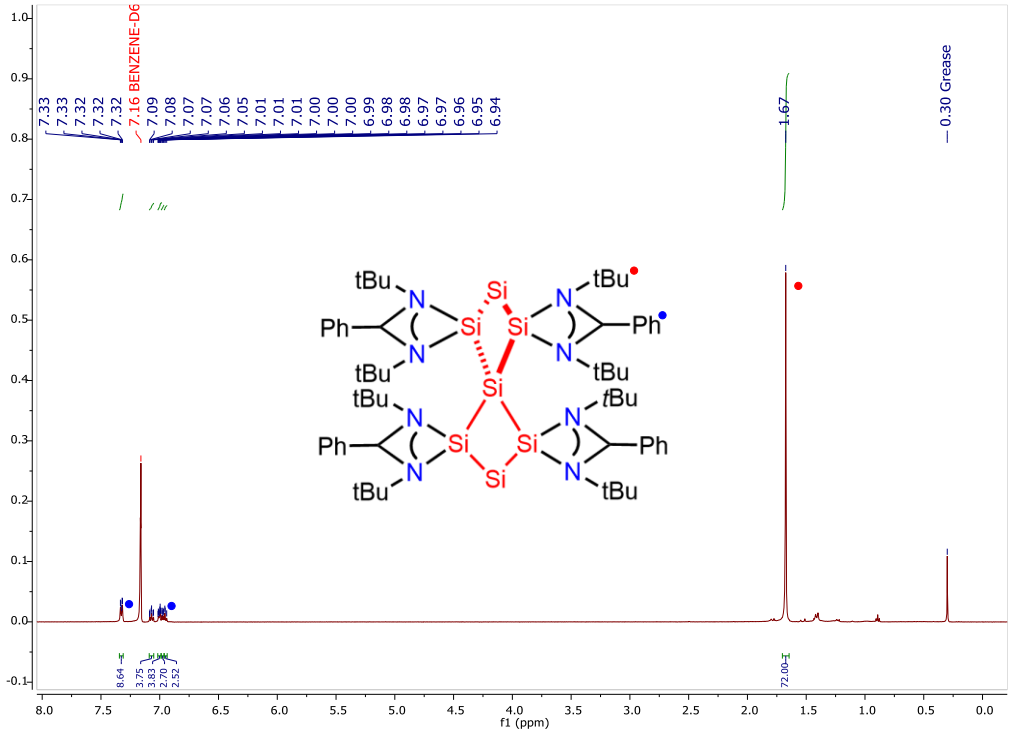

Figure A1.1 ^{1}H NMR spectrum of **2.4** in d-benzene

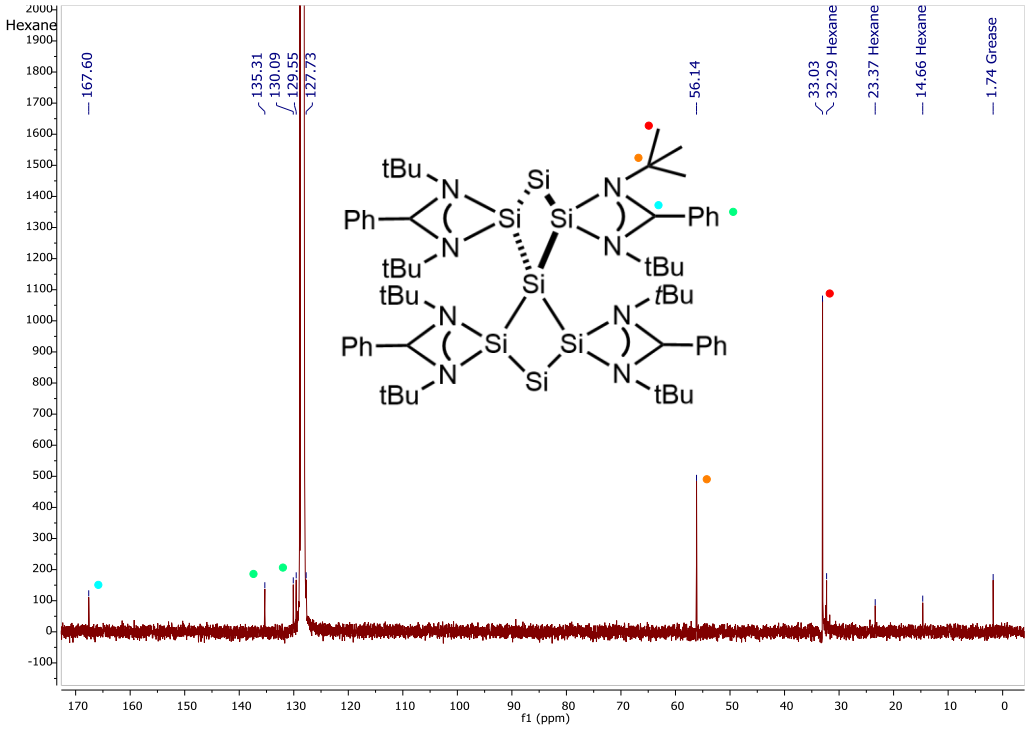

Figure A1.2 ^{13}C NMR spectrum of **2.4** in d-benzene

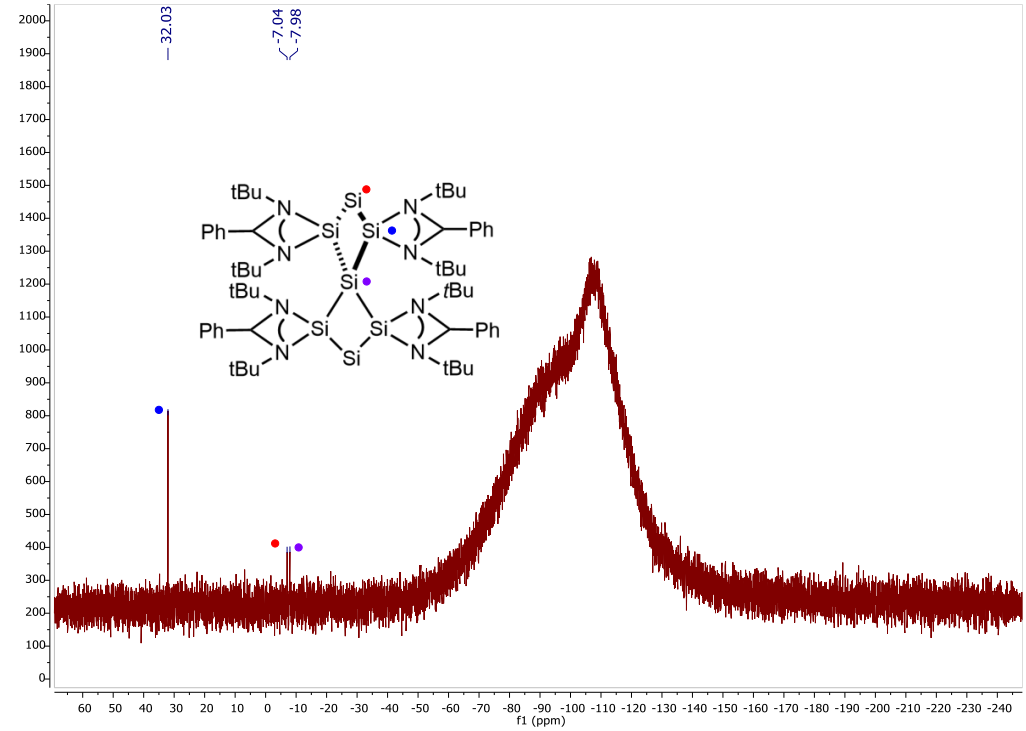

Figure A1.3 $^{29}Si\{^{1}H\}$ NMR spectrum of **2.4** in d-benzene

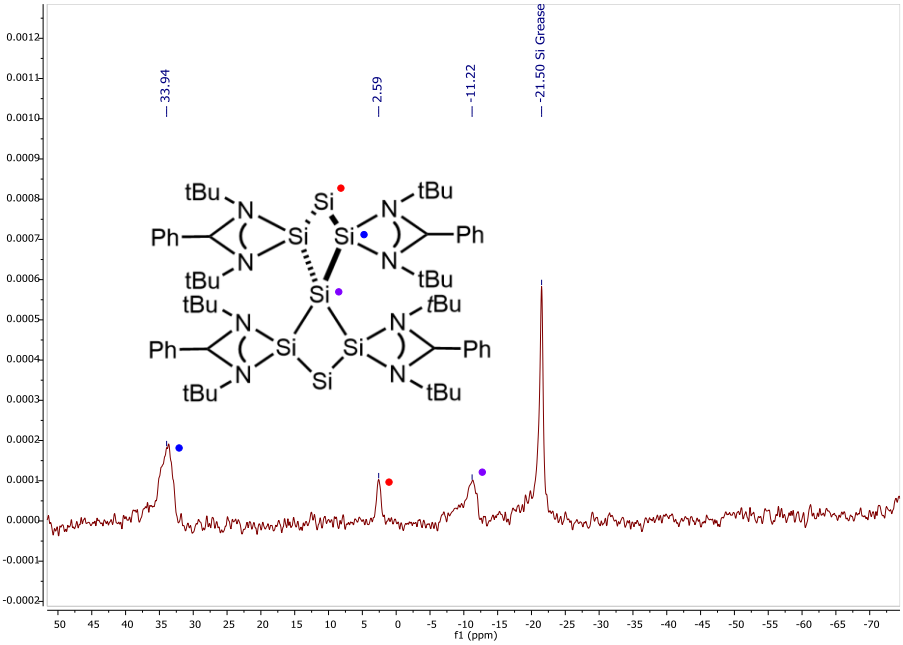

Figure A1.4 CP-MAS $^{29}Si\{^{1}H\}$ NMR spectrum of **2.4**

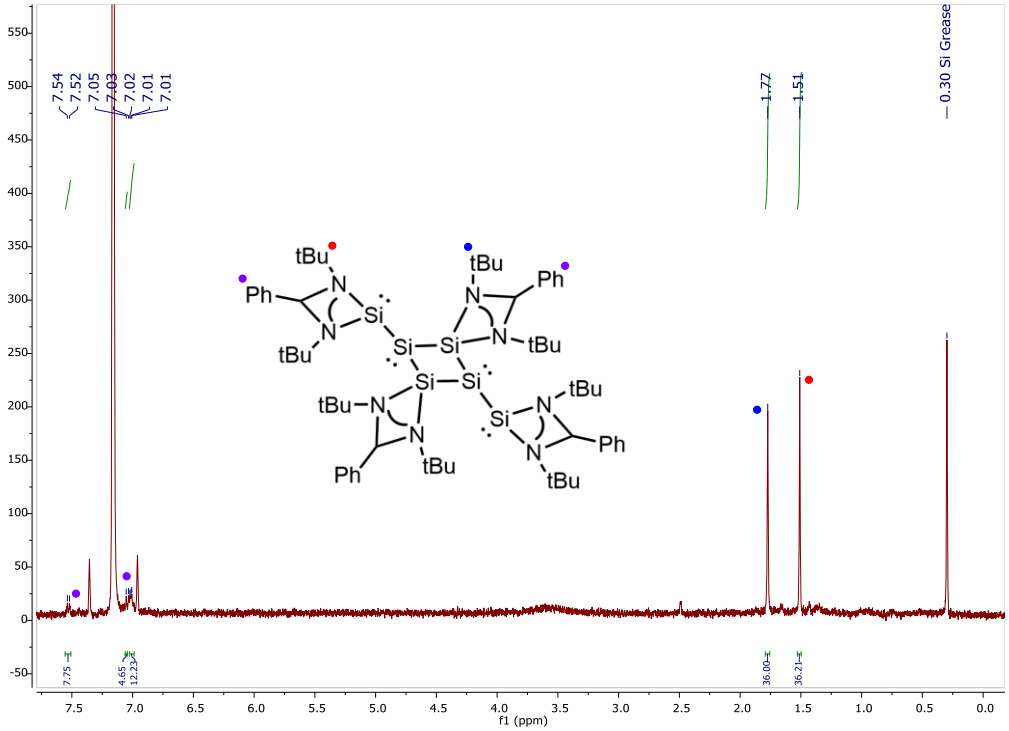

Figure A1.5 ^{1}H NMR spectrum of **2.5** in d-benzene

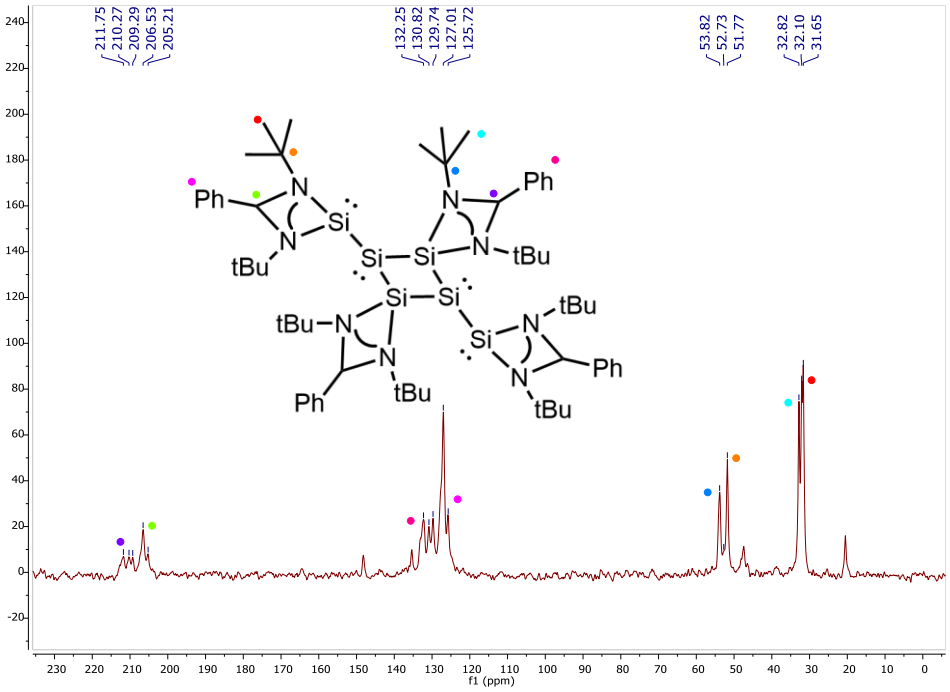

Figure A1.6 CP-MAS ^{13}C NMR spectrum of **2.5**

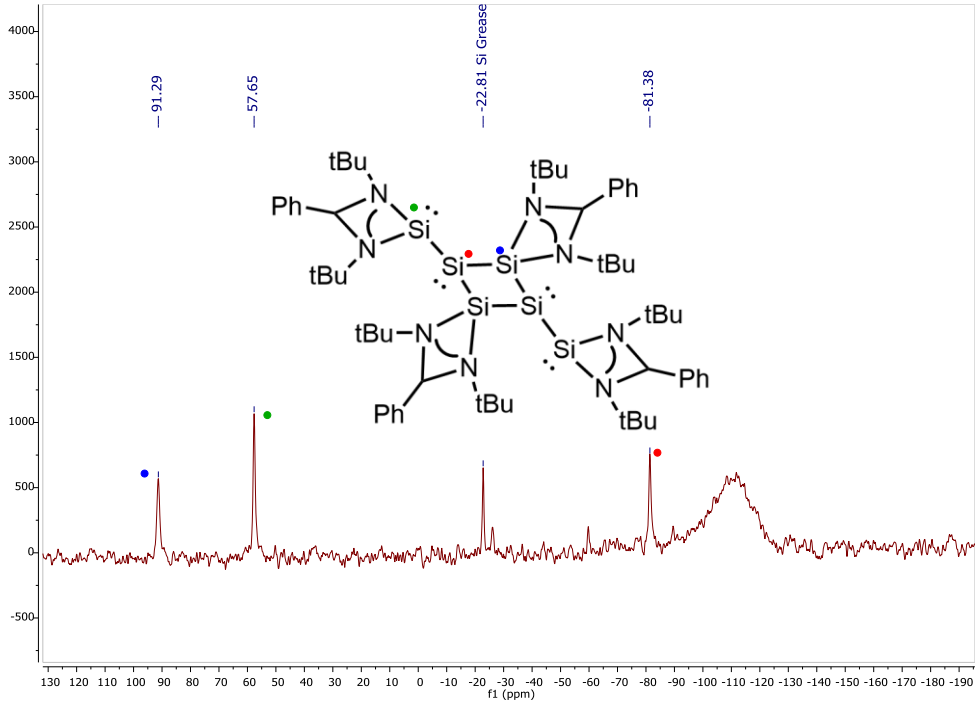

Figure A1.7 CP-MAS $^{29}Si\{^{1}H\}$ NMR spectrum of **2.5**

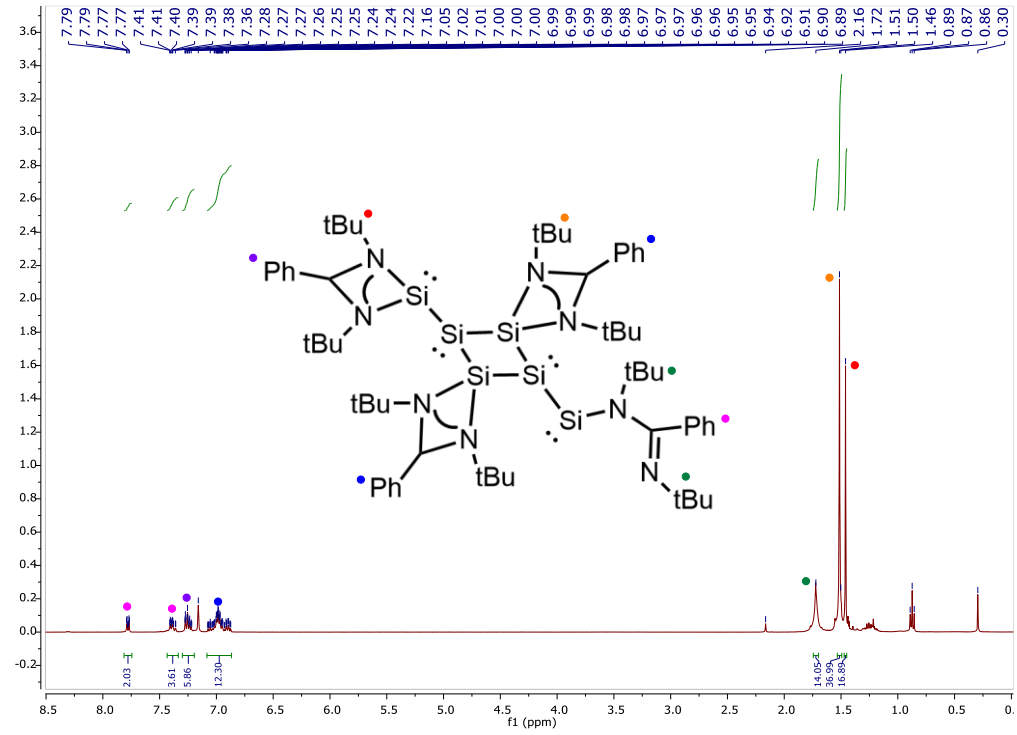

Figure A1.8 ^{1}H NMR spectrum of **2.6** in d-benzene

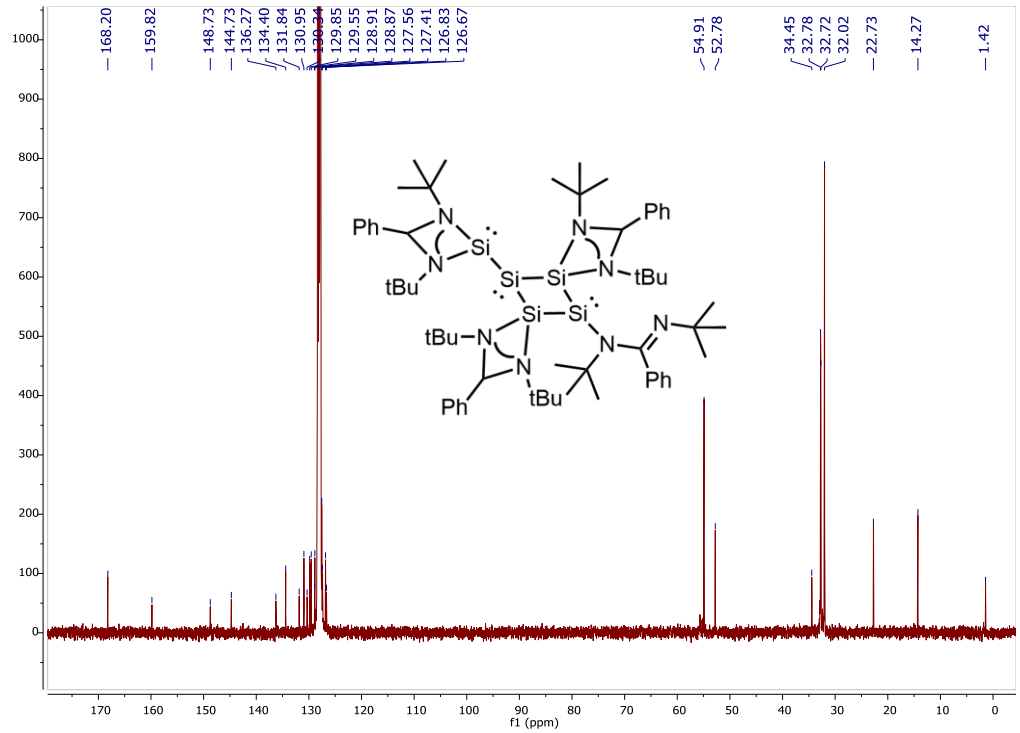

Figure A1.9 ^{13}C NMR spectrum of **2.6** in d-benzene

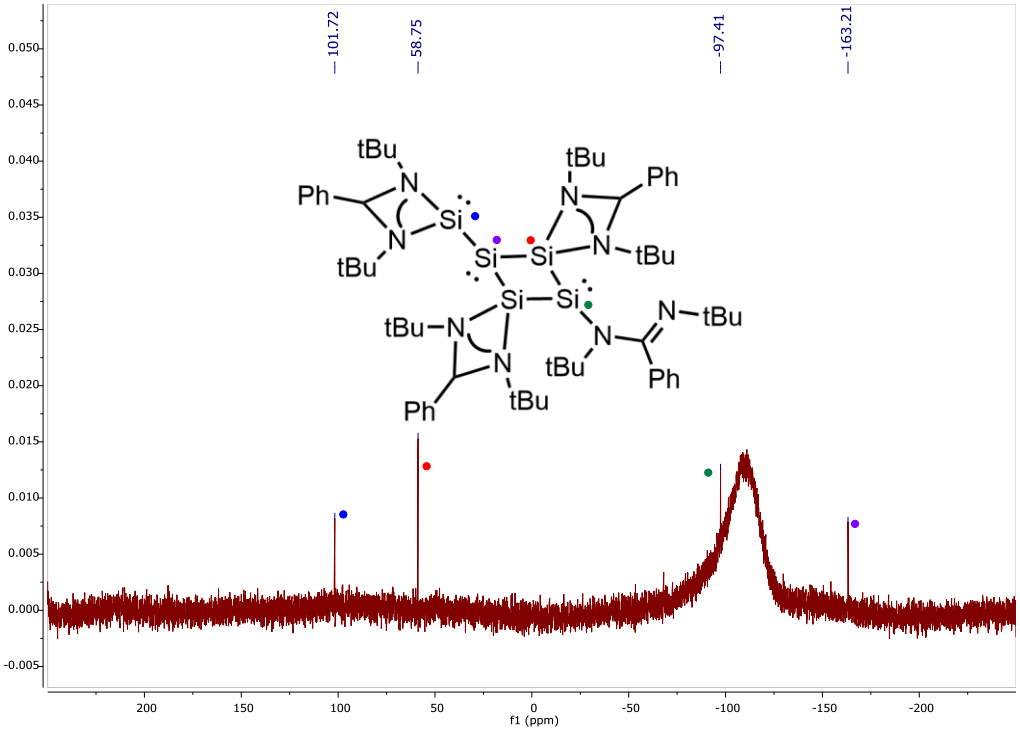

Figure A1.10 ^{29}Si{^{1}H} NMR spectrum of **2.6** in d-benzene

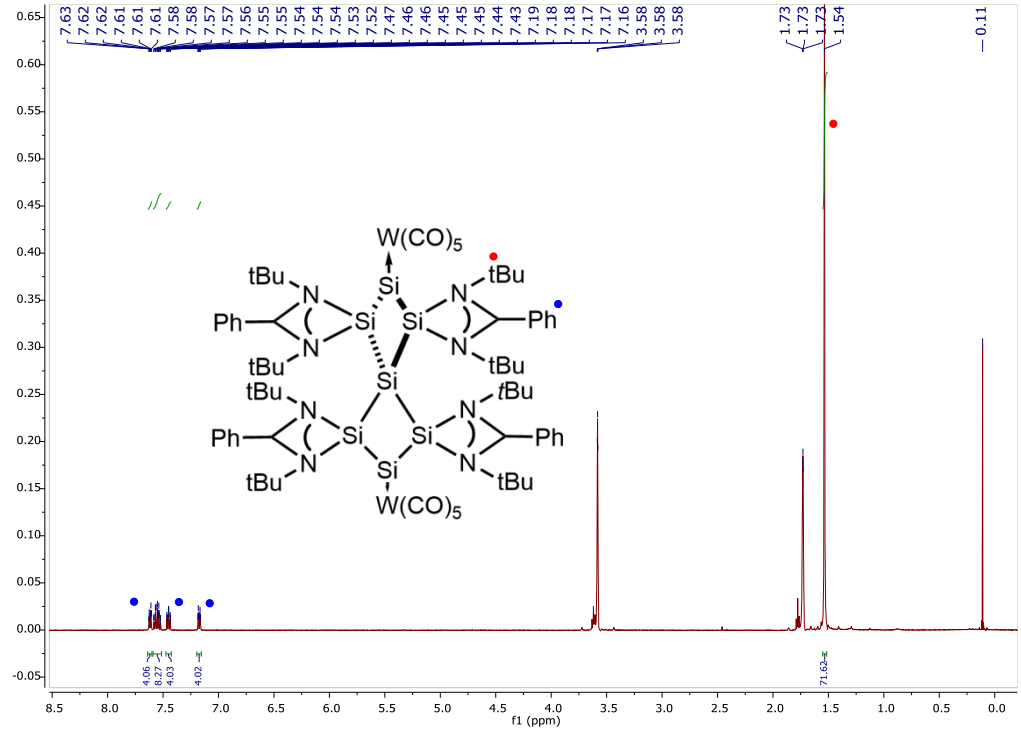

Figure A1.11 ^{1}H NMR spectrum of **2.7** in d8-THF

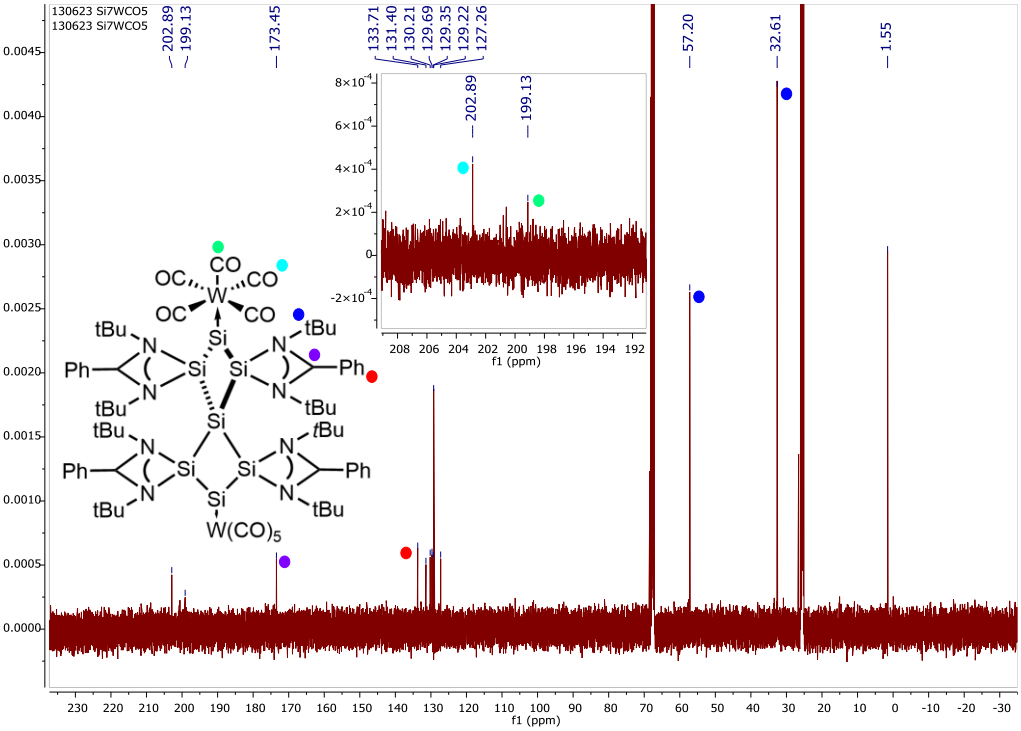

Figure A1.12 ^{13}C NMR spectrum of **2.7** in d8-THF

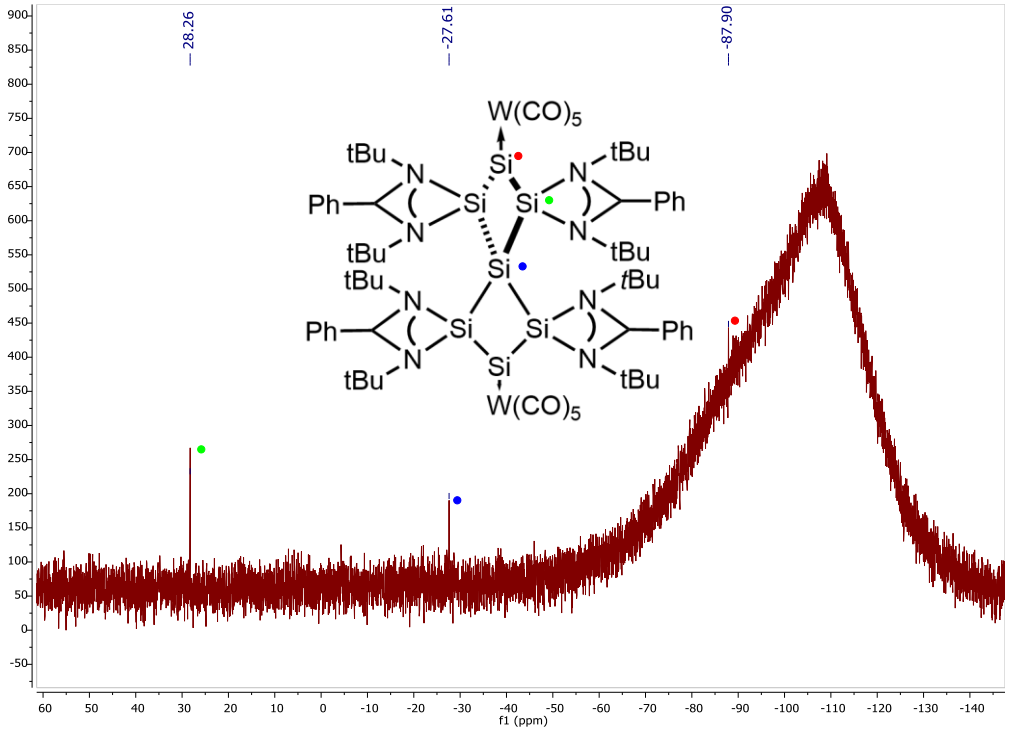

Figure A1.13 $^{29}Si\{^{1}H\}$ NMR spectrum of **2.7** in d8-THF

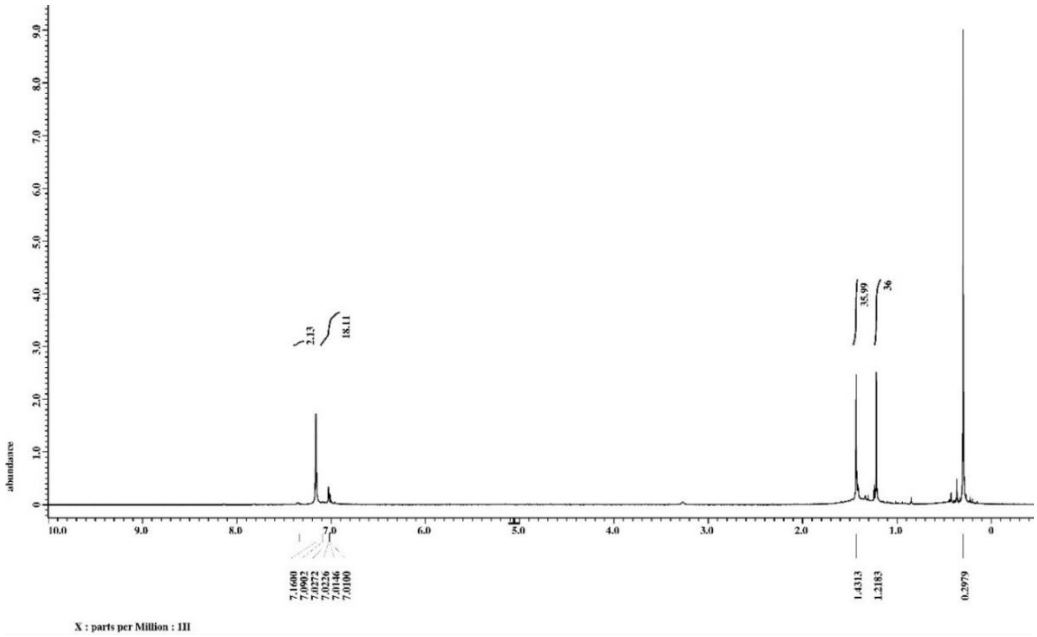

Figure A1.14 ^{1}H NMR spectrum of **3.2** in d-benzene

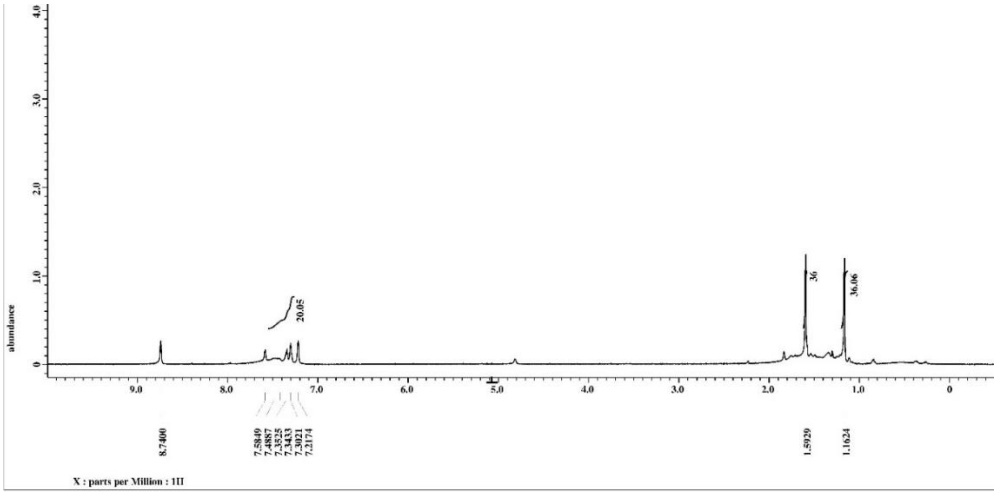

Figure A1.15 ^{1}H NMR spectrum of **3.2** in d-pyridine

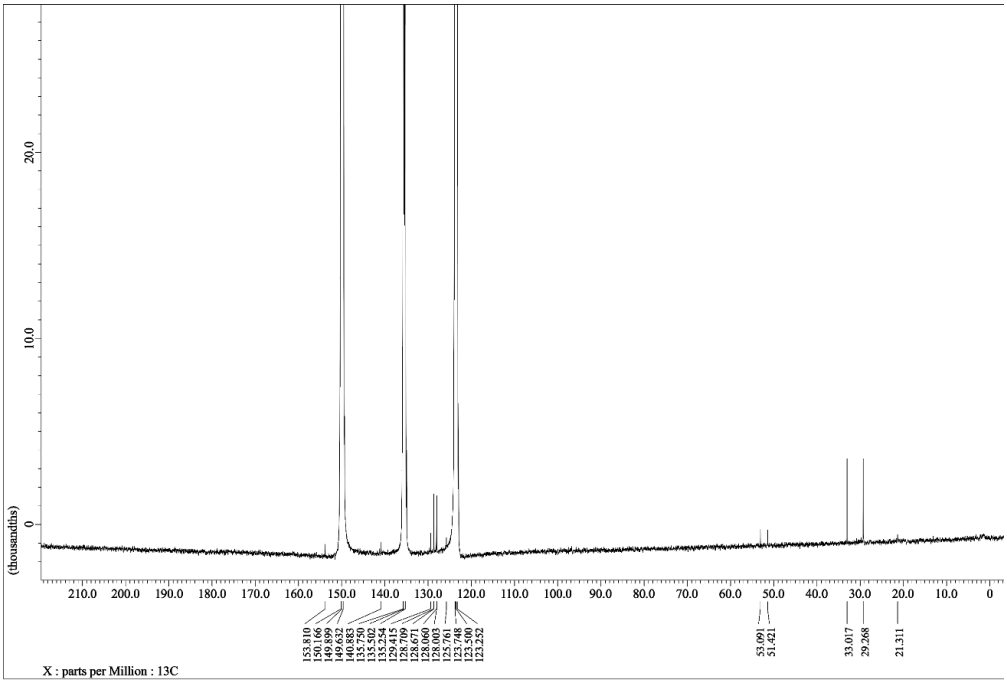

Figure A1.16 ^{13}C NMR spectrum of **3.2** in d-pyridine

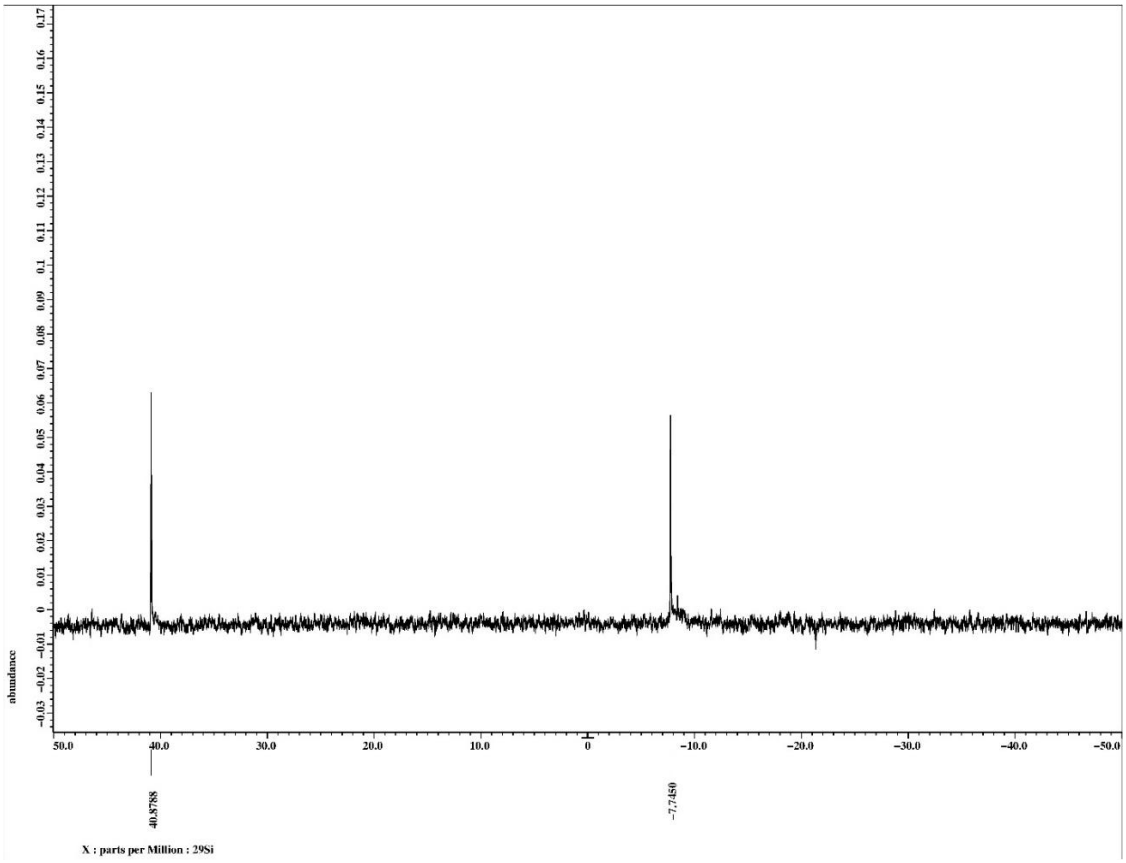

Figure A1.17 $^{29}Si\{^{1}H\}$ NMR spectrum of **3.2** in d-benzene

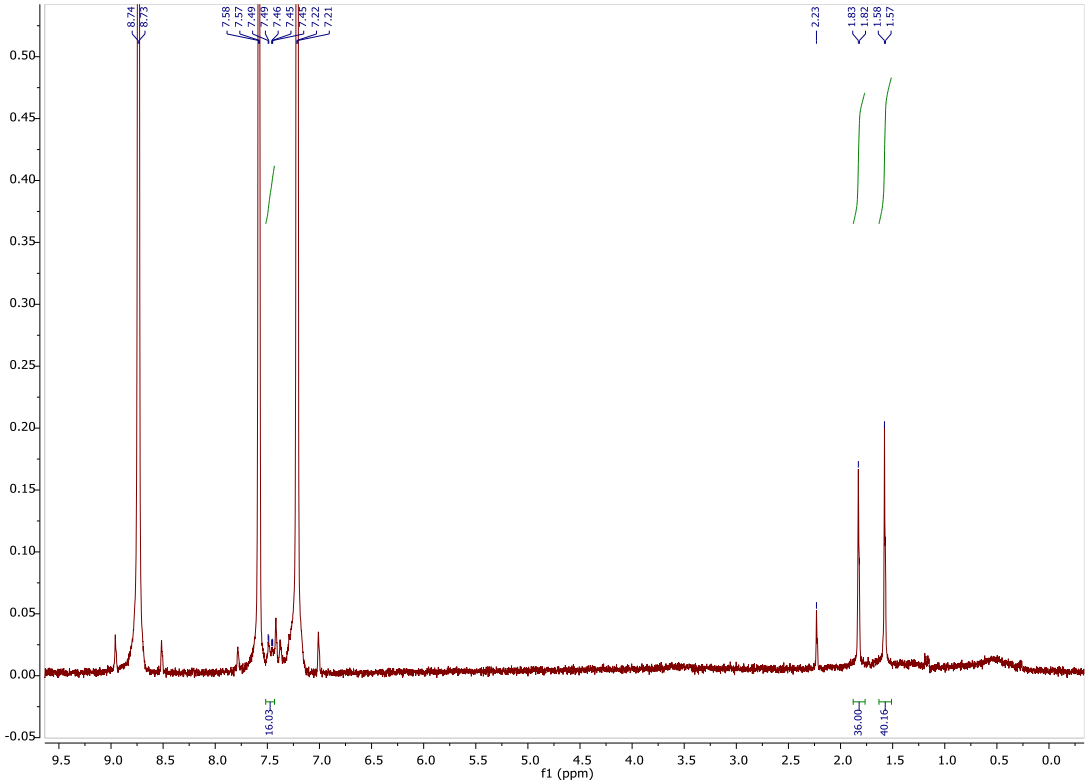

Figure A1.18 $^{29}Si\{^{1}H\}$ NMR spectrum of **3.3** in d-pyridine

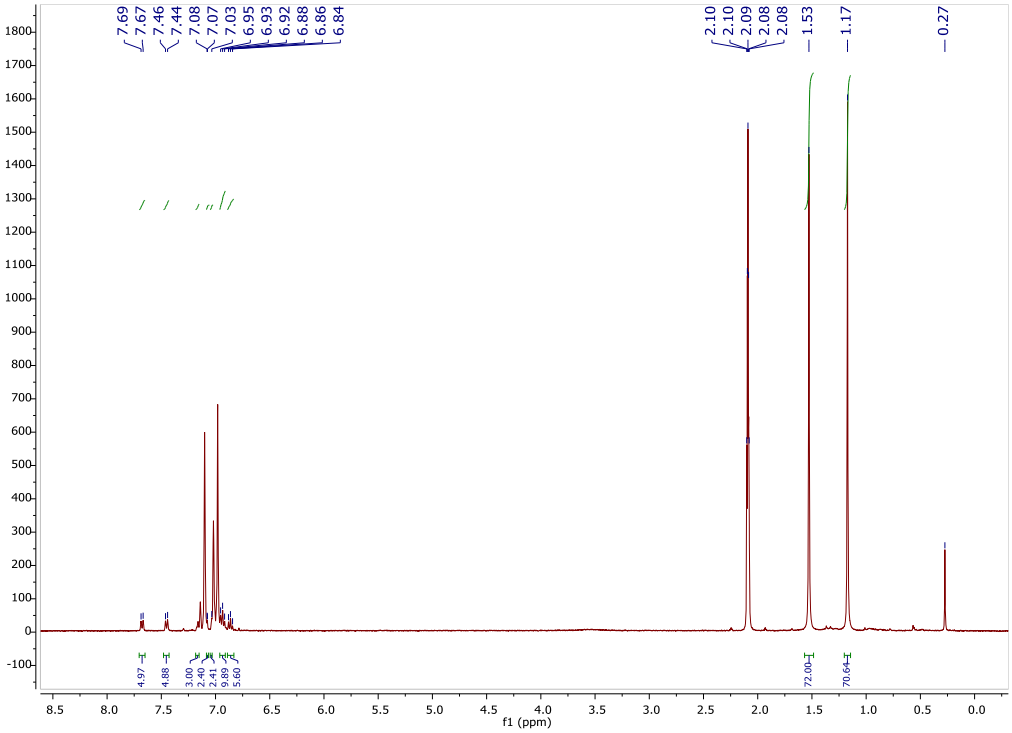

Figure A1.19 ^{1}H NMR spectrum of **3.4** in d-benzene

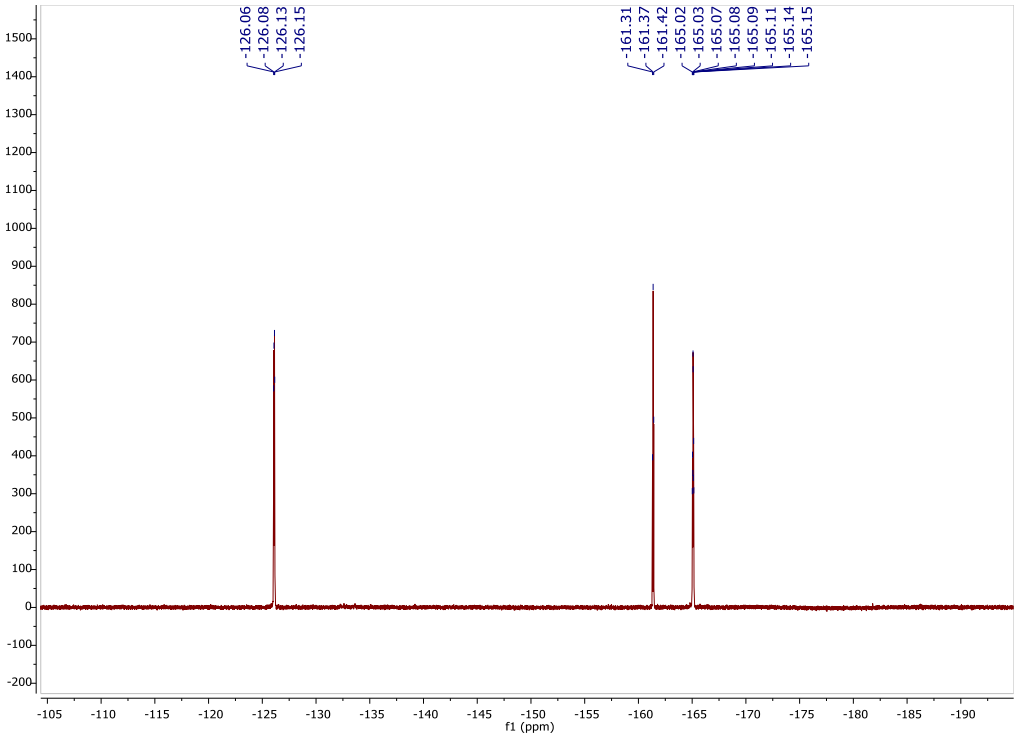

Figure A1.20 $^{19}F\{^{1}H\}$ NMR spectrum of **3.4** in d-benzene

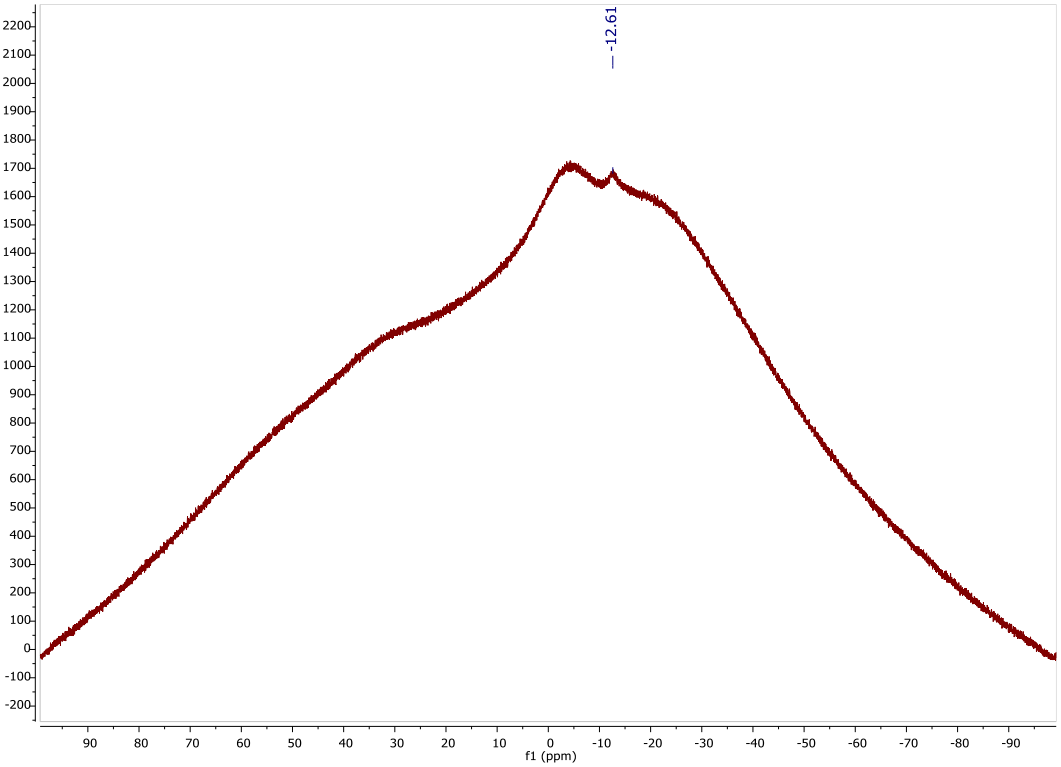

Figure A1.21 $^{11}B\{^{1}H\}$ NMR spectrum of **3.4** in d-benzene

A.2 Computational Data

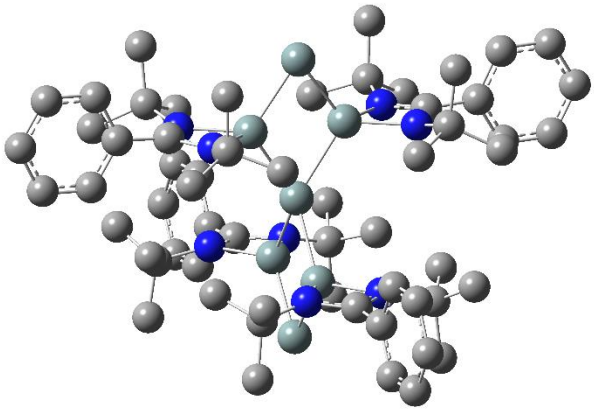

Figure A2.1 Optimized Structure of compound **2.4**

Natural bond orbital (NBO) analysis at M06-2X/def2-SVP level

Bond type	Occupancy	Polarization	Hybridization	Bond Length(Å)	WBI
σ-Bonding-Si_1Si_2	1.90	Si_1: 40.72% Si_2: 59.28%	Si_1: $sp^{6.83}$ Si_2: $sp^{1.07}$	2.26	1.31
σ-Bonding-Si_2Si_4	1.94	Si_2: 47.03% Si_4: 52.97%	Si_2: $sp^{1.75}$ Si_4: $sp^{3.00}$	2.36	0.90
σ-Bonding-Si_1Si_3	1.90	Si_1: 40.71% Si_3: 59.29%	Si_1: $sp^{6.83}$ Si_3: $sp^{1.07}$	2.26	1.31
σ-Bonding-Si_3Si_4	1.94	Si_3: 47.00% Si_4: 53.00%	Si_3: $sp^{1.75}$ Si_4: $sp^{2.99}$	2.36	0.90
σ-Bonding-Si_4Si_5	1.94	Si_4: 53.01% Si_5: 46.99%	Si_4: $sp^{2.99}$ Si_5: $sp^{1.76}$	2.36	0.90
σ-Bonding-Si_4Si_6	1.94	Si_4: 53.00%	Si_4: $sp^{2.99}$	2.36	0.90

		Si_6: 47.00%	Si_5: $sp^{1.75}$		
σ-Bonding-Si_5Si_7	1.90	Si_5: 59.30% Si_7: 40.70%	Si_5: $sp^{1.07}$ Si_7: $sp^{6.83}$	2.26	1.31
σ-Bonding-Si_6Si_7	1.90	Si_6: 59.30% Si_7: 40.70%	Si_6: $sp^{1.07}$ Si_7: $sp^{6.83}$	2.26	1.31
3C-Bonding-$Si_2Si_1Si_3$	1.88	Si2: 26.07% Si1: 47.84% Si3: 26.09%	Si2: $p^{1.00}$ Si1: $p^{1.00}$ Si3: $p^{1.00}$	--	--
3C-Bonding-$Si_5Si_7Si_6$	1.88	Si5: 25.28% Si7: 48.50% Si6: 26.22%	Si5: $p^{1.00}$ Si7: $p^{1.00}$ Si6: $p^{1.00}$	--	--
Lone pair-Si_1	1.91	--	$sp^{0.33}$	--	--
Lone pair-Si_7	1.91	--	$sp^{0.33}$	--	--

Table A2.1. NBO results of compound **2.4** at M06-2X/def2-SVP theory

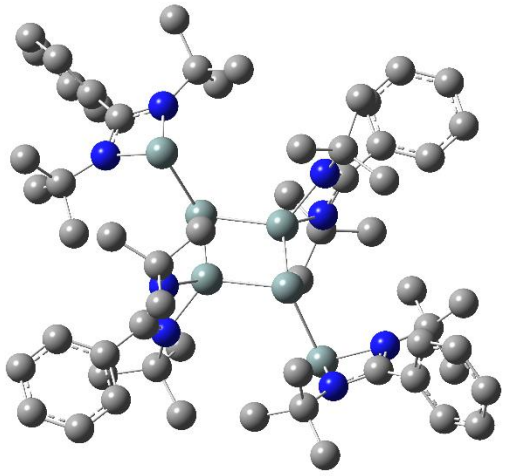

Figure A2.2 Optimized Structure of compound **2.5**

Natural bond orbital (NBO) analysis at M06-2X/def2-SVP level

Bond type	Occupancy	Polarization	Hybridization	Bond Length(Å)	WBI
σ-Bonding-Si_1Si_2	1.84	Si_1: 43.69% Si_2: 56.31%	Si_1: $sp^{6.17}$ Si_2: $sp^{7.26}$	2.42	0.90
σ-Bonding-Si_2Si_3	1.91	Si_2: 44.41% Si_3: 55.59%	Si_2: $sp^{7.11}$ Si_3: $sp^{1.37}$	2,33	1.06
σ-Bonding-Si_2Si_4	1.91	Si_2: 44.38% Si_4: 55.62%	Si_2: $sp^{7.23}$ Si_4: $sp^{1.41}$	2.33	1.06
σ-Bonding-Si_3Si_5	1.91	Si_3: 54.74% Si_5: 45.26%	Si_3: $sp^{1.41}$ Si_5: $sp^{6.68}$	2.32	1.07
σ-Bonding-Si_4Si_5	1.91	Si_4: 54.71% Si_5: 45.29%	Si_4: $sp^{1.36}$ Si_5: $sp^{6.44}$	2.31	1.10
σ-Bonding-Si_5Si_6	1.85	Si_5: 57.37%	Si_5: $sp^{6.63}$	2.41	0.90

		Si_6: 42.63%	Si_6: $sp^{6.22}$		
Lone pair-Si_1	1.93	--	$sp^{0.37}$	--	--
Lone pair-Si_2	1.76	--	$sp^{0.57}$	--	--
Lone pair-Si_5	1.72	--	$sp^{0.65}$	--	--
Lone pair-Si_6	1.94	--	$sp^{0.37}$	--	--

Table A2.2 NBO results of compound **2.5** at M06-2X/def2-SVP theory

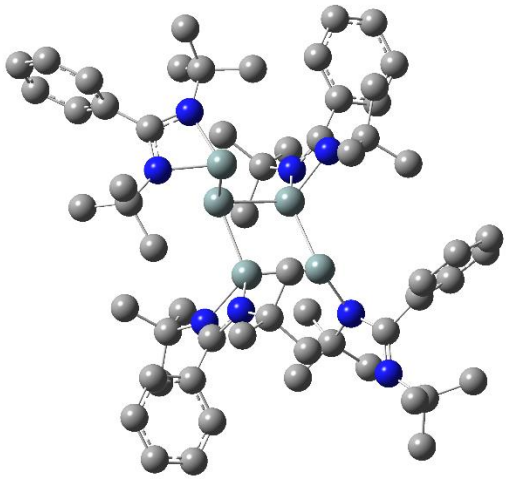

Figure A2.3 Optimized Structure of compound **2.6**

Natural bond orbital (NBO) analysis at M06-2X/def2-SVP level

Bond type	Occupancy	Polarization	Hybridization	Bond Length(Å)	WBI
σ-Bonding-Si_1Si_2	1.86	Si_1: 43.04% Si_2: 56.96%	Si_1: $sp^{6.35}$ Si_2: $sp^{6.71}$	2.43	0.90
σ-Bonding-Si_2Si_3	1.90	Si_2: 43.58% Si_3: 56.42%	Si_2: $sp^{7.69}$ Si_3: $sp^{1.44}$	2.34	1.03
σ-Bonding-Si_2Si_5	1.89	Si_2: 43.68% Si_5: 56.32%	Si_2: $sp^{8.03}$ Si_5: $sp^{1.38}$	2.35	1.01
σ-Bonding-Si_3Si_4	1.89	Si_3: 51.81% Si_4: 48.19%	Si_3: $sp^{1.84}$ Si_4: $sp^{2.06}$	2.28	1.13
π-Bonding-Si_3Si_4	1.67	Si_3: 17.63% Si_4: 82.37%	Si_3: $sp^{16.71}$ Si_4: $sp^{8.41}$		

σ-Bonding-Si_4Si_5	1.93	Si_4: 46.53% Si_5: 53.47%	Si_4: $sp^{2.13}$ Si_5: $sp^{1.58}$	2.29	1.13
Lone pair-Si_1	1.94	--	$sp^{0.36}$	--	--
Lone pair-Si_2	1.77	--	$sp^{0.54}$	--	--

Table A2.3 NBO results of compound **2.6** at M06-2X/def2-SVP theory

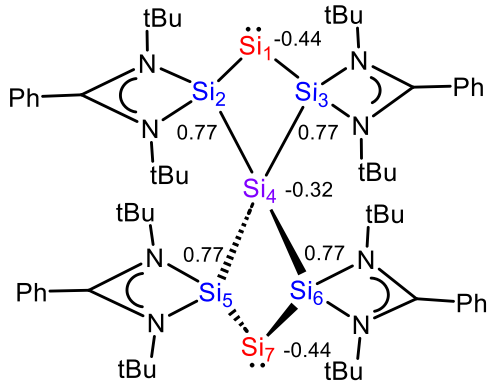	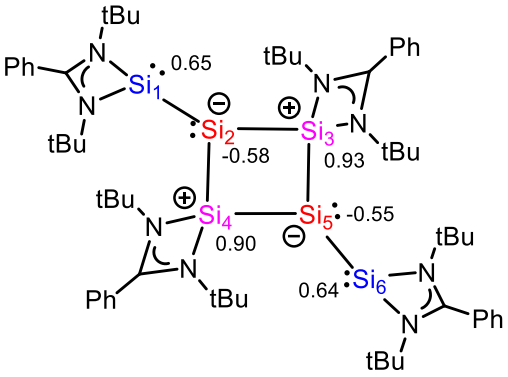
2.4	**2.5**
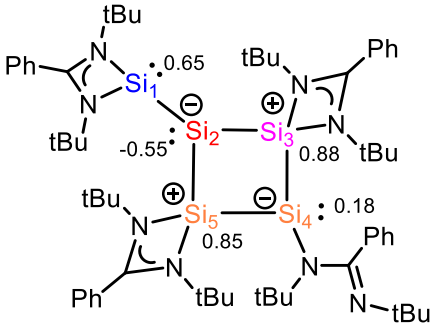	
2.6	

Table A2.4 Selected NPA charges for silicon centers of compounds **2.4**, **2.6** and **2.7** at M06-2X/def2-SVP theory

a) b)

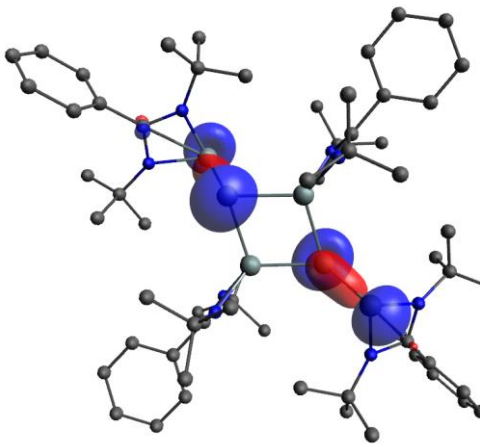

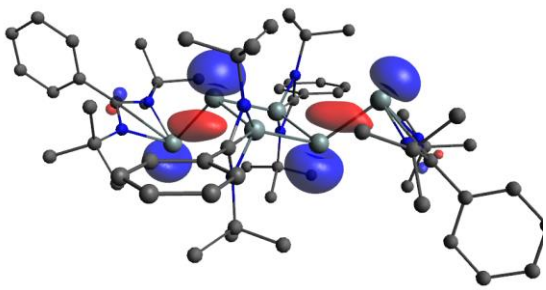

Figure A2.4 The HOMO of compound **2.5** a) top view b) side view

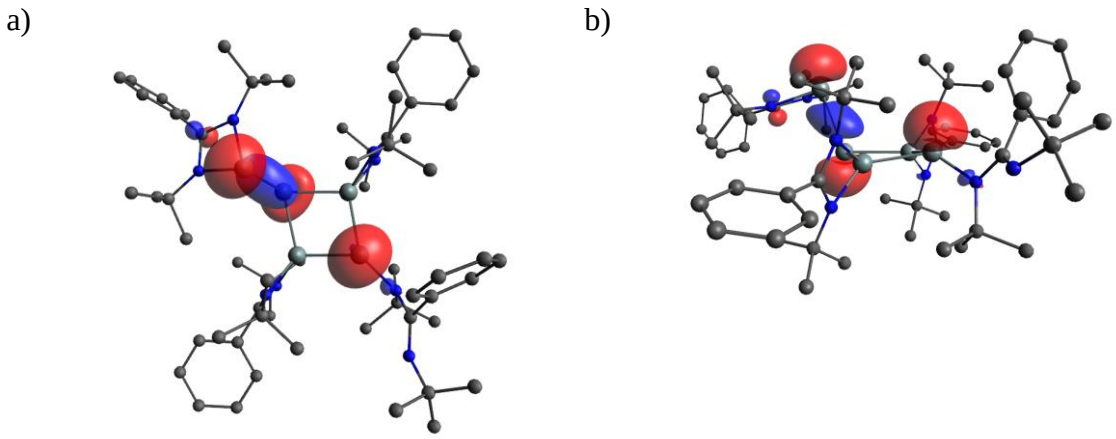

Figure A2.5 The HOMO of compound **2.6** a) top view b) side view

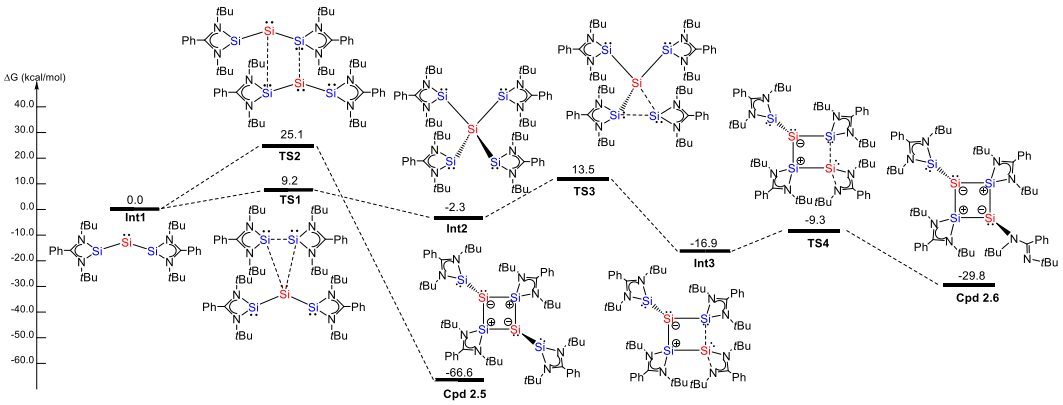

Figure A2.6 Mechanistic study for the formation of compounds 2.5 and 2.6 and formation of Int2

M06-2X /def2-SVP

Compound 2.4

C	12.07125700	10.04291800	11.55031600
C	12.32908700	8.53684500	11.42081000
H	13.03420100	8.34155700	10.59868400
H	11.39332800	7.98547200	11.23730100
H	12.75953600	8.15767500	12.35826300
C	13.36637600	10.72700300	12.01216400
H	14.17483500	10.54129800	11.28884700
H	13.66854700	10.33604300	12.99518100
H	13.22258900	11.81490500	12.08996200
C	11.63352000	10.62967600	10.20246600
H	12.36823300	10.34399100	9.43472100
H	11.58713200	11.72686300	10.22871900
H	10.65123900	10.24611300	9.89651000
C	10.36789000	11.24268700	13.01910700
C	10.18446300	12.51757100	12.27175900
C	11.05381600	13.59817000	12.43749200
H	11.89346200	13.51915300	13.13050000
C	10.84381100	14.77306600	11.71543600
H	11.52285000	15.61684300	11.84509800
C	9.77015600	14.86875000	10.83104700
H	9.60862000	15.78875400	10.26750000
C	8.90207100	13.78791200	10.66639900
H	8.06183300	13.86170800	9.97468700
C	9.10700900	12.61309000	11.38471200
H	8.43534100	11.75965000	11.26530600
C	9.21458800	11.78439400	15.22688300
C	10.31984300	12.58891700	15.92675500
H	9.90317200	13.14835900	16.77803500
H	10.77090400	13.31285100	15.23204600
H	11.10419700	11.91040700	16.29403200
C	8.15191600	12.74358400	14.67635900
H	7.63635600	13.22596900	15.52036700
H	7.40240900	12.21169300	14.07553500
H	8.59608400	13.53619100	14.05908500
C	8.59080800	10.81961800	16.24241800
H	8.04861900	11.38268400	17.01716500
H	9.38432400	10.22839100	16.72055500
H	7.89958000	10.11557700	15.75263300
C	13.17976800	4.73361400	14.92481000
C	13.00968600	5.26870600	13.49789000
H	13.75940600	4.81651700	12.83105900
H	13.14394800	6.35950500	13.49792500
H	12.00108900	5.05711400	13.10891000
C	14.51473000	5.24494200	15.48604600
H	15.34852600	4.91005100	14.85050000
H	14.68307500	4.85548900	16.50096900
H	14.51128900	6.34460400	15.52161500
C	13.17546600	3.19988100	14.92647300
H	13.92303300	2.84078700	14.20325600
H	12.19550700	2.80033600	14.63369000
H	13.43927500	2.79051700	15.91108900
C	11.66499000	5.08450500	16.94515100
C	12.00128400	3.89400700	17.77403200
C	13.10590300	3.88351800	18.62888100
H	13.74680800	4.76427900	18.69958800
C	13.38342000	2.74681300	19.38830300
H	14.24612500	2.73902300	20.05579700
C	12.56113300	1.62473100	19.29490100
H	12.78041800	0.73722100	19.89014300

C	11.45733800	1.63661900	18.44022300
H	10.81334400	0.75926800	18.36653000
C	11.17592400	2.76847000	17.67998100
H	10.31519600	2.79089400	17.00736600
C	10.33804300	6.49134600	18.60609400
C	11.48279900	7.12771800	19.40809100
H	11.10049600	7.54784800	20.35075000
H	11.95134600	7.93196000	18.82145400
H	12.24647200	6.37560000	19.65580800
C	9.72595300	5.33869000	19.41183400
H	9.22564800	5.75216200	20.30041900
H	10.49011900	4.62968400	19.75811800
H	8.98012500	4.78782000	18.82368500
C	9.28147100	7.56522200	18.31963700
H	8.79916200	7.88268500	19.25657700
H	8.51370800	7.19518500	17.62180500
H	9.76252000	8.43603700	17.85259700
C	9.87063200	3.13694500	12.14673400
C	9.68936900	3.13358600	13.66937100
H	9.85687300	2.12218100	14.06956200
H	8.66655900	3.45073300	13.91667600
H	10.38320800	3.83734100	14.15588700
C	11.22755600	2.53081300	11.76742100
H	11.32292900	1.54447900	12.24584200
H	12.05915500	3.16021400	12.11070900
H	11.32323700	2.38684700	10.68265000
C	8.74271700	2.30853300	11.51423700
H	8.76484800	1.27756300	11.89877000
H	8.85986000	2.26670500	10.42120500
H	7.76708100	2.75829500	11.75159700
C	9.91967800	5.12691200	10.55470500
C	10.70245200	4.57173900	9.41606500
C	10.10127900	3.81075400	8.41093400
H	9.02910000	3.60952100	8.44890800
C	10.87558500	3.31193200	7.36324100
H	10.40596300	2.71756400	6.57835300
C	12.24472000	3.57197400	7.31912000
H	12.84763200	3.18064100	6.49847500
C	12.84420400	4.33276900	8.32445500
H	13.91524800	4.53681600	8.29080100
C	12.07611900	4.83283900	9.37237000
H	12.53235700	5.42962300	10.16579200
C	9.00293900	7.27449500	9.53249800
C	10.16831500	7.56211900	8.57763500
H	9.88702600	8.39287700	7.91314100
H	10.40459600	6.69467500	7.94652900
H	11.07493100	7.85253600	9.12472700
C	7.81258000	6.71883100	8.73701900
H	7.46824300	7.45919800	7.99905600
H	6.98259000	6.48009100	9.41861600
H	8.10212200	5.80668000	8.19441500
C	8.56283000	8.55982600	10.24348400
H	8.35015200	9.34807400	9.50546400
H	9.33613300	8.91473300	10.94296200
H	7.65254700	8.36203400	10.82673300
C	5.33647800	9.49135100	14.26973500
C	6.29852100	9.91832200	13.15452400
H	5.91040900	10.80967200	12.63870800
H	6.40136700	9.10094600	12.42700500
H	7.30168900	10.13629000	13.55401300
C	5.04090800	10.67173900	15.20326300
H	4.70407400	11.52753900	14.59914400
H	5.93586500	10.97699000	15.76134000
H	4.24467500	10.43614700	15.92235900
C	4.02880400	8.99954200	13.63215800
H	3.57570500	9.79824600	13.02549800
H	3.30540300	8.70963500	14.40864900

H	4.22839600	8.12996100	12.98830400
C	5.67080000	7.70777100	16.06049700
C	4.75092700	8.18736500	17.12873200
C	3.38760300	7.88395300	17.11691300
H	2.97187900	7.28054100	16.30784000
C	2.56469100	8.35413200	18.14052600
H	1.49999500	8.11704500	18.13127700
C	3.10080200	9.12424200	19.17185600
H	2.45480700	9.49049900	19.97100800
C	4.46359000	9.42686100	19.18217600
H	4.88387600	10.02936700	19.98857000
C	5.28932500	8.96013900	18.16310900
H	6.35764400	9.18923200	18.15902400
C	6.22478800	5.36199700	16.89117100
C	4.97998100	4.59538800	16.42075800
H	4.90774100	3.62866700	16.94183200
H	5.03615900	4.41469700	15.33696800
H	4.06720500	5.16917000	16.63964400
C	6.11445000	5.64576000	18.39450800
H	6.17330800	4.69282500	18.94158200
H	5.15838800	6.12092600	18.65273800
H	6.93040400	6.29238400	18.74339600
C	7.46709500	4.51296700	16.59578200
H	7.46462700	3.60663900	17.22013900
H	8.39266200	5.08061800	16.78099600
H	7.46523900	4.21718700	15.53727000
N	11.05610400	10.18586300	12.60032500
N	9.82143500	10.93937900	14.19184100
N	12.08006300	5.31425000	15.70383700
N	10.84888300	6.07308500	17.29549700
N	9.72582700	4.53644500	11.72941800
N	9.34873900	6.32601500	10.59766300
N	5.98702900	8.36539900	14.94973100
N	6.36929400	6.57763600	16.08211000
Si	10.71178700	9.24907800	14.22924000
Si	12.39650500	8.90867800	15.69445600
Si	11.18609800	7.00219600	15.66051800
Si	9.40429600	7.28803400	14.14224300
Si	8.63354000	5.98182300	12.33602900
Si	6.41071900	5.67220200	12.58779500
Si	7.08314100	6.92352900	14.34379900

Compound 2.5

C	2.38325100	8.57083300	8.38479200
C	1.53161700	7.95089200	9.50037900
H	0.86298000	7.18259100	9.08150900
H	0.92646700	8.70171700	10.02660100
H	2.19008200	7.47040500	10.23881300
C	3.18746900	9.76017000	8.92408300
H	3.86915600	10.13838000	8.14668800
H	3.79665100	9.43605300	9.78101400
H	2.52911600	10.57182500	9.26345400
C	3.36868900	7.51980300	7.86588000
H	2.84165300	6.61875400	7.52027800
H	4.06816500	7.24622500	8.66910400
H	3.95172000	7.92596000	7.02361600
C	0.37890000	9.61577300	7.20080700
C	-0.32556900	10.25657300	8.34808700
C	0.10513700	11.49228400	8.83893100
H	0.96221600	11.98246600	8.37613400
C	-0.57123800	12.09783600	9.89629400

H	-0.23493300	13.06571800	10.27038300
C	-1.67560900	11.47007000	10.47172100
H	-2.20368500	11.94458800	11.30003200
C	-2.10297900	10.23322100	9.98802800
H	-2.96224100	9.73572300	10.43975800
C	-1.43236600	9.62796100	8.92738000
H	-1.75135400	8.65460100	8.55256200
C	-1.23419300	10.16495800	5.29004100
C	-1.49636900	11.59630200	5.77443700
H	-1.88700600	11.62381600	6.80061500
H	-2.24238200	12.06717700	5.11774300
H	-0.57249500	12.19269300	5.73208500
C	-2.47086800	9.28886100	5.52010100
H	-2.71016800	9.20728200	6.58997000
H	-2.29974800	8.28210800	5.10990400
H	-3.34037500	9.72702400	5.00751700
C	-0.93179600	10.18474400	3.78914600
H	-1.80348400	10.56844800	3.23981800
H	-0.71986500	9.16313600	3.43479100
H	-0.05492400	10.80978600	3.56596600
C	6.71274100	10.23931100	2.59489500
C	6.05271500	10.29185000	1.21136700
H	5.90735500	11.32856500	0.87801400
H	5.07227200	9.79360100	1.25058000
H	6.68665300	9.78546100	0.46602100
C	6.92577400	8.77211900	2.97429900
H	7.38134300	8.68895900	3.97289000
H	7.58902100	8.28409900	2.24401800
H	5.95995200	8.23818100	2.98450200
C	8.06676800	10.95960600	2.57085200
H	7.97149300	11.99184600	2.20750800
H	8.76016200	10.42820700	1.90183700
H	8.50304400	10.97950600	3.58056900
C	5.39569800	12.03936600	3.82228900
C	5.83357200	13.26906100	3.10006400
C	5.19587900	13.64866500	1.91508900
H	4.38444400	13.02973000	1.52546100
C	5.57890000	14.81696100	1.25889500
H	5.07496200	15.11248200	0.33755300
C	6.59910500	15.61088400	1.78351600
H	6.89660600	16.52660500	1.27038800
C	7.23855600	15.23414900	2.96494400
H	8.03802900	15.85275300	3.37534000
C	6.85691600	14.06602600	3.62295900
H	7.35654000	13.76102800	4.54489000
C	3.77813800	13.01415000	5.53703200
C	2.51880100	12.33631700	6.09152600
H	1.88642000	11.96393800	5.27016200
H	1.94256000	13.06014100	6.68804300
H	2.77897100	11.47594900	6.72968000
C	3.33519500	14.16729400	4.62750800
H	4.17357500	14.80248300	4.31335400
H	2.62143700	14.79925500	5.17643600
H	2.83295500	13.77459800	3.73110000
C	4.62808000	13.55318000	6.69515900
H	4.93696600	12.72735200	7.35277200
H	4.06114500	14.28814400	7.28672400
H	5.53204000	14.04607400	6.30732200
N	1.54624800	8.97582300	7.24399000
N	-0.06051600	9.57124500	5.94450700
N	5.81873300	10.79532700	3.60617400
N	4.52636400	11.98267900	4.82470700
Si	1.43938200	8.56229000	5.39459300
Si	2.86036900	9.51806700	3.81353500
Si	4.82869100	10.10472100	5.08552300
C	0.04281900	3.04891500	2.63938000
C	-1.23538300	2.61886800	1.90766300

H	-1.82275500	1.93497100	2.53857300
H	-0.99144700	2.09778100	0.96941300
H	-1.85291400	3.49910000	1.67702200
C	0.91438500	1.82272100	2.93796600
H	1.76326300	2.10130900	3.57956000
H	1.31079400	1.42820200	1.99012000
H	0.35182300	1.01688100	3.42753000
C	0.84662000	4.01219900	1.76182500
H	0.28007300	4.93994300	1.58230900
H	1.06529100	3.54778000	0.78788700
H	1.79070600	4.28620000	2.25968100
C	-0.74499500	3.41797800	5.03350500
C	-0.74118000	2.02002500	5.55451800
C	0.40637700	1.51273800	6.17267200
H	1.27874400	2.16044400	6.28746900
C	0.43244400	0.19413800	6.62165300
H	1.32980800	-0.19840600	7.10201300
C	-0.68503100	-0.62428500	6.45216900
H	-0.66213100	-1.65783800	6.80086700
C	-1.83217400	-0.12060400	5.83905900
H	-2.70769100	-0.75823700	5.70841500
C	-1.86181800	1.19991000	5.39225000
H	-2.75823400	1.60394500	4.91691300
C	-1.54756100	4.72547600	7.05695200
C	-0.35573700	4.44437800	7.98157700
H	-0.10314700	3.37495000	7.98652400
H	-0.59917000	4.73879400	9.01415000
H	0.52328300	5.01280800	7.64064100
C	-2.75151800	3.86528400	7.46173400
H	-3.58600300	4.02809400	6.76373500
H	-3.08352100	4.13786700	8.47481600
H	-2.49770800	2.79651100	7.46591800
C	-1.92948900	6.20362200	7.17113000
H	-1.08041900	6.84806400	6.88068200
H	-2.21383400	6.43531900	8.20851800
H	-2.78014400	6.43370300	6.51264100
C	5.06143000	5.25961300	3.52240400
C	6.41128200	5.06044500	2.82311200
H	6.32078900	4.48836100	1.89009700
H	7.07759100	4.50238800	3.49699200
H	6.88144800	6.02815700	2.59860900
C	4.34678000	3.90919000	3.67441200
H	3.38824000	4.05063200	4.19858800
H	4.96868700	3.20836800	4.25183600
H	4.15385500	3.46216700	2.68602200
C	5.29512100	5.87049400	4.90825500
H	5.78227100	6.85402400	4.82937400
H	5.93648300	5.20665900	5.50577500
H	4.33806000	6.00006500	5.43538100
C	3.80393800	6.22622900	1.52233200
C	4.56878200	5.64491300	0.38505300
C	4.24764000	4.38612300	-0.12894400
H	3.40506000	3.83342800	0.29087900
C	5.00064200	3.85195100	-1.17290700
H	4.75215200	2.86789000	-1.57256700
C	6.06813700	4.57448000	-1.70706900
H	6.65518100	4.15460900	-2.52514400
C	6.38525500	5.83332500	-1.19597100
H	7.21998000	6.39869900	-1.61254400
C	5.63963000	6.36847100	-0.14758100
H	5.88674800	7.34623600	0.27288600
C	1.98746700	7.53872800	0.30631900
C	1.80350200	6.55712100	-0.85667700
H	2.75140200	6.33304000	-1.36378300
H	1.12389000	7.00465700	-1.59649100
H	1.35811300	5.61540400	-0.50485600
C	2.77065600	8.76960700	-0.16659000

H	3.77578300	8.48225000	-0.51158400
H	2.86271400	9.49210600	0.65835300
H	2.24622600	9.25318700	-1.00456000
C	0.61537500	7.98438800	0.82176600
H	0.03545200	7.13048700	1.20449000
H	0.04734900	8.46269600	0.01103300
H	0.73775800	8.71072700	1.63937900
N	-0.30948000	3.80655000	3.83730900
N	-1.18391700	4.50550300	5.65810100
N	4.17659000	6.18637600	2.80221600
N	2.67353600	6.91971000	1.44837700
Si	-0.86997000	5.61617700	4.12550000
Si	1.30852500	6.29715000	4.90115400
Si	2.69983100	7.24763900	3.32015300

Compound 2.6

C	3.99749400	14.21295100	9.80979800
C	4.48544500	14.82472500	11.12914300
H	3.83107700	14.55075600	11.96766600
H	4.49394500	15.92236400	11.05190900
H	5.50723100	14.48235400	11.35026100
C	2.54152900	14.61147700	9.54110300
H	2.18857700	14.12201600	8.62195700
H	2.45907600	15.70343300	9.42173000
H	1.88839400	14.31292200	10.37289600
C	4.87208400	14.72914800	8.66456900
H	5.92493900	14.45045300	8.82510600
H	4.80896300	15.82623900	8.60239100
H	4.54368900	14.29940000	7.70234800
C	3.65675600	11.82600000	10.61873600
C	2.87506600	12.04144200	11.87167700
C	3.51723500	12.13421800	13.11038100
H	4.60727000	12.08695700	13.15535400
C	2.76923300	12.29568000	14.27587300
H	3.27465300	12.36711800	15.24004100
C	1.37785900	12.36711200	14.20842100
H	0.79326000	12.49192700	15.12111400
C	0.73409900	12.28049700	12.97353500
H	-0.35406000	12.33566000	12.91899400
C	1.47964400	12.11707600	11.80774300
H	0.98741900	12.03276600	10.83606800
C	3.89781100	9.29225800	10.63039800
C	4.13864200	8.35749300	9.44169500
H	3.32318000	8.44722500	8.70634900
H	4.20342100	7.31522300	9.79008500
H	5.08216000	8.61009300	8.93280000
C	4.98257400	9.06025400	11.69061600
H	5.97500300	9.26834100	11.26476000
H	4.95970000	8.01984400	12.04886400
H	4.82415700	9.72271800	12.55393900
C	2.51144300	8.99256700	11.21430700
H	2.34085000	9.50775400	12.16896700
H	2.42043100	7.91071600	11.39445400
H	1.72784900	9.29471600	10.50336200
C	6.05797900	7.56149200	6.01904400
C	6.41814300	6.40244800	6.95673800
H	6.07012500	6.60732900	7.98008800
H	7.51227500	6.29467800	6.98078200
H	5.99437500	5.44607300	6.62362900
C	6.36920700	7.17729900	4.56695600
H	5.81770400	6.27062400	4.27476700
H	7.44454700	6.97420200	4.44718400
H	6.08471900	7.98868100	3.87867100

C	6.87846200	8.79359600	6.41268300
H	6.63547100	9.64607700	5.76076700
H	7.95092800	8.56954100	6.31809200
H	6.67653700	9.09598400	7.45156000
C	3.54090300	7.19855800	6.06255700
C	3.46306400	5.71799700	6.19713400
C	3.36481100	5.12372400	7.45745900
H	3.36416300	5.75299900	8.34899200
C	3.27596200	3.73719000	7.56517800
H	3.19760500	3.27346800	8.54934500
C	3.29107900	2.94456800	6.41724100
H	3.22403900	1.85912700	6.50347200
C	3.39070300	3.53902700	5.15883000
H	3.39987100	2.92047200	4.26047300
C	3.47234000	4.92528900	5.04548800
H	3.53263500	5.40170800	4.06439700
C	1.06896000	7.79960400	5.98608800
C	0.73680600	7.84700500	7.48294000
H	1.25781300	7.04016300	8.02140500
H	-0.34507500	7.72220600	7.64031800
H	1.04760900	8.81692200	7.90119700
C	0.58009600	6.48281500	5.37017100
H	0.93482000	6.38583900	4.33313900
H	-0.51968300	6.48739400	5.35863500
H	0.90580300	5.60262100	5.93954300
C	0.37202600	8.96192400	5.27629700
H	0.73107800	9.91939500	5.68218000
H	-0.71419700	8.90060500	5.43432000
H	0.57337500	8.93228100	4.19578600
C	2.94092700	9.50136000	1.61779800
C	1.83750900	10.46329800	2.06046200
H	1.75654200	10.49814200	3.15415000
H	0.86928700	10.14346200	1.64628400
H	2.05951000	11.48240700	1.70579800
C	2.63431500	8.09041200	2.14147500
H	3.40948000	7.39228400	1.80032900
H	1.64999200	7.75242500	1.77757900
H	2.61194100	8.09440700	3.24268800
C	2.94685500	9.50541500	0.08143700
H	3.24869000	10.49671100	-0.29131600
H	1.93008700	9.29932300	-0.28397700
H	3.62421600	8.74986000	-0.32836600
C	5.43070900	9.57179200	1.57149400
C	6.53730600	10.59909400	1.56870800
C	6.44485800	11.66347800	0.66683800
H	5.53836100	11.77084700	0.06715100
C	7.50761100	12.55199500	0.51061700
H	7.43721500	13.36289700	-0.21640900
C	8.65724700	12.40652900	1.28651000
H	9.48959300	13.10243400	1.16834000
C	8.73011200	11.38290900	2.23320800
H	9.61368500	11.28493200	2.86604400
C	7.67703400	10.48018300	2.37104900
H	7.72854400	9.68174600	3.11416900
C	6.60614800	7.83991600	0.25806000
C	7.37473800	8.80712200	-0.65818200
H	6.67324000	9.43124500	-1.23257100
H	7.97261200	8.22092100	-1.37240400
H	8.05831400	9.46947500	-0.11257500
C	5.93741600	6.78324700	-0.63596900
H	5.35205000	6.08830000	-0.01758700
H	6.68691200	6.21412200	-1.20631000
H	5.25196900	7.26539900	-1.34918400
C	7.58030600	7.12565600	1.20301400
H	8.09884500	7.84655500	1.85033900
H	8.33692200	6.57397600	0.62449600
H	7.03594200	6.41279600	1.83915900

C	6.07231600	14.24132100	4.89010800
C	6.42678300	15.64187500	5.40403500
H	6.04593800	16.44047800	4.75387900
H	7.52223300	15.73098100	5.43842300
H	6.03868800	15.79824300	6.42087500
C	6.45290800	14.11020900	3.41243200
H	6.25022900	13.08880400	3.05607500
H	7.52436600	14.31631600	3.27239400
H	5.88154800	14.82352300	2.79759800
C	6.84282300	13.20132000	5.70835500
H	6.59973600	13.27622400	6.77851800
H	7.92353300	13.36040700	5.58181700
H	6.59763600	12.18334500	5.37004600
C	3.55695100	14.63278900	4.73903500
C	1.08086600	14.06241500	4.72900700
C	0.64536600	15.17898900	3.77214200
H	0.96269500	16.17311200	4.11284800
H	-0.45259500	15.18045200	3.70811200
H	1.04871000	15.00442000	2.76369100
C	0.69414900	14.41673100	6.16944800
H	0.95019600	13.58127900	6.83835700
H	-0.38725600	14.60861300	6.23745700
H	1.22402700	15.32119100	6.50472400
C	0.37971200	12.76536500	4.32383800
H	0.59357700	12.52099900	3.27474900
H	-0.70724600	12.87037200	4.44996400
H	0.72516300	11.93444800	4.95722800
N	4.14063600	12.75981500	9.80488600
N	4.00168700	10.64959600	10.10282800
N	4.64031300	7.94253200	6.12815400
N	2.51300400	8.00766800	5.80723800
N	4.23164400	10.02550400	2.15000000
N	5.51278900	8.41527800	1.04329200
N	4.64128500	13.92536200	5.03679900
N	2.52479300	13.79307300	4.65644300
Si	5.01211400	11.46585700	8.69184000
Si	3.14396500	11.27991600	7.14483800
Si	3.66097800	9.51050400	5.70695800
Si	4.47685100	10.58627400	3.86380100
Si	3.64068000	12.32324100	5.10376800
C	3.50308900	16.10867700	4.55314000
C	3.42169700	18.87493700	4.22059900
C	3.40026100	16.94247200	5.66983500
C	3.56607900	16.65845400	3.27013100
C	3.52835000	18.04161600	3.10661300
C	3.35612200	18.32488100	5.50104200
H	3.36691500	16.50083000	6.66827000
H	3.63979200	15.99890600	2.40332700
H	3.58005700	18.47122700	2.10532100
H	3.27499200	18.97573900	6.37259700
H	3.39038600	19.95758100	4.09025700

Int-1

G= -2255.776445 Hartree

--- C	1.85386400	16.25438200	12.34824300
C	2.12971200	15.26860900	13.48997600
H	1.26055700	14.63281000	13.70602600
H	2.37398700	15.82896000	14.40463300
H	2.98576300	14.62563000	13.23618000
C	0.56711100	17.04278500	12.62490900
H	0.36341700	17.73306400	11.79327400
H	0.66438900	17.62555900	13.55331000
H	-0.28907100	16.36228000	12.73749500

C	3.03223900	17.22704900	12.23638400
H	3.97174600	16.67872900	12.07327300
H	3.12266000	17.82371200	13.15528800
H	2.88301500	17.91482100	11.38897400
C	1.09533900	14.49954000	10.65969400
C	0.28437600	13.59089600	11.52085100
C	-1.05031300	13.89004100	11.81214600
H	-1.50318600	14.78994000	11.39130700
C	-1.79875700	13.03473800	12.61874600
H	-2.84044000	13.27086600	12.84085900
C	-1.21816200	11.87704600	13.13737400
H	-1.80498700	11.20805700	13.76855100
C	0.11314000	11.57590600	12.84938200
H	0.57054500	10.67347600	13.25738500
C	0.86384300	12.43039900	12.04378000
H	1.91148800	12.21177200	11.82587500
C	0.85040100	13.38058200	8.38077400
C	-0.62453700	12.99303100	8.55274000
H	-0.79584100	12.41464000	9.47034700
H	-0.93963000	12.37266100	7.70050600
H	-1.25719700	13.89293700	8.57944700
C	1.74003900	12.13681600	8.50676300
H	2.79668200	12.41683500	8.37954000
H	1.47042300	11.39403800	7.74038100
H	1.61432000	11.66928100	9.49399700
C	1.04190000	13.99661200	6.99060900
H	0.41152000	14.89156800	6.87747300
H	0.76941500	13.26849600	6.21299800
H	2.09549700	14.28496100	6.84680700
C	7.26412500	13.47295500	6.51990600
C	8.45191900	13.54726900	5.55408100
H	8.16220700	13.35464200	4.51292400
H	9.18786600	12.78380400	5.84470800
H	8.93886900	14.53186000	5.61003000
C	6.48083600	12.17415200	6.29428400
H	5.63582600	12.11741800	6.99610900
H	7.13238600	11.30163700	6.45002700
H	6.09177300	12.13315600	5.26550900
C	7.78881800	13.52241800	7.95700800
H	8.35045900	14.45196300	8.12863600
H	8.45411400	12.66698000	8.14106400
H	6.95843600	13.48359800	8.67757800
C	5.81660000	15.17912800	5.28711000
C	6.28479800	15.01272600	3.88486400
C	5.66956600	14.06511200	3.06030000
H	4.83050600	13.48176000	3.44470600
C	6.12494500	13.87562500	1.75699400
H	5.64556400	13.13337900	1.11746100
C	7.18945600	14.63537700	1.27147700
H	7.54436500	14.48686500	0.25070000
C	7.79935300	15.58594900	2.09024200
H	8.63128600	16.18122000	1.71173600
C	7.35148700	15.77325900	3.39618100
H	7.83457200	16.50441800	4.04710700
C	4.03759800	16.98378500	5.02069600
C	3.40399700	16.50194000	3.71092600
H	4.15683100	16.28279700	2.94219100
H	2.74081900	17.28700200	3.31958200
H	2.80183200	15.59862000	3.88891400
C	4.98945500	18.15625900	4.75775400
H	5.45394800	18.48412600	5.69944600
H	4.43655100	19.00416700	4.32768900
H	5.78052100	17.87244000	4.04910300
C	2.93339700	17.43105700	5.97706700
H	2.23180000	16.60964400	6.18153600
H	2.37130900	18.26788300	5.53941700
H	3.35198000	17.75968100	6.94038100

N	1.76273200	15.57825200	11.05539400
N	1.27282800	14.39823200	9.34304400
N	6.34754600	14.61424600	6.37247700
N	4.76161900	15.89678700	5.69789900
Si	2.22935100	16.05557200	9.25864600
Si	4.37400900	14.91202400	9.46278400
Si	5.04335900	15.37486300	7.46448200

TS1

G= -4222.181187 Hartree

C	11.46919500	9.54250300	11.89777500
C	11.21668800	8.08394500	11.50518600
H	11.26582700	7.96866100	10.41054900
H	10.21831600	7.75509200	11.84033100
H	11.96374000	7.41994300	11.96715400
C	12.90398500	9.92192200	11.50787400
H	13.07392100	9.65246800	10.45473200
H	13.63152100	9.37565700	12.12669600
H	13.09134700	10.99874700	11.61124000
C	10.47684300	10.45145200	11.16165900
H	10.57892300	10.33061800	10.07219100
H	10.66632300	11.50769800	11.40118500
H	9.44537000	10.20117200	11.44778400
C	11.54999600	10.59525700	14.20916200
C	12.24951200	11.88071300	13.90773100
C	13.63468200	12.01832600	14.04212900
H	14.23239400	11.16322400	14.36238700
C	14.25133500	13.23465200	13.75176200
H	15.33257400	13.33231200	13.85846400
C	13.49012300	14.32091900	13.32173700
H	13.97444500	15.27127300	13.09263300
C	12.10782900	14.19041800	13.18571100
H	11.50776200	15.03810000	12.85177800
C	11.49029200	12.97652600	13.47966300
H	10.40709900	12.87022300	13.38726100
C	10.97841300	10.90395300	16.67370900
C	12.39511500	10.80928800	17.24738200
H	12.42836400	11.21502400	18.27031000
H	13.11230800	11.37234100	16.63194400
H	12.69445800	9.75159300	17.26655000
C	10.49764600	12.36007200	16.64786500
H	10.38119500	12.73160700	17.67700600
H	9.52273900	12.42562400	16.14163300
H	11.21063500	13.01596300	16.13056900
C	10.03760800	10.07778500	17.55315400
H	10.05457700	10.44670800	18.58929900
H	10.34797800	9.02005400	17.54303400
H	9.00515100	10.14006000	17.17532400
C	13.98450900	7.25066900	16.03870800
C	14.10549600	8.22712600	14.86463800
H	15.14765500	8.31281400	14.52270700
H	13.73576000	9.21648500	15.17387100
H	13.48064800	7.88930000	14.02177200
C	14.83529700	7.76154000	17.20875200
H	15.85548700	7.94920100	16.84217400
H	14.90261700	7.02995000	18.02442500
H	14.44216200	8.70285000	17.61691700
C	14.49516700	5.86395500	15.62042800
H	15.55366100	5.91494600	15.32298500
H	13.89961900	5.47957000	14.78028100
H	14.40919600	5.15747400	16.45988900
C	11.86947200	6.70788900	17.36742900

C	12.47740500	6.38780100	18.69004700
C	12.63918800	7.38919400	19.65123600
H	12.27895900	8.39828600	19.43735400
C	13.25579100	7.09781200	20.86623300
H	13.37813900	7.88131800	21.61539100
C	13.71871300	5.80694000	21.12313200
H	14.20413600	5.58041800	22.07355700
C	13.55863900	4.80491000	20.16550000
H	13.91792300	3.79446900	20.36585900
C	12.93788500	5.09368300	18.95129600
H	12.80229300	4.31377100	18.19840800
C	9.43495200	5.94926200	17.63410900
C	9.58467300	5.86476500	19.15606600
H	8.61279200	5.57224500	19.57871100
H	9.86494400	6.83767800	19.58528200
H	10.32720600	5.12022100	19.46901200
C	9.15722600	4.55337000	17.06073500
H	8.27376000	4.11014200	17.54493500
H	10.02208500	3.89378900	17.23028400
H	8.96710300	4.61685500	15.97810900
C	8.24630800	6.86952500	17.32809500
H	7.32028900	6.41676400	17.71497400
H	8.12779100	7.01395400	16.24366400
H	8.38247900	7.85157400	17.80493200
C	11.03230900	3.75268100	11.67404200
C	10.43704000	3.28951400	13.00730500
H	11.13551900	2.59950700	13.50258200
H	9.47809400	2.77429300	12.84927400
H	10.27371300	4.15244300	13.67195800
C	12.38092200	4.42615600	11.94871300
H	13.07057400	3.70046500	12.40598400
H	12.24029000	5.25956100	12.65278600
H	12.84130900	4.79346300	11.02088100
C	11.21867800	2.53700100	10.75723700
H	11.76292600	1.75486600	11.30625000
H	11.79698300	2.77751200	9.85502300
H	10.24212400	2.12843000	10.45515000
C	9.88372300	5.13665000	9.84899800
C	10.77627300	4.84929300	8.69529900
C	10.38217500	3.91511800	7.73089200
H	9.41178900	3.42342000	7.82673400
C	11.22926900	3.60851200	6.66997700
H	10.92187500	2.87375000	5.92460100
C	12.47054500	4.23829600	6.56165900
H	13.13281100	3.99837900	5.72860300
C	12.86342300	5.17360700	7.51786000
H	13.83095200	5.67011000	7.43305600
C	12.02087100	5.47655200	8.58708800
H	12.32097400	6.20769900	9.33992400
C	8.02671000	6.64955200	8.86200900
C	8.69560600	6.68378100	7.48705800
H	8.14628600	7.40240300	6.86243000
H	8.66547900	5.70791000	6.98589800
H	9.74227200	7.01420400	7.54578100
C	6.59216000	6.13045300	8.72161200
H	6.02749300	6.76183200	8.02005300
H	6.07526600	6.15276700	9.69340300
H	6.59685800	5.09727900	8.34374800
C	8.01432600	8.06949700	9.43914100
H	7.42864600	8.74073900	8.79343200
H	9.03979900	8.45750000	9.51570800
H	7.56996600	8.07069900	10.44445400
C	5.70410900	10.00968200	13.56535300
C	6.69018700	10.16854800	12.40486400
H	6.92166300	11.23056400	12.23576800
H	6.26093600	9.75287400	11.47991000
H	7.62142600	9.63235300	12.64615700

C	6.30192400	10.66961800	14.81330700
H	6.53935500	11.72124900	14.58987300
H	7.23484800	10.15413900	15.09086200
H	5.60223900	10.65591500	15.65946900
C	4.36701600	10.66475200	13.19655300
H	4.51633000	11.72703100	12.95038900
H	3.65593200	10.60633200	14.03340500
H	3.92947200	10.15875700	12.32281800
C	4.75872600	7.88029900	14.58650900
C	4.11397600	8.41112100	15.82341400
C	2.76319700	8.77318300	15.83160800
H	2.17246100	8.65714200	14.92058500
C	2.17861000	9.27407600	16.99385700
H	1.12529200	9.55824400	16.99279300
C	2.93853100	9.40926400	18.15560200
H	2.47948600	9.79871000	19.06558800
C	4.28575600	9.04653300	18.15296600
H	4.88306300	9.15089500	19.05992100
C	4.87338200	8.55276000	16.98994200
H	5.92956400	8.27568600	16.97194700
C	4.18932600	5.40142800	14.72598000
C	2.69527400	5.48277400	15.06630300
H	2.33171800	4.49167900	15.37652300
H	2.12245700	5.80329400	14.18345500
H	2.50311300	6.18449700	15.88890900
C	5.00216300	5.07958800	15.98759500
H	4.69167000	4.10741000	16.40010800
H	4.84233100	5.84498700	16.76166300
H	6.07509300	5.03868200	15.74454600
C	4.40248900	4.29567600	13.68808400
H	4.06577400	3.32939500	14.09002200
H	5.46762000	4.21382800	13.42141700
H	3.83295900	4.51531100	12.77241500
N	11.25976300	9.61623700	13.34681400
N	10.94066400	10.28304100	15.35249400
N	12.54707100	7.18737100	16.31857600
N	10.62130000	6.48939400	16.95574300
N	10.07856400	4.72380000	11.10679300
N	8.71016300	5.77856900	9.83008600
N	5.53121400	8.56452700	13.74339900
N	4.66851300	6.64080000	14.11034600
Si	9.99743900	8.84393300	14.55749900
Si	11.11776900	6.77611500	15.12538700
Si	7.75778700	6.29559700	13.51523500
Si	8.44531200	5.43608900	11.64397600
Si	5.65718600	7.08362500	12.53443100

TS2

G= -4511.512933 Hartree

C	1.56330300	8.87790200	9.25013600
C	0.45014100	8.41631300	10.19811300
H	0.02483900	7.46336700	9.85042300
H	-0.35485000	9.16208600	10.26056800
H	0.85681500	8.27035900	11.20981500
C	2.15789100	10.20962400	9.72963900
H	2.82568300	10.60774100	8.95228100
H	2.73809500	10.04750000	10.64963300
H	1.37913200	10.95155200	9.94801500
C	2.66985200	7.82151500	9.21958600
H	2.26834500	6.84649500	8.91041200
H	3.12123300	7.72369500	10.21660100
H	3.45299300	8.09966300	8.50103400

C	0.07498200	9.73272300	7.35451100
C	-0.71193100	10.77653800	8.06957200
C	-0.18805800	12.05499800	8.29260400
H	0.80767100	12.29742600	7.91687100
C	-0.93935200	13.01059600	8.97194100
H	-0.52777800	14.00732000	9.13634400
C	-2.21589200	12.69441400	9.43904200
H	-2.80233600	13.44351100	9.97303400
C	-2.74175100	11.42193700	9.22133800
H	-3.73865300	11.17093900	9.58596100
C	-1.99365500	10.46555600	8.53545200
H	-2.39673800	9.46539900	8.36213100
C	-0.81641600	9.97431500	4.98634800
C	-0.51403900	11.47798800	4.98223000
H	-0.92643900	12.00533800	5.85052700
H	-0.93589100	11.93583700	4.07614900
H	0.57960500	11.58680600	4.95062600
C	-2.31691100	9.69124100	5.10152300
H	-2.73523800	10.12112100	6.02274800
H	-2.48608300	8.60377600	5.09436900
H	-2.84920700	10.13337800	4.24647900
C	-0.29295000	9.41204600	3.66069200
H	-0.83350600	9.89727800	2.83440400
H	-0.45654100	8.32837600	3.58917100
H	0.77999500	9.62468200	3.53970900
C	6.64301600	10.50652200	1.69636800
C	5.98193000	11.43412300	0.66913800
H	6.22845800	12.48973100	0.84206000
H	4.88885600	11.31956100	0.70801300
H	6.32665100	11.16776400	-0.34126700
C	6.45849900	9.05692400	1.23750400
H	6.81679400	8.35086500	2.00186600
H	7.03312900	8.89513400	0.31282700
H	5.39753700	8.82640000	1.04572800
C	8.14398700	10.80996900	1.79980200
H	8.31216700	11.85994800	2.07704200
H	8.64074100	10.62983400	0.83477800
H	8.60512400	10.16299000	2.56080400
C	5.81406800	11.72515000	3.76215200
C	5.88177500	13.14073300	3.29676500
C	4.72205500	13.73767800	2.78985200
H	3.80460800	13.14737900	2.72917400
C	4.75087900	15.06092900	2.35385800
H	3.84505600	15.52119800	1.95668400
C	5.93633400	15.79348800	2.42192600
H	5.95845300	16.82936300	2.08020600
C	7.09357200	15.20155400	2.92854400
H	8.02038700	15.77403900	2.98649100
C	7.06730200	13.87855900	3.36666100
H	7.96625800	13.41725700	3.77993800
C	5.00274300	12.02558100	6.15503600
C	5.12011500	11.03521700	7.31477800
H	4.48501200	10.15937800	7.11690500
H	4.78774800	11.50985700	8.24984400
H	6.15624400	10.68845400	7.43452100
C	3.53125300	12.41860300	5.96869900
H	3.42723300	13.13247600	5.13849200
H	3.14355100	12.89797600	6.88142200
H	2.92929300	11.53192000	5.72678400
C	5.83616200	13.27415300	6.47135800
H	6.90865500	13.02843600	6.48625800
H	5.55489300	13.65318600	7.46496500
H	5.66788200	14.07933600	5.74448000
N	1.05697300	8.99411900	7.87457200
N	-0.09908100	9.30894300	6.09743600
N	6.02277700	10.62794500	3.01873600
N	5.47379500	11.30991400	4.97059400

Si	1.25613600	8.03279200	6.29850400
Si	3.60298000	9.30509800	3.43349100
Si	5.73511500	9.45529500	4.53028000
C	0.38467900	3.52636000	2.93783300
C	-0.38445100	2.29135900	2.45461800
H	-0.25705300	1.43521800	3.13088900
H	-0.00897100	1.99707800	1.46324000
H	-1.45838000	2.51408500	2.36601700
C	1.85132300	3.16519800	3.20987900
H	2.40393600	4.06562900	3.51968500
H	2.31420600	2.75783300	2.29644000
H	1.93079900	2.40739400	4.00383200
C	0.33713700	4.61378000	1.85738600
H	-0.70176700	4.90292800	1.64138000
H	0.80639600	4.24982600	0.93109500
H	0.89092200	5.50687900	2.19891100
C	-0.68571500	3.62785800	5.25514000
C	-0.86294700	2.18013700	5.56881200
C	0.20533700	1.48545100	6.14672500
H	1.12407300	2.02715400	6.38447200
C	0.08686700	0.12430400	6.42227500
H	0.92249300	-0.41280200	6.87319100
C	-1.09805500	-0.54818800	6.12258800
H	-1.19040400	-1.61380000	6.33791500
C	-2.16486500	0.14180400	5.54638600
H	-3.09094600	-0.38348600	5.30839800
C	-2.04820900	1.50251200	5.26777600
H	-2.87399200	2.04276000	4.80088800
C	-1.69195600	4.72296200	7.32158700
C	-1.10631400	3.77948500	8.37885600
H	-1.25309900	2.72371700	8.11349800
H	-1.59959600	3.95685400	9.34623300
H	-0.02843400	3.96851600	8.49659300
C	-3.16532700	4.38371300	7.05761800
H	-3.56447200	5.04163400	6.27137600
H	-3.76123200	4.52459200	7.97193800
H	-3.27782100	3.33854700	6.73780600
C	-1.59801900	6.16302900	7.84022700
H	-0.55645700	6.41757800	8.08207600
H	-2.22570200	6.27822600	8.73690700
H	-1.93966100	6.87572000	7.07078500
C	6.02518300	5.26673400	2.82334000
C	7.38749600	5.41251400	2.13477900
H	7.37295600	5.02816500	1.10538900
H	8.14221200	4.84377600	2.69763700
H	7.69819100	6.46828300	2.11910000
C	5.56393500	3.80401400	2.79828700
H	4.57867400	3.72594400	3.27997900
H	6.27789400	3.17321000	3.34808400
H	5.49578800	3.41890200	1.77189300
C	6.15321300	5.70729600	4.28329200
H	6.50735800	6.74499800	4.35625900
H	6.86899700	5.05781100	4.80724900
H	5.18108800	5.63617600	4.79718900
C	4.53775100	6.13832700	0.94658500
C	5.10464600	5.42638200	-0.23445000
C	4.64553100	4.15021300	-0.58143900
H	3.86791400	3.67895800	0.02287800
C	5.16942400	3.49389100	-1.69253000
H	4.80712600	2.49917300	-1.95588200
C	6.15304200	4.10862100	-2.46866700
H	6.56180900	3.59435800	-3.33971300
C	6.61338500	5.37960200	-2.12834000
H	7.38369200	5.86268100	-2.73101600
C	6.09275800	6.03582700	-1.01342600
H	6.45638100	7.02512400	-0.73185200
C	2.54917700	7.35456300	-0.10413600

C	2.16696000	6.25569900	-1.10393900
H	3.01323700	5.95218800	-1.73342600
H	1.37299800	6.63172700	-1.76573800
H	1.78525000	5.37197400	-0.57223300
C	3.24582000	8.50579000	-0.83617800
H	4.19110300	8.16823500	-1.28762400
H	3.46006300	9.31885800	-0.12922900
H	2.60095800	8.89880000	-1.63631600
C	1.27362500	7.87562000	0.56613800
H	0.74479800	7.05886500	1.07981500
H	0.60202000	8.30841400	-0.18904300
H	1.51649700	8.65428300	1.30606900
N	-0.20579200	4.12923800	4.12963500
N	-0.93206500	4.66501800	6.06962700
N	5.01525700	6.13680100	2.19991800
N	3.41091400	6.85512600	0.97164200
Si	-0.44508400	5.94316500	4.71387800
Si	1.60451800	5.90535100	5.99412100
Si	3.50994500	7.06909100	2.83163400

Int2

G= -4222.19945 Hartree

C	11.54850900	9.85778500	10.86566200
C	11.84379700	8.35935900	10.71743000
H	12.27806900	8.15120000	9.72780800
H	10.92743000	7.76296100	10.84445200
H	12.56246900	8.03814600	11.48770600
C	12.88590600	10.60981200	10.93306200
H	13.50154800	10.36802500	10.05340800
H	13.43458100	10.31239500	11.83976600
H	12.73147700	11.69767000	10.94701300
C	10.73650000	10.36322100	9.66763100
H	11.27888000	10.14295300	8.73561100
H	10.58533100	11.45021000	9.71975700
H	9.75520200	9.87374500	9.62027500
C	10.49994300	11.10387200	12.81047500
C	10.36205300	12.47301200	12.23844100
C	11.36259800	13.43793100	12.39343800
H	12.28556500	13.17828600	12.91556100
C	11.18200200	14.72095000	11.87985900
H	11.96607400	15.46964000	12.00175800
C	10.00074100	15.04732700	11.21294300
H	9.85843900	16.05370600	10.81640600
C	9.00410300	14.08513400	11.04942700
H	8.08130400	14.33701400	10.52491700
C	9.18529200	12.79972800	11.55653600
H	8.41370600	12.03644800	11.43325900
C	10.13273600	11.55436600	15.30296000
C	11.49043600	12.01681100	15.85198800
H	11.35544000	12.53421800	16.81386600
H	11.97658100	12.71305700	15.15291300
H	12.14862600	11.14920200	16.00354900
C	9.23204900	12.77706200	15.07845600
H	8.97192600	13.20163500	16.05934500
H	8.30019300	12.50537300	14.56696600
H	9.72974100	13.56327500	14.49658800
C	9.48768000	10.61151100	16.32588400
H	9.21687000	11.16799100	17.23637200
H	10.19783800	9.81739100	16.60189600
H	8.59002500	10.12355100	15.91534300
C	13.29185100	5.39165000	15.33354100

C	13.14054100	5.92178400	13.90269400
H	14.04172300	5.68920500	13.31470400
H	13.00882700	7.01438100	13.92017900
H	12.25808800	5.49114200	13.40445400
C	14.39601300	6.19290700	16.03881600
H	15.34699400	6.09099600	15.49440100
H	14.54704400	5.82741300	17.06518500
H	14.12022700	7.25651700	16.07824200
C	13.68140800	3.90726100	15.30340000
H	14.54533800	3.78816800	14.63293000
H	12.86485100	3.28213200	14.92117700
H	13.97228600	3.53032100	16.29224800
C	11.43570600	5.09083500	17.07015100
C	11.93116600	3.90965700	17.83196300
C	12.99451300	4.01089100	18.73479100
H	13.45639000	4.98320300	18.91692000
C	13.45738200	2.87667700	19.39960500
H	14.28596300	2.96095300	20.10423200
C	12.86352700	1.63652500	19.16331100
H	13.23039900	0.74872300	19.68050900
C	11.79782800	1.53321100	18.26913800
H	11.32962200	0.56512800	18.08552900
C	11.32932500	2.66698300	17.60800400
H	10.49439600	2.59985400	16.90691200
C	9.62622700	5.95993700	18.62117100
C	10.59678300	6.40750900	19.72410600
H	10.03832700	6.68456900	20.63110000
H	11.17053800	7.28246400	19.38238700
H	11.29477400	5.60207300	19.99165100
C	8.91686400	4.67219300	19.05541100
H	8.31461700	4.86881300	19.95538700
H	9.64072500	3.88306000	19.30107500
H	8.24895600	4.30295900	18.26654200
C	8.60545200	7.08226300	18.39132700
H	7.94076300	7.17905800	19.26316500
H	8.00013800	6.88678600	17.49306600
H	9.12611100	8.04135800	18.24237200
C	10.64963600	3.14484100	12.35722100
C	10.45689500	3.09085300	13.87856400
H	10.90018200	2.17059100	14.28825800
H	9.38322400	3.09917700	14.12377900
H	10.91835800	3.96396500	14.36478700
C	12.11864500	2.89766200	11.99544700
H	12.44357800	1.93240100	12.41260100
H	12.76461800	3.68563600	12.40365200
H	12.25838700	2.85746800	10.90641800
C	9.77397600	2.05585100	11.71999500
H	10.01020600	1.07453800	12.15872300
H	9.94463600	1.98987300	10.63650400
H	8.71172100	2.27766200	11.90435600
C	9.97118200	4.95643500	10.71622300
C	10.58891500	4.45548300	9.45600500
C	9.88496300	3.63562300	8.56810700
H	8.86869300	3.32202500	8.81458300
C	10.48082200	3.21954600	7.37882100
H	9.92827900	2.57878900	6.69014400
C	11.78002200	3.62293700	7.06915800
H	12.24313500	3.30092900	6.13527800
C	12.48793700	4.43412300	7.95610300
H	13.50528300	4.74767800	7.71777700
C	11.89633700	4.84621800	9.14876400
H	12.44030200	5.48002100	9.85272900
C	8.37516900	6.74706900	9.82323500
C	9.22255000	7.06513600	8.58333100
H	8.68857900	7.81464100	7.98069700
H	9.38578800	6.18372300	7.95020800
H	10.20046300	7.48110200	8.85604000

C	7.10429300	6.00025500	9.39208600
H	6.50744800	6.62668200	8.71199700
H	6.49671000	5.75412600	10.27481000
H	7.35925500	5.06873200	8.86569100
C	7.96294700	8.04798700	10.52273900
H	7.49946500	8.73679300	9.79975300
H	8.82477900	8.54208800	10.99765100
H	7.23040000	7.83035500	11.31464100
C	5.80961100	10.21337400	14.72012400
C	6.73201400	10.63912200	13.57009300
H	6.52051700	11.67801000	13.27467000
H	6.57054500	9.98888900	12.69587800
H	7.79014100	10.55254100	13.86099100
C	5.85670900	11.24524500	15.85286800
H	5.58851700	12.23736300	15.45903400
H	6.86165800	11.30705800	16.29002500
H	5.14174000	10.99495400	16.64862500
C	4.37619900	10.11105700	14.17839600
H	4.07934100	11.06119200	13.70894600
H	3.66032600	9.89521900	14.98366000
H	4.32018700	9.31213600	13.42330200
C	5.72428100	8.01313500	15.98029700
C	4.73702200	8.32820000	17.05113200
C	3.37066500	8.07877600	16.88649600
H	3.00674800	7.67514600	15.93960500
C	2.48068000	8.34880400	17.92454200
H	1.41562500	8.15412000	17.79072700
C	2.95102000	8.86519800	19.13230100
H	2.25389700	9.07089900	19.94593000
C	4.31203500	9.12265900	19.29719400
H	4.68157100	9.53005300	20.23931300
C	5.20289300	8.85939900	18.25831900
H	6.27060800	9.05880500	18.37389100
C	5.84052900	5.46020700	16.12829900
C	4.65215300	4.93487200	15.30950900
H	4.43513900	3.89068300	15.58102000
H	4.88625500	4.98252000	14.23627100
H	3.75054300	5.53443500	15.50284400
C	5.49225500	5.40523800	17.62237700
H	5.42913400	4.34975800	17.92580600
H	4.52525400	5.87417300	17.84469200
H	6.26129500	5.89076100	18.23608700
C	7.05968900	4.57492000	15.84265300
H	6.89801400	3.56450900	16.24879200
H	7.97804800	5.00043400	16.27609700
H	7.21533600	4.49239600	14.75627600
N	10.81244900	9.99105700	12.13141900
N	10.36034600	10.76009800	14.08779600
N	12.01405000	5.65078100	16.01113500
N	10.33174700	5.80111800	17.34126400
N	10.19511400	4.48245600	11.95006300
N	9.08086300	5.93845800	10.82696900
N	6.29821600	8.89479300	15.14930800
N	6.18256800	6.80797500	15.65322000
Si	11.07664900	9.02353900	13.74956500
Si	10.84592200	7.15554600	16.10603800
Si	9.41340400	7.29021500	14.14300100
Si	8.73958200	5.49073000	12.64968800
Si	6.98940300	7.49097900	14.06539700

TS3

C	-3.83826400	-0.66270400	0.88322900
C	-3.36772400	-0.03036200	2.19710400
H	-4.15854000	0.63527900	2.57396500
H	-2.44820000	0.55794200	2.05165000
H	-3.16828100	-0.81018800	2.94867600
C	-5.14866500	-1.41522900	1.14857800
H	-5.84197100	-0.73974500	1.67115900
H	-4.97261100	-2.29121200	1.79025000
H	-5.63948200	-1.74769800	0.22483200
C	-4.06905100	0.43762600	-0.16196000
H	-4.83380500	1.14955300	0.18562800
H	-4.41479200	-0.00015800	-1.11146300
H	-3.13311800	0.98665100	-0.34894800
C	-2.72728300	-2.42184500	-0.57055000
C	-3.92564400	-3.10055000	-1.13913200
C	-4.53806500	-4.15577900	-0.45473200
H	-4.10551300	-4.50966100	0.48316200
C	-5.69281900	-4.74162900	-0.96632500
H	-6.16555600	-5.56622700	-0.43089600
C	-6.24944900	-4.26985700	-2.15631900
H	-7.15879100	-4.72490900	-2.55155600
C	-5.64184600	-3.21718100	-2.83983900
H	-6.07446000	-2.84539900	-3.76966000
C	-4.47920100	-2.63554700	-2.33605200
H	-3.99552100	-1.81142800	-2.86488700
C	-0.86906800	-3.67903800	-1.74191100
C	-1.26038100	-5.04397100	-1.15779200
H	-0.66771600	-5.83555400	-1.64032700
H	-2.32120500	-5.26775900	-1.33247700
H	-1.06350400	-5.07918800	-0.07769200
C	-1.29836800	-3.62663200	-3.21345000
H	-0.79528000	-4.43174400	-3.76969400
H	-1.01529400	-2.66829400	-3.66422500
H	-2.38196800	-3.76706800	-3.32395800
C	0.65501700	-3.52507900	-1.67120000
H	1.12474800	-4.29143500	-2.30664900
H	1.01546200	-3.63892400	-0.63830400
H	0.96581500	-2.52735000	-2.01314400
C	1.78775500	-3.62085800	2.60004600
C	0.91206000	-2.93640100	3.65119800
H	0.61875800	-3.65812700	4.42818100
H	0.00931100	-2.52204600	3.18370100
H	1.46121900	-2.10629800	4.11851600
C	0.97725800	-4.73114700	1.92240200
H	0.66557100	-5.49068300	2.65550700
H	1.56997300	-5.22718000	1.13818000
H	0.08119600	-4.28944700	1.46330200
C	3.00716900	-4.22274300	3.31145000
H	2.65281300	-4.82032500	4.16427900
H	3.66299600	-3.42900800	3.69830600
H	3.59850800	-4.88192600	2.66353600
C	3.15687100	-2.51914500	0.76313700
C	4.33332700	-3.43099700	0.71371600
C	4.28023900	-4.58468800	-0.07458000
H	3.37819800	-4.79423200	-0.65379700
C	5.37314500	-5.44775200	-0.12538700
H	5.32754000	-6.34597000	-0.74297400
C	6.52349800	-5.16288400	0.61066100
H	7.37888500	-5.83894600	0.57075600
C	6.57865300	-4.01285400	1.39891200
H	7.47617400	-3.78926100	1.97751700
C	5.48702300	-3.14868800	1.45139600

H	5.52082600	-2.25365200	2.07570100
C	3.83982900	-0.79902200	-0.96867800
C	4.68223800	-1.77770300	-1.80005400
H	5.16083400	-1.21972200	-2.61868800
H	4.04217600	-2.55636500	-2.24204900
H	5.47595300	-2.26383100	-1.21911900
C	4.75626000	0.14538900	-0.17942800
H	5.40889100	0.71595800	-0.85818700
H	5.39506800	-0.42790900	0.50888100
H	4.15165700	0.85203700	0.40808900
C	2.97769000	0.01077000	-1.93792400
H	3.63233200	0.59755200	-2.60011100
H	2.30837700	0.70284800	-1.41144800
H	2.35021600	-0.65174300	-2.55225600
C	0.29259100	1.29134800	4.59772100
C	1.72010600	0.99157100	4.13703500
H	2.23406300	0.36746400	4.88330600
H	2.28531000	1.92750900	4.00822800
H	1.70688500	0.45283300	3.17620600
C	-0.49143700	-0.01399600	4.76036100
H	0.00310300	-0.68164500	5.48231600
H	-0.55598700	-0.51687800	3.78431900
H	-1.50850800	0.19244700	5.12560700
C	0.36235700	2.04467600	5.93443100
H	1.02126700	1.49160400	6.62012900
H	-0.61843200	2.13890600	6.41806200
H	0.78482900	3.05019400	5.78754800
C	-1.47341500	2.76427100	3.52604900
C	-2.31240300	3.06927000	4.72405700
C	-2.06454200	4.22806100	5.46861600
H	-1.25088400	4.89215500	5.17093800
C	-2.83196800	4.51775000	6.59447900
H	-2.63023200	5.42204600	7.17060600
C	-3.85010700	3.64889300	6.98889800
H	-4.45071700	3.87561100	7.87112800
C	-4.09405200	2.48782500	6.25663000
H	-4.88566800	1.80291800	6.56391100
C	-3.32757100	2.19787900	5.12850500
H	-3.51642700	1.29192100	4.55153200
C	-2.57306800	4.27321900	1.81376700
C	-4.01234600	3.97970800	2.25649500
H	-4.69988400	4.64364500	1.71203000
H	-4.16537500	4.14536900	3.33084000
H	-4.27474600	2.93826800	2.01721400
C	-2.14465000	5.66884600	2.28801500
H	-2.77524800	6.43870400	1.81825400
H	-1.09633100	5.85279600	2.00944200
H	-2.24644800	5.76891300	3.37687300
C	-2.51564100	4.23304600	0.28962500
H	-3.18432700	4.99149500	-0.14250000
H	-2.80838900	3.24466900	-0.08900700
H	-1.49603500	4.43654300	-0.06963000
C	-0.53241600	0.50121700	-4.33799900
C	-1.73799700	-0.08071300	-3.59087600
H	-2.28053800	-0.78119800	-4.24383100
H	-2.42520500	0.72413300	-3.28676700
H	-1.40605800	-0.61927800	-2.68824400
C	0.35758600	-0.64500700	-4.83019200
H	-0.21407400	-1.30995400	-5.49566600
H	0.72385200	-1.23468800	-3.97749300
H	1.21953400	-0.26430600	-5.39387300
C	-1.04480400	1.32141500	-5.53065900
H	-1.74135300	0.71388100	-6.12803700
H	-0.22727300	1.64210400	-6.19003900
H	-1.58087400	2.21207000	-5.16873300
C	1.16165900	2.23025600	-3.53985300
C	1.87652400	2.49142500	-4.82313300

C	1.47998700	3.59048900	-5.59641800
H	0.66678100	4.22529400	-5.23718300
C	2.10529900	3.86218000	-6.80904200
H	1.78660200	4.71848000	-7.40539400
C	3.13787000	3.03856200	-7.26204200
H	3.63164200	3.25276400	-8.21112600
C	3.53332900	1.94019500	-6.50126100
H	4.33809600	1.29254900	-6.85225200
C	2.90241800	1.66387800	-5.28728500
H	3.20698700	0.80176200	-4.69278700
C	2.10263100	4.01217300	-1.93201400
C	1.24879800	5.06056500	-1.21199200
H	1.88771800	5.86724600	-0.82444800
H	0.73030200	4.60878600	-0.35216200
H	0.50260600	5.48742600	-1.89804300
C	2.92808200	4.70971900	-3.01748200
H	3.58430500	5.44364300	-2.52770400
H	2.29029300	5.24754200	-3.73158100
H	3.56289400	4.00786200	-3.57529000
C	3.06296500	3.36300700	-0.92660000
H	3.67528400	4.13350600	-0.43455000
H	3.73434000	2.65824900	-1.43694400
H	2.50142600	2.82246800	-0.14960700
N	-2.75251700	-1.53744400	0.42036100
N	-1.46307000	-2.57381700	-0.96637800
N	2.13313900	-2.59971700	1.60647400
N	2.93306500	-1.47277400	-0.03404300
N	-0.33292300	2.07693300	3.52958300
N	-1.63705700	3.24668900	2.29115900
N	0.18365800	1.32783500	-3.36011700
N	1.17965700	2.98958900	-2.44223900
Si	-0.84181000	-1.25816000	0.31768300
Si	1.29785000	-1.03489300	0.84650000
Si	-0.00473900	0.88114800	0.16363300
Si	0.14862700	2.71702200	1.81192400
Si	-0.44879600	2.22732300	-1.82574900

Int3

C	11.75737500	10.00949800	14.02288900
C	11.78320700	9.36300100	12.63622300
H	12.50871500	9.87515200	11.98735700
H	10.78875300	9.40681100	12.16966300
H	12.07039000	8.30451400	12.71950100
C	13.14701600	9.92859600	14.66117000
H	13.88560900	10.46946900	14.04839200
H	13.44993300	8.87583300	14.74039400
H	13.13446100	10.37831200	15.66698000
C	11.34385400	11.47968200	13.88141800
H	11.98140900	11.94710200	13.11661900
H	11.47321800	12.04202200	14.81500600
H	10.29843400	11.56745000	13.55532700
C	10.27031200	9.43742400	16.00305300
C	10.19917200	10.75879400	16.68550000
C	11.09923500	11.06010500	17.71121800
H	11.84335200	10.31872000	18.00959900
C	11.03248400	12.29417600	18.35514200
H	11.73734900	12.52753500	19.15422600
C	10.06154500	13.22474300	17.98419500
H	10.00650800	14.18801800	18.49326200
C	9.16163400	12.92342500	16.96106800
H	8.40274000	13.64977400	16.66684500
C	9.23311700	11.69533100	16.30772000
H	8.54404100	11.45984400	15.49510500

C	8.71143000	8.06608900	17.44827000
C	8.86037300	8.90777900	18.72388200
H	8.13332600	8.54261900	19.46396300
H	8.66003200	9.97391900	18.55659800
H	9.86623100	8.80150900	19.15600800
C	7.38088600	8.40215300	16.76192600
H	6.55304500	8.28454000	17.47958300
H	7.20799400	7.73490200	15.90245600
H	7.38571200	9.44487400	16.40369400
C	8.71294100	6.58564900	17.84248000
H	7.82793600	6.37530200	18.46101100
H	9.60684800	6.33683800	18.42976300
H	8.68078400	5.94475400	16.95013200
C	14.43567000	6.07349700	13.20449900
C	13.29516500	5.58812300	12.31462000
H	13.65138500	5.41357800	11.28877600
H	12.48325100	6.32908100	12.28187400
H	12.85966900	4.65359300	12.69507600
C	15.08419700	7.31418000	12.57993100
H	15.46413500	7.06389900	11.57844700
H	15.92962300	7.67782600	13.17985700
H	14.34780000	8.12359600	12.47649700
C	15.46609400	4.94201300	13.32635500
H	15.73630300	4.58103300	12.32302400
H	15.03447800	4.10177500	13.89043400
H	16.38728200	5.27596000	13.82116500
C	14.41557500	6.81519300	15.63012500
C	15.86640500	7.12299000	15.82549000
C	16.34057700	8.42963500	15.66757800
H	15.64465100	9.22268600	15.38900700
C	17.68967700	8.71699000	15.86755700
H	18.04992800	9.73877800	15.74120200
C	18.57501700	7.70188300	16.22875100
H	19.63081600	7.92737800	16.38559400
C	18.10842300	6.39728000	16.38822500
H	18.79713200	5.59943800	16.66940900
C	16.75981000	6.10879200	16.18721000
H	16.39118900	5.08815600	16.30791200
C	13.61477600	7.01613700	18.02745800
C	14.22104400	8.39055300	18.33483400
H	14.10070400	8.62173500	19.40372000
H	13.70998300	9.16532200	17.74390800
H	15.29279500	8.42850400	18.09924200
C	14.44774700	5.90601000	18.68271200
H	14.39464400	5.99589000	19.77805500
H	15.50435600	5.96771500	18.39205100
H	14.05251000	4.92098100	18.39341900
C	12.19520300	6.95324500	18.58607600
H	12.19593300	7.11125800	19.67442700
H	11.75736500	5.96394600	18.37940300
H	11.56194800	7.71247100	18.10600600
C	7.88726600	2.21973200	12.72519700
C	8.15985400	2.26856300	14.23190600
H	7.94872100	1.29001700	14.68750900
H	7.53846900	3.03360100	14.71718400
H	9.21385800	2.52417300	14.42333700
C	8.76778700	1.13229200	12.09157500
H	8.54766600	0.14868500	12.53405900
H	9.82944600	1.36810800	12.25543200
H	8.58281500	1.06868900	11.00894100
C	6.40939600	1.88376700	12.48440600
H	6.14573600	0.98883000	13.06793000
H	6.20051600	1.66971900	11.42778100
H	5.75921000	2.70951100	12.80656100
C	8.13094000	4.02527700	10.96098400
C	7.16276800	3.55401100	9.93013700
C	5.85254100	4.04482300	9.97088000

H	5.59059400	4.77610900	10.74091600
C	4.92184700	3.62132500	9.02605700
H	3.90224000	4.00863000	9.05748400
C	5.29176500	2.70625600	8.03831000
H	4.56041700	2.37391900	7.29981300
C	6.59748300	2.21958400	7.99345800
H	6.88950500	1.50611900	7.22138100
C	7.53405000	2.64402000	8.93681500
H	8.55761100	2.26490000	8.90625300
C	9.30611100	5.89287700	9.70294800
C	10.22014700	5.15906000	8.71172900
H	10.52897400	5.83398600	7.89881200
H	9.69544700	4.30201500	8.26518400
H	11.11745300	4.79063900	9.23078000
C	8.04490800	6.39340500	8.98746100
H	8.32200700	7.20443100	8.29705200
H	7.32196100	6.78014000	9.72255800
H	7.56237800	5.60207200	8.39842200
C	10.05571500	7.09506900	10.28250100
H	10.34681600	7.78952400	9.48064600
H	10.96499900	6.76318300	10.80697500
H	9.42325100	7.61635800	11.01495700
C	6.59557900	10.09147400	12.79604800
C	8.09526400	10.11901700	12.49613000
H	8.38610800	11.07465300	12.03409000
H	8.35490800	9.30479500	11.80125000
H	8.67481700	9.95924000	13.41900000
C	6.25047900	11.22832400	13.76780800
H	6.73741200	12.15706800	13.43376500
H	6.60425000	10.98700500	14.78105300
H	5.16972900	11.41406000	13.82316800
C	5.80838000	10.27183800	11.49085000
H	6.04744400	11.24054400	11.02590500
H	4.72654300	10.24360600	11.68738600
H	6.05768800	9.46528700	10.78607000
C	5.28235900	8.31663000	14.05282100
C	4.10365000	9.11278300	14.50409300
C	2.99417700	9.23530500	13.66128700
H	3.00779800	8.74897500	12.68334700
C	1.88239800	9.97377400	14.06670400
H	1.02082600	10.06630500	13.40385800
C	1.87302900	10.59073200	15.31693400
H	1.00279700	11.16667000	15.63517700
C	2.97786200	10.46930800	16.16125900
H	2.97226500	10.94922300	17.14095000
C	4.08939000	9.73427800	15.75702700
H	4.95612600	9.63398700	16.41211300
C	4.55388100	5.95435400	14.67168300
C	3.45287100	5.58942700	13.66677200
H	2.83627600	4.76464900	14.05485700
H	3.90278500	5.27644000	12.71306300
H	2.79599400	6.45146700	13.47990000
C	3.92632300	6.36777200	16.00751300
H	3.47556400	5.48338400	16.48153500
H	3.13838500	7.12240800	15.88235800
H	4.69624900	6.76826100	16.68375900
C	5.46079000	4.74319400	14.89575700
H	4.87079600	3.86446900	15.19706800
H	6.21606700	4.95930500	15.66644800
H	6.00614300	4.50312600	13.96900500
N	10.82095100	9.20706100	14.81768800
N	9.80778800	8.28193700	16.48228800
N	13.82994200	6.39954200	14.50623800
N	13.48055000	6.81127200	16.58089100
N	8.26878800	3.53244100	12.19577900
N	9.00696100	5.01094000	10.83065400
N	6.33813600	8.77352900	13.37178100

N	5.41467500	6.99676800	14.11444100
Si	10.41031100	7.32918100	14.93548300
Si	12.27584900	5.80967800	15.47270900
Si	8.75875600	6.18801600	13.93772800
Si	9.82152100	4.61776500	12.52851300
Si	6.82533600	7.00804000	12.82059200

TS4

C	2.63134800	-2.07866600	1.71971700
C	3.46974800	-1.18119400	0.80614700
H	4.53326600	-1.22863300	1.08459800
H	3.12807200	-0.13675600	0.87367300
H	3.35042800	-1.49476200	-0.24189500
C	3.23945600	-3.48317600	1.75794800
H	4.26235300	-3.42415000	2.15849600
H	3.29318700	-3.90743400	0.74538900
H	2.66518100	-4.16572000	2.39955500
C	2.59897700	-1.47415200	3.12857500
H	3.62264000	-1.37437800	3.51960700
H	2.02877700	-2.11223500	3.81996300
H	2.13611400	-0.47674100	3.09338200
C	0.18536600	-2.77174400	1.39903900
C	0.05214800	-3.92228000	2.34024100
C	0.13989000	-5.23006300	1.84966800
H	0.31182200	-5.39598500	0.78568600
C	0.00057100	-6.31023600	2.71684600
H	0.07293300	-7.32706300	2.32871000
C	-0.23571200	-6.09353900	4.07525700
H	-0.34762700	-6.94144200	4.75251100
C	-0.33098800	-4.79200900	4.56432700
H	-0.51987900	-4.61648100	5.62420600
C	-0.18592200	-3.70653900	3.70011100
H	-0.26459500	-2.68710200	4.07812900
C	-2.24313200	-2.42929900	0.68407500
C	-2.70552000	-3.88646600	0.80492400
H	-3.79780800	-3.91796800	0.67940900
H	-2.46852600	-4.31707500	1.78689500
H	-2.25405700	-4.51455500	0.02440800
C	-2.77881700	-1.62462000	1.87498800
H	-3.87941200	-1.66145200	1.88463600
H	-2.45553200	-0.57121200	1.80845900
H	-2.40751700	-2.05459500	2.81906500
C	-2.76985600	-1.83429200	-0.62433400
H	-3.86901000	-1.86649500	-0.64569900
H	-2.37825100	-2.39272400	-1.48826200
H	-2.44817800	-0.78507300	-0.71773300
C	3.50080300	-0.39275900	-3.37578700
C	2.74403000	0.63092000	-4.23957300
H	3.45577100	1.36110800	-4.65237000
H	1.99306000	1.17389300	-3.65219700
H	2.23849500	0.12285200	-5.07518400
C	4.18965900	0.31901800	-2.20749400
H	4.83227700	1.13462000	-2.57386000
H	4.82092400	-0.38902300	-1.64902200
H	3.43702700	0.73734800	-1.52354700
C	4.58064700	-0.98591500	-4.29611100
H	5.11559800	-0.14466100	-4.75965600
H	4.13455300	-1.58567700	-5.10210700
H	5.32298600	-1.59597400	-3.76987500
C	2.61983400	-2.72863800	-2.81180500
C	3.92059000	-3.45838100	-2.99472000
C	4.84146800	-3.48234600	-1.94218800
H	4.61970600	-2.94013900	-1.02182800

C	6.03439600	-4.19321200	-2.06435800
H	6.74358700	-4.20734000	-1.23535400
C	6.32074800	-4.88176400	-3.24284700
H	7.25578500	-5.43521500	-3.34105100
C	5.40806200	-4.85652400	-4.29778600
H	5.63096900	-5.38506200	-5.22594900
C	4.21272000	-4.15148000	-4.17249300
H	3.50836800	-4.11504000	-5.00503200
C	1.14471500	-4.73529600	-2.42838900
C	2.02648400	-5.50163400	-1.43420100
H	1.61145100	-6.50612400	-1.25558700
H	2.05859700	-4.96111000	-0.47752800
H	3.05541800	-5.62071600	-1.80059800
C	1.15504200	-5.44428300	-3.79188000
H	0.63785700	-6.41288100	-3.71429700
H	2.17712600	-5.63871500	-4.13966200
H	0.63178000	-4.82871900	-4.53792700
C	-0.29955000	-4.72244500	-1.91392800
H	-0.66878600	-5.74186200	-1.71946400
H	-0.95359600	-4.24142700	-2.65724500
H	-0.35538300	-4.12406100	-0.99416300
C	-1.92501200	2.48945600	-3.30223500
C	-2.60277000	1.23175200	-2.75183900
H	-3.39334900	0.90199200	-3.44167200
H	-3.05190600	1.42692100	-1.76733600
H	-1.87200500	0.41515900	-2.65270800
C	-1.29219600	2.15759200	-4.66044300
H	-2.06406400	1.83458400	-5.37522200
H	-0.55962500	1.34422600	-4.54315900
H	-0.78757500	3.04132700	-5.07902100
C	-2.97581700	3.59516600	-3.46359200
H	-3.83435000	3.19180500	-4.02060500
H	-2.59233200	4.46045200	-4.02000300
H	-3.33098500	3.93844000	-2.48102500
C	-0.06839000	3.92294900	-2.35018000
C	-0.36863900	5.23827600	-2.98040500
C	-1.18348500	6.14963200	-2.30183800
H	-1.58719900	5.87978000	-1.32335400
C	-1.47722900	7.38399500	-2.87834600
H	-2.11044000	8.09484000	-2.34569300
C	-0.96609300	7.70764600	-4.13534700
H	-1.19975400	8.67273400	-4.58731600
C	-0.15513600	6.79768800	-4.81459300
H	0.24641200	7.05023700	-5.79696500
C	0.14766300	5.56626700	-4.23741200
H	0.79330900	4.85513800	-4.75643600
C	2.06319800	4.46047500	-1.07484600
C	2.58681600	5.53210500	-2.04005700
H	3.48196800	5.99648100	-1.60073500
H	1.85275000	6.32754100	-2.22260600
H	2.86950500	5.08252900	-3.00372200
C	1.48638700	5.12210200	0.18119600
H	2.25294700	5.73896000	0.67436500
H	1.12908800	4.36048800	0.88955500
H	0.63751100	5.77226100	-0.07949000
C	3.22540600	3.54286200	-0.68997000
H	4.00249500	4.12014400	-0.16871300
H	3.66618000	3.08916400	-1.58916700
H	2.87609100	2.73898600	-0.02373400
C	-0.62859000	1.28478500	4.75516500
C	0.76028100	1.90678000	4.58465900
H	1.46566100	1.46354400	5.30250800
H	0.71618100	2.99236300	4.75600100
H	1.13871500	1.73304300	3.56501000
C	-0.55199200	-0.23141500	4.53596700
H	0.15222000	-0.69483300	5.24537100
H	-0.21675100	-0.44217600	3.50614200

H	-1.54607900	-0.68433700	4.68225100
C	-1.13272500	1.57895300	6.17365100
H	-0.37080200	1.25818700	6.89960700
H	-2.06418000	1.04525200	6.40391600
H	-1.30220700	2.65749800	6.30604700
C	-2.78368000	1.75262200	3.48075300
C	-3.83053500	1.43546700	4.49344700
C	-4.19771500	2.41319000	5.42661400
H	-3.70424100	3.38683300	5.40122800
C	-5.18614100	2.14540700	6.36823200
H	-5.47260900	2.91283400	7.08879000
C	-5.81115000	0.89636300	6.39076400
H	-6.58549500	0.68686700	7.13021000
C	-5.44372400	-0.08162300	5.46892300
H	-5.92644100	-1.05973000	5.48615900
C	-4.45635600	0.18712000	4.51947200
H	-4.16151400	-0.57449800	3.79668200
C	-4.20886100	2.43462200	1.47560900
C	-5.26172000	3.16837200	2.31617500
H	-6.06013300	3.53628500	1.65453500
H	-4.81073800	4.03283600	2.82649200
H	-5.72258500	2.51558000	3.06959100
C	-4.79631900	1.13139400	0.92322500
H	-5.68493400	1.33937000	0.30836700
H	-5.09449400	0.46547100	1.74694000
H	-4.04888200	0.61173900	0.30635500
C	-3.79079900	3.33828200	0.30970100
H	-4.62959700	3.46262100	-0.39131800
H	-2.93584800	2.90069300	-0.23184600
H	-3.48483000	4.32823900	0.67909200
N	1.28328700	-2.06936000	1.14381400
N	-0.78647200	-2.27794800	0.63092500
N	2.51755600	-1.37096600	-2.84088100
N	1.50280400	-3.33035900	-2.54042100
N	-0.86840900	2.85545700	-2.34715000
N	1.04087300	3.60161100	-1.68795700
N	-1.47352200	1.85689300	3.70964100
N	-2.98359900	2.13221600	2.21903000
Si	0.35435900	-0.93222300	-0.05975400
Si	0.65039600	-1.05505400	-2.50787800
Si	0.12119300	1.21212100	0.72597400
Si	0.45042600	1.81681700	-1.43508900
Si	-1.16824700	2.70291200	2.03948200

Table A2.5 Optimized geometries of compounds **2.4**, **2.5** and **2.6** and related transition states and intermediates.

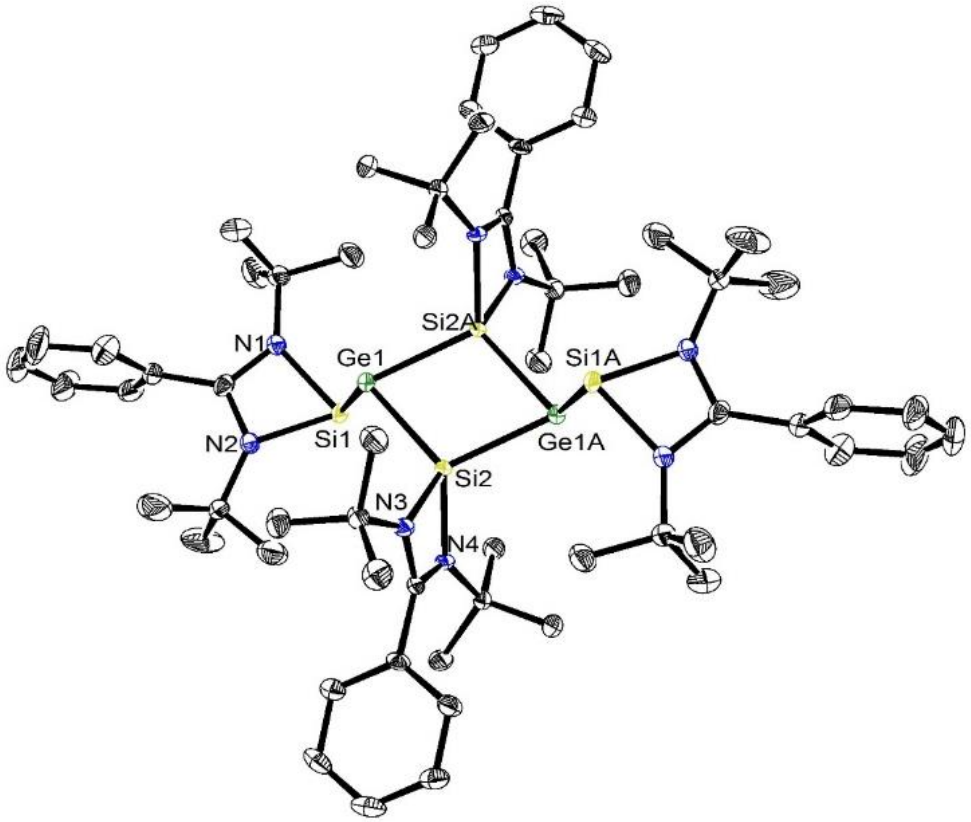

Bond	X-ray crystallographic data (Å)	Optimized geometric data at M06-2X/6-311G(d) level of theory (Å)
Ge1-Si2	2.3852(11)	2.4098
Ge1-Si2A	2.3844(11)	2.4070
Ge1-Si1	2.4673(13)	2.4907

Table A2.6 Comparison of X-ray crystallographic data and optimized geometric data of compound **3.2**

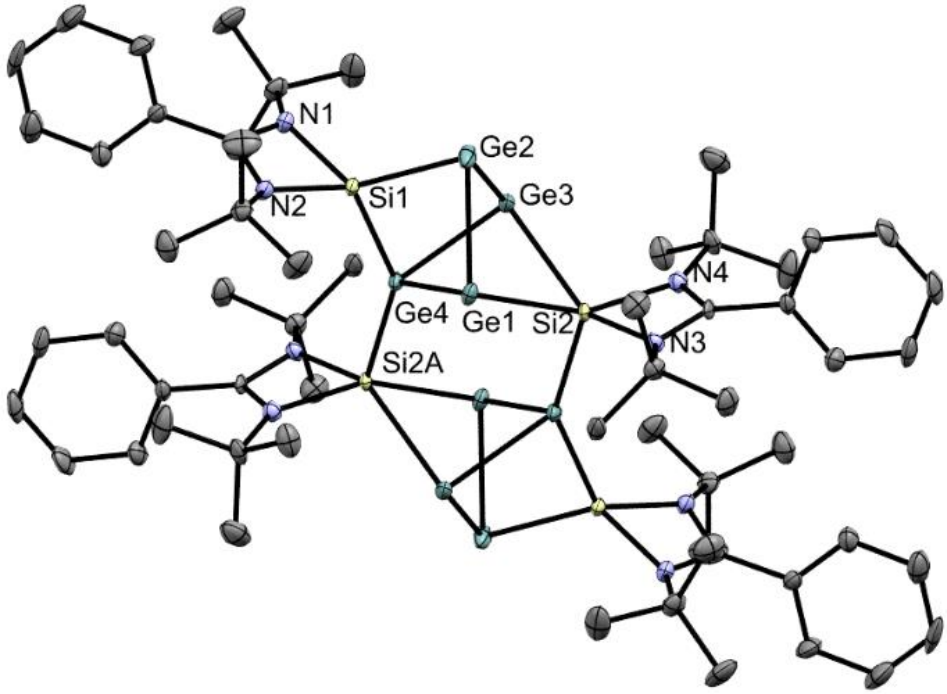

Bond	X-ray crystallographic data (Å)	Optimized geometric data at M06-2X/def2-SVP level of theory (Å)
Ge1-Ge2	2.5338(7)	2.568
Ge2-Ge3	2.5335(7)	2.565
Si1-Ge2	2.4012(11)	2.415
Ge4-Ge1	2.4735(7)	2.501
Ge4-Ge3	2.4810(6)	2.489
Si2-Ge1	2.5249(12)	2.539
Si2-Ge3	2.5503(11)	2.592

Table A2.7 Comparison of X-ray crystallographic data and optimized geometric data of compound **3.3**

Orbital[a]	Occ.[b]	Contribution from atoms to the orbital	Atomic orbitals
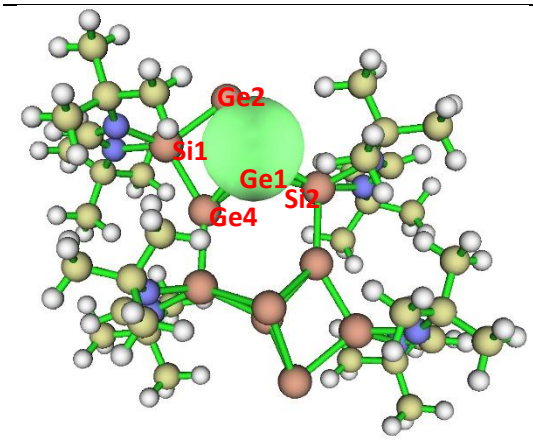	1.73	100% Ge1	70.78% *s* + 29.08% *p*
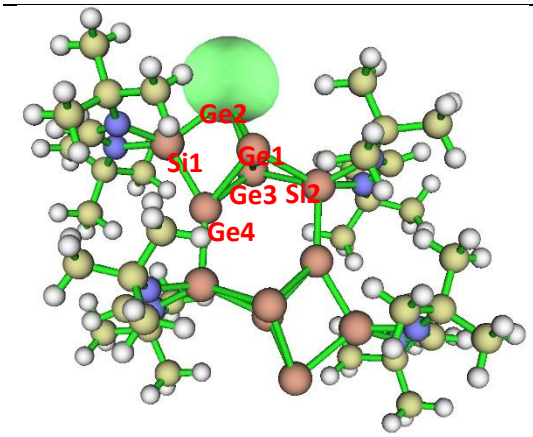	1.93	100% Ge2	74.65% *s* + 25.72 % *p*
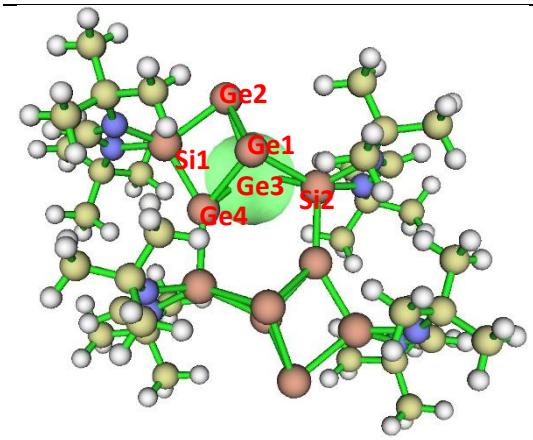	1.75	100% Ge3	69.89 % *s* + 30.0 % *p*

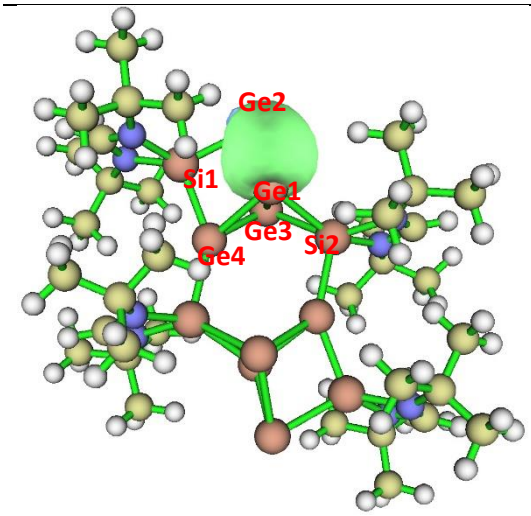	1.63	54.87% Ge1 + 45.13% Ge2	Ge1: 11.74 % *s* + 87.57 % *p* Ge2: 7.80 % *s* + 91.22 % *p*
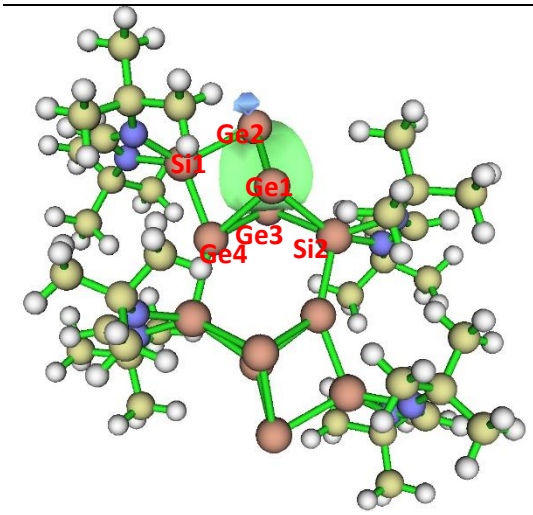	1.63	46.11% Ge2 + 53.89% Ge3	Ge2: 8.65 % *s* + 90.36 % *p* Ge3: 12.39 % *s* + 86.92 % *p*
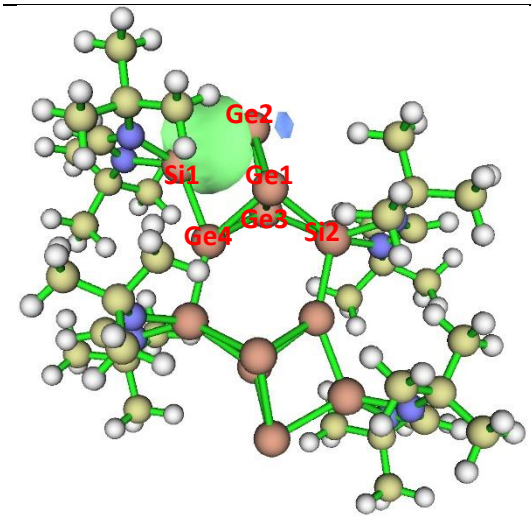	1.91	63.08% Si1 + 36.92% Ge2	Si1: 44.44% *s* + 55.37% *p* Ge2: 8.88% *s* + 90.41% *p*

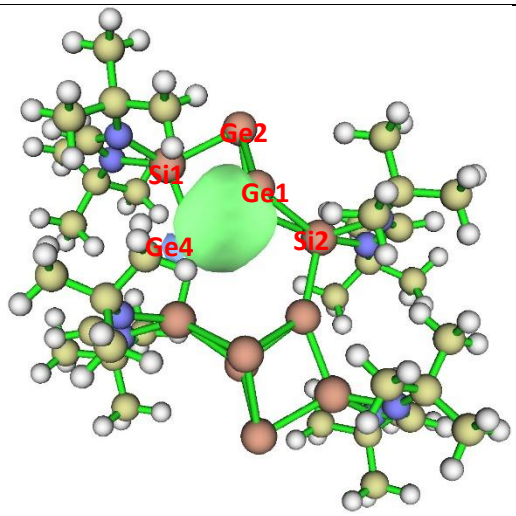	1.79	56.24% Ge4 + 43.76% Ge1	Ge4: 15.10% *s* + 84.50% *p* Ge1: 11.63% *s* + 87.71% *p*
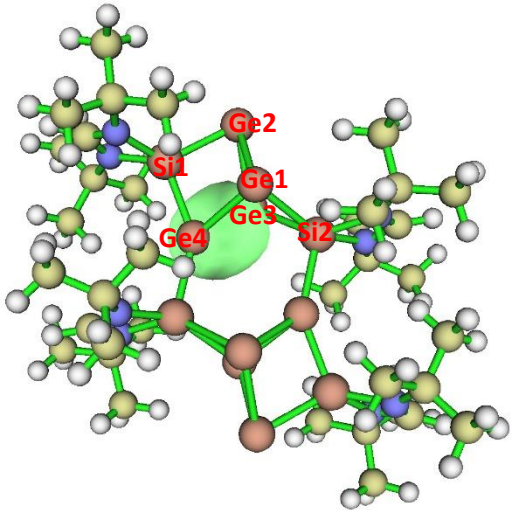	1.81	58.66% Ge4 + 41.34% Ge3	Ge4: 23.89% *s* + 75.76% *p* Ge3: 11.55% *s* + 87.91% *p*
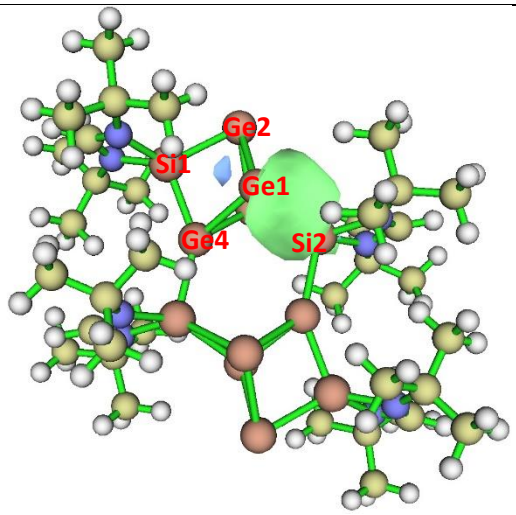	1.48	55.38% Si2 + 44.62% Ge1	Si2: 27.47% *s* + 72.10% *p* Ge1: 6.21% *s* + 93.16% *p*

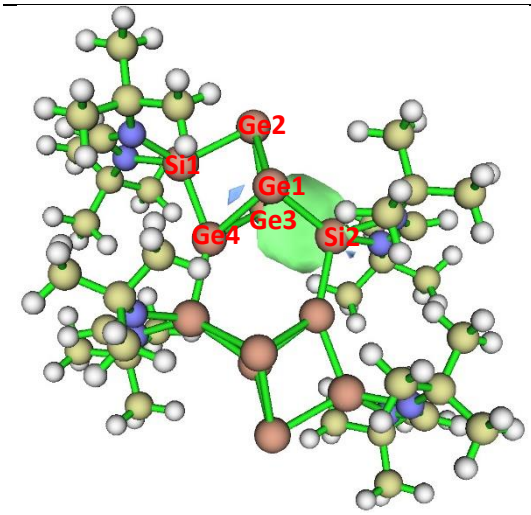	1.47	56.43% Si2 + 43.57% Ge3	Si2: 27.47% *s* + 72.10% *p* Ge3: 6.21% *s* + 93.16% *p*

[a] For generating of the NBO plot files, -Ph substituents are truncated by –H groups. [b] Occ. = Occupancy

Table A2.8 NBO results of compound **3.3** at M06-2X/def2-SVP theory

	Ge1-Ge2	Ge2-Ge3	Ge1-Ge3
$\rho(r)$ (eÅ^{-3})	0.059	0.060	0.046
$\nabla^2\rho(r)$ (eÅ^{-5})	-0.008	-0.011	0.015
η_{BCP}	0.64	0.67	0.54

Table A2.9 Electron density $\rho(r)$, Laplacian $\nabla^2\rho(r)$ and η_{BCP} ($\eta = |\lambda_3|/ \lambda_1$; λ_i is the eigenvalues of the Hessian matrix) at the Ge1-Ge2, Ge2-Ge3 and Ge1-Ge3 bond critical points (BCPs) of compound **3.3**

	Si1-Ge2
$\rho(r)$ (eÅ^{-3})	0.074
$\nabla^2\rho(r)$ (eÅ^{-5})	-0.018
η_{BCP}	0.61

Table A2.10 Electron density $\rho(r)$, Laplacian $\nabla^2\rho(r)$ and η_{BCP} ($\eta = |\lambda_3|/ \lambda_1$; λ_i is the eigenvalues of the Hessian matrix) at the Si1-Ge2 bond critical point (BCP) of compound **3.3**

	Si2-Ge1	Si2-Ge3
$\rho(r)$ (eÅ^{-3})	0.061	0.056
$\nabla^2\rho(r)$ (eÅ^{-5})	-0.021	-0.013
η_{BCP}	0.72	0.65

Table A2.11 Electron density $\rho(r)$, Laplacian $\nabla^2\rho(r)$ and η_{BCP} ($\eta = |\lambda_3|/ \lambda_1$; λ_i is the eigenvalues of the Hessian matrix) at the Si2-Ge1 and Si2-Ge3 bond critical points (BCPs) of compound **3.3**

	Ge4-Ge1	Ge4-Ge3
$\rho(r)$ (eÅ^{-3})	0.066	0.067
$\nabla^2\rho(r)$ (eÅ^{-5})	-0.017	-0.016
η_{BCP}	0.69	0.68

Table A2.12 Electron density $\rho(r)$, Laplacian $\nabla^2\rho(r)$ and η_{BCP} ($\eta = |\lambda_3|/ \lambda_1$; λ_i is the eigenvalues of the Hessian matrix) at the Ge4-Ge1 and Ge4-Ge3 bond critical points (BCPs) of compound **3.3**

Bond	Atom(1)	Contr. %	Hybrid Type	Atom(2)	Contr. %	Hybrid Type	Occu-pancy	Wiberg bond index
Ge1-Si2 (σ)	Ge1	51.4	$sp^{2.08}$	Si2	48.6	$sp^{2.19}$	1.85	1.04
Ge1-Si2 (σ*)	Ge1	48.6	$sp^{2.08}$	Si2	51.4	$sp^{2.19}$	0.21	
Ge1-Si2A (σ)	Ge1	50.9	$sp^{2.23}$	Si2A	49.1	$sp^{2.14}$	1.85	1.05
Ge1-Si2A (σ*)	Ge1	49.1	$sp^{2.23}$	Si2A	50.9	$sp^{2.14}$	0.19	
Ge1A-Si2 (σ)	Ge1A	50.9	$sp^{2.23}$	Si2	49.1	$sp^{2.14}$	1.85	1.05
Ge1A-Si2 (σ*)	Ge1A	49.1	$sp^{2.23}$	Si2	50.9	$sp^{2.14}$	0.19	
Ge1A-Si2A (σ)	Ge1A	51.4	$sp^{2.08}$	Si2A	48.6	$sp^{2.19}$	1.85	1.04
Ge1A-Si2A (σ*)	Ge1A	48.6	$sp^{2.08}$	Si2A	51.4	$sp^{2.19}$	0.21	

Ge1-Si1 (σ)	Ge1	65.3	$sp^{1.76}$	Si1	34.7	$sp^{6.83}$	1.85	0.86
Ge1-Si1 (σ*)	Ge1	34.7	$sp^{1.76}$	Si1	65.3	$sp^{6.83}$	0.23	
Ge1A-Si1A (σ)	Ge1A	65.3	$sp^{1.76}$	Si1A	34.7	$sp^{6.83}$	1.85	0.86
Ge1A-Si1A (σ*)	Ge1A	34.7	$sp^{1.76}$	Si1A	65.3	$sp^{6.83}$	0.23	
Ge1 LP	Ge1	-	*p*	-	-	-	1.22	-
Ge1A LP	Ge1A	-	*p*	-	-	-	1.22	-
Si1 LP	Si1	-	$sp^{0.36}$	-	-	-	1.94	-
Si1A LP	Si1A	-	$sp^{0.36}$	-	-	-	1.94	-

Table A2.13 NBO results of compound **3.2** at M06-2X/6-311G(d) theory

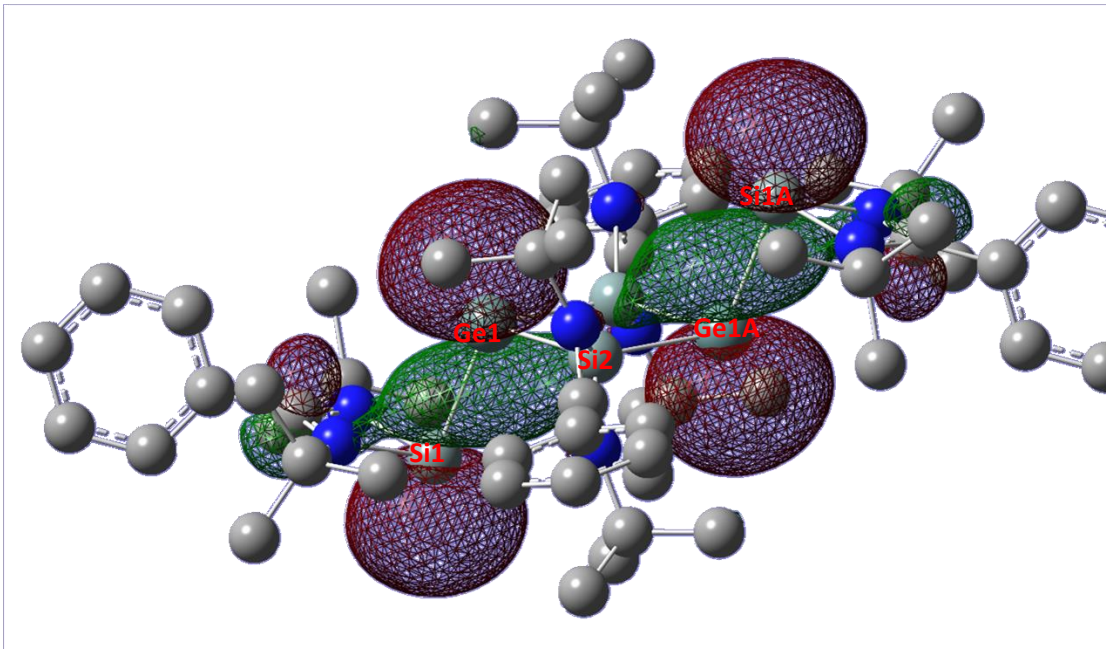

(a) HOMO

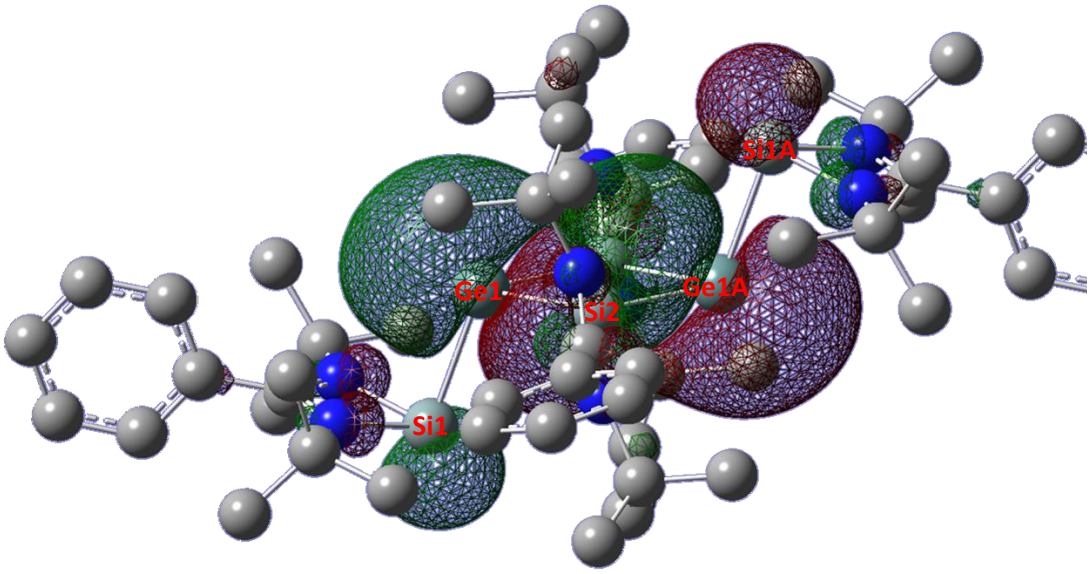

(b) HOMO-1

Figure A2.7 The HOMO and HOMO-1 of compound **3.2**

Compound **3.3**
M06-2X/6-311G(d)

Atomic Number	Coordinates (Angstroms) X	Y	Z
6	2.649397	-4.909951	-0.055342
6	2.649397	-4.909951	1.477561
1	3.665712	-4.909951	1.875052
1	2.144335	-5.804248	1.856422
1	2.128461	-4.025875	1.851593
6	3.447073	-6.104641	-0.589509
1	3.503744	-6.063573	-1.680105
1	2.955411	-7.038911	-0.304854
1	4.461159	-6.125824	-0.187862
6	1.204282	-5.010749	-0.548531
1	0.611041	-4.162859	-0.187667
1	0.745681	-5.934960	-0.186517
1	1.164789	-5.014678	-1.641087
6	4.376905	-3.100072	-0.534836
6	5.601816	-3.693957	0.069121
6	6.492410	-4.432174	-0.708463
1	6.277705	-4.588698	-1.760681
6	7.636492	-4.975357	-0.134232
1	8.324742	-5.550664	-0.743062
6	7.894199	-4.782375	1.219224
1	8.786374	-5.205443	1.666902
6	7.006975	-4.046106	1.998411
1	7.207602	-3.891908	3.052538
6	5.862968	-3.502505	1.425630
1	5.169175	-2.914989	2.019142
6	5.278769	-0.893663	-1.429680
6	6.225864	-1.364232	-2.539948
1	6.815685	-2.221831	-2.210611
1	6.920143	-0.566181	-2.817979
1	5.652999	-1.652384	-3.424584
6	6.070531	-0.506647	-0.175728
1	5.384058	-0.301113	0.649568
1	6.656190	0.395755	-0.372745
1	6.762309	-1.292871	0.129952
6	4.499045	0.331255	-1.917150
1	3.849028	0.066180	-2.756251
1	5.196025	1.102651	-2.255547
1	3.874173	0.740429	-1.118193
6	2.319798	3.173812	1.185533
6	1.463097	2.691963	2.358114
1	0.445711	3.086262	2.296777
1	1.905108	3.017454	3.302571
1	1.407558	1.600659	2.367621
6	3.718801	2.554099	1.287379
1	3.646843	1.463617	1.287862
1	4.209220	2.870878	2.211908
1	4.345241	2.867747	0.446926
6	2.417525	4.702731	1.227558
1	3.141363	5.097755	0.513608
1	2.739710	5.005585	2.226818
1	1.447113	5.163287	1.031371
6	1.884131	2.967884	-1.316774
6	2.542414	4.198304	-1.828704
6	3.902888	4.207539	-2.125200
1	4.483821	3.300676	-1.997560

6	4.502517	5.373024	-2.587863
1	5.561930	5.379996	-2.817139
6	3.743816	6.526803	-2.760091
1	4.212973	7.434379	-3.122605
6	2.383704	6.516231	-2.466112
1	1.791753	7.414979	-2.597050
6	1.782611	5.354300	-1.997358
1	0.725425	5.338310	-1.751857
6	1.021893	1.936557	-3.476181
6	2.174579	2.420599	-4.362770
1	2.310796	3.501608	-4.318999
1	1.957094	2.155483	-5.400395
1	3.113418	1.938987	-4.079112
6	-0.232667	2.777227	-3.736381
1	-1.065808	2.401152	-3.138233
1	-0.510316	2.722375	-4.792715
1	-0.059515	3.827696	-3.487747
6	0.723207	0.471920	-3.798989
1	1.599301	-0.160960	-3.641819
1	0.410725	0.377588	-4.841532
1	-0.084419	0.093909	-3.167246
32	1.662167	-0.938208	0.385944
7	3.161029	-3.640531	-0.572557
7	4.278741	-1.921630	-1.142975
7	1.660789	2.678001	-0.035097
7	1.364701	1.982706	-2.044066
14	2.452477	-2.208695	-1.605296
14	0.739572	1.103803	-0.493096
6	-2.649397	4.909951	0.055342
6	-2.649397	4.909951	-1.477561
1	-3.665712	4.909951	-1.875052
1	-2.144335	5.804248	-1.856422
1	-2.128461	4.025875	-1.851593
6	-3.447073	6.104641	0.589509
1	-3.503744	6.063573	1.680105
1	-2.955411	7.038911	0.304854
1	-4.461159	6.125824	0.187862
6	-1.204282	5.010749	0.548531
1	-0.611041	4.162859	0.187667
1	-0.745681	5.934960	0.186517
1	-1.164789	5.014678	1.641087
6	-4.376905	3.100072	0.534836
6	-5.601816	3.693957	-0.069121
6	-6.492410	4.432174	0.708463
1	-6.277705	4.588698	1.760681
6	-7.636492	4.975357	0.134232
1	-8.324742	5.550664	0.743062
6	-7.894199	4.782375	-1.219224
1	-8.786374	5.205443	-1.666902
6	-7.006975	4.046106	-1.998411
1	-7.207602	3.891908	-3.052538
6	-5.862968	3.502505	-1.425630
1	-5.169175	2.914989	-2.019142
6	-5.278769	0.893663	1.429680
6	-6.225864	1.364232	2.539948
1	-6.815685	2.221831	2.210611
1	-6.920143	0.566181	2.817979
1	-5.652999	1.652384	3.424584
6	-6.070531	0.506647	0.175728
1	-5.384058	0.301113	-0.649568
1	-6.656190	-0.395755	0.372745

1	-6.762309	1.292871	-0.129952
6	-4.499045	-0.331255	1.917150
1	-3.849028	-0.066180	2.756251
1	-5.196025	-1.102651	2.255547
1	-3.874173	-0.740429	1.118193
6	-2.319798	-3.173812	-1.185533
6	-1.463097	-2.691963	-2.358114
1	-0.445711	-3.086262	-2.296777
1	-1.905108	-3.017454	-3.302571
1	-1.407558	-1.600659	-2.367621
6	-3.718801	-2.554099	-1.287379
1	-3.646843	-1.463617	-1.287862
1	-4.209220	-2.870878	-2.211908
1	-4.345241	-2.867747	-0.446926
6	-2.417525	-4.702731	-1.227558
1	-3.141363	-5.097755	-0.513608
1	-2.739710	-5.005585	-2.226818
1	-1.447113	-5.163287	-1.031371
6	-1.884131	-2.967884	1.316774
6	-2.542414	-4.198304	1.828704
6	-3.902888	-4.207539	2.125200
1	-4.483821	-3.300676	1.997560
6	-4.502517	-5.373024	2.587863
1	-5.561930	-5.379996	2.817139
6	-3.743816	-6.526803	2.760091
1	-4.212973	-7.434379	3.122605
6	-2.383704	-6.516231	2.466112
1	-1.791753	-7.414979	2.597050
6	-1.782611	-5.354300	1.997358
1	-0.725425	-5.338310	1.751857
6	-1.021893	-1.936557	3.476181
6	-2.174579	-2.420599	4.362770
1	-2.310796	-3.501608	4.318999
1	-1.957094	-2.155483	5.400395
1	-3.113418	-1.938987	4.079112
6	0.232667	-2.777227	3.736381
1	1.065808	-2.401152	3.138233
1	0.510316	-2.722375	4.792715
1	0.059515	-3.827696	3.487747
6	-0.723207	-0.471920	3.798989
1	-1.599301	0.160960	3.641819
1	-0.410725	-0.377588	4.841532
1	0.084419	-0.093909	3.167246
32	-1.662167	0.938208	-0.385944
7	-3.161029	3.640531	0.572557
7	-4.278741	1.921630	1.142975
7	-1.660789	-2.678001	0.035097
7	-1.364701	-1.982706	2.044066
14	-2.452477	2.208695	1.605296
14	-0.739572	-1.103803	0.493096

Compound **3.4**
M06-2X/def2-SVP

Atomic Number	Coordinates (Angstroms) X	Y	Z
6	-5.302262	1.297229	-2.580671
6	-5.444652	-0.222820	-2.431056
1	-4.560654	-0.641499	-1.921348

1	-5.536632	-0.697533	-3.420115
1	-6.347817	-0.470195	-1.851508
6	-6.574622	1.888004	-3.199033
1	-7.483662	1.565457	-2.675484
1	-6.652626	1.551810	-4.243170
1	-6.529432	2.986873	-3.194050
6	-4.116515	1.617310	-3.494494
1	-3.965379	2.704609	-3.564123
1	-4.303801	1.218186	-4.501494
1	-3.188791	1.171579	-3.107816
6	-5.717488	1.962977	-0.158024
6	-7.191421	1.750556	-0.065931
6	-7.680949	0.505023	0.339573
1	-6.979542	-0.283457	0.621513
6	-9.054987	0.279927	0.397111
1	-9.431017	-0.693542	0.715308
6	-9.943928	1.299981	0.058670
1	-11.019577	1.124838	0.106869
6	-9.457352	2.545735	-0.338177
1	-10.150562	3.345656	-0.601424
6	-8.084010	2.770868	-0.405867
1	-7.697893	3.738966	-0.731032
6	-5.199600	2.756723	2.196232
6	-5.924503	4.101779	2.065669
1	-6.047402	4.559537	3.058230
1	-6.923923	3.978856	1.625529
1	-5.335932	4.787022	1.437491
6	-6.040305	1.769459	3.013898
1	-5.541037	0.790196	3.060584
1	-7.047306	1.637747	2.596773
1	-6.149252	2.149316	4.040275
6	-3.868908	2.986038	2.914648
1	-4.061930	3.347682	3.934631
1	-3.258082	3.731803	2.387107
1	-3.284595	2.056465	2.977626
6	2.767748	3.453671	2.285176
6	1.874215	4.701324	2.283281
1	2.272756	5.447554	1.578453
1	1.848472	5.152837	3.286237
1	0.846171	4.454630	1.983356
6	2.242104	2.401421	3.269714
1	1.237087	2.057972	2.994706
1	2.198903	2.829368	4.281838
1	2.911299	1.527898	3.286065
6	4.174782	3.855239	2.745381
1	4.878234	3.014316	2.666876
1	4.111219	4.146000	3.803965
1	4.580321	4.709561	2.188700
6	3.500718	3.040987	-0.132322
6	4.739073	3.865469	-0.203437
6	5.975893	3.330843	0.166089
1	6.027003	2.305007	0.535241
6	7.125269	4.108351	0.067270
1	8.090322	3.690489	0.358640
6	7.042891	5.422810	-0.396985
1	7.944803	6.032250	-0.470353
6	5.808370	5.958094	-0.760568
1	5.741012	6.985919	-1.119562
6	4.654133	5.179904	-0.666565
1	3.682858	5.590716	-0.950473
6	3.383496	2.209400	-2.545936

6	4.910415	2.188869	-2.696745
1	5.372150	3.176133	-2.568457
1	5.151871	1.832984	-3.709036
1	5.358527	1.489446	-1.973695
6	2.789588	3.320812	-3.418408
1	1.693448	3.325041	-3.337278
1	3.066217	3.165715	-4.471977
1	3.171893	4.302923	-3.101617
6	2.859774	0.840813	-2.994007
1	3.303897	0.049038	-2.370653
1	3.132262	0.663369	-4.045059
1	1.766597	0.774022	-2.900661
32	-1.808025	0.469593	-0.314336
32	-0.784962	2.307821	1.038730
32	-1.853480	4.044106	-0.523137
32	-0.574870	2.145974	-1.680574
7	-4.994326	1.890172	-1.270575
7	-4.891785	2.217534	0.857632
7	2.738841	2.844920	0.941952
7	2.946777	2.400295	-1.153179
14	-3.388088	2.191860	-0.307166
14	1.449472	1.870079	-0.084879
6	5.302366	-1.297370	2.580576
6	5.444762	0.222687	2.431043
1	4.560763	0.641402	1.921367
1	5.536759	0.697345	3.420127
1	6.347924	0.470083	1.851500
6	6.574759	-1.888187	3.198832
1	7.483772	-1.565622	2.675243
1	6.652826	-1.552047	4.242981
1	6.529562	-2.987055	3.193795
6	4.116665	-1.617498	3.494442
1	3.965530	-2.704799	3.564020
1	4.304002	-1.218426	4.501453
1	3.188923	-1.171743	3.107833
6	5.717505	-1.963059	0.157898
6	7.191456	-1.750761	0.065816
6	7.681105	-0.505317	-0.339812
1	6.979777	0.283185	-0.621886
6	9.055165	-0.280344	-0.397318
1	9.431290	0.693054	-0.715620
6	9.944007	-1.300428	-0.058709
1	11.019672	-1.125378	-0.106879
6	9.457309	-2.546093	0.338270
1	10.150441	-3.346037	0.601652
6	8.083947	-2.771106	0.405919
1	7.697735	-3.739130	0.731191
6	5.199535	-2.756725	-2.196370
6	5.924455	-4.101778	-2.065877
1	6.047263	-4.559531	-3.058451
1	6.923915	-3.978857	-1.625831
1	5.335942	-4.787027	-1.437649
6	6.040191	-1.769433	-3.014051
1	5.540878	-0.790195	-3.060749
1	7.047186	-1.637668	-2.596926
1	6.149156	-2.149297	-4.040423
6	3.868813	-2.986044	-2.914730
1	4.061796	-3.347650	-3.934734
1	3.258028	-3.731840	-2.387184
1	3.284476	-2.056483	-2.977649
6	-2.767815	-3.453724	-2.285042

6	-1.874261	-4.701362	-2.283126
1	-2.272755	-5.447562	-1.578240
1	-1.848560	-5.152926	-3.286060
1	-0.846205	-4.454638	-1.983265
6	-2.242237	-2.401508	-3.269651
1	-1.237221	-2.058014	-2.994696
1	-2.199059	-2.829504	-4.281755
1	-2.911459	-1.528006	-3.286022
6	-4.174861	-3.855340	-2.745171
1	-4.878324	-3.014424	-2.666689
1	-4.111333	-4.146162	-3.803741
1	-4.580364	-4.709636	-2.188424
6	-3.500731	-3.040910	0.132455
6	-4.739133	-3.865316	0.203621
6	-5.975930	-3.330599	-0.165850
1	-6.026983	-2.304756	-0.534995
6	-7.125359	-4.108021	-0.066981
1	-8.090395	-3.690086	-0.358306
6	-7.043058	-5.422487	0.397269
1	-7.945012	-6.031860	0.470676
6	-5.808559	-5.957863	0.760793
1	-5.741261	-6.985696	1.119779
6	-4.654269	-5.179759	0.666743
1	-3.683012	-5.590647	0.950600
6	-3.383453	-2.209188	2.546018
6	-4.910371	-2.188579	2.696836
1	-5.372151	-3.175833	2.568634
1	-5.151806	-1.832597	3.709097
1	-5.358455	-1.489199	1.973727
6	-2.789584	-3.320563	3.418566
1	-1.693445	-3.324846	3.337427
1	-3.066198	-3.165377	4.472125
1	-3.171935	-4.302680	3.101851
6	-2.859670	-0.840590	2.993988
1	-3.303780	-0.048837	2.370596
1	-3.132124	-0.663070	4.045036
1	-1.766494	-0.773843	2.900608
32	1.808040	-0.469571	0.314338
32	0.784953	-2.307763	-1.038763
32	1.853490	-4.044094	0.523037
32	0.574902	-2.145994	1.680546
7	4.994365	-1.890238	1.270462
7	4.891772	-2.217561	-0.857747
7	-2.738869	-2.844910	-0.941847
7	-2.946753	-2.400187	1.153270
14	3.388099	-2.191850	0.307087
14	-1.449464	-1.870042	0.084904

Table A2.14 Optimized geometries of compounds **3.2** and **3.3**

A.3 X-ray Crystallographic Data

Crystallographic data for **2.4**: $C_{72}H_{104}N_8Si_7$; M = 1278.26; triclinic *P* -1; *a* = 15.3763(14) Å, *b* = 15.3866(17) Å, *c* = 27.8566(18) Å; α =83.745(4)°, β = 83.819(3)°, γ = 64.633(3)°; *V* = 3785.9(7) Å^3; *Z* = 2; ρ_{calcd} = 1.121 g cm^{-3}; 28868 measured reflections; 13235 independent reflections; 736 refined parameters; R_1 = 0.0978, wR_2 = 0.2097 ($I > 2\sigma(I)$).

Crystallographic data for **2.5**: $C_{74}H_{108}N_8Si_6$; M = 1278.22; monoclinic *P* 1 21/c 1; *a* = 11.8359(17) Å, *b* = 17.048(2) Å, *c* = 18.222(3) Å; α =90°, β = 91.926(4)°, γ = 90°; *V* = 3674.7(9) Å^3; *Z* = 2; ρ_{calcd} = 1.155 g cm^{-3}; 7561 measured reflections; 7561 independent reflections; 451 refined parameters; R_1 = 0.0797, wR_2 = 0.1985 ($I > 2\sigma(I)$).

Crystallographic data for **2.6**: $C_{65}H_{104}N_8Si_5$; M = 1138.01; monoclinic *P* 1 21/c 1; *a* = 13.4477(12) Å, *b* = 23.674(2) Å, *c* = 21.774(2) Å; α =90°, β = 94.560(3)°, γ = 90°; *V* = 6910.0(12) Å^3; *Z* = 4; ρ_{calcd} = 1.094 g cm^{-3}; 65656 measured reflections; 14465 independent reflections; 810 refined parameters; R_1 = 0.0945, wR_2 = 0.1790 ($I > 2\sigma(I)$).

Crystallographic data for **2.7**: $C_{94}H_{140}N_8O_{16}Si_7W_2$; M = 2202.46; monoclinic *C* 1 2/c 1; *a* = 22.0507(10) Å, *b* = 17.9656(8) Å, *c* = 26.7083(13) Å; α =90°, β = 97.712(2) °, γ = 90°; *V* = 10484.9(8) Å^3; *Z* = 4; ρ_{calcd} = 1.395 g cm^{-3}; 111396 measured reflections; 13874 independent reflections; 632 refined parameters; R_1 = 0.0677, wR_2 = 0.1659 ($I > 2\sigma(I)$).

Crystallographic data for **3.3**: $C_{74}H_{108}N_8Si_4Ge_2$; M = 1367.22; monoclinic *P*1 21/*c*1; *a* = 11.8909(17) Å, *b* = 17.158(2) Å, *c* = 18.316(2) Å; α =90°, β = 91.698(4)°, γ = 90°; *V* = 3735.3(9) Å^3; *Z* = 2; ρ_{calcd} = 1.216 g cm^{-3}; 56423 measured reflections; 8889 independent reflections; 411 refined parameters; R_1 = 0.0560, wR_2 = 0.1170 ($I > 2\sigma(I)$).

Crystallographic data for **3.4**: $C_{81}H_{116}Ge_8N_8Si_4$; M = 1894.89; triclinic *P* -1; *a* = 12.07180(10) Å, *b* = 13.99550(10) Å, *c* = 14.92650(10) Å; α =113.6632(5)°, *β* = 96.9458(6)°, *γ* = 102.2063(6)°; *V* = 2197.13(3) $Å^3$; *Z* = 1; ρ_{calcd} = 1.432 g cm^{-3}; 29249 measured reflections; 7735 independent reflections; 489 refined parameters; R_1 = 0.0570, wR_2 = 0.1467 ($I > 2\sigma(I)$).

A.4 Other Spectroscopic Data

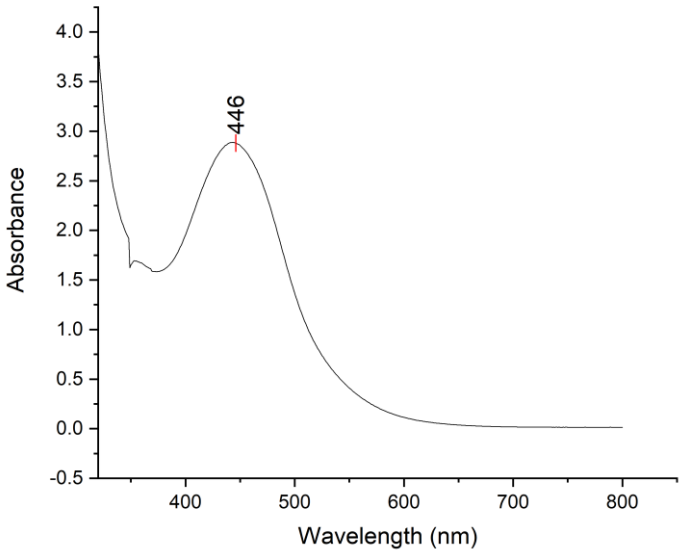

Figure A4.1 UV-vis spectrum of **2.4** in benzene

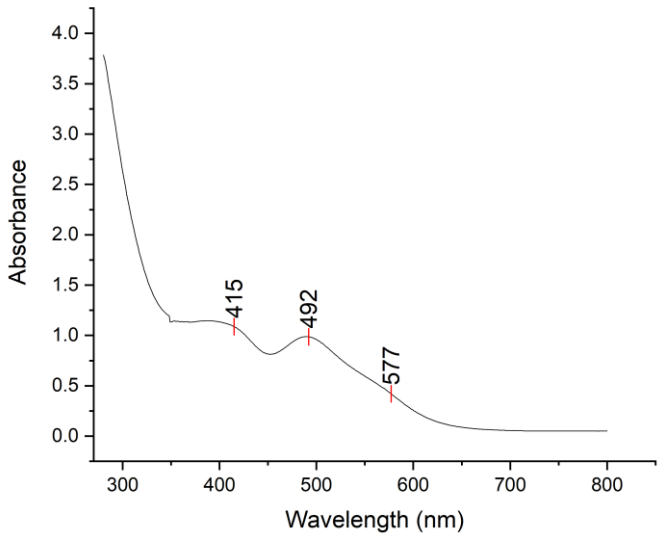

Figure A4.2 UV-vis spectrum of **2.5** in benzene

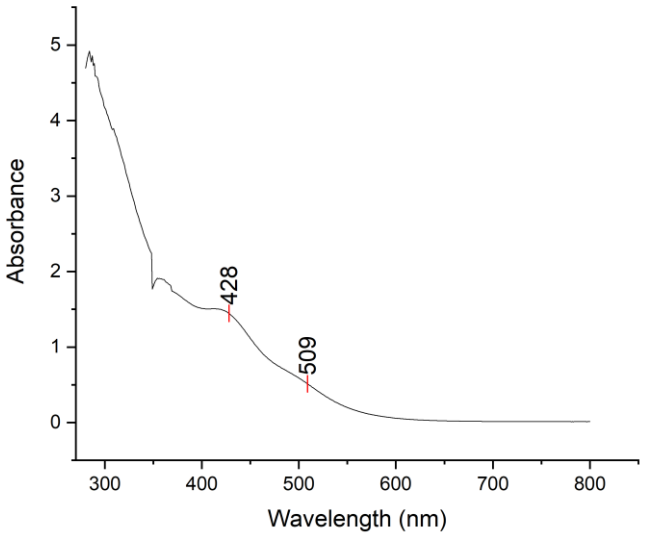

Figure A4.3 UV-vis spectrum of **2.6** in benzene

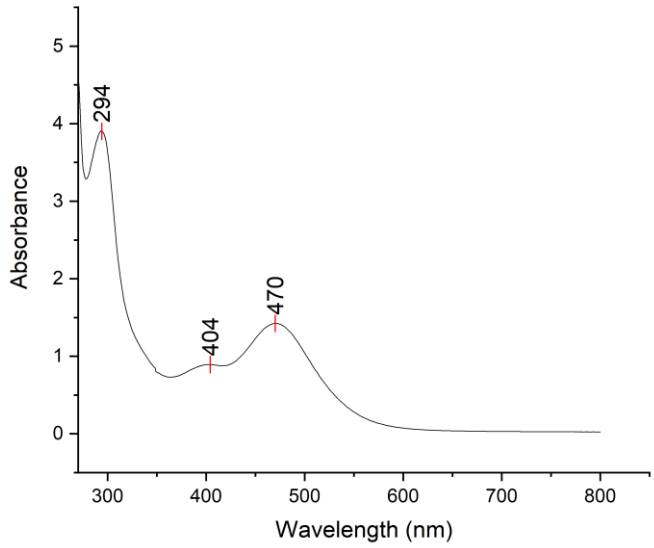

Figure A4.4 UV-vis spectrum of **2.7** in THF

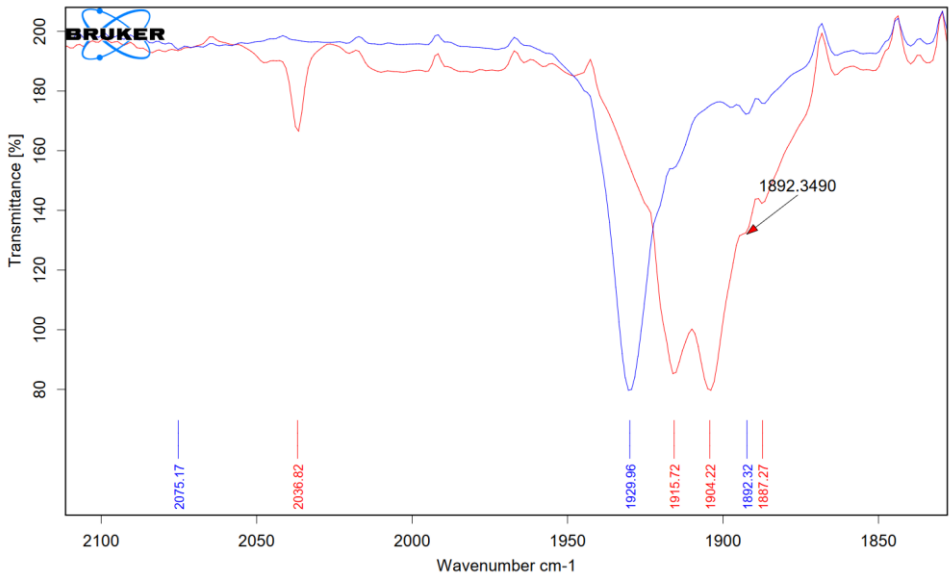

Figure A4.5 FT-IR spectrum of W(CO)THF (blue) and **2.7** (red) in THF

Point Energy Dispersive Spectroscopy Data:

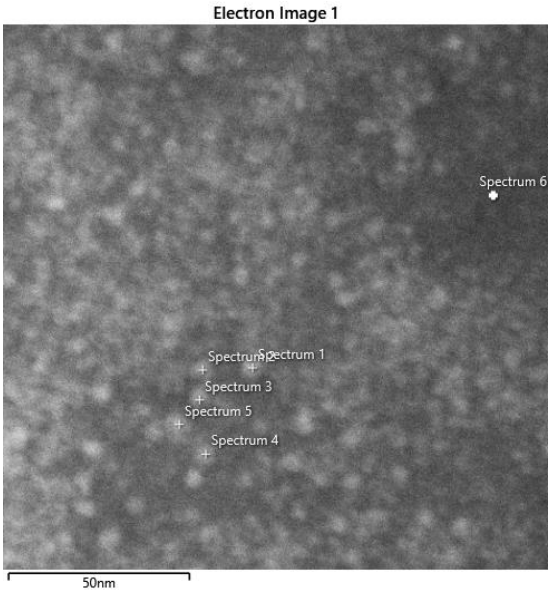

Figure A4.6 HAADF electron micrograph of area used for EDS point analysis, each point corresponding to the following spectrums

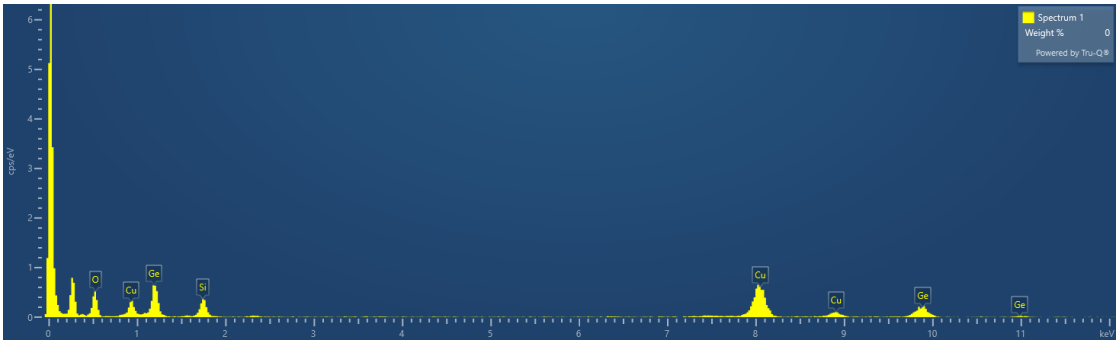

Figure A4.6.1 EDS point analysis of germanium nanoparticles Spectrum 1

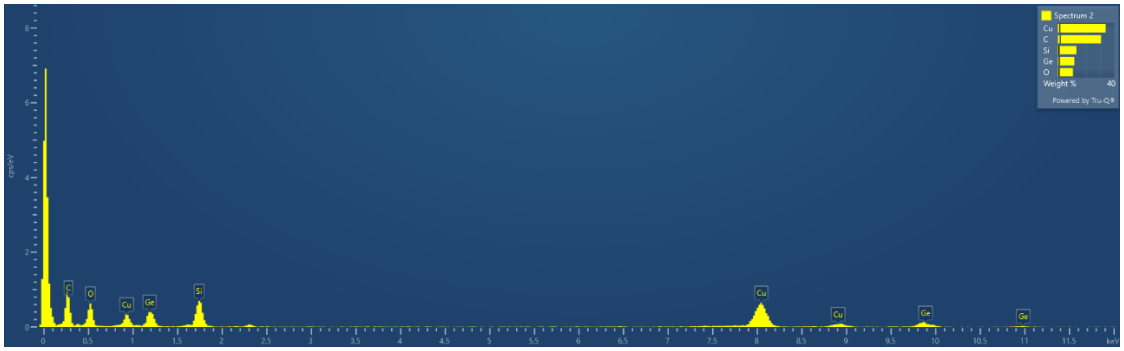

Figure A4.6.2 EDS point analysis of germanium nanoparticles Spectrum 2

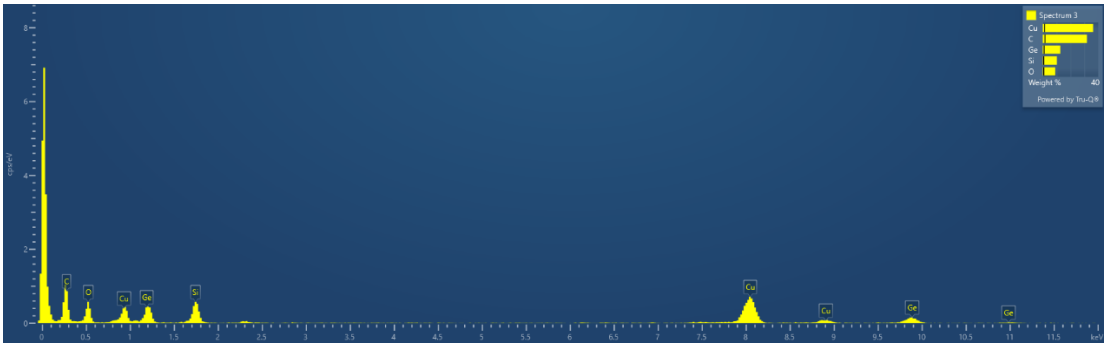

Figure A4.6.3 EDS point analysis of germanium nanoparticles Spectrum 3

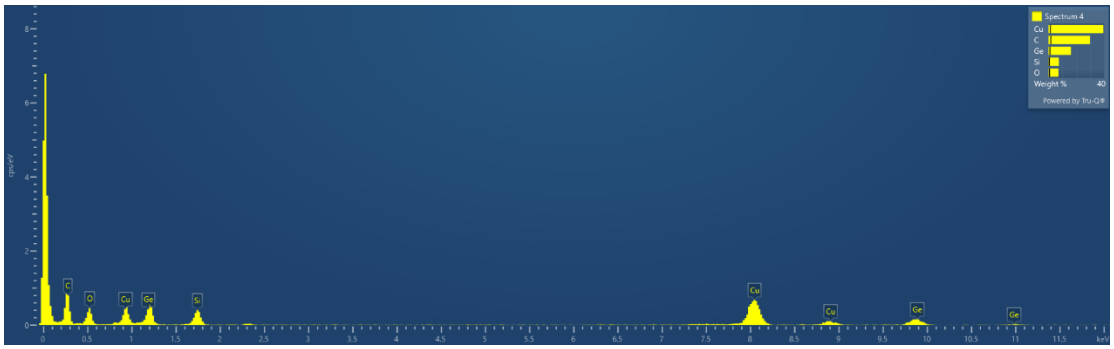

Figure A4.6.4 EDS point analysis of germanium nanoparticles Spectrum 4

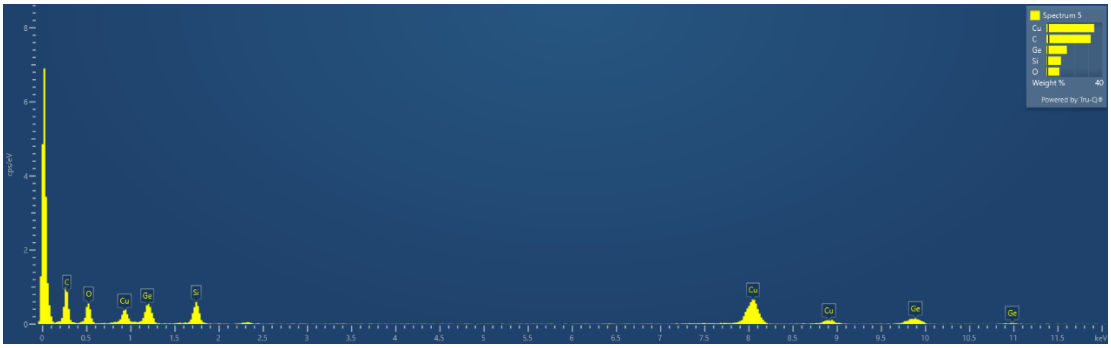

Figure 4.6.5 EDS point analysis of germanium nanoparticles Spectrum 5

Figure A4.6.6 EDS point analysis of germanium nanoparticles Spectrum 6

Point EDS measurements of nanoparticles show definitively the presence of germanium in the nanoparticles as evidenced by spectrums 1-5.

Spectrum 6 was the point EDS measurement for empty space, as observed from the micrograph, showing no germanium while providing meaningful background data, corresponding to the silicate and formvar coating and copper from the TEM copper grid.

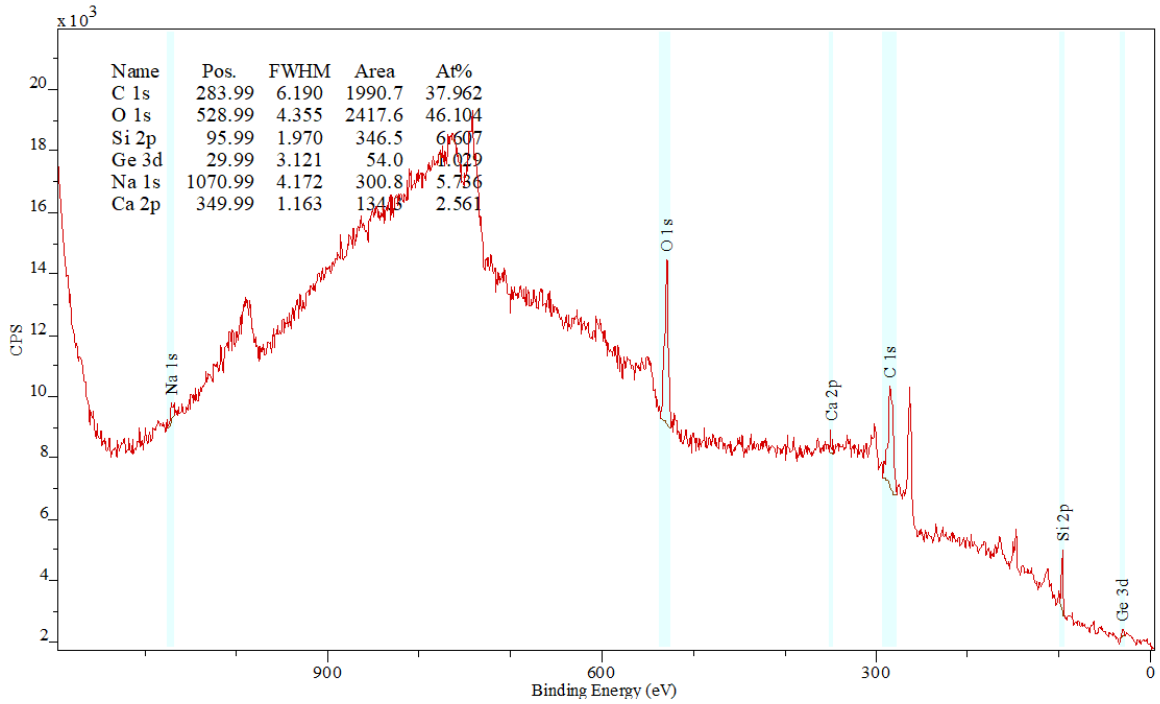

Figure A4.7XPS Survey spectra for 7th day samples. Spectrum was collected with an Al source (1486.69 eV), 3 scans, pass energy 50 eV. Referenced to adventitious carbon at 284.4 eV.

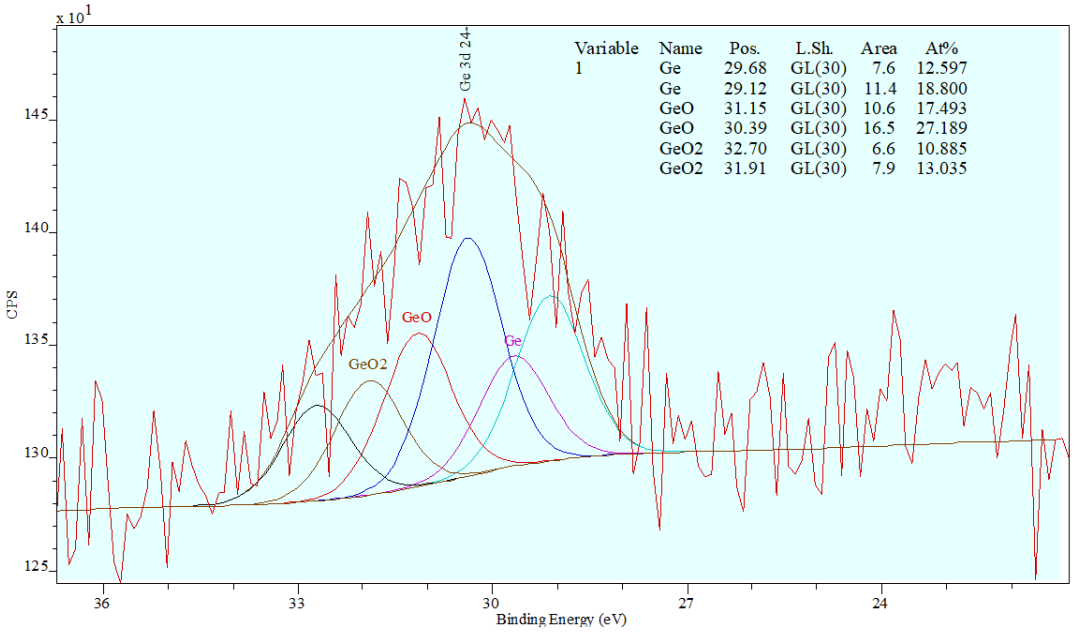

Figure A4.8 Representative Ge 3d XPS data for 7th day samples. Spectrum was collected with an Al source (1486.69 eV), 50 scans, pass energy 20 eV.

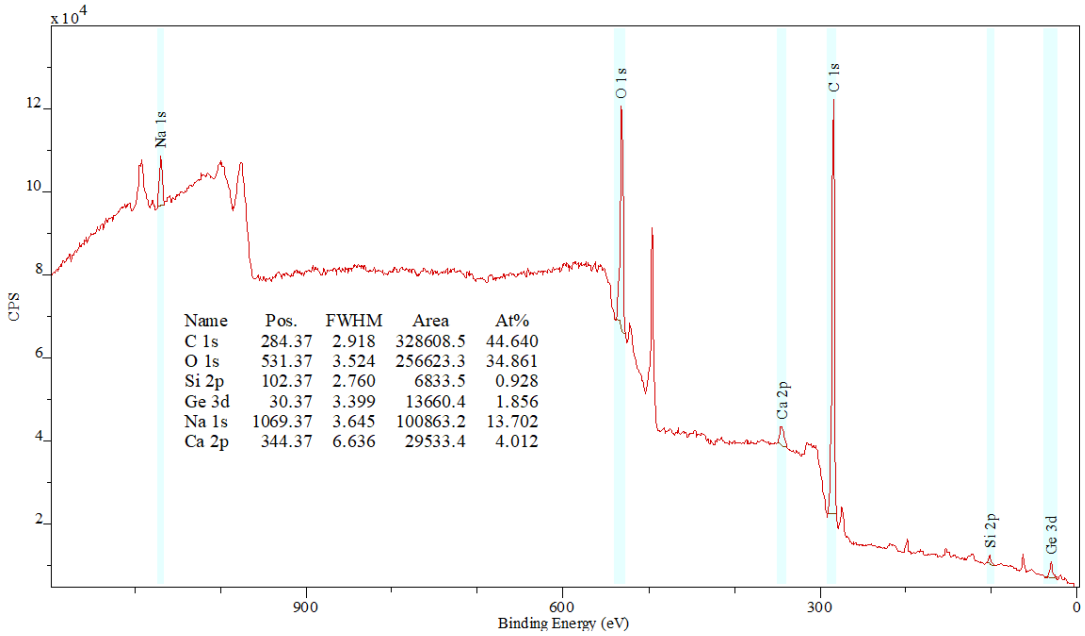

Figure A4.9 XPS Survey spectra for 12th day samples (methanol used was stored over molecular sieves). Spectrum was collected with an Al source (1486.69 eV), 3 scans, pass energy 50 eV. Referenced to adventitious carbon at 284.4 eV.

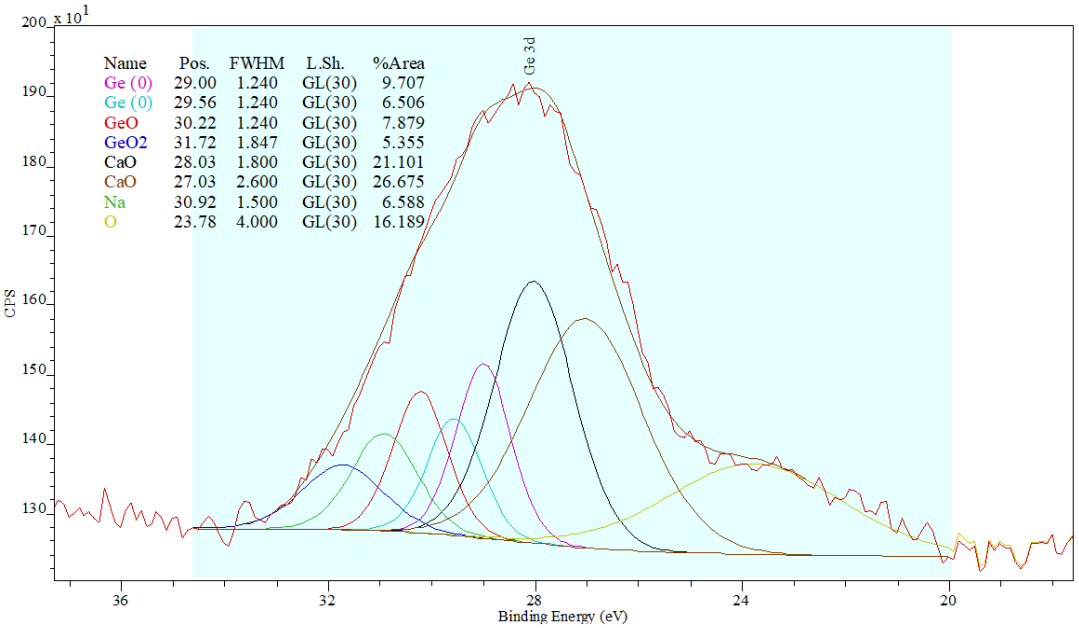

Figure A4.10 Representative Ge 3d XPS data for 12th day samples (methanol used was stored over molecular sieves). Spectrum was collected with an Al source (1486.69 eV), 50 scans, pass energy 20 eV.

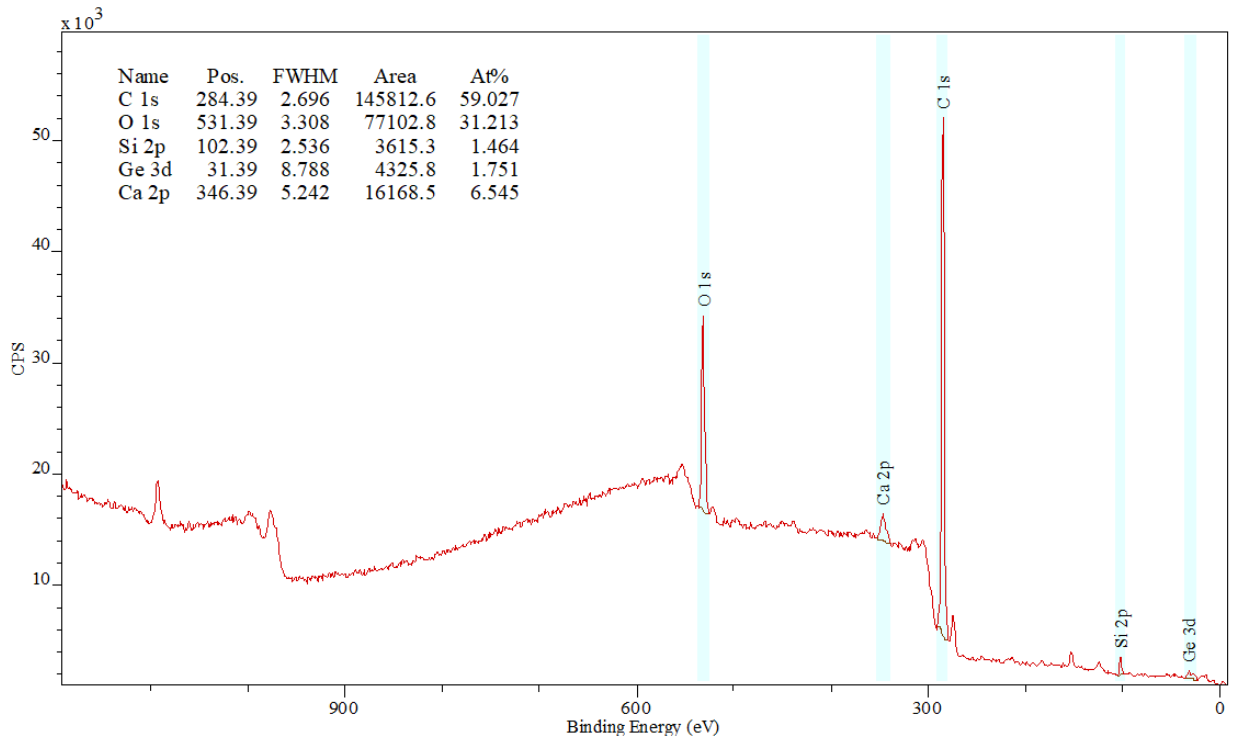

Figure A4.11 XPS Survey spectra for 12th day samples (using redistilled methanol). Spectrum was collected with an Al source (1486.69 eV), 3 scans, pass energy 50 eV. Referenced to adventitious carbon at 284.4 eV.

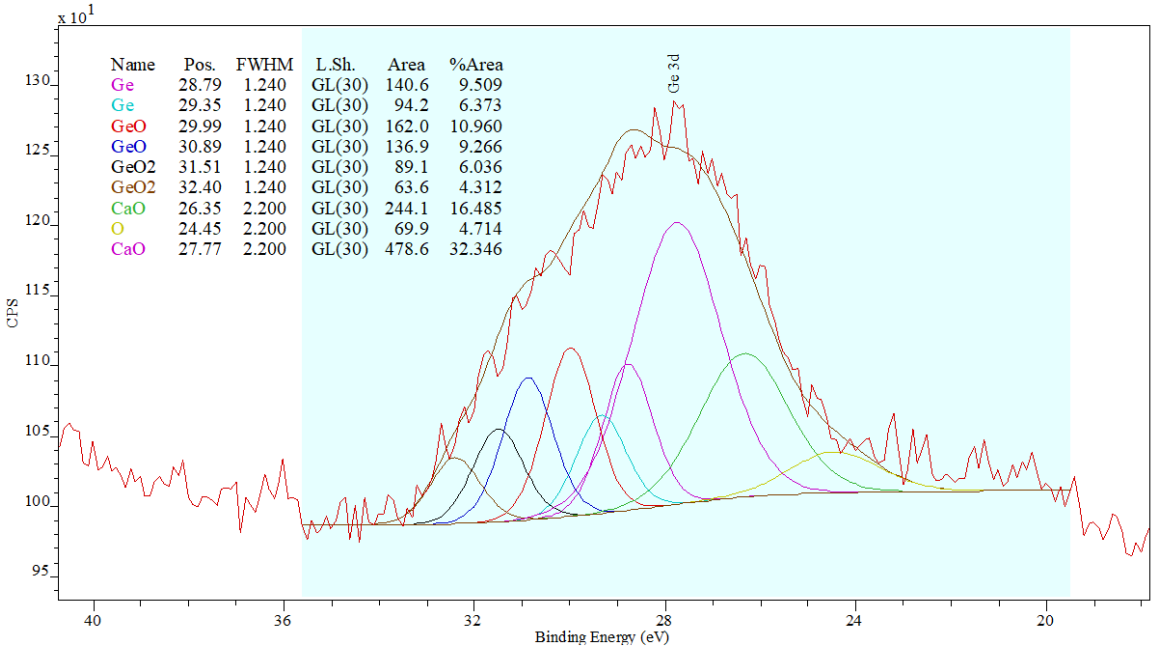

Figure A4.12 Representative Ge 3d XPS data for 12th day samples (using redistilled methanol). Spectrum was collected with an Al source (1486.69 eV), 50 scans, pass energy 20 eV.

High Resolution Transmission Electron Microscopy (HRTEM) Image

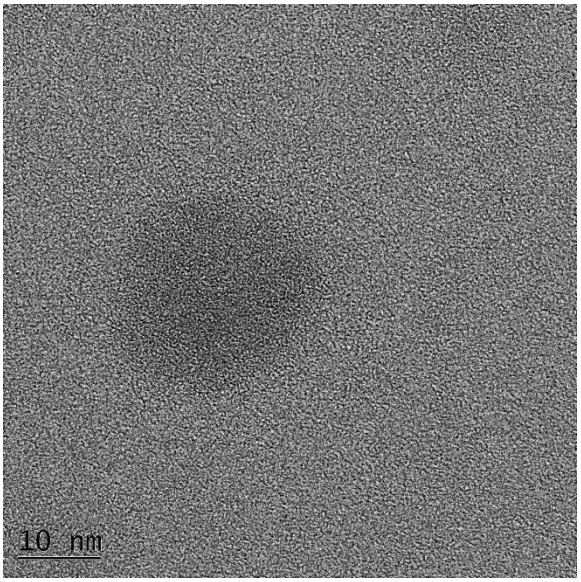

Figure A4.13 HRTEM Image of Germanium nanoparticle (10^{th} day sample)

Raman Spectroscopy of Nanoparticles

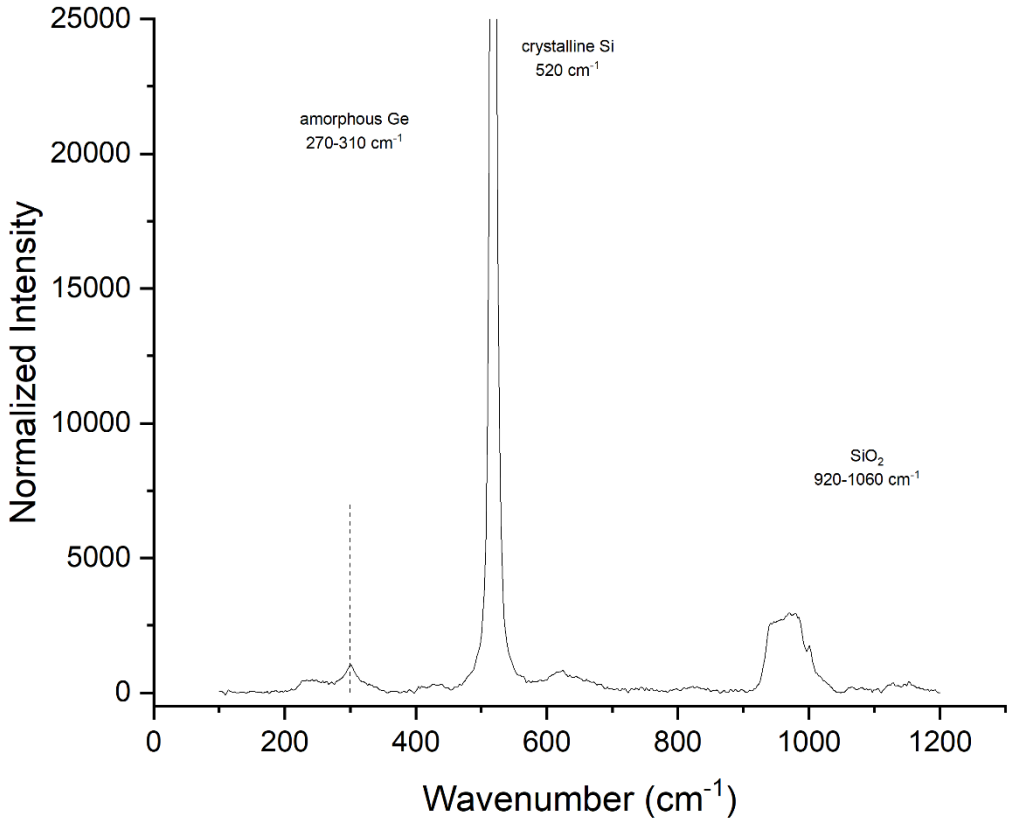

Figure A4.14 Raman spectrum of deposited Ge nanoparticles (12th day) onto a crystalline silicon wafer. Excitation wavelength: 514 nm. A broad peak at 270-310 cm^{-1} was observed, which corresponds to amorphous germanium.[55]